MOLECULAR CHARACTERIZATION OF TERRESTRIAL ORGANIC CARBON IN SOME ORGANIC-RICH SOILS IN THE NORTHERN LATITUDES

Eleanor Yvonne Swain

A thesis submitted to Newcastle University in partial fulfilment of the requirements for the degree of Doctor of Philosophy in the Faculty of Science, Agriculture and Engineering

School of Civil Engineering and Geosciences
Drummond Building
Newcastle University
United Kingdom

February 2013

Declaration

I hereby certify that the work presented in this thesis is my original research work, with the exception of the Ryggmossen samples presented in Chapters 4 and 5. The experiment set up and subsequent peat core and litter sampling was carried out by Dr. Lisa Belyea, Dr. Kathryn Allton, Dr. Chris Laing (Queen Mary, University of London), and subsequently extracted by Dr. Aminu Muhammad (Newcastle University). Carbohydrate and elemental analysis of the Ryggmossen samples were performed by Dr. Greg Cowie (University of Edinburgh, UK), however all interpretation of the data is my own. Wherever contributions of others are involved, every effort is made to indicate this clearly, with due reference to the literature, and acknowledgement of collaborative research and discussions. No part of this work has been submitted previously for a degree at this or any other university.

Eleanor Yvonne Swain

Abstract

Northern peatlands store around one third of the global soil carbon, however over the past 100 years significant areas of these peats and peaty gley soils have been drained and planted with coniferous forest. Afforestation could accelerate peat decay due to land disturbance causing the peatland to become a net carbon source, alternatively carbon may accumulate due to increased carbon fixation, causing the peatland to remain a net carbon sink. Despite the global importance of these mechanisms, our understanding of the fate of soil carbon stores in afforested carbon-rich soils (i.e. peaty gley and peat soils) remains unclear.

Peat and litter were analysed using thermally assisted hydrolysis and methylation (THM) in the presence of ^{13}C-labelled and unlabelled tetramethylammonium hydroxide (TMAH) which revealed the distribution, degradation transformations and turnover rates of vascular plant- and *Sphagnum*-derived phenols in carbon-rich soil profiles. The studied sites included afforested peaty gley soils under a first- and second-rotation Sitka spruce plantation, unplanted moorland, and self seeded Sitka spruce on unprepared moorland, all of which are located in Kielder Forest, northern England. A pristine peatland in central Sweden was also extensively sampled to assess the carbon related processes occurring in carbon-rich soils prior to afforestation. The effects of afforestation on total carbon stocks were also investigated.

The establishment of coniferous forests on peaty gley soils led to a net accumulation of soil carbon during the second rotation, surpassing the moorland carbon capacity. Whilst the encroachment of Sitka spruce on to open moorland via self seeding has resulted in a decreased carbon stock. The phenol composition of soil horizons displayed a maximum lignin content at deep soil across the afforested sites caused primarily by the horizon inversion that occurred prior to planting.

Sphagnum acid THM products were identified across the peatland and serve as putative biomarkers for the contribution of *Sphagnum*-derived organic matter in peats and afforested peatlands, as well as showing potential to provide information on peatland oxic conditions. *Sphagnum* phenols accumulate preferentially in the anoxic saturated peat, suggesting changes introduced via land-use change or climate change could affect the water table, and thus increase the potential peat decomposition, and the subsequent loss of carbon in peatlands.

Acknowledgements

My first acknowledgement goes to my supervisor, Dr. Geoff Abbott, whom I thank for his support, great advice and encouragement throughout the years of my PhD.
I'm highly indebted to Forest Research and NERC, for the funding of my 3 year PhD studentship. I would also like to thank my supervisors in industry; Dr. Mike Perks, and Dr. Elena Vanguelova for all of their help and guidance throughout the course of this project.

Thanks to Ian Harrison, Paul Donohoe, Berni Bowler, Phil Green and Yvonne Hall for all of their technical advice and assistance over the last 4 years in the lab and office. Thanks also to Dr. Tim Filley from the Department of Earth & Atmospheric Sciences, Purdue University, USA, for his supply of ^{13}C-TMAH.

I am also indebted to Dr. Sharon Mason, who provided me with the assistance I required at the start of my project, providing me with my first set of samples and guiding me through the array of new techniques. Thank you to everyone in the lab and office that has been there throughout my PhD for their help and friendship over the years.

I must also acknowledge the late Dr. Elizabeth Sulzman (Oregon State University, USA). For without her passion and enthusiasm in soil science, I may never have ventured further into the complex and intriguing word of soil science as a young undergraduate student. Elizabeth, you are a true inspiration.

Many thanks to my parents and sister for both their financial and emotional support throughout my many years at university.

Last but by no means least, my partner Paul Reed. You have the patience of a saint, and your support knows no limits. You got me through it! Thank you.

Contents

LIST OF FIGURES

LIST OF TABLES

Chapter 1:

Introduction & Literature Review

1 Introduction & Literature Review

1.1 Introduction

Over the past 100 years the Earth's climate has warmed on average *ca* 0.6 ºC as a direct result of increasing greenhouse gases (GHG) in the atmosphere, notably carbon dioxide (CO_2), which has risen from 280 ppmv 100 years ago to 379 ppmv in 2005 (IPCC, 2007). These changes are caused for the large part by human activities including the combustion of fossil fuels and land-use change (Watson and Noble, 2005). Furthermore, the Intergovernmental Panel on Climate Change (IPCC) project a further temperature increase of 1.4-5.8 ºC between 1990 and 2100, assuming a range of climate sensitivities (IPCC, 2001a). The increasing threat of climate change led to the Kyoto Protocol to be enacted in 1997, whereby as part of the United Nations Framework Convention on Climate Change (UNFCCC), Annex one Parties (including the UK) would commit to reducing GHG emissions. Annex one Parties can sequester carbon (C) to contribute to reducing GHG emissions via Land Use, Land-use Change and Forestry (LULUC) activities (Article 3.3), including afforestation (IPCC, 2001b)[1].

In Britain, the largest land use change in the past 100 years, has been the introduction of conifer plantations in the uplands, with 315,000 ha of shallow peatlands planted with coniferous forest (Hargreaves et al., 2003). This establishment of forest plantations on land that was previously not forest, is known as afforestation. Despite the positive effect of CO_2 incorporation into new plant biomass, afforestation of peaty soils involves land disturbance in order to obtain the desired environment for conifers; including drainage, ploughing, mounding and fertilisation (Minkkinen et al., 2008). These land preparation mechanisms can intensify rates of oxidation due to improved aeration and lowered water table, which can increase carbon losses to the atmosphere (Farmer and Nisbet, 2004; Zerva et al., 2005; Mason et al., 2009).

Globally, more than twice as much carbon is held in soils compared to vegetation or the atmosphere (Batjes, 1996). However, a recent study using data from the National Soil Inventory of England and Wales, concluded that between 1978 and 2003, carbon was lost from soils at a mean rate of 0.6% yr^{-1}, which increased to >2% yr^{-1} in soils with

[1] The text of the UNFCCC, and its Kyoto Protocol are available at http://unfccc.int/; the reports of the IPCC are available at http://www.ipcc.ch/.

carbon contents greater than 100 g kg^{-1} (10% TOC) (Bellamy et al., 2005).
Peats are the most significant terrestrial carbon pool in Britain, accounting for *ca* 50% of the total carbon stock (Milne and Brown, 1997), located almost entirely in the uplands; currently defined as land >300 m above sea level (Atherden, 1992). However, detailed bioclimatic modelling scenarios carried out by Clark et al., (2010a; 2010b; 2010c) revealed that under climate change, British upland altitude thresholds will retreat, reducing upland areas by up to 51%, increasing the vulnerability of peatlands and their associated carbon stocks.

Two components of the recalcitrant carbon pool are lignin and tannins which are quantitatively the second and fourth most abundant biopolymers in terrestrial biomass respectively (Crawford, 1981; Hernes and Hedges, 2000), and therefore their contribution to soil organic matter (SOM) is significant. As a result, previous studies have used lignin as an in indicator for predicting litter turnover in different soils, under different environmental conditions (e.g. Mason et al., 2009; Nierop et al., 2001; Nierop, 2001). Due to the difficulties quantifying tannins caused by the lack of one single analytical technique to simultaneously track their dynamics coupled with lignin phenols in litter and soils, there is little detailed information on tannin amounts, structures, and possible transformations (Nierop and Filley, 2008). However, with the introduction of ^{13}C-labelled TMAH, this limitation is being overcome (Section 1.2.10).

The second most common soil type for afforestation in the UK (after peaty gleys/podzols) were the peats (Vanguelova, 2012); which are dominated by *Sphagnum* mosses (Weng and Chapple, 2010). *Sphagnum* could potentially incorporate more carbon in both dead and alive *Sphagnum* biomass, than any other genus of plant (Clymo and Hayward, 1982). Despite being the dominant peat forming plant, and therefore being most at risk from the afforestation on peats, there has been little research into the impact of afforestation on this carbon store at both the bulk and molecular level.

It is critically important to understand the rate of organic matter turnover after afforestation for its net effect on atmospheric CO_2, as well as its effect on long term soil sustainability and carbon sequestration. In order to obtain a clearer picture of the processes occurring after afforestation, it is vital to understand the range of both lignins and polyphenolic compounds (e.g. from peat mosses) present prior to land use change.

1.2 Literature Review

1.2.1 Soil Organic Carbon

The carbon cycle can be separated into a simple, three compartmental system consisting of an oceanic (38,000 Pg C), an atmospheric (760 Pg C), and a terrestrial pool (8060 Pg C) (Pg = 10^{15} g) (Lal, 2004). The terrestrial compartment consists of the geologic (5000 Pg C), pedologic (2500 Pg C) and biotic pools (560 Pg C), with climate, geology and land management the primary controls on the quantity of carbon held within this compartment. These pools are interconnected, with carbon constantly cycling between them (Lal, 2004).

The pedologic (soil) pool receives carbon primarily as CO_2 from the atmosphere via the biotic pool. CO_2 is converted into terrestrial biomass and either sequestered as SOM by biochemical and physical stabilisation processes, or released back to the atmosphere as CO_2 and CH_4 via respiration (Kay and Angers, 2000; Dawson and Smith, 2007; Lorenz et al., 2007). The amount of carbon held within a soil (carbon stock) is based on the balance between these biomass inputs from the biotic pool, and respiration outputs (Post et al., 1982), with carbon sequestered only when there is an additional transfer of carbon from the atmosphere to soils and thus a contribution to climate change mitigation (Powlson et al., 2008) as requested by the IPCC (IPCC, 2000). The rapid turnover of the biotic pool has a major influence on whether the soil acts as a source or a sink to carbon (Milne and Brown, 1997).

Soil organic carbon (SOC) is an important component of SOM, contributing *ca* 60% (1550 Gt C) to the pedologic pool of 2500 Gt (Post et al., 2001; Lal, 2004). Fresh SOC is added to the soil as leaf, wood and root litter and root exudates of plants and soil microbes, and undergoes decomposition, forming a natural decomposition continuum through the soil profile. During decomposition, between 60 and 80% of labile OM are converted to CO_2 (González-Pérez et al., 2004), most of which occurs in the first year of litter decomposition (active fraction; with a residence time of <10 years). The remaining material is transformed into the intermediate OM pool, which is more recalcitrant, and has a residence time of decades to a hundred years, and finally into the most stable pool which may have a turnover time of >1000 years (slow/refractory fraction) (Trumbore, 1997; von Lützow et al., 2006; Lorenz et al., 2007). The refractory OM pool is

responsible for the long term stabilisation of carbon in soils (von Lützow et al., 2006). The mechanisms controlling SOC stabilisation include; the selective preservation due to the structural composition, the spatial inaccessibility, and interactions with mineral surfaces and metal ions (Sollins et al., 1996; Six et al., 2002; von Lützow et al., 2006).

The turnover of SOM and thus SOC depends upon several factors including the quality and chemical quality of the carbon (labile or refractory), climate and soil properties such as clay content, soil moisture, pH and nutrient status, and site conditions (Dixon et al., 1994; Trumbore, 1997; Jandl et al., 2007), of which several of these factors can be influenced by afforestation and subsequent forest management (Jandl et al., 2007). However, recent studies have shown that the so-called recalcitrant carbon displays a large potential to degrade, especially under elevated temperature scenarios, whilst fresh relatively labile components can act to inhibit the activity of the enzymes that degrade the substrate, introducing the concept that relatively fresh SOC can contribute to the recalcitrant pool (von Lützow et al., 2006; Karhu et al., 2010; Kleber et al., 2011).

1.2.2 Kyoto Protocol

Under the terms of the Kyoto Protocol, the 36 nations that make up the Annex 1 countries are committed to reducing emissions by 5.2% from the 1990 base year level over the period 2008-2012; with the UK committed to reduce GHG emissions by 12.5% (Kyoto Protocol, 1997). Under Article 3.3 of the Kyoto Protocol, afforestation can be used to sequester carbon in order to offset carbon emissions (IPCC, 2001b). According to Lal (2004), global carbon sequestration has the potential to off-set fossil fuel emissions by 5 to 15%. Carbon sequestration however, is not a recent proposal; utilising the soils capability to sequester carbon from the atmosphere was first suggested by Dyson in 1977 (Metzger and Benford, 2001).

The Kyoto Protocol discusses the carbon sequestration potential after afforestation and reforestation of 0.4-4.5 t C ha^{-1} in above and below ground biomass in boreal and temperate regions. However there is no discussion of potential soil carbon stock changes in previously non-cultivated land (i.e. peatland and moorland) (IPCC, 2000). The rules for the Kyoto Protocol, including Article 3.3 were further elaborated in the Marrakech Accords in 2001. Stating that "Each Party included in Annex I shall account for all changes in the following carbon pools: above-ground biomass, below-ground

biomass, litter, dead wood, and soil organic carbon. A Party may choose not to account for a given pool in a commitment period, if transparent and verifiable information is provided that the pool is not a source." However this still allows for soil carbon stocks to be estimated; often based on low resolution soil surveys with estimated soil types and depths, thereby utilising unreliable data (UNFCCC, 2001; Lindsay, 2010). Section 1.2.3 provides evidence of the variability incurred from estimating carbon stocks.

Cannell (1999) has reported the questionable effect of growing trees to sequester carbon in line with the Kyoto Protocol's LULUC activities. Suggesting that whilst sandy soils have the potential to sequester carbon via increased SOC and biomass, the majority of plantations in the UK occur on peat and peaty gley soils. In contrast to sandy soils, peat soils whilst indeed they will display a degree of carbon sequestration in the first 1-2 rotations of conifer plantation, they will in the long term (>100 years) lose more carbon that can be sequestered by the forests planted on them (Cannell et al., 1993; Ball et al., 2011). Cannell (1999) concluded that LULUC activities within the UK were simply "buying time" thereby delaying global warming, but the eventual release of the carbon was inevitable.

1.2.3 Peatland

Peatlands are widespread across the northern circumpolar area, and at a global scale are considered an important SOC sink (Gorham, 1991), with carbon accumulating in northern peatlands since the end of the last ice age in the Holocene (Charman, 2002). The southern limits of these peatlands in North America is approximately 40°N latitude, and 50°N latitude in Eurasia (Tarnocai and Stolbovoy, 2006). Early estimates of the global land cover of peatlands were conservatively estimated at 0.82% of Earth's land surface (Taylor, 1964). However, recent estimates suggest that northern peatlands alone cover approximately 2.4% of the Earth's land surface, and store approximately 547 Pg of organic carbon (Yu et al., 2010), which equates to approximately 35% of the global soil carbon (Post et al., 1982; Oades, 1988). Previous estimates have been considerably lower; 300 Pg C (Sjors, 1980), 249 Pg C (Armentano and Menges, 1986), and 455 Pg C (Gorham, 1991), highlighting the uncertainty in peatland carbon storage.

The characterisation of peatlands varies regionally based on differing peatland factors. For example, Canada characterises peatlands based primarily on their hydrological regimes, whereas Russia uses a vegetation classification, and Finland uses a combination of hydrological, nutrient status and peat margin gradients (Tarnocai and Stolbovoy, 2006). The classification of peat in the UK has evolved from the Avery soil classification (1980), characterising peatland according to their vegetation (Kennedy, 2002). Peatlands can be further divided according to their hydrological regimes; bog peatlands which receive all their water from precipitation, and fen peatlands which are formed under the influence of ground- and/or surface-water supply. Peatland landscapes can display a composite of these types; for example, upland blanket bogs are often interspersed with nutrient poor fens, and raised bogs can grade into fringing 'lagg' fens (JNCC, 2011). Owing to the complex and numerous definitions that can be applied to different factors of peatland ecosystems, it has been suggested that the generic term peatland be used to avoid confusion about conditions that may or may not be present at a particular site (Bridgham et al., 1996).

Peat is defined as the partially decomposed remains of plants and soil organisms which have accumulated at the surface of the soil profile, resulting in a typical carbon content of ~52% total organic carbon in UK peat (Lindsay, 2010). Carbon accumulation occurs owing to the increased rate of input of organic material from the surface compared to the rate of decomposition, due to in part the low temperatures (Gorham, 1991; Minkkinen et al., 2008), and the oxygen constraints on the degrading enzymes (Freeman et al., 2001b). However the rates of carbon sequestration on peatlands are a complex balance between carbon inputs and carbon outputs (Post et al., 1982), with minor changes in plant communities, the temperature and precipitation regimes, the water table and the soil chemistry (Holden et al., 2007), potentially having a significant effect on the carbon storage dynamics (Belyea and Malmer, 2004). Although there has been extensive research into the sensitivity of peatlands to climate change, findings have shown that peatland dynamics are non-linear and this non-linearity makes predicting the response of these habitats to a changing climate difficult (Belyea, 2009; Clark et al., 2010b). A literature review carried out by Belyea (2009), revealed three possible non-linear pathways of peatland development; an initial sensitivity to changing conditions which can results in a multitude of development pathways, long periods of little change followed by a drastic change occurring under weak or steady environmental forcings

(e.g. temperature, precipitation and albedo), and the response of peatlands to external forcings at unexpected frequencies (Belyea, 2009).

1.2.4 Sphagnum

Peatlands are either classed as bogs or fens, depending on their hydrology; ombrotrophic bogs receive all of their water and subsequently all of their nutrients from precipitation, whereas minerotrophic fens receive base-rich water that has passed over mineral soils (Clymo, 1983). The succession of fens to bogs is often accompanied by the invasion of *Sphagnum* species (Andrus, 1986; van Breemen, 1995). Litter produced by the peat-forming moss, *Sphagnum*, is the dominant input of organic carbon into ombrotrophic bogs and some minerotrophic fens. Considered an intermediate between planktonic algae and vascular species (Clymo, 1970), *Sphagnum* mosses, although devoid of lignin phenols (Weng and Chapple, 2010), biosynthesize other phenylpropanoids including *trans*-sphagnum acid (*p*-hydroxy-β-[carboxy-methyl]-cinnamic acid); Fig. 1.1; (Rasmussen et al., 1995). These phenolics are connected via ether bonds to cell wall polymers and act both as structural support components and as inhibitors of microbial decomposition of the organic substrate (van der Heijden, 1994; Verhoeven and Liefveld, 1997; Freeman et al., 2001a).

Sphagnum can manipulate its environment, including increasing the peat acidity due to a high cation exchange capacity, allowing *Sphagnum* to dominate at the expense of other species (van Breemen, 1995). The anoxic and acidic conditions created by the growth and expansion of *Sphagnum* species significantly reduce the microbial degradation of both the *Sphagnum* species and the other peat forming species (Verhoeven and Liefveld, 1997) further enhancing the carbon sequestration capacity of peats.

Sphagnum tissue is regarded as extremely recalcitrant due to the high content of sphagnum acid in the cell walls (Rudolph and Samland, 1985), decomposing more slowly than the leaves of most other plants (Rochefort et al., 1990; Johnson and Damman, 1991). Therefore, it is imperative to understand the distinctive biochemistry of *Sphagnum* and its degradation pathways in order to elucidate the dynamics of organic carbon degradation in peat.

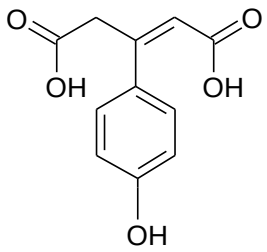

Fig. 1.1: The structure of *p*-hydroxy-*β*-[carboxymethyl]-cinnamic acid (sphagnum acid).

1.2.5 Sphagnum Characterisation

Alkaline cupric oxide (CuO) oxidation of 15 species of *Sphagnum* moss released large quantities of unsubstituted *p*-hydroxyl phenolic compounds as well as sphagnum acid (Williams et al., 1998). Alkaline CuO oxidation has also been utilised to characterise lignin in vascular species (Hedges and Parker, 1976; Hedges and Mann, 1979a; Hedges et al., 1982; Kögel, 1986), however lignin phenols with a C3 side chain are lost during the CuO treatment. These side chains are retained when tetramethylammonium hydroxide (TMAH) thermochemolysis is used (Hatcher et al., 1995; Filley et al., 2000) (Section 1.2.9). van der Heijden et al. (1997) have identified six thermochemolysis products of sphagnum acid, including phenolic acids with C3 side chains (van der Heijden et al., 1997). Therefore thermochemolysis is advantageous over CuO oxidation when detailed structural information is required (Wysocki et al., 2008).

1.2.6 Land-Use Change

Approximately 1.5 x 10^5 km^2 of northern peatlands have been drained for forestry (Paavilainen and Päivänen, 1995), which is approximately 3.8% of the total area of northern peatlands (4 x 10^6 km^2; Yu et al., 2011). Globally, forest soils hold around two thirds (*ca* 787 Pg C) of the total carbon stored in forest ecosystems (1146 Pg) (Dixon et al., 1994) and, with the residence time of soil carbon exceeding that of plant biomass (von Lützow et al., 2006), this makes soil carbon more stable and therefore more significant to the long term storage of carbon than plant biomass (Jones and Alison, 2004).

In order to optimise the productivity of forest stands established on peats and peaty gley soils, land preparation including drainage, ploughing and fertilisation is carried out

(Biggs, 1979; Minkkinen et al., 2008). The extensive ground preparation accelerates the oxidation of the stored carbon due to a disturbed soil structure and broken soil aggregates, lowered water table, decreased soil moisture and peat aeration (Tiessen and Stewart, 1983; Hillman, 1992; Mojeremane et al., 2010). These physical changes can enhance carbon losses to the atmosphere as CO_2 (von Arnold et al., 2005), as well as to ground water via dissolved organic matter (DOM) (Baker et al., 2008) and particulate organic matter (POM) (Evans and Warburton, 2010). Conversely, the growth of conifers has been shown to enhance the carbon sink through increased biomass, litter and root input (Farmer and Nisbet, 2004; Zerva et al., 2005). Furthermore, Byrne and Farrell (2005) have shown that afforestation does not always lead to increased soil CO_2 emissions.

Studies on the effects of afforestation on SOC stocks have also resulted in conflicting results, for example, several studies have shown no change after afforestation (Davis et al., 2003; DeGryze et al., 2004; Peri et al., 2010), whereas other groups found increases (Guo and Gifford, 2002; Morris et al., 2007) while some have found a decrease in SOC stocks (Alberti et al., 2008). These SOC changes after afforestation are primarily controlled by the soil type, plant type, climate, previous land use, and the time after afforestation (e.g. Guo and Gifford, 2002; Paul et al., 2002). Several other studies however, observed an initial decline in SOC stocks after afforestation, then a recovery to and even exceeding pre-afforestation levels (Paul et al., 2002; Hu et al., 2008).This pattern has also been observed in the specific study of afforestated Sitka spruce (*Picea sitchensis* (Bong.) *Carr*.) on peats and peaty gley soils (Hargreaves et al., 2003; Zerva et al., 2005). However, the time it took for SOC stocks to recover varied significantly; Hargreaves et al. (2003), showed that after afforestation the soil can return to a carbon sink in under 10 years after the plantation of the first rotation. However, Zerva et al. (2005) showed that the carbon storage did not recover to pre-afforestation levels until the second rotation. These studies indicate that the conclusions reached by Cannell (1999) (Section 1.2.2), may not be entirely justified, and that further research into the effect of afforestation on peaty gley soils is required.

The contribution of recalcitrant compounds, including lignin and tannin, to SOC and their role in the carbon cycle and carbon stabilisation are significant (Mason et al., 2009) but are often left out of carbon studies. Therefore key information about these compounds after afforestation is still limited.

1.2.7 Lignin

Latin: *lignum* = wood

After cellulose and hemicellulose, the biopolymer lignin is the most abundant biopolymer in vascular species (Crawford, 1981; Gold et al., 1989), and accounts for approximately a third of the organic carbon in the biosphere (Boerjan et al., 2003). A complex aromatic polymer (Fig. 1.2), lignin comprises 30% of the mass of woody species and lesser amounts in non-woody species (Adler, 1977). Lignins are chemically connected to cellulose and hemicellulose in the cell walls to provide mechanical strength to vascular plants and allow for the conduction of water and nutrients (Sarkanen and Hergert, 1971).

Lignins are biosynthesised by the oxidative co-polymerisation of mainly three hydroxycinnamyl alcohol monomers differing in their degree of methoxylation; *p*-coumaryl, coniferyl, and sinapyl alcohols (Fig. 1.3). These monolignols lead to *p*-hydroxyphenyl (P), guaiacyl (G) and syringyl (S) units of lignin respectively, via the enzymic dehydrogenation of the respective alcohols (Adler, 1977). There are further precursor alcohols, albeit much less abundant, which can contribute to the lignin macromolecule, including 5-hydroxyguaiacyl nuclei (5-hydroxyconiferyl) identified in some tropical grasses and a variety of temperate and tropical woody angiosperms (Suzuki et al., 1997) and more recently in non-woody angiosperms (del Río et al., 2007). The chemical composition and structure of lignin can vary widely between different vascular plant groups, and therefore can provide an excellent vegetation indicator. Lignin can be divided into three main groups based on their structural monomer units; gymnosperm, angiosperm and grass lignin (non-woody) (Higuchi, 1980).

Gymnosperms are dominated by guaiacyl-based lignin, which are less susceptible to decomposition compared to syringyl-based lignins that dominate hardwoods (angiosperms) (Sarkanen and Hergert, 1971; Boerjan et al., 2003). Non-woody species are dominated by cinnamyl lignin derivatives (*p*-coumaric acid and ferulic acid) in addition to smaller quantities of guaiacyl and syringyl lignin derivatives (Clifford et al., 1995).

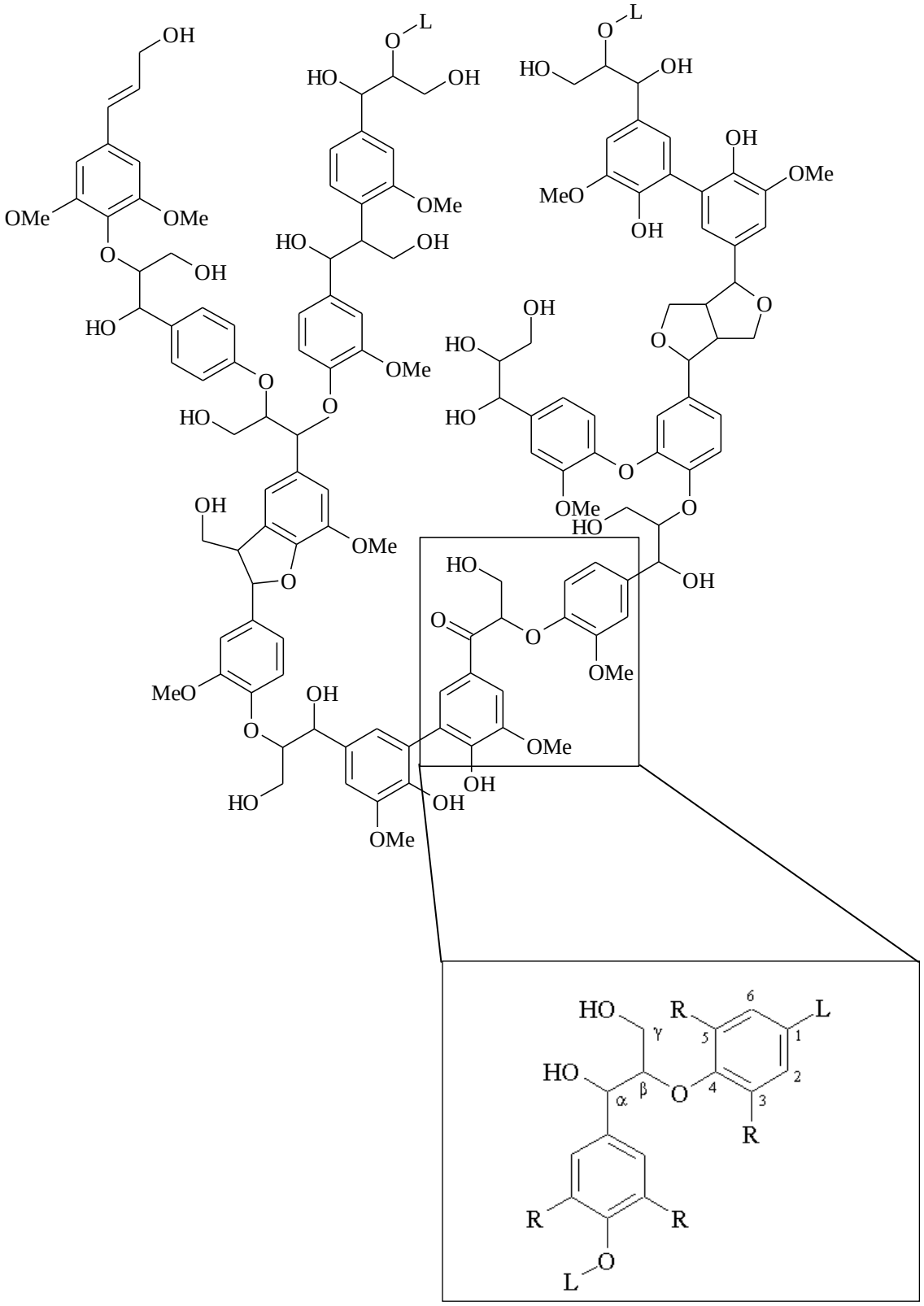

Fig. 1.2: A schematic representation of lignin (reproduction of Dorrestijn, 2000; L = lignin biomacromolecule). The box displays the dominant β-O-4 linkage found in the lignin biopolymer.

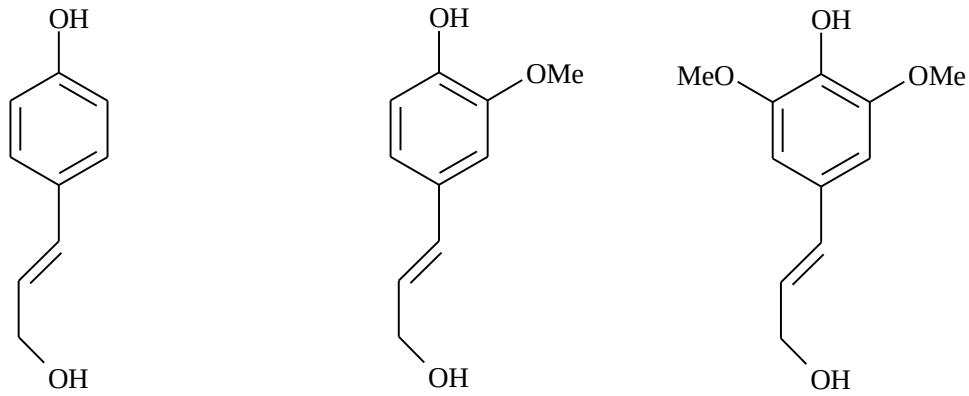

p-coumaryl alcohol coniferyl alcohol sinapyl alcohol

Fig. 1.3: Three main precursor alcohol monomers that form lignin; *p* -coumaryl, coniferyl and sinapyl.

The lignin monomers methoxyphenyl propanoid units are linked primarily via alkyl–aryl ether bonds (β-O-4) (contributing 60% and 46% of linkages in gymnosperms and angiosperms respectively (Dorrestijn et al., 2000)); a covalent bond formed between the β carbon position, on the alkyl side chain and the phenolic oxygen atom found on the fourth carbon of the aromatic phenol ring (Fig. 1.2) (Adler, 1977). In addition, there are up to twelve other bond types occurring in lignin, including the more resistant carbon–carbon linkages namely, β-5, β-β, β-1, and 5-5, which are more prevalent in gymnosperm vegetation because of the availability of the C5 position for coupling (contributing 30% and 21% of linkages in gymnosperms and angiosperms respectively) (Dorrestijn et al., 2000; Boerjan et al., 2003; Kishimoto et al., 2010), that account for the structural complexity of softwood lignins (Vane et al., 2003).

The complexity of this three-dimensional biopolymer of high molecular weight coupled with the heterogeneous intramolecular bonds, forms the basis for why lignin is considered a recalcitrant molecule (Crawford, 1981), and therefore considered to be a major contributor to the stable carbon pool in soils; accumulating in SOM with respect to other more labile compounds (Dignac et al., 2005). However, based on a critical overview of the literature available, it appears that the chemical recalcitrance of the lignin polymer does not necessarily lead to its long-term stabilisation, specifically in aerobic soils (e.g. Kiem and Kögel-Knaber, 2003; Dignac et al., 2005; Bahri et al., 2006; Kalbitz et al., 2006; Marschner et al; 2008; Klotzbücher et al., 2011; Dungait et al., 2012). For example, compound-specific ^{13}C analysis of lignin CuO oxidation products

indicated that lignin turnover was faster than that of bulk SOC (Heim and Schmidt, 2007). Thus, a relatively rapid turnover of soil incorporated lignin is possible (<38 years) (Rasse et al., 2006; Heim and Schmidt, 2007).

Lignin degradation is limited to a handful of microorganisms which are able to produce the specific oxidoreductases that are necessary for lignin cleavage (Kirk and Farrell, 1987). Microbial degradation of lignin is an aerobic process performed predominantly by wood decaying fungi (basidiomycetes), of which there are three main groups, the soft rot, brown rot and white rot (Kirk and Farrell, 1987).

White rot fungi are the only microorganisms capable of completely mineralising lignin to CO_2 and water (Gold et al., 1989). White rot degradation residues are characterised as having undergone extensive side chain oxidation and aromatic ring cleavage (Umezawa and Higuchi, 1987; Srebotnik et al., 1997). Brown rot fungi are capable of mineralising the methoxyl groups of lignins (Kirk and Farrell, 1987), resulting in the enrichment in hydroxylated phenyl (catechol derivatives) substituents as a result of methoxyl demethylation or demethoxylation with only a small degree of side chain oxidation (Filley et al., 2000). Fig. 1.4 illustrates the three main changes that occur as a result of this oxidative attack by fungi; side chain oxidation, demethylation/demethoxylation and ring cleavage.

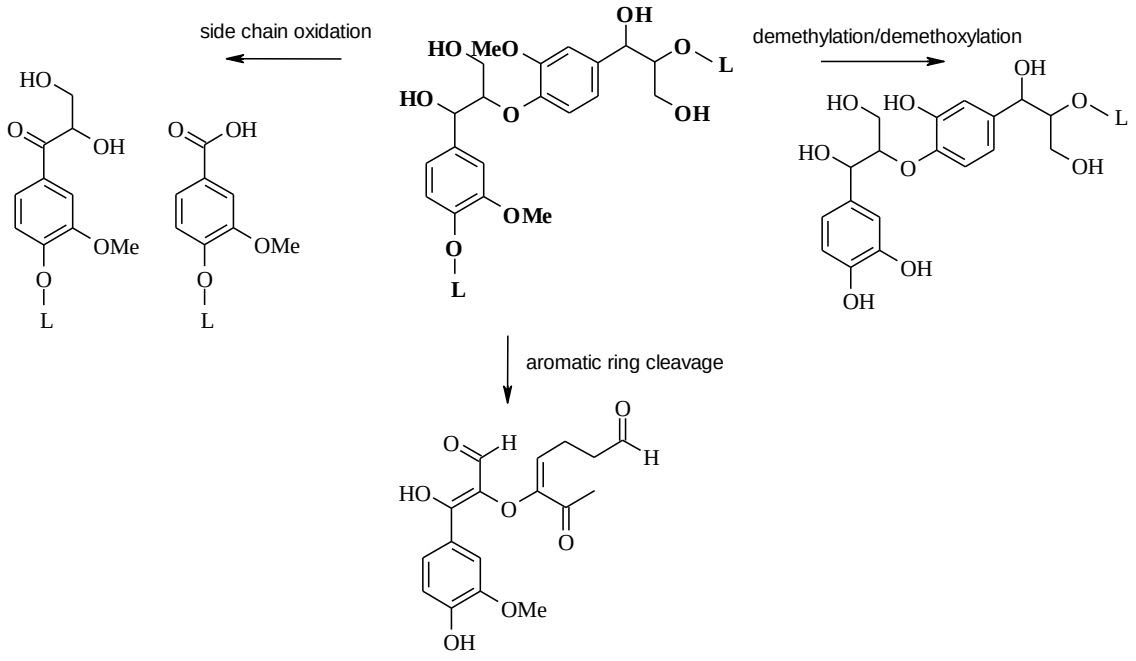

Fig. 1.4: The main chemical changes that occur during fungal degradation of guaiacyl lignin (reproduction of Filley et al., 2000; L = lignin biomacromolecule).

1.2.8 Lignin Characterisation

Extensive lignin research has been carried out since 1865, when F. Schulze first coined the term lignin, however the research was primarily focused on the lignin biomacromolecule structure and biosynthesis (see Adler 1977, and references therein). The discovery of the taxonomic separation of lignin by Bibbs in 1958 paved the way for the discussion and analyses of lignin as vascular vegetation markers (gymnosperm/angiosperm), primarily using the cupric oxide method (CuO) (Hedges and Parker, 1976; Hedges and Mann, 1979b; Hedges et al., 1982; Kögel, 1986).

The oxidation of lignin with CuO yields eight major reaction products; six vanillyl and syringyl phenols in the forms of aldehydes, ketones and carboxylic acids, and ferulic and *p*-coumaric acid (Hedges and Parker, 1976). Hedges and Mann (1979a) utilised these products to provide information on the vegetation source (S/V; C/V ratios), degradation state [Ad/Al], and the yield of lignin (Λ) in the sample.

Despite providing information on the vegetation source and degradation state of the lignin, the CuO technique does not provide any structural information (Dijkstra et al., 1998), for example, the propyl side chain which indicates intact lignin phenols is not retained (Hatcher et al., 1995; Filley et al., 2000). Together with the lack of structural information, the CuO technique is extremely time consuming and is best suited to organic poor samples (Hatcher et al., 1995; Wysocki et al., 2008), and has therefore received less attention over the past 20 years, as new techniques have been introduced.

Pyrolysis in combination with gas chromatography and mass spectrometry ((Py)-GC-MS) has also been utilised to analyse the lignin biomacromolecule in soils (e.g. Dijkstra et al., 1998; Vancampenhout et al., 2009; Wang et al., 2009). The non-volatile lignin macromolecule is thermally treated in the absence of oxygen, which yields smaller, more volatile fragments that are amenable to GC (Kaal and Janssen, 2008). However, benzenecarboxylic acids are not released upon pyrolysis due to the decarboxylation of these products (Saiz-Jimenez, 1994; Klingberg et al., 2005). To overcome this and aid the structural identification of macromolecules, thermochemolysis in the presence of tetramethylammonium hydroxide (TMAH) was introduced as a pyrolytic degradation technique with in-situ derivatisation (Challinor, 1989). The methylating agent TMAH prevents the decarboxylation of products and results in the in situ generation of methyl

esters of carboxylic acids, making the molecules amenable to GC (Challinor, 1989; Kaal and Janssen, 2008). When coupled to an MS, electron impact mass spectra (EI-MS) of each of the eluted compounds can be recorded so that compounds can be identified.

Lignin undergoes heat-induced bond dissociation to give reduced molecular mass compounds which reflect the composition of the original polymer (del Río et al., 1996). The exact reaction mechanism is not fully understood, however Clifford et al. (1995) demonstrated that the dominant reaction with TMAH is mainly a thermally assisted chemolytic degradation rather than degradation induced by pyrolytic bond cleavage, leading to the widely used abbreviation THM; thermally assisted hydrolysis and methylation (e.g. Challinor 2001; Joll et al., 2003; Tanczos et al., 2003). TMAH is currently the most common reagent used for THM, accounting for over 90% of published THM applications (Shadkami and Helleur, 2010).

1.2.9 THM in the Presence of TMAH

THM cleaves primarily the dominant β-O-4 linkage, however this extends to all propyl-aryl ether linkages (Hatcher et al., 1995), with the mechanism proposed described by Filley et al. (1999). Although the proportion of these linkages varies according to the type of wood, typically more than two-thirds of the linkages in lignin are aryl ether linkages (Pandey and Kim, 2011). Therefore although Geib et al. (2008) stated that THM detects chemical modification of the entire lignin fraction of the sample, THM in fact provides an indication of the relative abundance of aryl ether linkages remaining intact in the macromolecular network (McKinney and Hatcher, 1996; Klotzbücher et al., 2011). So far, however, there has been no discussion on the quantitative recovery of lignin after THM, primarily due to the lack of understanding of the reaction mechanisms (Kaal and Janssen, 2008). However, there are a handful of lignin model compound studies that have shown that THM provides characteristic products retaining the structural attributes of β-aryl ether, β-5, β-β subunits and cinnamyl alcohol end groups (Filley et al., 1999; Kuroda et al., 2002; Kuroda and Nakagawa-Izumi, 2005).

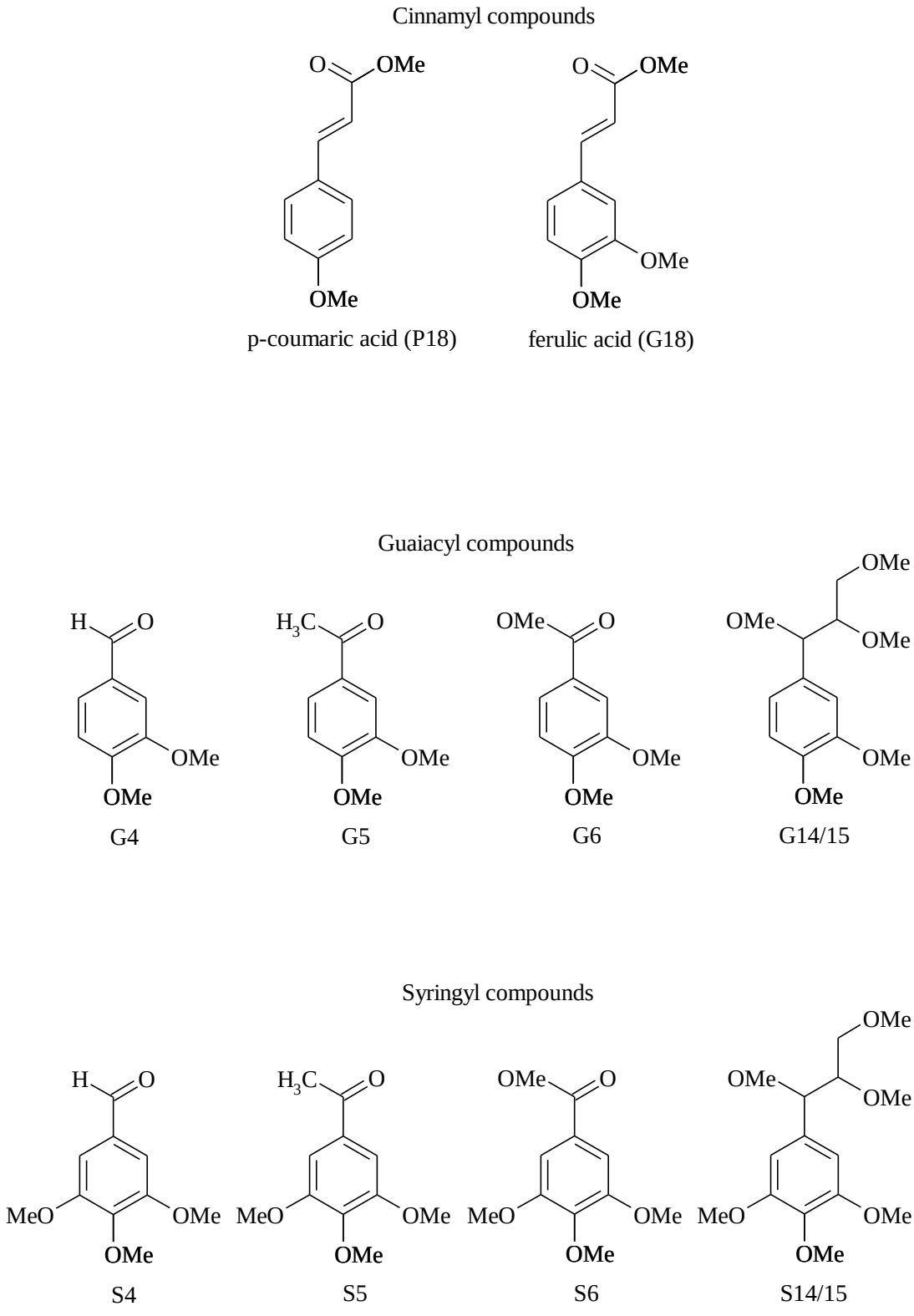

Fig. 1.5: Dominant permethylated aromatic compounds released by TMAH thermochemolysis.

For highly coalified lignin and extensively degraded lignin, the ability for TMAH to depolymerise lignin is limited due to the extensive loss of the β-O-4 bond or the adjacent hydroxyl groups on the propyl side chain (Hatcher, 1990; Filley et al., 1999). Therefore, the total yield of lignin monomers released from fresh and degraded samples is dependent, in part, on the extent and type of alteration of the lignin macromolecule and not solely dependent upon the concentration of lignin present in the sample. It is also important to consider the varying degree of dominant linkages including β-O-4, β-5, and β-β that occur in differing plant sources as well as changing with degradation, which will influence the relative decomposition rates of syringyl, guaiacyl and cinnamyl phenols (Vane et al., 2001). Due to the specific bond cleavage of TMAH, THM has been suggested to be best suited to the analysis of fresh and mildly altered plant fractions (i.e. litter (L), fermentation (F) and humified (H) organic horizons, and carbon-rich A soil horizons) (Filley et al., 2006).

The THM of lignin yields a large suite of lignin phenols; the eight major reaction products are analogous to the eight CuO oxidation products, with the additional release of the intact lignins; *threo/erythro* 1-(3,4-dimethoxyphenyl)-1,2,3-trimethoxypropane (G14/15) and *threo/erythro* 1-(3,4,5-trimethoxyphenyl)-1,2,3-trimethoxypropane (S14/15) (Fig. 1.5) (Hedges and Parker, 1976). Where *threo* and *erythro* are prefixes used to distinguish diastereomers. The lignin proxies introduced for CuO products by Hedges and Mann (1979a) (Section 1.2.8), can also be used for the THM products (Hatcher et al., 1995; Wysocki et al., 2008; Klotzbücher et al., 2011).

1.2.10 ^{13}C-Labelled TMAH

The major limitation of TMAH thermochemolysis is that it does not distinguish between the original methoxyl groups of lignin and those added during derivatisation (Filley et al., 2000). This shortcoming makes it impossible to determine whether or not lignin residues have undergone demethylation during microbial decay or even if the compound is indeed a lignin product. However the introduction of ^{13}C-labelled TMAH in 1999, methylates phenolic acids and phenols using ^{13}C-labelled methyl groups, has allowed the distinction between lignin, altered lignin and non-lignin phenols (Filley et al., 1999). This technique has been successfully used to analyse a variety of biopolymers, SOM and DOM (Filley et al., 2000; Filley et al., 2002; Frazier et al., 2005;

Filley et al., 2006; Nierop and Filley, 2007; Mason et al., 2012). With the use of ^{13}C-TMAH thermochemolysis together with unlabelled TMAH, it was found that after correcting for contributions of non-lignin phenols and altered lignin; lignin proxies; Λ, F/P, [Ad/Al], and Γ, were severely influenced by non-lignin phenols, Nierop and Filley (2007) found that the total yield of lignin in two sandy soil profiles under oak forest was reduced by 16-46% after correcting for tannin and poly-hydroxyl compounds. By contrast, S/G and C/G remained similar (Nierop and Filley, 2007).

Fig. 1.6 demonstrates the advantage of using ^{13}C-labelled TMAH to differentiate between lignin, demethylated lignin and non-lignin phenols. Both syringic acid (lignin source) and gallic acid (tannin source) produce the same 3,4,5-trimethoxybenzoic acid methyl ester (S6) derivative when methylated with unlabelled TMAH, with a molecular weight of 226. Using ^{13}C-labelled TMAH, syringic acid has a molecular weight of 228, indicating the methylation of two hydroxyl groups, whereas gallic acid has a molecular weight of 230, indicating the methylation of four hydroxyl groups by ^{13}C-TMAH. This highlights how mass spectral interpretation can be used to determine the % ^{13}C-labelled methyl groups added and therefore allow for the successful determination of source input (Filley et al., 1999; Filley et al., 2006). The principal limitation of ^{13}C-labelled TMAH, is that fully demethylated syringic acid is indistinguishable from gallic acid; the main building block of hydrolysable tannins (Nierop and Filley, 2007).

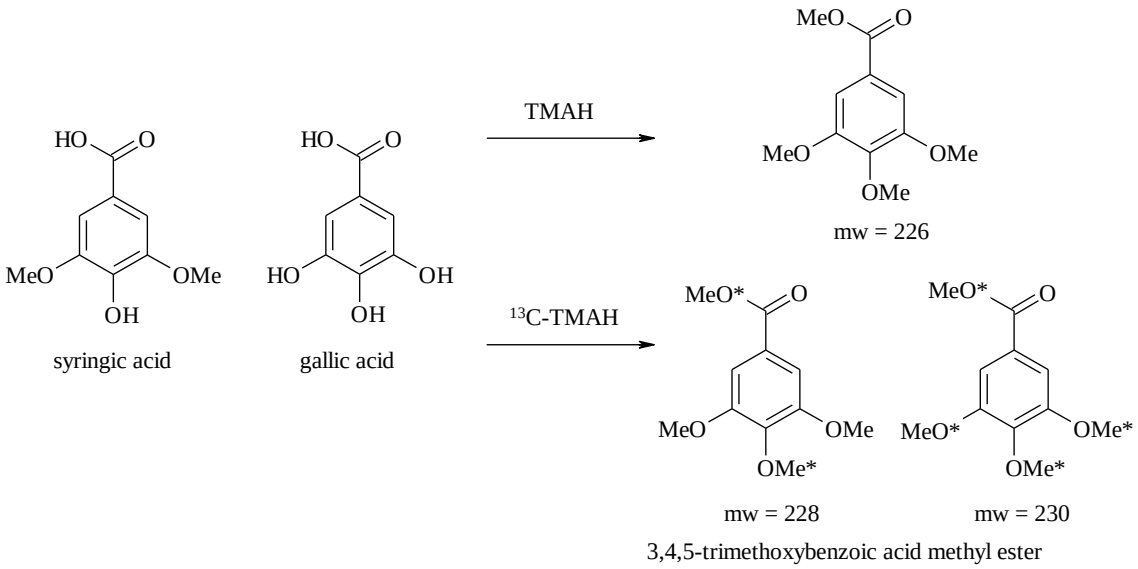

Fig. 1.6: Reaction schematic showing how ^{13}C-labelled TMAH can be used to distinguish between source inputs with similar structure but different origin (i.e. syringic acid (lignin) and gallic acid (tannin)). Asterisks indicate ^{13}C-labelled methyl groups.

The use of ^{13}C-labelled TMAH can also differentiate between sources which could potentially have a high input from non-lignin sources including G6 and G18. For example, 3-hydroxy-4-methoxybenzoic acid methyl ester (lignin-derived or a possible intermediate in the Cannizzaro reaction described below) can be distinguished from 3,4-dihydroxybenzoic acid methyl ester (microbially demethylated lignin or other phenolic acids - protocatechuic acid), which are both methylated to form 3,4-dimethoxybenzoic acid methyl ester (G6). Also, the 3-(3-methoxy, 4-hydroxy-phenyl)-3-propenoic acid methyl ester (lignin-derived) can be differentiated from 3-(3,4-dihyroxyphenyl)-3-propenoic acid methyl ester (microbially demethylated lignin or other phenolic acids - caffeic acid) which are methylated to form (*E*)- 3-(3,4-dimethyoxyphenyl)-3-propenoic acid methyl ester (G18) (Nierop and Filley, 2007).

It must be noted that a Cannizzaro type reaction might affect the THM method, in which a disproportionation of the aldehyde occurs, resulting in production of the corresponding methoxybenzoic acid methyl ester and methoxybenzyl alcohol methyl ether (Hatcher and Minard, 1995; Tanczos et al., 1999). This could particularly affect the lignin proxies that incorporate methoxybenzoic acid methyl esters, such as acid/ aldehyde ratios [Ad/Al], indicating the relative state of lignin oxidation. This reaction could contribute to understanding the results of Hatcher et al. (1995) and Klotzbücher et al. (2011), that for the same lignin sample, a higher [Ad/Al] was measured for the TMAH products compared to the CuO products. It has also been shown that CuO can depolymerise lignin more completely than THM, as CuO cleaves not only the β-O-4 linkage, but also some of the C-C linkages (Goñi and Hedges, 1992). Therefore CuO method may be able to access a larger part of the unaltered, non-oxidised lignin structure (Klotzbücher et al., 2011), resulting in a lower [Ad/Al].

Due to the large range of analytical methods, and no standard method for THM in the presence of ^{13}C-labelled or unlabelled TMAH, lignin concentrations reported in the literature vary and may not be comparable with each other (Hättenschwiler and Vitousek, 2000; Klingberg et al., 2005). However, thermochemolysis-GC-MS as an analytical technique bears many advantages over the other methods, primarily, this technique is faster than other methods, sample pre-treatment is virtually absent, and TMAH can take place under milder conditions than traditional pyrolysis resulting in fewer secondary reactions, allowing the original structure to be established (Kaal and Janssen, 2008).

1.2.11 Tannin

Tannin, a water soluble polyphenol, can exceed lignin concentrations in leaves, bark and needles, accounting for up to 40% dry weight (Kraus et al., 2003). Tannins are secondary metabolites, and as with lignins, are unique to vascular plants. Tannins can be divided into two main groups; hydrolysable (gallo- and/or ellagi-) tannins (HT) and condensed tannins (proanthocyanidins) (CT) (Bate-Smith, 1977; Hernes and Hedges, 2004). CTs are present in ferns, gymnosperms and half of all woody angiosperms, whilst HTs can be found in 15 of the 40 orders of dicot angiosperms (Harborne, 1997; Nierop et al., 2005).

CTs are composed of flavan-3-ols joined with C-C linkages, with monomers distinguishable by the number of hydroxyl groups on the B ring; di-hydroxy and tri-hydroxy B ring indicates procyanidins (PC) and prodelphinidins (PD), respectively (Fig. 1.7). As with the lignin macromolecular structure, the diversity of condensed tannin monomers reveals a heterogeneous structure of high molecular weight. HTs are composed of gallic acid or hexahydroxydiphenic acid esters, linked to a central sugar moiety with ester linkages (Fig. 1.7) (Kraus et al., 2004).

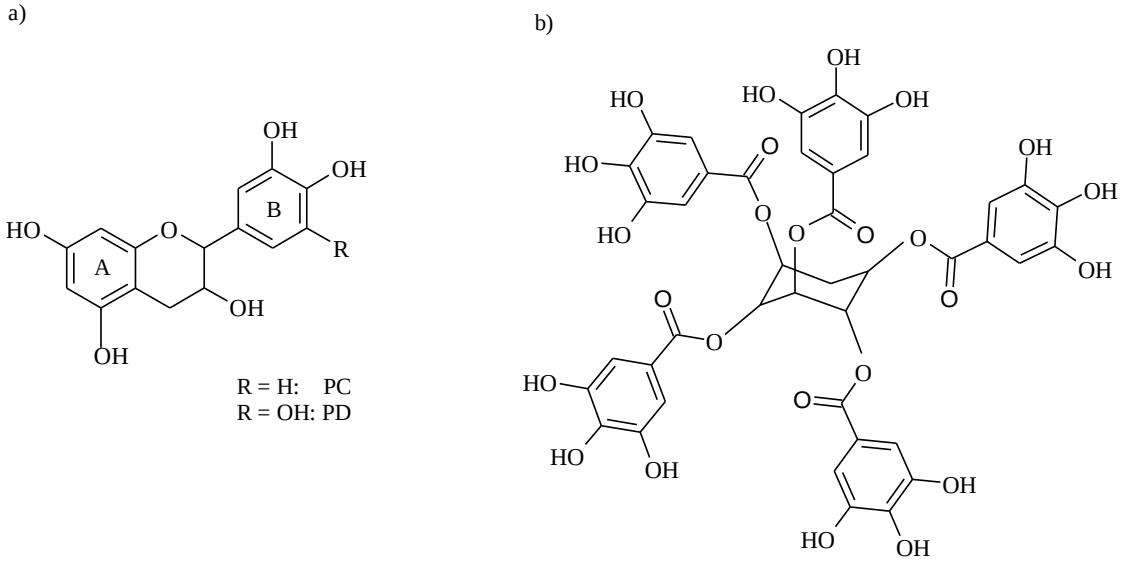

Fig. 1.7: The chemical structure of (a) condensed tannins and (b) hydrolysable tannins. R = H: epicatechin, R=OH: epigallocatechin (Behrens et al., 2003; Nierop et al., 2005). Where PC = procyanidins and PD = prodelphinidins.

Tannins have a significant effect on soil degradation dynamics (Lorenz et al., 2000), due to in part their ability to inhibit microbial degradation, and also in part to their role in herbivore and insect defence (Schultz et al., 1992). However, some microbes are resistant to the tannins, with CTs conveying more resistance to microbial attack than HTs (Bate-Smith and Swain, 1962; Bhat et al., 1998).

Owing to the lack of one single analytical technique to simultaneously track lignin and tannin, the fate of tannins within soils remains largely unknown (Nierop et al., 2005). However, the introduction of ^{13}C-labelled TMAH in 1999 has allowed the concurrent analysis of both lignin and tannin phenols (Filley et al., 1999). As a result, it is important to determine accurately the concentrations and inputs of tannins together with lignins within soils to provide a better understanding of the importance of tannins in ecosystem processes.

1.2.12 Carbohydrates

Carbohydrates are an important constituent of living biomass, that are formed during photosynthesis and are the primary source of metabolic energy in living matter, incorporating carbon, hydrogen, oxygen and solar energy. Carbohydrates can occur as monosaccharides (simple sugars), oligosaccharides (short chain monosaccharides 2-10), and polysaccharides (large polymer carbohydrates) (Brett and Waldron, 1996).

Carbohydrates are ubiquitous and abundant in soils, and therefore are potentially useful in elucidating sources, processes and pathways of organic matter in soils (Jia et al., 2008). However, carbohydrates have been used relatively infrequently for organic matter source discrimination and degradation patterns in carbon-rich soils (van Smeerdijk and Boon, 1987; Moers et al., 1989; Jia et al., 2008).

Neutral monosaccharides account for 10 to 20% of SOM (Cheshire, 1979; Amelung et al., 1996; Puget et al., 1999; Karroum et al., 2004), despite being amongst the most easily biodegradable substrates in soils. Literature also indicates that the age of sugar carbon atoms may be as old or even older than that of bulk SOC, and therefore contribute to the recalcitrant SOM pool (Gleixner et al., 1999; Gleixner et al., 2002; Kögel-Knabner, 2002; De Leeuw et al., 2006; Derrien et al., 2006). It has been suggested that the relative preservation of sugars could be due to either of several

preservation factors: physical or physico-chemical preservation, combination in humic substances (Derrien et al., 2006; von Lützow et al., 2006), or the continuous recycling of the sugars by microbes (Sauheitl et al., 2005).

Primarily utilised to analyse complex and inextractable compounds, such as lignins, TMAH has also shown to have the potential to recover entrapped carbohydrates and identify simple sugars (Fabbri and Helleur, 1999; Schwarzinger, 2003; Tanczos et al., 2003; Estournel-Pelardy et al., 2011). Fabbri and Helleur (1999) discovered that reducing sugars form methylated saccharinic acid (deoxyaldonic acid) methyl esters under THM conditions. Although THM does not analyse the hemicellulosic carbohydrate pool and individual carbohydrates as observed with acid hydrolysis, it can analyse a cellulose pool that is ordinarily hidden to acid hydrolysis, making THM an ideal tool for complex mixtures (Estournel-Pelardy et al., 2011).

1.3 Aims and Objectives of this Thesis

Recent land use changes within the UK, have seen an increase in the afforestation of carbon rich peat and peaty gley soils with conifers (Cannell et al., 1993). However, little is known about the effects afforestation will have on SOM properties, phenolic transformations and decomposition products. This study investigates the soil carbon stocks, phenolic and polyphenolic biomarker stocks and their dynamics in a pristine peat and after the afforestation of these peat and peaty gley soils with Sitka spruce. This will provide valuable knowledge of carbon cycle dynamics at the molecular level allowing us to investigate how refractory lignin and tannins are, and begin to understand whether or not afforested soils have the potential to become sources of carbon dioxide rather than being carbon sinks.

The study was divided into four sub-projects, each with specific aims:

1) Carbon stock and phenolic distributions in peaty gley soils afforested with Sitka spruce (Chapter 3).

   This sub-project assessed and compared the within and between site variations in phenolic content with increasing soil depth in three different peaty gley soils in Northumberland (UK) a) an un-forested moorland, b) a first rotation Sitka spruce afforested moorland, and c) a second rotation Sitka spruce afforested moorland. The objectives were to:

   (i) examine the effects of afforestation on peaty gley soils carbon stocks within the soil profiles, in order to understand the long term effects (~100 years) of afforestation on soil carbon stocks; and

   (ii) characterise and analyse changes in THM product composition with depth, to test for the persistence of lignin phenols in the first and second rotation Sitka spruce stands, which will inform on the processes occurring after afforestation.

2) *Sphagnum* biomarkers from a typical northern latitude peatland, Ryggmossen (Sweden) (Chapter 4) and the geochemical composition of *Sphagnum* peat cores spanning arange of environmental conditions from Ryggmossen (Chapter 5). This sub-project, used a pristine peatland to confirm the identity of *Sphagnum* biomarkers and to determine the role of these peat moss phenolics on the turnover of soil organic carbon, and their use as *Sphagnum* biomarkers within afforested peat. The objectives were to:

   (i) confirm the identity of *Sphagnum* biomarkers,

   (ii) characterize the phenolic biochemistry of *Sphagnum*; the dominant peat forming species, and

   (iii) analyse changes in THM product composition with peat depth, to test for persistence of the *Sphagnum* markers and to infer their extent of degradation relative to vascular plant-derived phenols as a function of distance from the water table.

3) The implications of the spreading of Sitka spruce away from the plantation area onto the adjacent peatland (known as the edge-effect) on the SOM, at both the bulk and molecular level (lignin, non-lignin phenolics and other organic compounds) (Chapter 6).

   This sub-project utilised ^{13}C-labelled TMAH to assess the impact of a Sitka spruce plantation on an adjacent peatland in Northumberland (UK). The soil sites investigated were sampled with increasing distance from the Sitka spruce plantation; a) forest-margin peat under the canopy of self-seeded Sitka spruce, b) forest-margin peat, and c) open peat. The objectives were to:

   (i) identify key vegetation biomarkers (including lignins and tannins) and evaluate the changes of the chemical characteristics as a function of depth,

   (ii) compare and evaluate the changes across the three sites to explore whether the adjacent forest and self seeded Sitka spruce affect the phenolic and SOC dynamics with soil depth, and

   (iii) further explore the potential of ^{13}C-TMAH thermochemolysis as a screening method for the rapid characterisation of biomacromolecules in SOM as a function of depth.

4) The research carried out for the above sub-projects allowed also an investigation in to the TMAH thermochemolysis analysis of carbohydrates in peat and soil (Chapter 7). Although carbohydrates have been used relatively infrequently for SOM source discrimination and degradation patterns in carbon-rich soils (van Smeerdijk and Boon, 1987; Moers et al., 1989; Jia et al., 2008), THM released these compounds from the soil and litter macromolecular structures in significant quantities. However it has been suggested that the presence of these methylated carbohydrates could be derived from the use of cellulose extraction thimbles (Mason, 2009). The objectives were to:

   (i) ascertain whether or not the extraction thimbles are a source of the methylated carbohydrates, and

   (ii) identify the carbohydrate derived products in the soil samples, and examine the usefulness of the technique of THM-GC-MS in the analysis of carbohydrates within soil and peat samples.

Chapter 2:

Methods & Sites

2 Methods & Sites

2.1 Standard Laboratory Procedures

Laboratory grade solvents, dichloromethane (DCM) and methanol (MeOH) were supplied by LSS Ltd. (UK) and distilled on a 50 plate Oldershaw column. All glassware was cleaned in a laboratory dishwasher (Miele 7783CD) with Lancerclean and Lancerinse (Lancer Ltd., UK) before being rinsed in 15 MΩ.cm deionised water and dried in an oven at 60 °C. Multiple rinsing with MeOH and DCM then took place before a final three washes in the solvent to be used.

Glass wool, extraction thimbles and anti-bumping granules were all pre-extracted with DCM:MeOH (93:7; v:v) in a Soxhlet apparatus for 24 h.

2.2 THM in the Presence of ^{13}C-Labelled and Unlabelled TMAH

On-line thermally assisted hydrolysis and methylation (THM) in the presence of unlabelled and ^{13}C-labelled tetramethylammonium hydroxide (TMAH) was performed using a pulsed mode open pyrolysis system, specifically a CDS 1000 pyroprobe unit (Chemical Data Systems, USA) fitted with a platinum coil and a CDS 1500 valved interface. ^{13}C-labelled TMAH was provided by Dr. Timothy Filley, synthesised according to published methods (Filley et al., 1999).

Approximately 1 mg of extracted organic sample and 20 mg of extracted mineral sample was weighed into a quartz pyrolysis tube plugged with pre-extracted silica wool. An internal standard, 5α-androstane was added to the samples to allow for accurate quantitative chromatographic analysis to be carried out on peaks within the chromatogram, and an aqueous solution of unlabelled or ^{13}C-labelled TMAH (25% w/w) was added to the sample immediately prior to THM. The pyroprobe interface was maintained at 340 °C and THM was carried out at 686 °C (actual 610 °C) for 10 s (20 °C/ms temperature ramp) with the products passing into an Hewlett-Packard 5890 gas chromatograph (GC) with an open split (40 mL/min) and a 60 m HP5-MS column (0.25 mm internal diameter, 0.25 μm film thickness; J&W Scientific, USA). Helium was used as carrier gas at a flow rate of 1 mL/min. The GC oven was programmed from 50 °C to 220 °C at a rate of 1.5 °C /min, where it was held isothermally for 1 min and

then raised to a final temperature of 320 °C at a rate of 15 °C/min, where it was held for 16 min. This GC temperature programme was used throughout unless otherwise stated (Chapter 5). The GC was linked to a Hewlett-Packard 5972 mass spectrometer (MS) (electron voltage 70 eV, source temperature 180 °C, multiplier voltage 2000V, interface temperature 320 °C), which was used to analyse the pyrolysis products. The data were obtained using a Hewlett-Packard Vectra 486 Chemstation computer, used in full scan mode (50-700 amu). Compound identification was based on the NIST98 mass spectral library, on ion fragmentation patterns and following the conventions described in other studies (van der Heijden, 1994; Clifford et al., 1995; Hatcher et al., 1995; Filley et al., 2000; Mason et al., 2009).

The slow increase in temperature of 1.5 °C /min from 50 °C to 220 °C of the GC oven allowed for improved peak separation, which ensured that determination of chromatographic peak area was as accurate as possible. Pyrolysis was carried out at 610 °C so that condensed tannins (CTs) could be cleaved to produce characteristic thermochemolysis products (Nierop et al., 2005). Clifford et al. (1995) has shown that pyrolysis at high temperatures yields similar results to low temperature THM, however gymnosperm sources such as Sitka spruce will contain these CTs (Harborne, 1997). THM temperature of 600 °C and 610 °C have also been used to unequivocally identify tannin markers in a soil profile under Corsican pine (Nierop and Filley, 2008) and Sitka spruce (Mason et al., 2009).

Excluding the changes in the GC programme for the Ryggmossen peat core samples (Section 2.7.6 and Chapter 5), the experimental conditions (temperature, ratio of TMAH to sample, solvent choice and contact time between sample and TMAH) were kept constant throughout each study, ensuring that consistent and meaningful results were obtained. This allowed the relationships between amounts of phenols with increasing burial depth to be made. Any site specific changes will be discussed in the respective chapters. The ratio of TMAH to sample was maintained at 5 μL/1 mg of organic samples and 10 μL/20 mg of mineral samples.

2.2.1 Aromatic Hydroxyl Contents

During thermochemolysis with ^{13}C-labelled TMAH, the acidic oxygen functional groups on the products are methylated by the ^{13}C-labelled methyl groups from the TMAH. Therefore, the number of ^{13}C-labelled methyl groups added to the TMAH thermochemolysis reaction products should be equivalent to the number of acidic oxygen functional groups on the molecule, and is measured as a difference in the mass of the molecular ion between unlabelled and ^{13}C-labelled THM products.

The percent aromatic hydroxyl content gives the proportion of hydroxyl groups initially present prior to methylation, and is displayed as the percent of one hydroxyl group present (%1 OH) or two hydroxyl groups present (%2 OH). In THM products where there are more than two methoxyl groups present, one, two or three of the observed methoxyl groups could have previously been hydroxyl groups, therefore the percent of one, two and three hydroxyl groups can be calculated (%1 OH, %2 OH, %3 OH). For example, after THM, G6 is observed as 3,4-dimethoxybenzoic acid methyl ester (Fig. 1.5), however, intact G6 is 3-hydroxy-4-methoxybenzoic acid methyl ester (i.e. one hydroxyl group). Therefore, if ^{13}C-labelled TMAH indicated that one of the two observed methyl groups were labelled, it can be assumed that the sample is intact lignin (i.e. 1 OH), if however there was the presence of two hydroxy groups, a non-lignin input would be identified. A typical soil will give a complex mixture of thermochemolysis products with inputs from both lignin and non-lignin phenols contributing to the G6 signal, therefore the percent hydroxyl content calculations can determine the percent of intact (one hydroxyl group) and non-lignin (two hydroxyl groups) phenols within a sample .

Percentage aromatic hydroxyl content was determined using equations and mass spectral methods set out in previous work (Filley et al., 1999; Filley et al., 2006; Mason et al., 2009). The key equations taken from Filley et al. (2006) are shown in Appendix A1. Unlabelled TMAH thermochemolysis of samples allowed the structures of products to be identified and to determine the appropriate baseline fragment ion ratios needed to accurately calculate percent ^{13}C following addition of the ^{13}C-labelled TMAH. Owing to limited amounts of the ^{13}C-labelled TMAH, it was not used throughout the thesis.

2.2.2 Mass Yields and Lignin Parameters

THM in the presence of unlabelled TMAH was used to determine the individual mass yields of thermochemolysis reaction products. 5α-androstane was used as an internal standard and a relative response factor (RRF) of 1 was assumed, allowing the semi quantitative measurements of the changing amounts of thermochemolysis products with increasing soil depth and across changing habitats. The percent aromatic hydroxyl content, was used to adjust unlabelled TMAH thermochemolysis mass yields, in order to distinguish between intact lignin, demethylated lignin and non-lignin phenolics (tannins) as outlined in Filley et al. (2006).

Lambda (Λ) is the sum of the amounts of the eight dominant lignin derived phenols (G4+G5+G6+S4+S5+S6+G18+P18) normalised to 100 mg of OC (Hedges and Mann, 1979b; Hedges et al., 1982; Kögel, 1986). Individual compound yields allow the relative degradation dynamics that govern the changes in Λ to be assessed. The S/G and C/G ratios are two lignin parameters that are the weight ratios of total syringyl and cinnamyl phenols, respectively to total guaiacyl phenols. The S/G ratio is used to assess vegetation input, reflecting the relative abundance of angiosperms (S/G > 0) and gymnosperms (S/G = 0), measured as the sum of the OC-normalised amounts of syringyl (S4+S5+S6) divided by the sum of the normalised amounts of guaiacyl (G4+G5+G6) phenols (Hedges and Mann, 1979b). Cinnamyl phenols are only produced in appreciable amounts by non-woody tissues of vascular plants, therefore the C/G ratio indicates the input of non-woody tissue, using the sum of the normalised amounts of cinnamyl (*p*-coumaric acid, P18 and ferulic acid, G18) divided by the sum of the normalised amounts of guaiacyl (G4+G5+G6) phenols (Hedges and Mann, 1979b). The acid/aldehyde ratio $[Ad/Al]_{G/S}$ records the state of oxidation for guaiacyl components (G6/G4) and syringyl components (S6/S4) and was determined as the sum of 3,4-dimethoxybenzoic acid methyl ester (G6) divided by 3,4-dimethoxybenzaldehyde (G4) or the sum of 3,4, 5-trimethoxybenzoic acid methyl ester (S6) divided by 3,4,5-trimethoxybenzaldehyde (S4) (Filley et al., 2006). $\Gamma_{G/S}$ records the relative lignin side chain oxidation, determined by 3,4-dimethoxybenzoic acid methyl ester (G6) divided by the sum of *threo/erythro* 1-(3,4-dimethoxyphenyl)-1,2,3-trimethoxypropane (G14/15) or 3,4,5-trimethoxybenzoic acid methyl ester (S6) divided by the sum of *threo/erythro* 1-(3,4,5-trimethoxyphenyl)-1,2,3-trimethoxypropane (S14/15) (Filley et al., 2006).

2.3 THM Reproducibility

Precision of manual integration was assessed by repeated (10x) integration of four selected peaks from a single TIC. Percent relative standard deviation ([std dev/mean]*100) varied from 1.5 to 3.5% with greater variability associated with smaller peaks.

The reproducibility of ^{13}C-labelling was assessed by repeated (4x) analysis of a sample with both unlabelled and ^{13}C-labelled TMAH (total of 8 analyses). Percent relative standard deviation of the total corrected lignin yield (Λ) varied 6.3%, whilst the standard error of the percent intact lignin phenols ranged from 0.36 to 2.51%.

Although the repeatability of THM has been raised as a concern (e.g. Kaal and Janseen, 2008), the reproducibility of quantitative results in this study has been shown to be relatively high.

2.4 Temperature Calibration of Pyroprobe

Thermochemolysis was performed on-line using a pulse mode open pyrolysis system fitted with a platinum coil probe and a valved interface (Section 2.2). When using THM, it is important to know the precise temperature at which pyrolysis of the samples is being carried out. However, the temperature of the coil pyroprobe indicated on the pyroprobe control unit will not reflect the exact temperature within the quartz tubes due to the insulating properties of the quartz tube and glass wool in which the samples are loaded.

In order to avoid pyrolysing at the wrong temperature, the pyroprobe was calibrated according to the method described by Bashir (1999) to determine the exact temperature of pyrolysis within the quartz tubes. To ensure the reproducibility, the pyroprobe should be periodically calibrated. The pyroprobe is calibrated using inorganic salts of known melting temperatures. The salts were placed in quartz tubes, mounted in the platinum coil of the pyroprobe and inserted in to a brass heating block, which was maintained at a temperature of 340 °C. The helium carrier gas flow rate was maintained at 2-10 mL/min. A glass window allowed the melting of salts to be observed under the microscope.

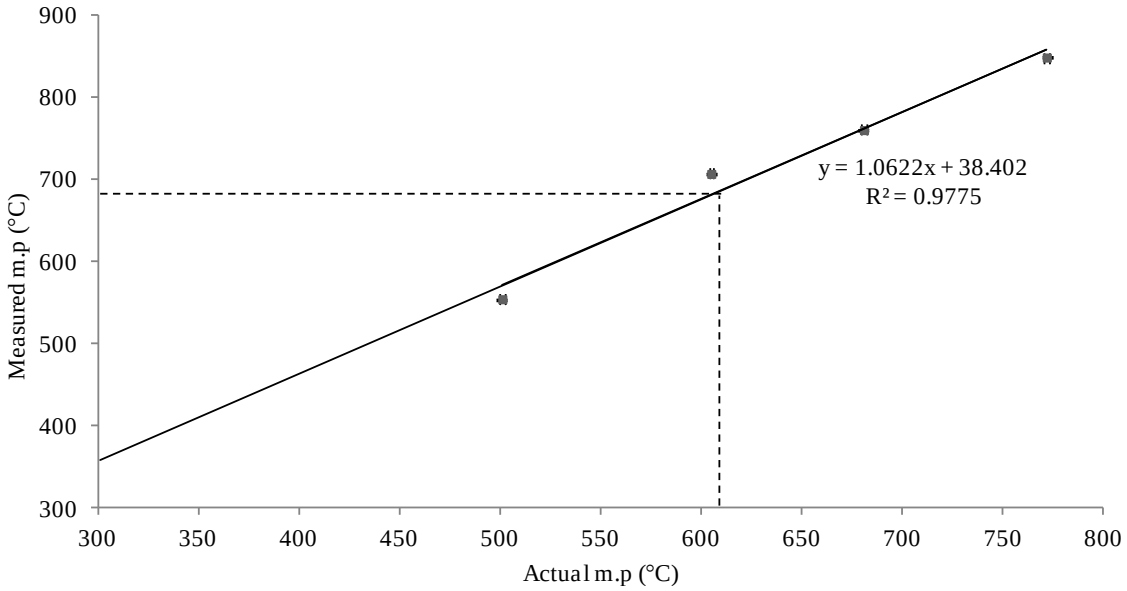

Fig. 2.1: Temperature calibration of pyroprobe. Displaying the mean actual and the equivalent mean observed melting points of four inorganic salts. Error bars represent the standard error of three replicates.

The salts selected were lead chloride (m.p 501 °C), lithium chloride (m.p 605 °C), potassium iodide (m.p 681 °C) and calcium chloride (m.p 772 °C). The probe was flashed at increasing temperatures and the observed melting point was recorded as displayed on the pyroprobe control panel. The average melting temperature of the four replicates of each salt was plotted against the actual known melting points (Fig. 2.1). THM temperatures in this study were therefore determined using the equation below;

$$y = 1.0622x + 38.402$$

(where y = observed temperature and x = actual temperature)

Calibration of the probe confirmed that an actual pyrolysis temperature of 610 °C in the quartz tube was indicative of an observed temperature of 686 °C on the pyroprobe interface. The previous pyroprobe calibration indicated that a pyrolysis temperature of 610 °C corresponded to an actual pyroprobe temperature of 735 °C (Mason, 2009), however this may be due to the different carrier gas used in the calibration carried out by Mason, or the use of a different platinum coil.

2.5 Bulk Density (D_b)

Soil bulk density is defined as the mass of a unit volume of dry soil. This volume includes solids, fragments and pores. A metal core of known volume (100 cm^3) was used to obtain an undisturbed soil sample from the clean face of a soil pit. In the laboratory, the soils were weighed, then oven dried at 60 °C for 48 hours and reweighed. The bulk density is calculated by dividing the dried sample weight by the sample volume, Eq. 2.1.

$$D_b = W_d / V_s \qquad \text{Eq. 2.1.}$$

Where D_b is the bulk density (g cm^3), W_d is the weight of oven dry soil (g) and V_s is the volume of soil (solids & pores) (cm^3). The stone content at all sites was minimal, therefore no correction for stone content was required.

2.6 Total Organic Carbon and Carbon Storage Determination

Total organic carbon (TOC) determination was performed using a modification of BS7755 (Section 3.8, 1995). Air dried soil (0.1 g) and litter (0.03 g) were weighed into porous ceramic TOC crucibles. HCl (1 mL:4 mM) was added to remove inorganic carbon and left for 4 h before oven drying at 65 ºC overnight. AR077 iron chips and SL266 tungsten accelerators were added and the TOC content was measured using the LECO-CS-244 analyser (Leco Corporation, USA). The analyser was calibrated using 1 g standard steel rings of known carbon content (Leco Corporation, USA) and evolved CO_2 was quantified using infrared detection. The weight of organic carbon (t C ha^{-1}) in each soil horizon could then be calculated using bulk density and horizon depth measurements, Eq. 2.2.

$$OC = d \times D_b \times TOC \qquad \text{Eq. 2.2.}$$

Where d is the depth (cm), D_b the bulk density (g cm^3) and TOC is the total organic carbon (%). (n.b. by maintaining TOC as a percent value, we avoid the conversion from g per cm^2 to t per ha).

2.7 Sites and Samples

2.7.1 Afforested Ecosystems

Owing to the increase of afforestation on peaty gley soils, it is important to study the changes in the distribution and degradation of lignin and tannins, to investigate whether these phenols are becoming stabilised and accumulating within the soil, or whether they are degrading faster than previously under the original land use.

Two soil profiles were sampled from Coalburn Forest, northwest England. The first site is an afforested Sitka spruce (*Picea sitchensis* (Bong.) *Carr.*) stand in its first rotation (SS1) and the second, is an unmanaged moorland site (ML). Both soil profiles were linearly deposited and experienced minimal bioturbation. A third soil profile was sampled from Harwood Forest, an afforested Sitka spruce stand in its second rotation (SS2), an area that had experienced horizon inversion prior to planting. Both Coalburn and Harwood Forests are located within Kielder Forest and are located 25 miles apart on the same acidic peaty gley soils (Fig. 2.2). Six soil profiles were sampled from a third site; Wark Forest, also located within Kielder Forest (Fig. 2.2). The profiles were taken across a chronosequence and comprised two soil profiles in open peat and four profiles in forest-margin peat, whereby the adjacent Sitka spruce plantation had begun to encroach on to the unprepared open peat via self seeding (i.e. edge effect). All three sites are underlain by the Tyne limestone formation, with peat deposits.

Fig. 2.2: A map of Kielder Forest and surrounding areas, in which the three afforested sites are located. The location of each site is marked by a red box; (CB) Coalburn Forest, (Wark) Wark Forest, and (HW) Harwood Forest. Inset map of Britain highlights area covered.

2.7.2 Coalburn Forest

Coalburn Forest is a small, 1.4 km^2 catchment located within Kielder Forest in the North of England, 55°05` N, 2° 28`W (elevation 300 m on a gentle slope, annual precipitation 1400 mm yr^{-1}; mean annual temperature 9.0 °C (Fig. 2.3) (Vanguelova et al., 2010). Previously, Coalburn was an extensive peatland (> 75% was peat bog) (Clayden and Hollis, 1984), the previous vegetation cover comprised molina grassland (*Dysopsis glechomoides*), and peat bog species including cotton grass (*Eriophorum spp.*), sphagnum mosses (*Sphagnum spp.*), rushes (*Juncus spp.*) and herbaceous plants (*Plantago spp.*) and was used for rough grazing for sheep (Robinson, 1998).

The soil type across the catchment varies from thick oligo-fibrous acidic peats (Long Moss and Winter Hill series) in the north (Clayden and Hollis, 1984) to thinner peat and cambic stagnohumic gley soils (Wilcocks 1 series) in the south east of the catchment.

Owing to the high elevation and restricted rooting depth, the site is vulnerable to wind throw. Coalburn forest was prepared and planted with Sitka spruce in the early 1970s by the Forestry Commission. The entire catchment was initially prepared for planting by ploughing with a D90 deep double mouldboard plough to cut furrows to 0.8-0.9 m depth approximately 4.5 m apart in 1972.

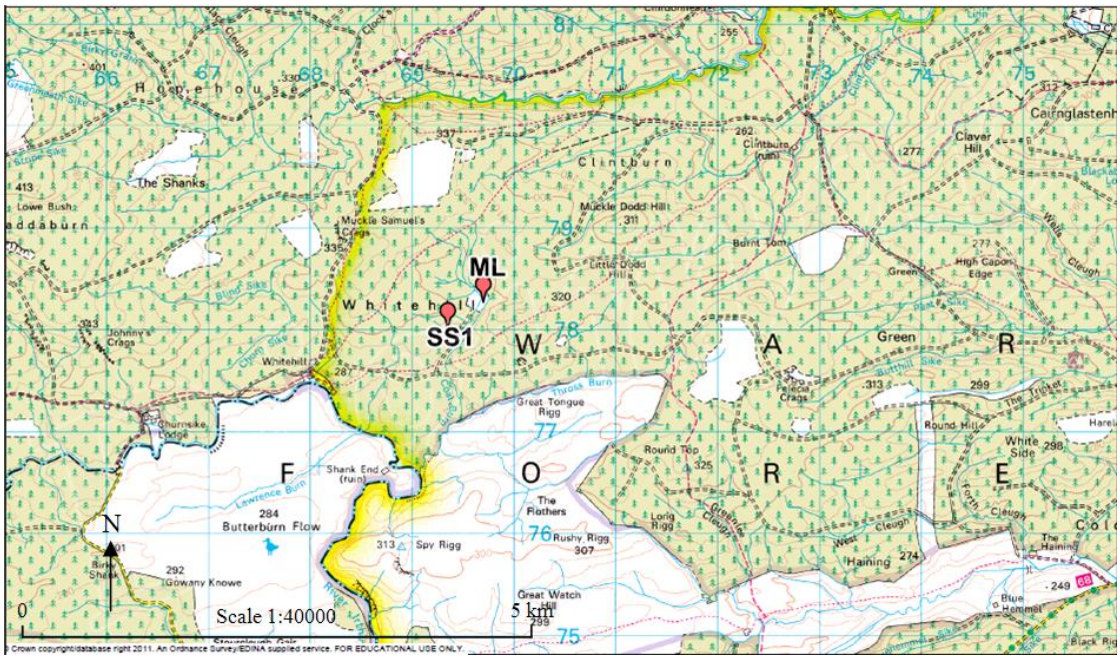

Fig. 2.3: A map of Coalburn Forest, including the two sites where soil profiles were sampled; the open undisturbed moorland (ML), and the Sitka spruce afforested (SS1) peaty gley soil cores.

The double furrow ploughing technique split the peat in half each side of the drain, creating a deep drain. The excavated material was used to construct elevated dry turf ridges and left to dry for a year. In spring 1973, the turf ridges were planted with Sitka spruce (*Picea sitchensis*) and some Lodgepole pine (*Pinus contorta)* at about 2 m spacing (Fig. 2.4b) (Robinson et al., 1998; Mounsey, 2000). There are now many small islands of peat remaining due to severe frost in the lower areas of the catchment (Fig. 2.4a), however these areas were kept to maintain a habitat for Black Grouse, resulting in 90% of the total area of Coalburn catchment now afforested (Chapman and Rose, 1991; Robinson et al., 1998). According to Robinson (1998), tree growth has been slow, only reaching full canopy closure after 23 years of growth, reflecting typical growth patterns for upland sites, with mature Sitka spruce reaching a height of between 7 and 12 m.

Coalburn Forest is currently one of ten Level II intensive long-term monitoring sites (ICP Level II plots) in the UK. Established in 1995, these plots provide information on the effects of air pollution and other factors on forest ecosystem structure and function (Vanguelova et al., 2010). Measurements at these sites include precipitation, interception, throughfall (i.e. the amount of precipitation reaching the forest floor), soil solution chemistry, litterfall biomass and chemistry, ground flora, and tree growth.

Two peat profiles were sampled from Coalburn Forest in May 2009, the sample locations are marked on the map in Fig. 2.3. Soil pits were dug with dimensions approximately 1 m x 1 m x 0.4 m. Soil samples were taken in triplicate within each soil horizon identified. At the moorland site (ML) the horizons were linearly deposited with horizon boundaries observed at: 0-4 (L+F), 4-15 (Hf), 15-27 (Hs), 27-42 (Ae) and 42+ (Bg) cm, located 299 m (AOD) (Fig. 2.5a). The afforested site profile (SS1) was also linearly deposited with horizon boundaries observed at: 0-5 (L+F), 5-20 (Hf), 20-28 (Ae) and 28+ (Bg) cm, sampled from the flat ribbon of land between the drain and the mound, located 386 m (AOD) (Fig. 2.5b). A small Hs horizon was also identified *ca* 18-20 cm, however the boundary between the Hf and Hs horizon was unidentifiable. Therefore, in line with the EU soil sampling protocol, the Hf and Hs layers were sampled together (FSCC, 2006). The organic soil horizons were identified according to the EU humus classification system, where Hf describes a histic organic horizon consisting almost entirely of practically unchanged plant remains (i.e. fibric), and Hs describes a histic organic horizon in advanced stage of decomposition (i.e. sapric) (Zanella et al., 2011).

Fig. 2.4: Photographs taken at Coalburn Forest at the (a) open moorland (ML) and (b) afforested Sitka spruce stand (SS1).

Fig. 2.5: Photographs taken at Coalburn Forest at the (a) moorland (ML) soil profile and (b) afforested (SS1) soil profile.

Soil cores (100 cm^3) were taken in triplicate from the horizontal face of the moorland soil pit in the centre of each soil horizon, so that the soil bulk density could be calculated. The bulk density measurements of the afforested soil were provided by Forest Research (FR), which were sampled in 2008. Samples were kept in glass jars which were sealed immediately after collection. Sitka spruce roots were also sampled from Coalburn Forest for THM analysis. The Coalburn Forest samples were analysed in triplicate with unlabelled TMAH.

2.7.3 Harwood Forest

Harwood Forest is a coniferous plantation of *ca* 5 km^2, situated in Northumberland National Park, 55°10`N, 2°3`W (Fig. 2.2). The forest sits on a gentle slope with an elevation between 200 and 400 m (AOD) with acidic peaty gley soils from the Wilcocks I Association. The Harwood site is a Sitka spruce afforested moorland that was first established in the 1930s, with a previous land cover of heather (*Calluna vulgaris*) and grasses (*Festuca ovina, Deschampsia flexuosa* and *Eriophorum vaginatum*). This site has experienced land preparation in the form of ploughing to a depth of 30 cm, and the soil formed into ridges prior to planting.

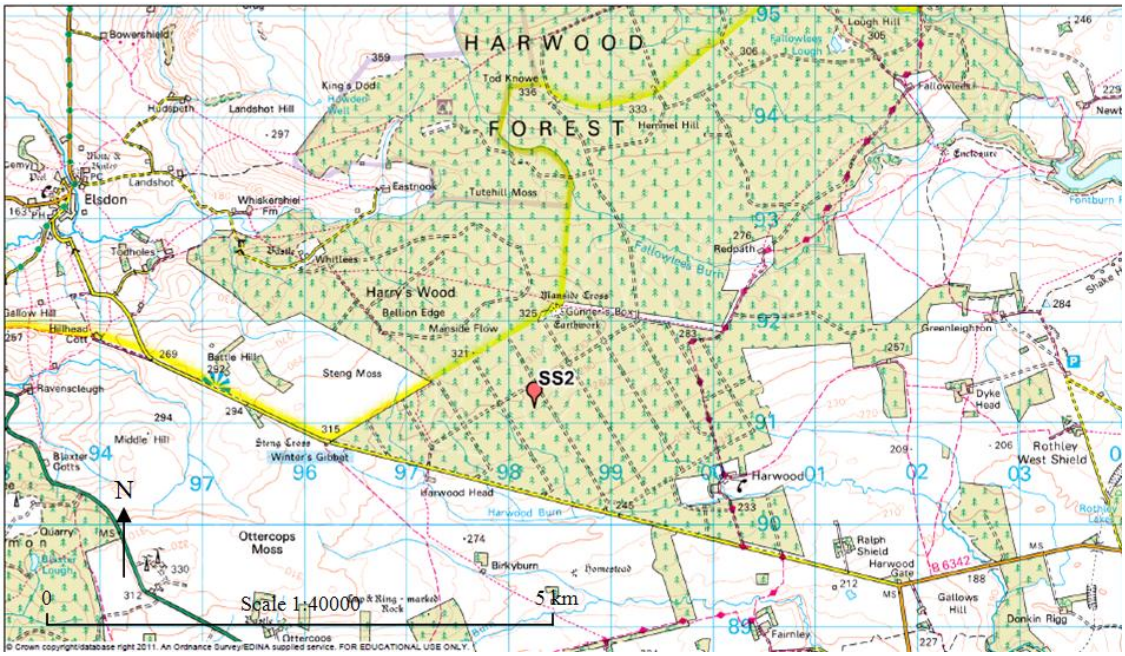

Fig. 2.6: A map of Harwood forest including the site where the SS2 soil profile was sampled; the second rotation Sitka spruce afforested moorland peaty gley soil core was sampled by S. Mason.

After the first stand, the soil was mounded, creating soil inversion down the profile. The forest is currently in its second stand, with the stand aged around 35 years old.
Soil cores were taken from Harwood using a manually driven soil corer with a slide hammer attachment (Giddings Machine Company, Inc., USA; 5.5 cm diameter), to a depth of 45 cm. Samples were taken in duplicate by Sharon Mason in July 2008. It is important to note that these samples were taken from a different core to the samples investigated by Mason et al. (2009), which is reflected in the different horizons, horizon depths, and TOC values. Soils were sampled at 5 cm increments at depths 0-5 (L+F), 10-15 (Hf), 15-20 (Hf2), 20-25 (Hs), 25-30 (Hs2), 30-35 (A), 35-40 (Hs3), 40-45 (Hs4) cm. Bulk density measurements were provided by Maurizio Mencuccini (Edinburgh University, UK). The sample location is marked on the map in Fig. 2.6. The Harwood samples were analysed in duplicate with unlabelled TMAH.

2.7.4 Wark Forest

Wark Forest, a 13.5 km^2 catchment located within Kielder Forest at 55°04`N, 2°18`W, (elevation 160-240 m AOD, annual precipitation 1350 mm yr^{-1}; Robinson et al., 1998; Fig. 2.2). Wark Forest consists primarily of Sitka spruce (*Picea sitchensis*), Norway spruce (*Picea abies*), and Lodgepole pine (*Pinus contorta*) established in the 1930s on moorland and enclosed pastures (Chapman and Rose, 1991; Peterken et al., 1992).

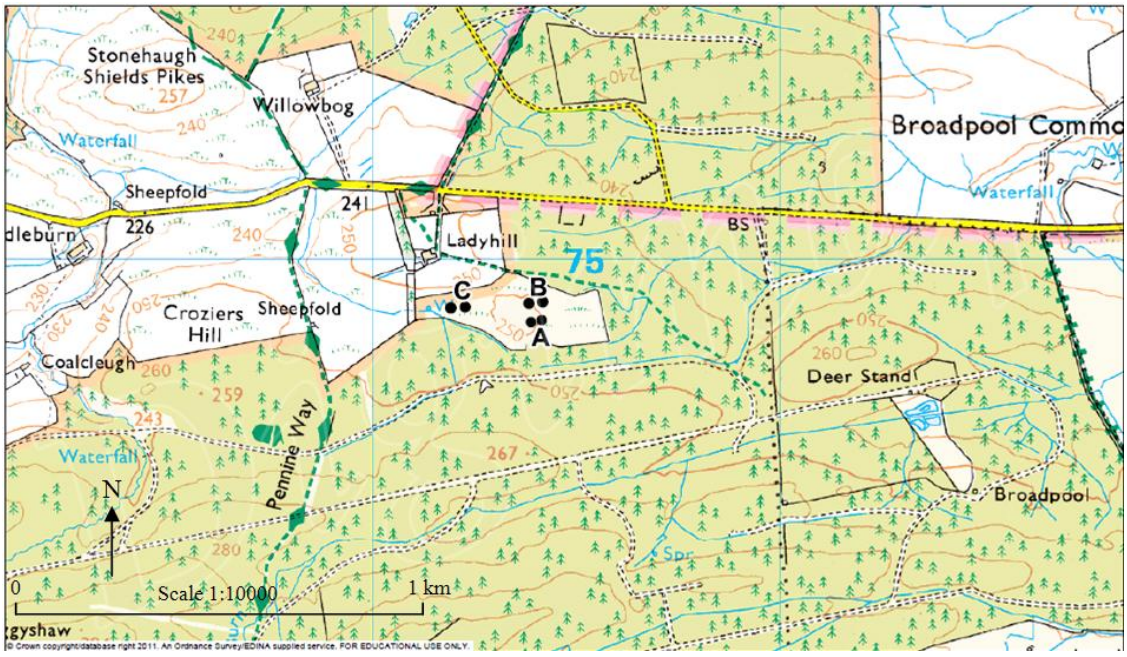

Fig. 2.7: A map of Wark Forest. The locations of all six sites are marked in bold where (A) forest-margin peat pits under the Sitka spruce canopy, (B) forest-margin peat pits and (C) open peat pits.

Fig. 2.8: Photographs taken at Wark Forest at the (a) forest-margin peat and (b) open peat looking back towards the forest-margin peat and afforested land on the horizon.

Fig. 2.9: Photographs taken at Wark Forest at the (a) forest-margin peat under Sitka spruce soil profile and (b) forest-margin peat soil profile.

Similar to the Coalburn Forest site, small pockets of moorland remain. Vegetation observed in Coom Rigg Moss, a pocket of unplanted moorland to the west of this site has a ground vegetation of heather and grasses (*Calluna vulgaris*, *Deschampsia flexuosa* and *Eriophorum vaginatum*), and was designated a National Nature Reserve in 1960 (Chapman and Rose, 1991). The area sampled is deposited with peat, and the surrounding coniferous forests have a deposit of Devensian till. Drains have been created in the coniferous plantation to make the soil more favourable for growing Sitka spruce, by reducing the water table and increasing aeration.

The site includes two soil profiles in an undisturbed open peat and four profiles in the forest-margin peat, the sample locations are marked on the map in Fig. 2.7. The forest-margin peat comprised two pits amongst self-seeded Sitka spruce but not situated underneath the canopy, and two pits located directly under the canopy of Sitka spruce. The soil profiles were entirely organic, with samples taken from the three ectorganic layers; the litter (L) horizon, the fibric histic (Hf) horizon and the sapric histic (Hs) horizon.

Two soil profiles were sampled beneath the canopy of self seeded Sitka spruce on the forest-margin peat. Horizon boundaries were identified at depths 0-13 (L), 13-30 (Hf), 30-50 (Hs) cm at pit one and 0-8 (L), 8-20 (Hf), 20-50 (Hs) cm at pit two, located at 167 and 191 m (AOD) respectively (Figs. 2.8a and 2.9a). These samples are labelled as forest-margin peat under SS. Two further profiles were sampled from the forest-margin peat this time away from the Sitka spruce canopy. Horizon boundaries were identified at depths 0-9 (L), 9-25 (Hf), 25-50 (Hs) cm at pit one and 0-8 (L), 8-20 (Hf), 20-50 (Hs) cm at pit two, located at 207 and 220 m (AOD) respectively (Fig. 2.9b). These samples are labelled as forest-margin peat. The third site sampled two profiles in the open peat. Horizon boundaries were identified at depths 0-4 (L), 4-26 (Hf), 26-50 (Hs) cm at pit one and 0-5 (L), 5-13 (Hf), 13-50 (Hs) cm at pit two, located at 234 and 238 m (AOD) respectively (Fig. 2.8b). The first open peat core was sampled in a hollow where the core was saturated, and the second core taken from a hummock with a lower water table.

Once in the laboratory, the litter (L) samples were divided in to green litter (Lg) and brown litter (Lb). Bulk density measurements were taken in triplicate from the Hs horizon of each pit. This bulk density value was therefore assumed for each peat profile. The Wark samples were analysed in duplicate with unlabelled and ^{13}C-labelled TMAH.

2.7.5 Pristine Peat Ecosystem

In order to understand the processes that occur within soil after the afforestation of peats, it is vital to have a thorough understanding of the processes occurring prior to afforestation. Litter produced by the peat-forming moss, *Sphagnum*, is regarded as extremely recalcitrant owing to the high content of sphagnum acid in the cell walls (Rudolph and Samland, 1985). It is therefore imperative to understand the distinctive biochemistry of *Sphagnum* and its degradation pathways in order to elucidate the dynamics of organic carbon degradation in peat prior to afforestation.

Intersite and down-core comparisons across the macrotopographic gradient from the bog centre to the peatland-forest will provide an unprecedented database for inferring processes of physical and chemical digenesis of peat SOM that is broadly representative of that for a wide class of peatlands in the boreal zone.

2.7.6 Ryggmossen Peatland

Peat forming plant samples and peat core samples were taken from Ryggmossen (60° 3`N, 17° 20`E; 60 m AOD) in the boreonemoral zone of central Sweden (annual precipitation 554 mm yr^{-1}; mean annual temperature 5.6 °C), see Fig. 2.10 (Bragazza et al., 2003). Ryggmossen is an ombrotrophic peat bog with total area *ca* 0.6 km^2 and has been designated a Nature Reserve since 1997.

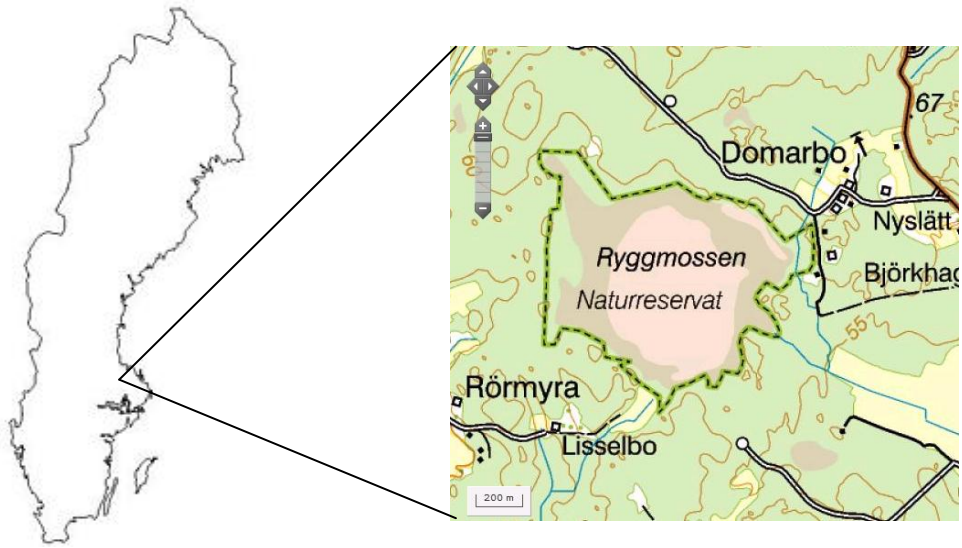

Fig. 2.10: The location and terrain map of Ryggmossen bog, Sweden.

The site has a well-developed hummock-lawn-hollow microtopography, typical of many northern peatlands, and has been largely undisturbed by human activity, even at the peatland-forest ecotone. The macrotopographic gradient from the bog centre to the peatland-forest ecotone shows increases in mineral cations and pH, a distinct succession of plant growth forms with highly contrasting traits, and marked changes in water table regimes (Bragazza et al., 2003). The developmental sequence at this site is broadly representative of that for a wide class of peatlands in the boreal zone. Proceeding from the centre to the edge, the macrotopographic gradient comprises four stages: bog plateau (BP), bog margin (BM), fen lagg (FL) and swamp forest (SF) (Table 2.1).

Table 2.1: The Ryggmossen peatland stage descriptions

Stage		Description
BP	Bog Plateau	Ombrogenous peatland with a distinct microtopography of dry *Sphagnum fuscum* hummocks and wet *Sphagnum balticum* hollows
BM	Bog Margin	A well drained ombrogenous peatland with low, open tree cover (*Pinus sylvestris*) and an understory of dwarf shrubs (*Calluna vulgaris*) with *S. fuscum* hummocks and *S. angustifolium* lawns
FL	Fen Lagg	A geogenous peatland with a diverse assemblage of graminoids (*Carex lasiocarpa, Phragmites australis*), peat mosses (*S. majus, S. fallax*) and other plant groups, with isolated *S. fuscum* hummocks in a matrix of *S. fallax* hollows
SF	Swamp Forest	A seasonally flooded woodland (*Pinus sylvestris, Betula pubescens*) with an understory of shrubs (*Salix aurita, Juniperus communis*) and forest mosses (*Polytrichum commune*), with wet patches of *S. angustifolium*.

A large number of samples were taken from both the litter and peat, across the peatland and down the peat profile. Samples were provided for this work as part of a collaboration with Dr. Lisa Belyea, Dr. Kathryn Allton, Dr. Chris Laing (Queen Mary University, London), and Dr. Greg Cowie (Edinburgh University). Additionally, Prof. Håkan Rydin and Dr. Gustaf Granath (both from Uppsala University, Sweden) provided help with species identification.

Living material was collected from the capitulum (i.e. the cluster of leaves at the top of the plant) of six different *Sphagnum* species; *S. angustifolium* (BM, FL), *S. balticum* (BP), *S. fallax* (FL), *S. fuscum* (BP, BM), *S. magellanicum* (BM) and *S. papillosum* (FL). These were sampled in order to investigate the phenolic differences between the

dominant *Sphagnum* species growing at the peatland. The capitulum samples were analysed in triplicate with unlabelled TMAH.

Living material was also collected from two non-*Sphagnum* moss species (*Polytrichum commune* and *Pleurozium schreberi*), one species of sedge (*Eriophorum vaginatum*), and several dwarf shrubs (*Andromeda polifolia, Calluna vulgaris, Empetrum nigrum, Rhododendron tomentosum, Vaccinium microcarpum*) from a field monitoring site in April 2008. The non-*Sphagnum* samples were analysed in duplicate with ^{13}C-labelled TMAH to investigate the geochemical fingerprints of the various non-*Sphagnum* peat forming species.

Nine litter samples (i.e. a section of stem just below the photosynthesising part), all dominated by *Sphagnum*, were also collected; for these samples, an attempt was made to separate out the *Sphagnum*, but small quantities of fungi, vascular plant roots and non-*Sphagnum* bryophytes are likely to be present (*S. angustifolium* from BM and SF; *S. balticum* from BP; *S. fallax* from FL; *S. fuscum* from BP and BM; *S. magellanicum* from BM and; *S. papillosum* from FL). The *Sphagnum*-dominated litter samples were analysed in duplicate with unlabelled and ^{13}C-labelled TMAH.

Eight peat cores (20 cm diameter, 30-50 cm long) were collected, one from a hummock and one from a hollow at each of the four stages (BP, BM, FL, and SF), to span the range of environmental conditions across the Ryggmossen peat. The cores were extracted intact by sequentially cutting the peat around a PVC pipe and then gently inserting the pipe; the process of alternately cutting and inserting the pipe was continued as far as possible, to a depth of 20-70 cm. The pipe was then dug out intact, sealed and transported upright. The cores were initially stored at 4 °C, then frozen at -18 °C, removed from their pipes and sectioned into contiguous 2 cm thick slices using a water-lubricated bandsaw. Samples were taken from each 2 cm interval using a holesaw attached to a power drill (2.9 cm diameter by 2 cm thick). For dry bulk density measurements, a sub-sample from each of these intervals was oven-dried at 80 °C for 8 hours (Vitt et al., 2009). For geochemical analyses, the samples were freeze-dried, and then milled to a fine powder using a freezer mill. Areal coverage (i.e. percent ground coverage) of living plants at each coring site was determined with quadrat surveys. The peat core samples were analysed in duplicate with unlabelled TMAH. Data loggers (Solinst Leveloggers) were placed at each coring station by Dr. Lisa Belyea and Dr.

Kathryn Allton one year prior to core extraction to measure the annual water table (WT) and the temperature fluctuation.

All Ryggmossen samples were extracted by Dr. Aminu Muhammad (see Section 2.8 for extract technique). Additionally, owing to the large number of the peat core samples they were analysed on a shorter GC programme; however the pyrolysis temperature was maintained at 610 °C. The shorter GC oven programme began at 40 °C where it was held for 4 minutes, then the temperature was increased from 40 °C to 90 °C at a rate of 4 °C /min, then at 2 °C/min to 150 °C and finally at 4.5 °C/min to 320 °C where it was held for 6 minutes.

2.8 Sample Preparation

Soils were returned to the laboratory within 24 h of collection and stored in the freezer prior to freeze-drying. Prior to analysis, the vegetation samples and peaty soils were cryo-milled to a fine powder using a Certiprep 6750 freezer mill (Spex Certiprep, USA). Mineral soils were ground to a fine powder using a pestle and mortar.

In the Harwood, Coalburn and Wark Forest samples, free lipids were removed upon Soxhlet extraction for 48 h using DCM:MeOH (93:7; v/v). The remaining solid residue was air dried for 48 h and stored in the freezer at -20 °C. The organic-soluble components were removed from the Ryggmossen samples (*Sphagnum* capitula, *Sphagnum* litter, *non-Sphagnum* litter and peat cores samples) by repeated ultrasonication and centrifugation in a 50 mL Teflon centrifuge tube using a mixture of DCM/MeOH (1:1; v/v).

2.9 Statistical Analyses

Statistical analysis was performed using Minitab 16 statistical software package (Minitab Inc., USA). The analysis of variance (ANOVA) was tested using the General Linear Model (GLM) method, which analyses a continuous response variable with at least one categorical factor with two or more levels to test for significant differences in the data using the p-value. Significant differences between means were evaluated at p-value of less than 0.05 (i.e. 95% confidence interval).

The data residuals are required to be normally distributed with roughly equal variances between factor levels for the GLM test to be reliable. This was tested with the Anderson-Darling Normality test. The residuals are the differences between the average for the treatment and the individual observation. The p-value must be greater than 0.05 for the residuals to be considered to have a reasonably normal distribution, however the nearer to 1.0 the better. If the residuals follow a significantly different distribution to a normal one ($p<0.05$) then the ANOVA model is not reliable. When the GLM displayed a significant difference ($p<0.05$), and the residuals were normally distributed ($p>0.05$), the Tukey's honestly significantly different test (HSD) was used to show significant differences, using a multiple comparison method.

Data which were not normally distributed were tested for significant differences ($p<0.05$) using the Kruskal-Wallis test. There is no Tukey's test equivalent, however a Mann-Whitney test can be used to determine pairwise differences. The standard error of the mean was calculated and displayed graphically as error bars or within the text (±).

Chapter 3:

Carbon Stock and Phenolic Distributions in Peaty Gley Soils Afforested With Sitka Spruce

3 Carbon Stock and Phenolic Distributions in Peaty Gley Soils Afforested With Sitka Spruce

3.1 Introduction

The moorland habitat in the UK is a rare and unique environment, characterised by open, often upland areas with acidic soils such as peat, and can be categorised into three main groups; heathland communities, mire or bog communities and acid grassland communities (Pearsall, 1971; Gimingham, 1972; Holden et al., 2007), comprising a significant amount of the total UK soil C pool (Billett et al., 2010). The UK has seen a substantial increase in upland tree cover over the past 100 years, with around 2.5 x 10^4 km^2 (20% of the UK's moorland land surface) now afforested with coniferous plantations, including 9% of UK upland deep peats, which has been the main cause of the net loss of moorland habitat over the past century (Cannell et al., 1993; Holden et al., 2007). Unfortunately, economic incentives are likely to encourage increased upland tree cover over the next 30 years (Brown et al., 2010); the IPCC has identified afforestation as a possible method of combating increasing CO_2 levels by storing carbon in soils and biomass, making afforestation a favourable land-use change option (IPCC, 2000); which in part has led to Scottish and English agencies aiming to meet new targets of increased afforestation but also for mixed broadleaf tree cover in the uplands (Natural England, 2009).

In order to optimise the productivity of forest stands established on peats and peaty gley soils, land preparation including drainage, ploughing and fertilisation is carried out (Biggs, 1979; Minkkinen et al., 2008), although mounding has replaced ploughing as a land preparation technique in recent years (Minkkinen et al., 2008). The extensive ground preparation accelerates the oxidation of the stored carbon due to disturbed soil structure and broken soil aggregates, lowered water table and decreased soil moisture (Tiessen and Stewart, 1983; Hillman, 1992; Mojeremane et al., 2010). These physical changes can enhance carbon losses to the atmosphere as CO_2 (von Arnold et al., 2005), as well as to ground water via dissolved organic matter (DOM) (Baker et al., 2008) and particulate organic matter (POM) (Evans and Warburton, 2010). Conversely, the growth of conifers has been shown to result in an enhanced carbon sink through increased

biomass, litter and root input (Farmer and Nisbet, 2004; Zerva et al., 2005). However, with global forest soils holding around two thirds (*ca* 787 Pg C) of the total carbon stored in forest ecosystems (1146 Pg C) (Dixon et al., 1994), coupled with the residence time of soil carbon exceeding that of plant biomass (Trumbore et al., 1990; Thuille et al., 2000), makes soil carbon more stable and therefore more important to the long term storage of carbon than plant biomass. In order to determine if afforested soils will become a sink or source of CO_2, a thorough understanding of the processes that control the stabilisation and release of carbon within soil, together with the long-term carbon turnover in soils after afforestation is required.

Previous studies on the effects of afforestation on soil organic carbon (SOC) stocks have provided contradictory results, with SOC changes after afforestation primarily controlled by the soil type, plant type, climate and previous land use (e.g. Guo and Gifford, 2002; Paul et al., 2002), although the majority of these studies were carried out on mineral soils. The specific study of afforestation of Sitka spruce (*Picea sitchensis* (Bong.) *Carr*.) on peat and peaty gley soils by Zerva et al. (2005), showed that the soil carbon storage recovered to pre-afforestation levels in the second rotation, with soil carbon storage values consistent with previous measurements at afforested sites (97 – 250 t C ha^{-1}) (Black et al., 2009). From a review study of 204 sites, Paul et al. (2002), showed that carbon accumulation is maximised by maintaining longer forest rotations; between 20 and 50 years. A forest rotation is defined by the number of years required to establish and grow trees to a specified size required for productive timber production, with the first rotation describing the initial planting and land-use change to forest, with any subsequent rotations (e.g. second, third) describing the successive plantations after each clearfelling (Ferris et al., 2000). Coniferous plantation rotations are typically around 40 years long from planting to clearfelling (Ferris et al., 2000).

Together with the SOC dynamics, a deeper understanding of the changes in phenolic distributions in soils following afforestation is also of upmost importance. After cellulose and hemicellulose, lignin and polyphenols such as tannins comprise the main biopolymers on Earth (Kögel-Knabner, 2002). Historically, lignin has always been considered to be the main contributor to the resistant carbon pool, and therefore accumulates in soil organic matter (SOM) with respect to other more labile compounds (Dignac et al., 2005). However, recent studies have shown that lignin is only preserved in the early stages of decomposition, and that later stages of lignin degradation can

occur at rates higher than overall litter decomposition (Kiem and Kögel-Knabner, 2003; Kalbitz et al., 2006). The softwood (gymnosperm) Sitka spruce trees that are extensively used for afforestation in the UK are characterised by the dominance of guaiacyl-based lignin, which are less susceptible to decomposition compared to syringyl-based lignins that dominate hardwoods (angiosperms) (Sarkanen and Hergert, 1971).

Thermally assisted hydrolysis and methylation (THM) in the presence of tetramethylammonium hydroxide (TMAH), also referred as TMAH thermochemolysis (e.g. Chefetz et al., 2000), has been successfully used to analyse peaty gley soils under grass (Huang et al., 1998; Mason et al., 2012) and under open moorland and afforested Sitka spruce (Mason et al., 2009). Key findings included the increased oxidation of lignin phenols with depth under grass, whereas under a second rotation of Sitka spruce, the composition of phenolic components significantly changed compared to the open moorland, indicating either a changing vegetation input, horizon inversion, root input or leaching, or a combination of these processes. However it is unknown what phenolic and carbon storage changes occur during the first rotation of the Sitka spruce, which is important to ascertain the processes that occur both directly after afforestation and into subsequent rotations, and whether or not these changes are coupled to carbon stock changes.

This chapter reports the effects of afforestation on peaty gley soils in a northern UK upland using TMAH thermochemolysis. The phenolic and SOC distributions and their quantitative changes were compared in soils beneath a first and second rotation spruce forest and an adjacent unforested moorland, in order to determine how a change in vegetation cover and stand maturity affects the soil carbon and phenolic depth profiles. The specific objectives of this chapter are to (i) examine the effects of afforestation of peaty soils on the soil carbon stocks within the soil profile, in order to evaluate the long term effects (~100 years) of afforestation on soil carbon stocks; and (ii) to characterise and analyse changes in thermochemolysis product composition with soil depth, to test for the persistence of lignin phenols in the first and second rotation Sitka spruce stands and to infer the processes occurring after afforestation.

3.2 Overview of Methods and Sites

3.2.1 Site Background

Two soil profiles were sampled from Coalburn Forest a small 1.5 km^2 catchment in Cumbria, northern England (Fig. 2.3). The first an afforested Sitka spruce stand in its first rotation (SS1) and second, an unmanaged moorland site (ML). Both soil profiles were linearly deposited (i.e. oldest horizon being the deepest horizon) and have experienced minimal bioturbation. A third soil profile was sampled from Harwood Forest, an afforested Sitka spruce stand in its second rotation (SS2), an area that had experienced horizon inversion prior to planting the second rotation (Fig. 2.6). Both Coalburn and Harwood Forests are located within Kielder Forest and are located 40 miles apart on the same acidic peaty gley soils from the Wilcocks I Association (cambic stagnohumic clay loam with humified peat topsoil 20-30 cm thick) (Fig. 2.2).

The Coalburn Forest moorland site is an undisturbed natural habitat, accounting for just 10% of the land cover at Coalburn Forest. These pockets of land are typically *Molina* glass lands, with *Eriophorum*, *Sphagnum*, *Juncus* and *Plantago* species also present. The Coalburn afforested site is a Sitka spruce afforested moorland that was established as an experimental plot in 1966. For five years, the site was subjected to rough grazing, followed by land preparation in 1972 and planting in 1973 of Sitka spruce. The land was prepared using a D90 peat plough. The forest is currently in its first stand, with the stand aged around 40 years old (Robinson et al., 1998).

Harwood Forest is a Sitka spruce afforested moorland that was first established in the 1930's, with a previous land cover of heather (*Calluna vulgaris*) and grasses (*Festuca ovina*, *Deschampsia flexuosa* and *Eriphorum vaginatum*) (Mason et al., 2009). This site has experienced land preparation in the form of ploughing to a depth of 30 cm, and the soil formed into ridges prior to planting. After the first stand, the soil was mounded, creating soil inversion down the profile so that a second Hs horizon appears below the A horizon. The forest is currently in its second stand, with the stand aged around 35 years old (Mason et al., 2009).

At Coalburn Forest, two soil pits was dug to a depth of 45 cm; one at the first rotation Sitka spruce site (SS1), and one at the unplanted moorland site (ML). Sitka spruce roots were sampled from Coalburn Forest for THM analysis. At the second rotation site (SS2)

in Harwood Forest, sampling took place on the flat ribbon of land between the drain and the mound. Detailed site and soil profile descriptions for Coalburn and Harwood Forest are presented in Chapter 2, Sections 2.7.2 and 2.7.3.

3.2.2 TMAH Thermochemolysis

On-line THM in the presence of unlabelled TMAH performed at 610 °C for 10 s (20 °C/ms temperature ramp) using the method set out in Chapter 2 (Section 2.2).

3.2.3 TOC & Carbon Storage

The total organic carbon (TOC) content was measured using the LECO-CS-244 analyser (Leco Corporation, USA). TOC measurements were taken in triplicate (n=3) for each of the ML and SS1 samples, and in duplicate (n=2) for the SS2 samples. Bulk densities (D_b) were obtained for the ML horizons using 100 cm^3 soil cores in May 2009. Bulk densities for the Coalburn Forest SS1 soil profile were sampled in five replicates per horizon in 2008 and provided by Dr. Elena Vanguelova (Forest Research). The Harwood Forest SS2 soil profile bulk density measurements were taken by Maurizio Mencuccini, (Edinburgh University, UK) as published in Zerva & Mencuccini., (2005).

The weight of organic carbon (OC t C ha^{-1}) in each horizon is calculated using equation 2.2 (Chapter 2). The TOC measurement also permits the normalisation of the amounts of phenols per 100 mg of organic carbon (OC) down the peat core (Hedges and Mann, 1979b; Hedges et al., 1982; Kögel, 1986).

3.2.4 Lignin Proxies

Lignin proxies were used as described in Chapter 2 (Section 2.2.2), with all phenol yields normalised to 100 mg of OC. Lambda (Λ) is the sum of the amounts of the 8 dominant lignin derived phenols (G4+G5+G6+S4+S5+S6+G18+P18) (Chapter 1, Fig. 1.5 for dominant lignin phenol structures) (Hedges and Mann, 1979b; Hedges et al., 1982). The S/G and C/G ratios are used to assess vegetation input; reflecting the relative abundance of angiosperms (S/G > 0), gymnosperms (S/G = 0), and non-woody tissue (C/G > 0). Whilst $[Ad/Al]_{G/S}$ and $\Gamma_{G/S}$ reveal the relative state of lignin oxidation.

3.3 Results and Discussion

3.3.1 Soil Organic Carbon

3.3.1.1 Total organic carbon

The TOC and organic carbon storage (t C ha^{-1}) for each horizon down the profile of the ML and the two SS soils are presented in Fig. 3.1 and Table 3.1. The organic horizons (L, F + Hf/s) across all sites have a significantly similar TOC value of 39.6 ± 1.6%, whilst the mineral horizons (Ae + Bg) have a significantly similar TOC value of 1.7 ± 0.3% ($p>0.05$). The ML and SS1 soils display a significant decrease between the deepest organic horizon and the upper mineral horizon, from 42.3 and 38.4% to 3.4 and 0.9% in the ML and SS1 soil respectively ($p<0.001$). This drop in TOC is also observed in the SS2 profile from 47.3% in the litter to 1.8% in the mineral A horizon, however this is followed by a significant increase to 45.8% in the buried H2 horizon ($p=0.022$).

This decrease of TOC from the organic horizons into the mineral horizons has also been observed in peaty gley soils of the Pennines and Kielder Forest (Huang et al., 1996; Mason, 2009), and attributed to the degradation of litter and incorporation into clay and minerals. The buried Hs2 horizon at SS2 highlights the horizon inversion that occurred prior to planting, causing the burial of an organic rich horizon below a mineral horizon.

The ML and SS1 soils have a similar depth of litter (L+F) and fibric histic (Hf) horizons, deviations occur at around 20 cm, where the ML soil displays a deep degraded peat (Hs) horizon (Table 3.1). The SS2 profile shows much deeper litter and Hf horizons, indicating an increased litterfall at the surface and the accumulation of humified organic soil. The A horizon along the chronosequence becomes shallower, decreasing from 15 cm depth in the ML to 5 cm in the SS2, which could be a sign of the increased disturbance at the sites, mixing the organic and mineral soils so that the mineral horizon boundaries becomes less well defined, and therefore appearing thinner. The absence of a buried organic horizon at SS1 confirms that the horizon inversion occurred after the clearfelling of the first stand to prepare the land for the second rotation (Mason et al., 2009), and therefore is only observed in SS2. This is consistent with the replacement of ploughing with mounding over the last 30 years (Minkkinen et al., 2008).

Table 3.1: The mean soil organic carbon contents and associated parameters for each horizon of the moorland and afforested Coalburn (ML, SS1) and Harwood (SS2) Forest soil profiles.

	Boundaries (cm)	TOC (wt %)	D_b (g cm^{-3})	OC (t C ha^{-1})	OC (% total)
ML (Moorland)					
L+F	0	32.0 b	0.11	14.1 ± 2.4	3.9
Hf	4	45.2 a	0.29	145.6 ± 11.8	39.9
Hs	15	42.3 ab	0.28	140.8 ± 18.4	38.6
Ae	27	3.4 c	1.14	58.6 ± 3.8	16.1
Bg	42	1.6 c	1.16	5.6 ± 0.2	1.5
	45			**364.8 A ± 36.6**	100.0
SS1 (1st rotation)					
SS Roots		42.8			
L+F	0	34.4 a	0.08*	13.8 ± 1.4	11.7
Hf	5	38.4 a	0.13*	64.8 ± 5.9	55.0
Hs	18	38.4 a	0.17*	13.1 ± 1.2	11.1
Ae	20	0.9 b	0.49*	3.42 ± 0.2	2.9
Bg	28	0.9 b	1.52*	22.7 ± 0.8	19.3
	45			**117.8 B ± 9.5**	100.0
SS2 (2nd rotation)					
L+F	0	47.3 a	0.11**	52.9 ± 0.9	10.9
Hf	10	35.4 a	0.34**	120.3 ± 35.3	24.8
Hs	20	42.5 a	0.34**	144.4 ± 19.7	29.8
A	30	1.8 b	1.30**	11.5 ± 0.00	2.4
Hs2	35	45.8 a	0.34**	155.7 ± 2.9	32.1
	45			**484.8 A ± 58.9**	100.0

* determined by Forest Research in 2008

** determined by Maurizio Mencuccini, (Edinburgh University, UK).

Means followed by the same letter are not significantly different (Tukey's HSD, $p<0.05$). SE of three replicates for ML and SS1 and 2 replicates for SS2

3.3.1.2 Bulk Density

Forest Research measured the bulk density of the first rotation Sitka spruce stand (SS1) soil profile in 1995 and again in 2008. The bulk density results revealed that over thirteen years, the ectorganic horizons (L+F+H), remained consistent; 0.125 and 0.127 g cm^{-3}, respectively. The mineral A and B horizons however showed an increase from 0.32 and 1.25 g cm^{-3} to 0.49 and 1.52 g cm^{-3}, respectively (Vanguelova, *unpublished data*). This increase in the mineral horizons is likely a result of compaction due to drying and shrinkage from the drainage of the soil (Holden et al., 2007). Assuming all other factors remained constant (i.e. TOC, horizon depths), this increasing bulk density would also increase the soil profile carbon storage from 65.8 to 104.0 t C ha^{-1}, representing an annual increase (ΔSOM) of 2.9 t C ha^{-1} $year^{-1}$. However, following compaction there would also be a degree of shrinkage in the soil depth, which would have a negative impact on the carbon storage.

The bulk density measurements in the ectorganic horizons decrease from 0.28 g cm^{-3} in the ML to 0.17 g cm^{-3} in the SS1. The bulk density then increases into the SS2 to 0.34 g cm^{-3} (Table 3.1). These results indicate an initial decrease of bulk density in the ectorganic horizons after afforestation, which could be due to the mechanical site preparation (Paul et al., 2002), and/or a decrease in the density of the original peat (Braekke, 1987); however with increasing time, enhanced bulk densities are most likely due to increasing compression and stabilisation of the soil (Holden et al., 2007) and an increased density of roots (Braekke, 1987), in addition to higher water table uptake by trees and peat drying and compaction (Vanguelova, *unpublished data*).

3.3.1.3 Organic Carbon Storage

The changes in mean mass of organic carbon in each horizon down to 45 cm are displayed as t C ha^{-1} and are shown in Fig. 3.1. This conversion from wt% to t C ha^{-1} highlights the importance of taking into consideration the boundary depths of the horizons and the relative bulk densities in addition to stone content.

The planting of Sitka spruce on the peaty gley soils led to a significant decrease in OC from 364.8 ± 36.6 t C ha^{-1} in the unplanted moorland (ML) to 117.8 ± 9.5 t C ha^{-1} in the first rotation stand (SS1) (Table 3.1). This represents an average annual decrease

(ΔSOM) of 6.2 t C ha^{-1} $year^{-1}$ over the first 40 years of the land-use change from moorland to forest, causing the soil to become a carbon source. Although this acute loss of carbon has previously been observed by Zerva et al. (2005), a loss of 5 t C ha^{-1} $year^{-1}$ is normally associated with heavily disturbed peaty gley soils which have been destumped and the whole peat horizon mixed with the mineral subsoil (E. Vanguelova, *pers. comm*.).

Previous measurements of carbon storage at Coalburn Forest by Forest Research found an average carbon storage of 199 t C ha^{-1} based on 30 sample pits (E. Vanguelova, *pers. comm*.). Therefore although observed at a higher than normal rate, the carbon loss has undoubtedly occurred after afforestation, and can be attributed to the accelerated decomposition of the SOM caused by the improved aeration, a direct result of drainage at the site (Zerva et al., 2005).

The introduction of the drainage ditches at Coalburn Forest resulted in increased streamflow and peak flows after afforestation at the catchment outlet, with streamflow levels only falling below pre-forestry levels several decades after afforestation, whilst peak flows were reduced as the drainage ditches deteriorated (Robinson, 1998). This increased stream flow during the first rotation could increase the loss of POM from the site and therefore enhance the loss of OC from the SS1 site. However, in an extensive literature study carried out by Paul et al. (2002), it was suggested that the soil carbon losses observed after afforestation (<10 year old) could be predominantly attributed to the lack of plant growth rather than soil disturbance, as land disturbance yielded no significant changes in soil carbon.

The significant increase of OC to 484.8 ± 58.9 t C ha^{-1} in the second rotation site (SS2) indicates the ability of the carbon stocks to recover approximately 80 years after initial afforestation and even exceed the carbon stock of the unplanted ML, once again becoming a carbon sink, supporting previous findings by Zerva et al. (2005) (Table 3.1 and Fig. 3.1c) ($p=0.001$). Before replanting, mounding was used to prepare the land prior to the second rotation (M. Mencuccini, *pers. comm*.), in agreement with the review paper by Paul et al. (2002), this land disturbance did not significantly reduce the OC into the second rotation as was seen for the first rotation, suggesting that the change from moorland to forest including the drainage of the soil, has a greater impact than the repeated disturbance during second rotation planting on the soil carbon.

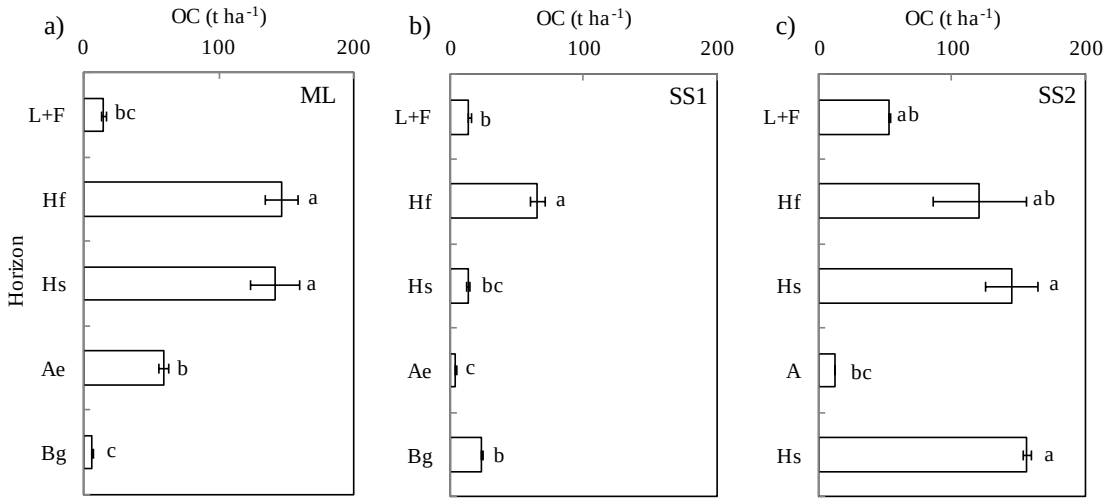

Fig. 3.1: Soil organic carbon contents (t C ha^{-1}) of the a) Coalburn ML, b) Coalburn SS1 and c) Harwood SS2 soils. Error bars represent the standard error of the mean for two (SS2) and three (ML+SS1) analytical replicates. Means followed by the same letter are not significantly different (Tukey's HSD, $p>0.05$).

OC storage in the litter of the SS2 soil was significantly larger than that of the SS1 and ML soil ($p=0.004$). The increased litter OC from the ML to the SS1 suggests an elevated litterfall after afforestation (Zerva et al., 2005), however the increased litter OC into the second rotation is unlikely to be a continued increase of litterfall due to similar ages of the two stands. Instead, the higher carbon storage could be a result of changing decomposition rates as the soil becomes more acidified. Furthermore, the amount of litterfall can be influenced by the forest age, and also biological influences (e.g. aphid infestations) (Pitman et al., 2010).

OC storage in the histic (Hf) horizons significantly decreased after afforestation as observed by Zerva and Mencuccini (2005), and Mason et al. (2009), however stocks displayed an increase into the second rotation ($p=0.045$).

The OC storage of 140.8 t C ha^{-1} in the humified (Hs) horizon in the ML was significantly similar to the OC storage of 144.4 t C ha^{-1} in the SS2. However there was also a buried Hs horizon with 155.7 t C ha^{-1} in SS2 (Hs2), resulting in a total Hs OC of 300.1 t C ha^{-1}, significantly higher than the ML soil ($p=0.001$) (Fig. 3.1). The significantly reduced carbon storage of the Hs horizon in the first rotation SS stand could be a reflection of increased decomposition rates as a result of the land preparation that occurred prior to planting the Sitka spruce (Zerva and Mencuccini, 2005), whilst

the SS2 profile shows that this OC content has recovered and exceeds the natural ML conditions. This decrease of Hs OC in the first rotation stand, followed by a subsequent increase in the second rotation has previously been observed in Harwood forest (Zerva and Mencuccini, 2005).

The OC content of the mineral horizons (A+B) significantly decreases from the ML soil to the first and second rotation soils, with 64.2, 26.1 and 11.5 t C ha^{-1}, respectively ($p=0.002$). This progressive decrease is coupled with the decrease in horizon depth across the three sites.

Paul et al. (2002) highlighted the importance of stratified sampling (i.e. disturbed and undisturbed soils) which would provide direct evidence oF the effect of site preparation during forest establishment on soil carbon. Disturbed soil from the mound was sampled at the Coalburn Forest site, however a visual assessment of the site drew attention to the large spatial variability of this area, and emphasised the need for a much larger scale sampling layout to account for the soil heterogeneity. It was evident that the soil had been lifted from the drain and laterally placed creating the mound. In effect, the soil profile had been laid out across the mound, exposing both the organic and mineral horizons. TOC measurements of the organic and mineral exposed soils were 11.4 ± 2.13 and 0.67 ± 0.04%, respectively, indicating major soil mixing on the mounds. Further work should be carried out using multiple sample points across the heavily disturbed mounds. Indeed, Forest Research is currently carrying out a detailed chronosequence experiment in Kielder Forest, with 26 stands of different ages; moorland, first and second rotation Sitka spruce, which employs a stratified soil sampling design with >30 sampling points per stand, taking into account the heterogeneity of the stands and calculating the difference between soil carbon stocks in mounds compared to undisturbed flat areas between tree mounds (E. Vanguelova, *pers. comm.*).

3.3.2 THM

3.3.2.1 Lignin Thermochemolysis Products

THM in the presence of TMAH of solvent-extracted powdered soil from Coalburn Forest ML causes decomposition of its polymeric network yielding a range of methylated phenolic and other oxygenated aromatic products (Fig. 3.2, Table 3.2).

Table 3.2: The main thermochemolysis products

Peak Label	Compound
P1	methoxybenzene
P2	4-methoxytoluene
G1	1,2-dimethoxybenzene
P3	4-methoxybenzeneethylene
1	cellulose derivative*
2	cellulose derivative*
3	cellulose derivative*
G2	3,4-dimethoxytoluene
I	4-isopropenyl phenol
4	cellulose derivative*
P4	4-methoxybenzaldehyde
P5	4-methoxyacetophenone
G3	3,4-dimethoxybenzeneethylene
1,2,4-TMB	1,2,4-trimethoxybenzene*
P6	4-methoxybenzoic acid methyl ester
1,3,5-TMB	1,3,5-trimethoxybenzene
MC1	methylated carbohydrate derivative*
G4	3,4-dimethoxybenzaldehyde
MC2	methylated carbohydrate derivative*
MC3	methylated carbohydrate derivative*
MC4	methylated carbohydrate derivative*
G5	3,4-dimethoxyacetophenone
P17	(*Z*)- 3-(4-methoxyphenyl)-3-propenoic acid methyl ester
G6	3,4-dimethoxybenzoic acid methyl ester
S4	3,4,5-trimethoxybenzaldehyde
G7	(*Z*)- 1-(3,4-dimethoxyphenyl)-2-methoxyethylene
G24	3,4-dimethoxybenzene acetic acid methyl ester
G8	(*E*)- 1-(3,4-dimethoxyphenyl)-2-methoxyethylene
G9	(*Z*)- 1-(3,4-dimethoxyphenyl)-3-methoxyprop-1-ene
G10	(*Z*)- 1-(3,4-dimethoxyphenyl)-3-methoxyprop-1-ene
P18	(*E*)- 3-(4-methoxyphenyl)-3-propenoic acid methyl ester
S5	3,4,5-trimethoxyacetophenone
S6	3,4,5-trimethoxybenzoic acid methyl ester
G13	(*E*)- 1-(3,4-dimethoxyphenyl)-3-methoxyprop-1-ene
S7	(*Z*)- 1-(3,4,5-trimethoxyphenyl)-2-methoxyethylene
S8	(*E*)- 1-(3,4,5-trimethoxyphenyl)-2-methoxyethylene
G14	*threo/erythro* 1-(3,4-dimethoxyphenyl)-1,2,3-trimethoxypropane
G15	*threo/erythro* 1-(3,4-dimethoxyphenyl)-1,2,3-trimethoxypropane
G18	(*E*)- 3-(3,4-dimethoxyphenyl)-3-propenoic acid methyl ester
S14	*threo/erythro* 1-(3,4,5-trimethoxyphenyl)-1,2,3-trimethoxybenzene
$C_{16:0}$ FAME	$C_{16:0}$ fatty acid methyl ester
S15	*threo/erythro* 1-(3,4,5-trimethoxyphenyl)-1,2,3-trimethoxybenzene
IS	5α-androstane

*see Chapter 7 for further interpretation of these compounds

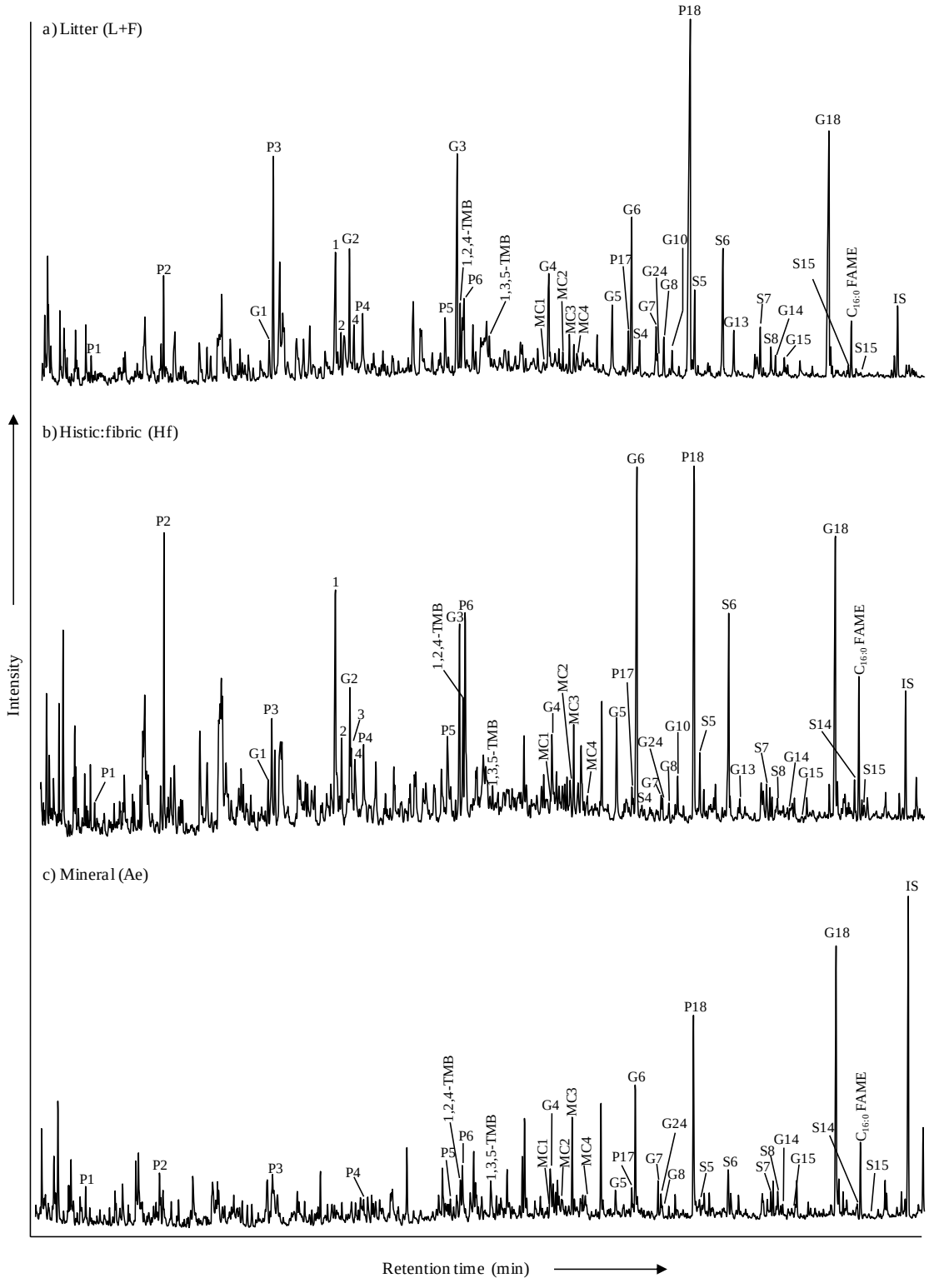

Fig. 3.2: Partial trace for the total ion current (TIC) of the thermochemolysis products from the (a) Litter (L+F), (b) Histic (fibric) (Hf) and (c) Mineral (Ae) horizons of the Coalburn Forest ML. Peak identities and symbols are listed in Table 3.2.

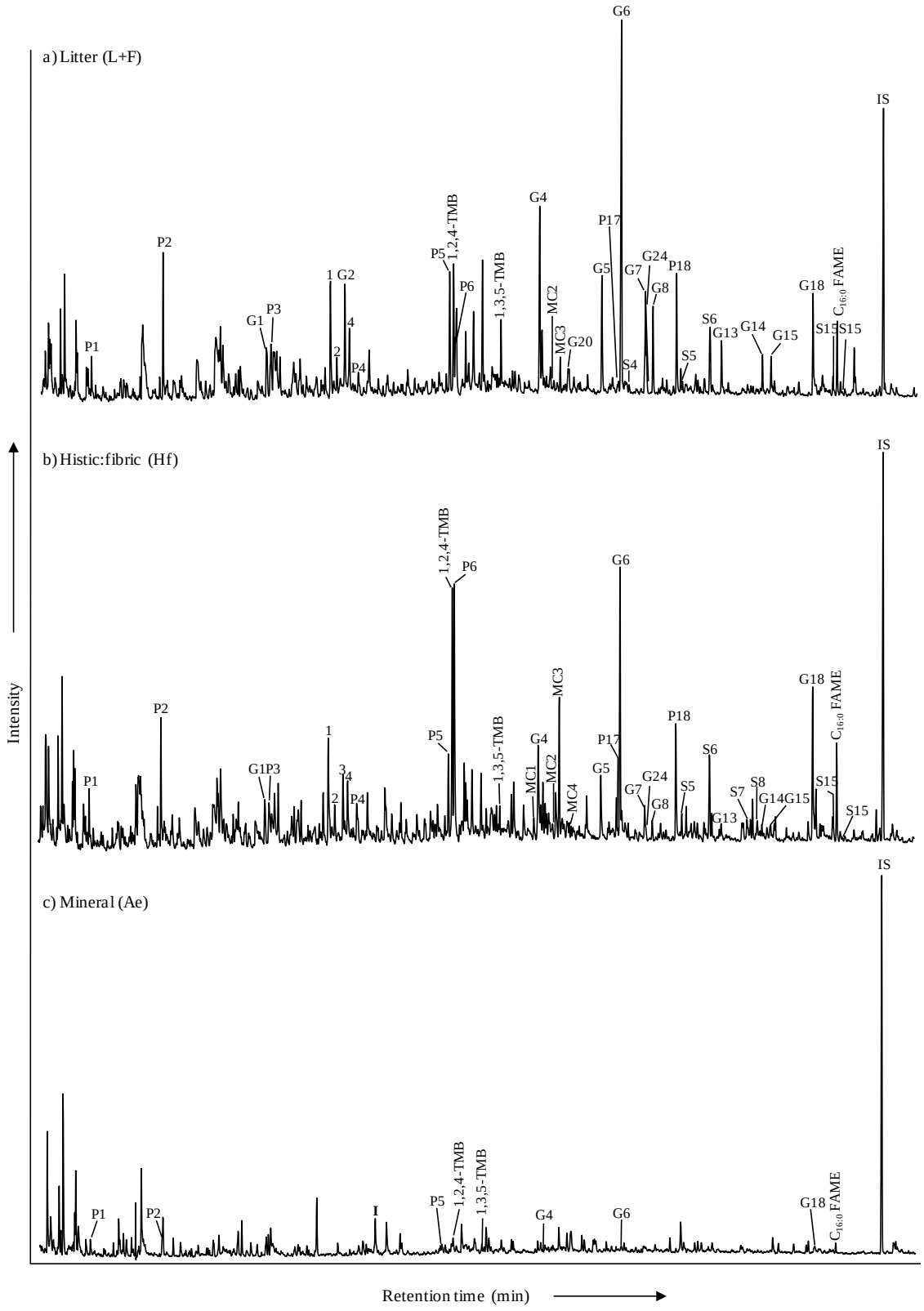

Fig. 3.3: Partial trace for the total ion current (TIC) of the thermochemolysis products from the (a) Litter (L+F), (b) Histic (fibric) (Hf) and (c) Mineral (Ae) horizons of the Coalburn Forest SS1. Peak identities and symbols are listed in Table 3.2.

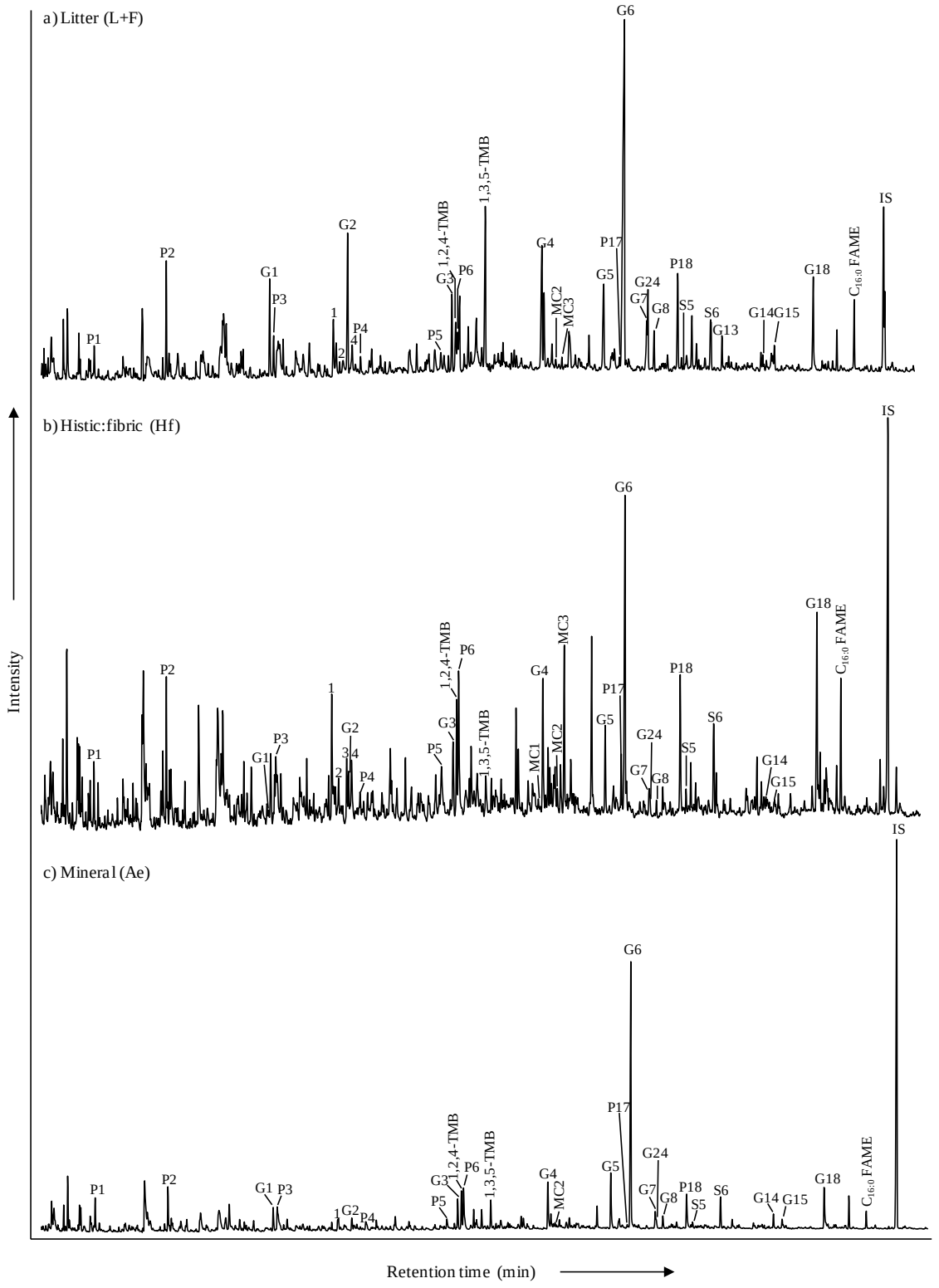

Fig. 3.4: Partial trace for the total ion current (TIC) of the thermochemolysis products from the (a) Litter (L+F), (b) Histic (fibric) (Hf) and (c) Mineral (Ae) horizons of the Harwood Forest SS2. Peak identities and symbols are listed in Table 3.2.

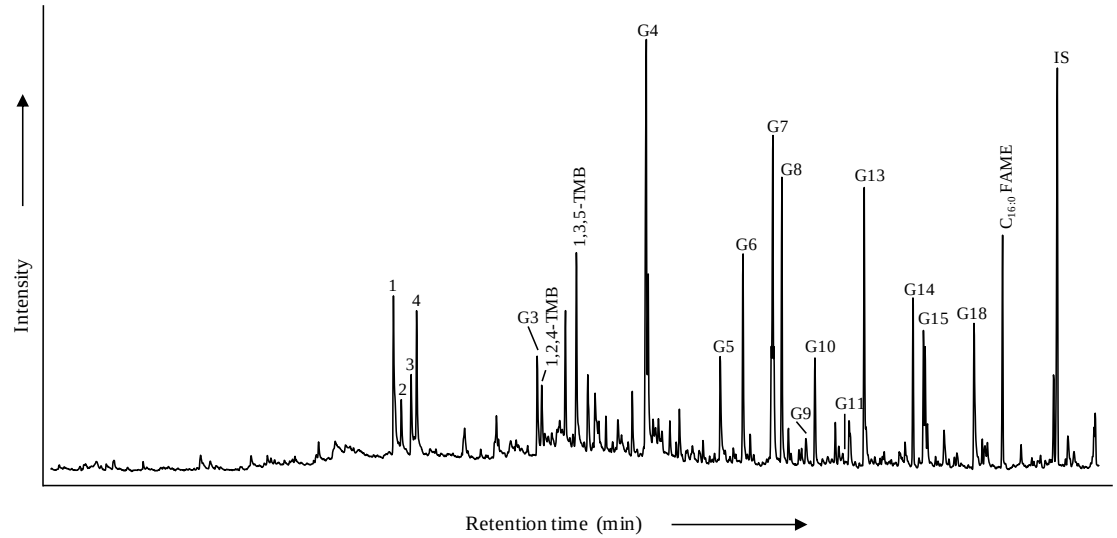

Fig. 3.5: Partial trace for the total ion current (TIC) of the thermochemolysis products from the Coalburn Forest Sitka spruce roots. Peak identities and symbols are listed in Table 3.2.

The most abundant THM components included *p*-coumaric acid (P18) and ferulic acid (G18), abundant down the ectorganic horizons and the mineral A horizon of the ML core (Fig. 3.2). The consistent dominance of P18 and G18 down core indicates a prolonged graminaceous input to the soil typical of a moorland habitat that has not undergone any recent vegetation or land-use changes (Hedges and Mann, 1979a).

There were also smaller amounts of other vascular plant-derived phenols produced during the thermochemolysis of the Coalburn Forest ML soil, including the methylated guaiacyl (G) lignin phenols 3,4-dimethoxytoluene (G2), 3,4-dimethoxybenzaldehyde (G4), 3,4-dimethoxyacetophenone (G5), 3,4-dimethoxybenzoic acid methyl ester (G6), and syringyl (S) lignin phenols 3,4,5-trimethoxyacetophenone (S5) and 3,4,5-trimethoxybenzoic acid methyl ester (S6) (Fig. 3.2). Relatively large quantities of *p*-hydroxyphenols were also observed in the organic horizons of the ML core, including 4-methoxytoluene (P2), 4-methoxybenzeneethylene (P3), 4-methoxybenzaldehyde (P4), 4-methyoxyaceophenone (P5), and 4-methoxybenzoic acid methyl ester (P6) (Fig. 3.2a and b). Small quantities of THM products *threo/erythro* 1-(3,4-dimethoxyphenyl)-1,2,3-trimethoxypropane (G14/15) and *threo/erythro* 1-(3,4,5-trimethoxyphenyl)-1,2,3-trimethoxybenzene (S14/15) are observed down the entire core of ML soils indicating the rapid side chain oxidation of lignin at the surface of the soil (Fig. 3.2).

The THM products identified from the organic horizons of the Coalburn Forest SS1 site are dominated by G6; indicating the presence of gymnosperm vegetation (Fig. 3.3a and

b). There were also smaller amounts of other vascular plant-derived phenols produced during the thermochemolysis of Coalburn Forest SS1 soil, including the methylated guaiacyl lignin phenols; 1,2-dimethoxybenzene (G1), 3,4-dimethoxytoluene (G2), 4-dimethoxybenzaldehyde (G4), 3,4-dimethoxyacetophenone (G5), (*E/Z*)- 1-(3,4-dimethoxyphenyl)-2-methoxyethylene (G7/G8), and 3,4-dimethoxybenzeneacetic acid methyl ester (G24); syringyl lignin phenols; 3,4,5-trimethoxyacetophenone (S5) and 3,4,5-trimethoxybenzoic acid methyl ester (S6) and the methyl esters of the cinnamyl (C) phenols; P18 and G18 (Fig. 3.3). 1,2,4-trimethoxybenzene (1,2,4-TMB) was also observed with a high abundance in the organic horizons; a thermochemolysis product which can be derived from both carbohydrates (Fabbri and Helleur, 1999) and condensed tannins (CT), specifically a procyanidin B ring (Nierop et al., 2005).

In the Hf horizon, the abundance of guaiacyl lignins has decreased so that they are of similar abundance to the cinnamyl phenols, an indication of the previous vegetation cover of grasses prior to planting (Fig. 3.3b). Small quantities of intact lignin phenols G14/15 and S14/15 are observed down the organic horizons of SS1 soil indicating the rapid side chain oxidation of lignin (Fig. 3.3). 4-isopropenyl phenol (**I**) was also observed in the Ae horizon, a pyrolysis product of sphagnum acid, an indication that *Sphagnum* species, albeit in small quantities have previously grown at this site (the pyrolysis products of sphagnum acid are discussed in more detail in Chapter 4). The A horizon shows very low abundances of lignin phenols (Fig. 3.3c), consistent with other peaty gley soils (Huang et al., 1998). As with the ML soil, the mineral Bg horizon does not contain any lignin phenols, an indication of the degradation of lignin phenols.

The THM products identified from the Harwood Forest SS2 soil revealed similar lignin phenols to those observed in the first rotation (SS1); however the dominant lignin phenol G6 persists into the mineral Ae horizon, an indication of the long term presence of the Sitka spruce vegetation growth at this site (Fig. 3.4a and b). G14/15 are observed throughout the SS2 profile with a marked absence of S14/15, indicating the inputs from the dominant gymnosperm vegetation. There were also smaller amounts of other vascular plant-derived phenols including primarily the methylated guaiacyl lignin phenols; G2, G4, G5, G7/G8, and G24, and the methyl esters of the cinnamyl phenols; P18 and G18 (Fig. 3.4). 1,3,5-trimethoxybenzene (1,3,5-TMB) was also observed with a high abundance in the litter, previously identified as a marker for condensed tannins

(Nierop et al., 2005). Although this product has been observed in cutan (McKinney et al., 1996), cutan is only found in drought-adapted plants (Boom et al., 2005), and therefore 1,3,5-TMB can be used as an unequivocal CT marker in these samples (Hernes and Hedges, 2004). Methylated carbohydrate (MC) thermochemolysis products were also observed throughout the samples (Figs. 3.2, 3.3 and 3.4). These compounds are discussed in more detail in Chapter 7.

THM in the presence of TMAH of the Soxhlet-extracted Sitka spruce roots yielded a wide range of guaiacyl phenols (Fig. 3.5). The large abundance of 1,3,5-TMB, indicates CTs are a major product from the THM of SS roots. C16:0 fatty acid methyl ester and four cellulose derived products (1-4) were also major components detected by GC-MS. These compounds are discussed in more detail in Chapter 7.

3.3.2.2 Lignin Yield (Λ)

Owing to the use of unlabelled TMAH, the differentiation between lignin, degraded lignin and non-lignin phenols (i.e. tannins) cannot be made. However tannin phenols as with lignin phenols are exclusive to vascular plants (Hernes and Hedges, 2004). Therefore the lignin yield (Λ) parameter represents an input from vascular plant rather than that solely from lignin.

In the ML and SS1, Λ decreases from the surface down through the organic horizons, decreasing to zero in the mineral B horizon. This decrease is most pronounced in the ML (decreasing from 2.60 ± 0.58 mg /100 mg OC in the litter to 0 mg in the Bg horizon), most of the decrease occurred in the litter and Hf horizons (Fig. 3.6a and b). For the SS2 core, the Λ profile was rather different, displaying an initial decrease from 0.77 ± 0.04 in the litter to 0.36 ± 0.08 mg/100 mg OC in the Hs horizon consistent with the ML and SS1 sites. However with increasing depth, Λ increases in the mineral A horizon to 2.49 ± 1.5 mg/100 mg OC, before decreasing again in the Hs2 horizon to 0.53 ± 0.01 mg/100 mg OC (Fig. 3.6c). The linear deposition of horizons in the ML and SS1 soils together with the progressive decrease in Λ with increasing burial depth suggests a relatively rapid decay of the lignin biopolymer in the upper organic horizons, with the mineral horizons containing only a few lignin monomers.

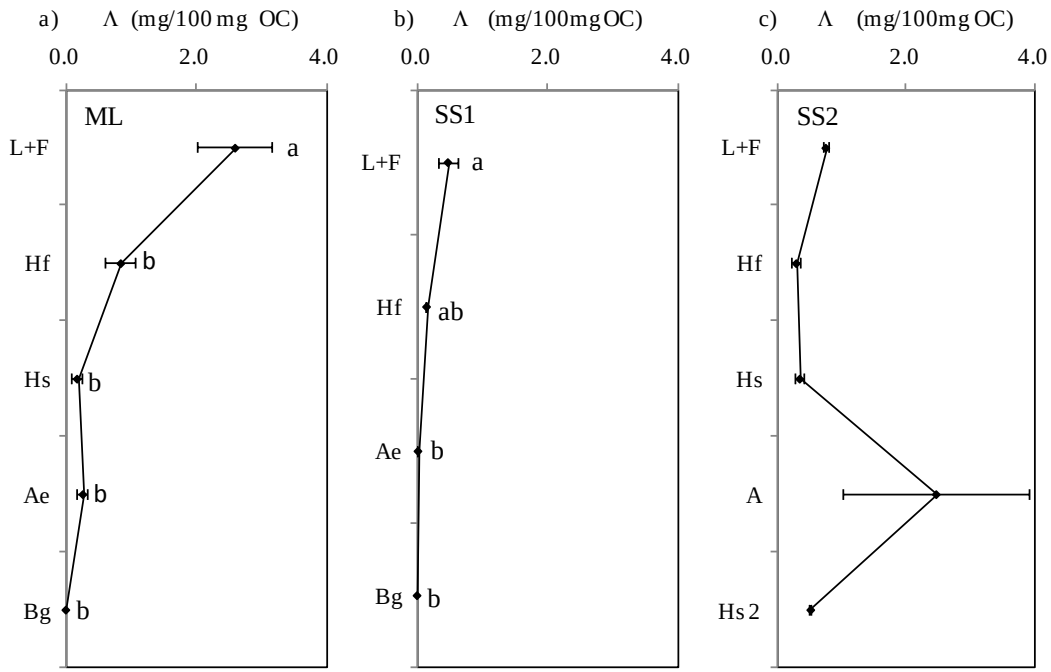

Fig. 3.6: The depth profile showing changes in the lignin content (Λ) (mg/100 mg OC) in (a) Coalburn ML, (b) Coalburn SS1 and (c) Harwood SS2 soil. The error bars indicate the standard error from three/two analytical replicates. Lettering indicates significant differences from the Tukey's test.

Tukey's test at the 95 % confidence level highlighted that the litter has a significantly higher Λ than the deeper horizons in the ML and the SS1 ($p<0.05$). These results are consistent with those from other studies and suggests that lignin may not be as refractory as conventionally perceived (Huang et al., 1998; Kiem and Kögel-Knabner, 2003; Bahri et al., 2006; Heim and Schmidt, 2007; Mason, 2009).

The Λ in the mineral A horizon at SS2 was higher than the organic horizons, although differences were not significant ($p=0.273$). This lambda maximum has previously been observed in the buried Hs2 horizon at this site, and was put down to either the horizon inversion that occurred prior to planting at this site, the input of root material, the leaching of phenolics or a change in vegetation (Mason et al., 2009).

THM of the SS roots reveals a lignin yield of 0.22 mg/100 mg OC, which will be contributing to the soil lignin yield down the profile. However, the THM product distribution and abundance from the SS roots does not match the TIC from the mineral A horizon of the SS1 or SS2 profile, primarily due to the lack of compounds 1-4, and low abundances of G4 in the soil, suggesting that the root input alone is not causing the lignin maximum (Figs. 3.3, 3,4 and 3.5). Zerva et al. (2005), found that the modelled

change in fine root biomass after afforestation increased from 2.4 to 3.6 t C ha^{-1} from the first rotation to second rotation stand, whilst the coarse root biomass decreased from 56.3 to 27.1 t C ha^{-1}, reflecting a total modelled decrease of 28 t C ha^{-1}. However, Rasse et al. (2006) has shown that root carbon has a longer residence time in soil compared to shoot carbon, which could be due to physical protection through mycorrhiza and root-hair activities, physico-chemical production particularly in deeper soil horizons, or the chemical interactions with metal ions. Further research is clearly needed at the molecular level to help unravel the fate of individual shoot and root compounds, such a cutins and suberins, throughout soil profiles.

The lignin maximum is not observed in the SS1 site, however the significant increase in dissolved organic matter (DOC) between 2002 and 2006 at Coalburn Forest (Vanguelova et al., 2010), coupled with the increased streamflow and peak flow levels due to the draining of the site after the land-use change (Robinson, 1998), would suggest that the leaching of phenolics is occurring under the first rotation. The change in vegetation input from grassy species at the moorland to gymnosperm litter at the forest occurred at both SS sites, and this change is reflected in the increased dominance of guaiacyl phenols at the surface with respect to cinnamyl phenols (Figs. 3.3 and 3.4) (see Section 3.3.2.3 for vegetation source proxy results and discussion). As the same changes have occurred at both sites, it is unlikely that the change in vegetation input is causing the lignin maximum at SS2. Therefore, the lignin maximum can be largely attributed to the horizon inversion that occurred between the first and second rotation at Harwood Forest. However root input could also be a contributory explanation.

Tukeys tests revealed that the SS2 profile exhibits a significantly larger yield of lignin monomers compared to SS1, with ML showing a medium lignin yield (Fig. 3.6). This suggests that after afforestation, the yield of lignin monomers is greatly reduced, most likely due to a combination of a reduced litter input (Paul et al., 2002), increased aeration and degradation (Guo and Gifford, 2002) and the increased DOC and streamflow experienced at this site (Robinson, 1998), however the yield increases in the second rotation to levels exceeding the ML, with the majority held deeper in the horizons of SS2 predominantly in mineral clay rich A horizon. Clay soils have been shown to be able to sequester the most stable C compared to other soil types (Villada et al., 2012).

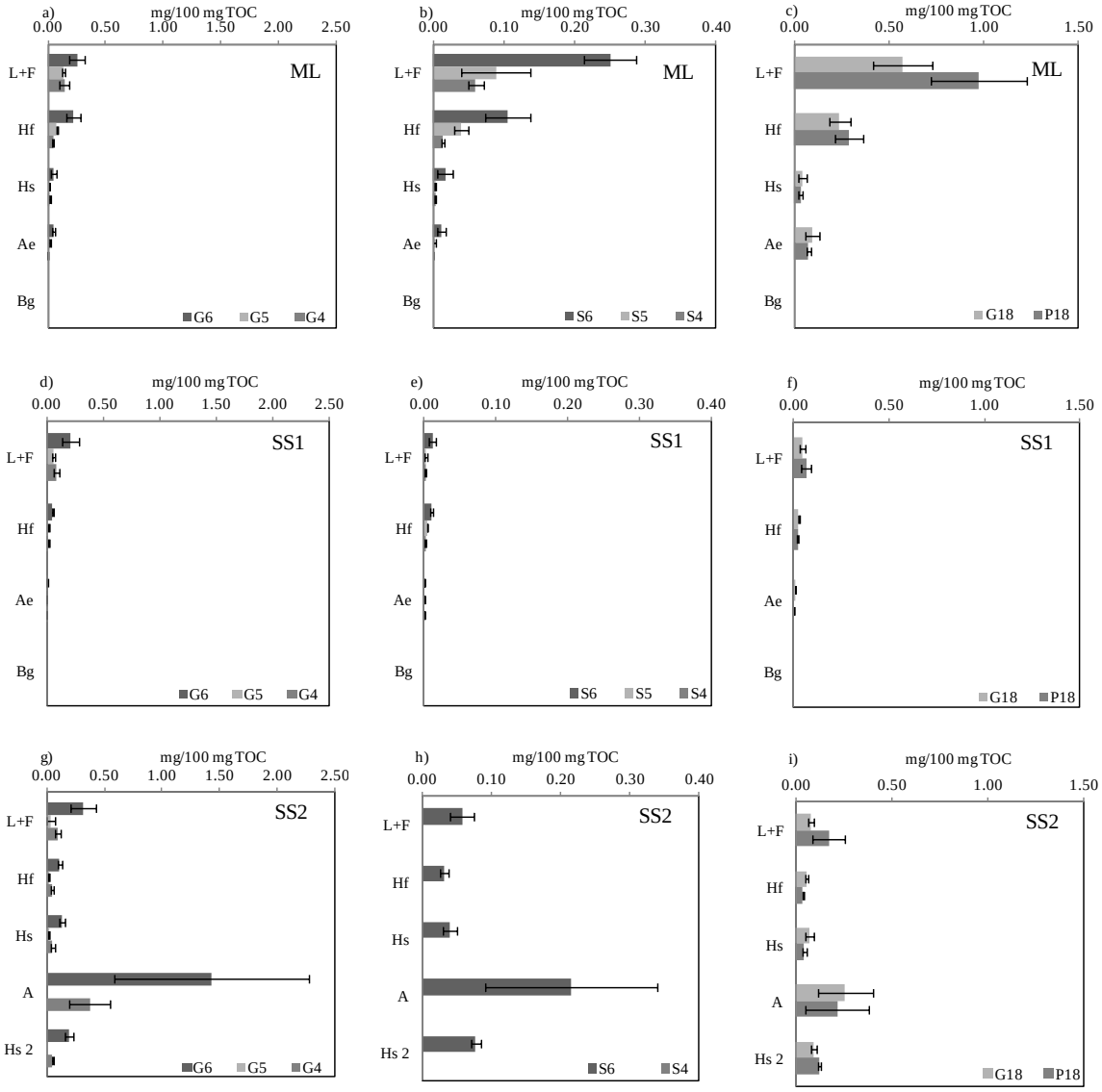

Fig. 3.7: Depth profile showing changes in yield of lignin phenols that contribute to the Λ parameter; ML soil (a) G phenols (b) S phenols (c) G18 and P18; SS1 soil (d) G phenols (e) S phenols (f) G18 and P18, and SS2 soil (g) G phenols (h) S phenols (i) G18 and P18. The error bars indicate the standard error from three/two analytical replicates.

Plotting the individual amounts of guaiacyl, syringyl and cinnamyl phenols that contribute to the Λ value allows the assessment of the changes in lignin monomer amounts that govern the changes in total lignin (Fig. 3.7). A progressive degradation of cinnamyl phenols (P18 & G18) is observed in the ML and SS1 soils (Fig. 3.7c and f), whereas the cinnamyl phenol amounts pass through a maximum in the SS2 soil (Fig. 3.4i). The guaiacyl (G) and syringyl (S) phenol yield in the SS2 also display a maximum at the A horizon (Fig. 3.7g and h), consistent with the Λ profile.

The absence of the syringyl aldehyde (S4) and S14/15 in the SS2 soil, indicates that the remaining syringyl phenols are highly degraded, with no fresh input of angiosperm vegetation, signifying the dominance of the guaiacyl containing gymnosperm Sitka spruce at this site. However, it is important to note that the S6 present at SS2 could be derived from gallic acid, which has been shown to occur in abundance in Sitka spruce needles (Hernes and Hedges, 2004).

In the ML soil, the mass of G and S phenols gradually decrease down the profile to almost zero in the deeper mineral horizons (Fig. 3.7a and b). The absolute amount of C phenols exceeds the G and S phenol yield, indicating the graminaceous input at the ML. In the SS1 soil, the mass of syringyl phenols remain constant in the litter and Hf horizons, which then reduce down to almost zero in the deeper mineral horizons (Fig. 3.7e). The G moieties, however, show a progressive decrease down the profile (Fig. 3.7d), evidence of their relatively recent introduction at the site. The low levels of S phenols relative to G phenols in the SS soils reflect the dominant gymnosperm input.

Of the aromatic compounds investigated, G14/15 and S14/15 represent the only true lignin phenols with intact β-O-4 linkages bearing adjacent hydroxyl groups, which are derived solely from lignin (Filley et al., 1999; Nierop and Filley, 2007). The aldehydes (G4 and S4) and the acids (G6 and S6) can be derived from non-lignin sources, such as tannins (Garnier et al., 2003). The remaining phenols are derived from the breakdown of lignin as a thermochemolysis by-product (Clifford et al., 1995; Filley et al., 1999). Therefore, it is important to consider that the yields shown in Fig. 3.7 will show both the lignin and non-lignin yield, which cannot be differentiated between without ^{13}C-labelled TMAH.

It must also be noted that the fractionation of lignin has been identified by Hernes et al. (2007). Hernes et al. displayed the preferential removal of acidic phenols from the process of dissolution and sorption from POM to DOM. This can result in elevated [Ad/Al] and C/G ratios, however is most significant when comparing between systems whereby leaching is a significant process, i.e. between POM in soils and DOM in riverine systems (e.g. Ertel et al., 1986).

3.3.2.3 Lignin Source Proxies

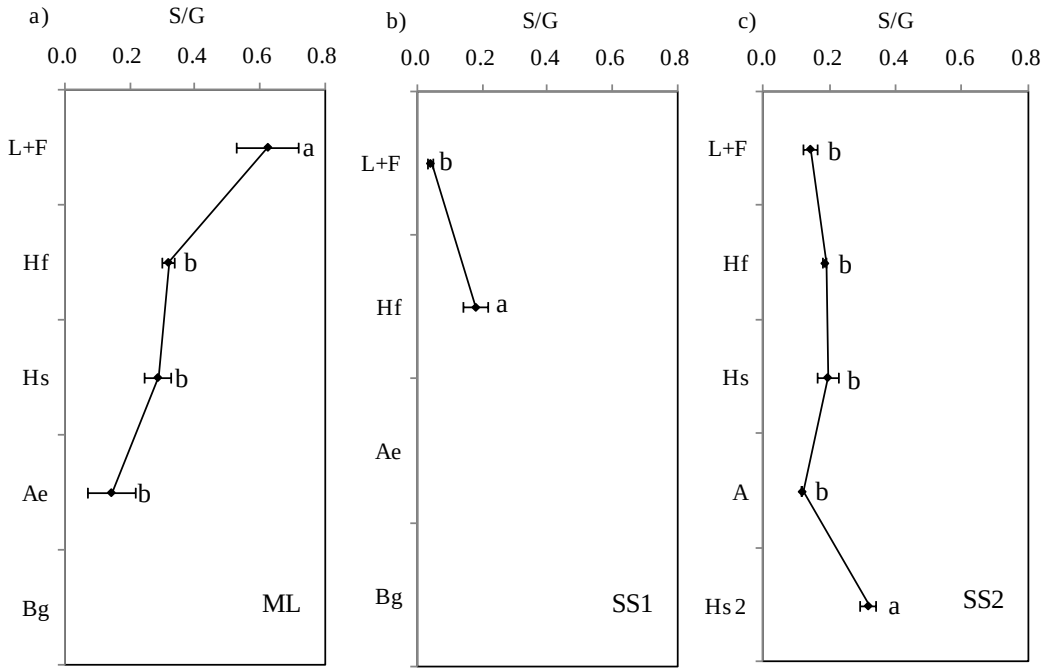

Fig. 3.8: The depth profile showing changes in the S/G ratio in (a) Coalburn ML, (b) Coalburn SS1 and (c) Harwood SS2 soil. The error bars indicate the standard error from three/two analytical replicates. Lettering indicates significant differences from the Tukey's test.

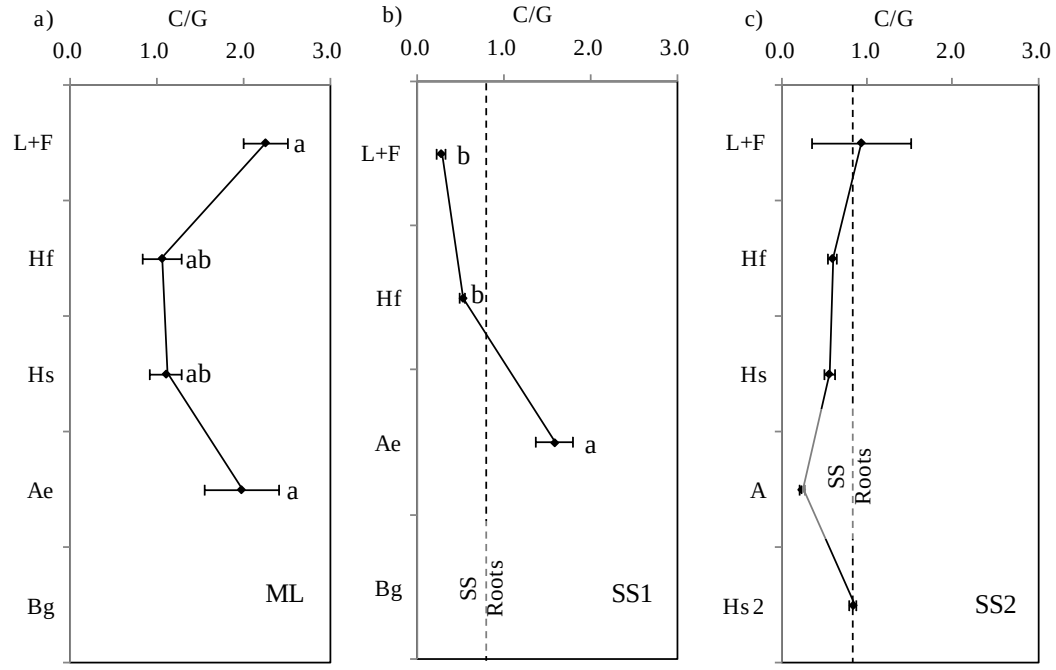

Fig. 3.9: The depth profile showing changes in the C/G ratio in (a) Coalburn ML, (b) Coalburn SS1 and (c) Harwood SS2 soil. The error bars indicate the standard error from three/two analytical replicates. Lettering indicates significant differences from the Tukey's test. The dashed line indicates the C/G ratio from the THM of SS roots (C/G = 0.09).

The ML soil profile shows a classic S/G degradation profile, significantly decreasing from 0.63 ± 0.1 in the L to 0.14 ± 0.07 in the Ae horizon (p=0.001) (Fig. 3.8a). It can be assumed that there has been no change in the vegetation over the course of humification at the moorland, therefore the structural changes in the lignin ratios are due to the biodegradation and humification processes, resulting in the transformation of SOM with a preferential degradation of syringyl over guaiacyl moieties (Chefetz et al., 2000).

The C/G ratio in the ML decreases from 2.3 ± 0.25 in the litter to 1.1 ± 0.2 in the Hf and Hs horizons, then the ratio increases again to 1.9 ± 0.4 in the A horizon, however these changes are not significant, (p=0.155) (Fig. 3.9a). The relatively high C/G values are an indication of an input of grass lignin with a large contribution of cinnamyl moieties, concomitant with the moorland habitat.

The SS1 profile shows significant increases in both the S/G (p=0.002) and C/G ratios (p=0.001) down the profile (Figs. 3.8b and 9b). The initial low values of the S/G and C/G ratios of only 0.04 ± 0.01 and 0.28 ± 0.05, respectively, is a direct result of the input of Sitka spruce litter to the upper horizons since afforestation (Figs. 3.8b and 9b). The S/G increases in the Hf horizon to 0.19 ± 0.04, a result of decreasing guaiacyl (Fig. 3.7a) and a constant syringyl (Fig. 3.7b) contribution, which could be due to the input from the grasses in the previous vegetation cover into the deeper horizons prior to afforestation. The S/G ratio in the mineral horizons could not be determined primarily due to very low/absence of syringyl phenols, thus preventing the calculation of accurate ratios. This is reflected in the low lignin content at increasing depth (Fig. 3.7). The C/G ratio increases into the Ae horizon to 1.6 ± 0.21 due to an increased proportion of cinnamyl phenols (Fig. 3.7c) to guaiacyl phenols (Fig. 3.7a). No lignin phenols were observed in the Bg horizon in both sites therefore no ratios could be calculated.

The SS2 profile has a statistically similar S/G ratio of 0.16 ± 0.02 down core, increasing only in the deepest Hs 2 horizon to 0.32 ± 0.03 (Fig. 3.8c). The C/G is also significantly similar down core; 0.64 ± 0.19 (Fig. 3.9c). The C/G ratio for SS roots produced a low ratio of 0.09 (marked on the profiles of SS1 and SS2 (Fig. 3.8)), which maybe the cause of the reduced C/G ratio at the SS2 profile.

Tukey's test at the 95% confidence level highlighted that both the S/G ratio and C/G ratio in the ML soil is significantly higher than at the SS1 and SS2 soils ($p<0.05$). This increase at the ML is due to the grassy vegetation prevailing at this site, whilst the

reduced S/G ratio under Sitka spruce is a direct result of a changing vegetation from cinnamyl and syringyl rich grasses to guaiacyl rich gymnosperms, with reduced C/G values reaching progressively deeper into the profile with increasing time from the land use change.

Fig. 3.10a shows that ML $[Ad/Al]_G$ values were lowest in the litter (1.5 ± 0.09) where no/little microbial degradation had yet occurred (Nierop and Filley, 2007). An increase of the $[Ad/Al]_G$ ratio in the Hf horizon to 5.1 ± 0.28 indicates increased oxidation of lignin (Nierop and Filley, 2008). However there is a subsequent significant decrease in the Hs and A horizons with an average $[Ad/Al]_G$ of 3.5 ± 0.3, which could be due to an input of fresh organic matter such as root material (Nierop and Filley, 2007), but could also be due to the preservation of lignin phenols as a result of anoxic conditions caused by a naturally higher water table than the afforested site (Robinson, 1998).

The two SS soils both show a statistically constant $[Ad/Al]_G$ ratio down core of 2.5 ± 0.3 and 3.2 ± 0.2, respectively (Figs. 3.10b and c). The horizon inversion observed at SS2 would expect to cause a lower $[Ad/Al]_G$ at the Hs 2 horizon due to the burial of fresher OM as observed by Mason et al. (2009), however this is not the case.

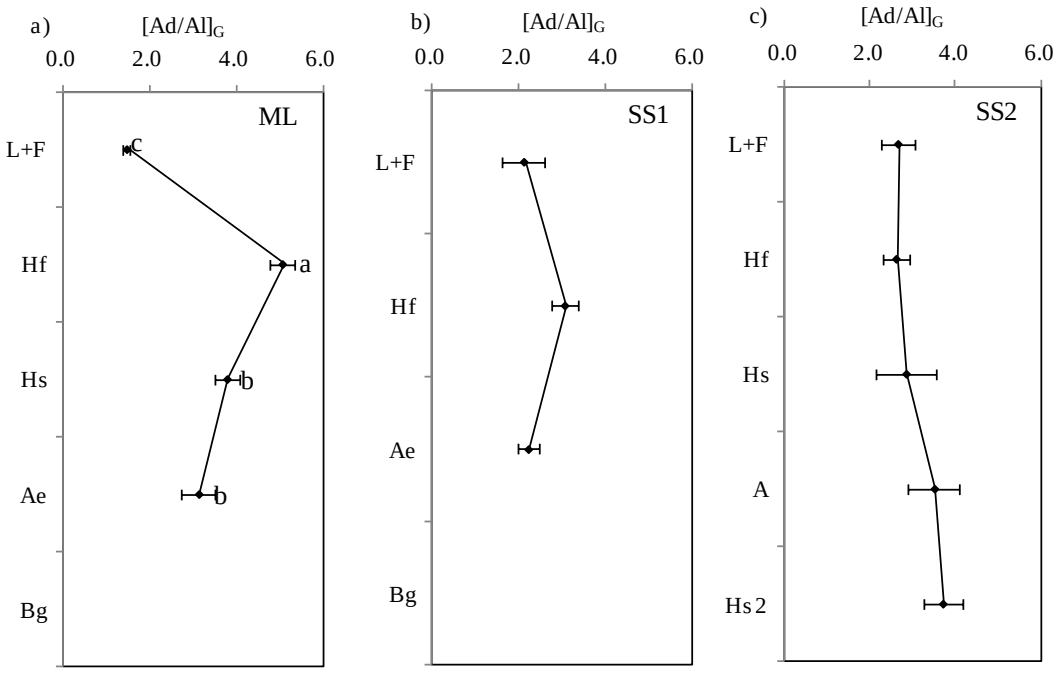

Fig. 3.10: The depth profile showing changes in the $[Ad/Al]_G$ ratio in (a) Coalburn ML, (b) Coalburn SS1 and (c) Harwood SS2 soil. The error bars indicate the standard error from three/two analytical replicates. Lettering indicates significant differences from the Tukey's test.

This suggests that after 40 years, the entire SS1 soil profile has degraded to the same degree, potentially due to the consistent oxic conditions down core, however measurements at Coalburn Forest have revealed the water table can be as shallow as 20 cm from the soil surface in the winter, subjecting shallow soils to anoxic conditions (E. Vanguelova, *pers. comm.*).

In the mineral Bg horizons of the ML and SS soil $[Ad/Al]_G$ ratios could not be determined primarily due to very low/absence of G4, thus preventing calculation of accurate values. The SS roots show a very low $[Ad/Al]_G$ ratio of 0.74, indicating very little microbial decay has occurred. There is no $[Ad/Al]_G$ decrease in the two SS profiles, suggesting that the input of SS roots cannot be detected over the bulk soil lignin signal. ANOVA revealed that ML had a significantly higher $[Ad/Al]_G$ ratio ($p<0.05$) compared to SS1, with the SS2 similar to both, indicating an input of fresh material at the SS1 site, which degraded over time into the second rotation.

The $[Ad/Al]_S$ ratio can also be used to illustrate the oxidation of the syringyl lignin phenols in soil. The $[Ad/Al]_S$ for the ML gave an average of 5.49 ± 0.89 in the ectorganic horizons only ($p>0.05$). The ratio could only be calculated for the Hf horizon in the SS1 soil due to the lack of S4 in the deeper horizons;7.7 ± 3.2 with the large error due to the small quantities of S4. The $[Ad/Al]_S$ ratio could not be calculated for SS2 due to the absence of S4. This further indicates the gradual oxidation and loss of syringyl phenols from the ML to the SS1 and finally completely lost from the SS2 soil.

The $\Gamma_{G/S}$ is another proxy to indicate lignin oxidation (Γ_G shown in Fig. 3.11).This proxy provides an indication of the extent of side-chain oxidation (Vane et al., 2001). The Γ_G shows a significant increase of side chain oxidation with increasing depth at the ML and first rotation stand (SS1) ($p<0.05$). The very low quantities/total absence of G14/15 in the deeper horizons at the ML and SS1 sites is due to the complete side chain oxidation. Fig. 3.11c shows that these phenols are present down the entire core of SS2 suggesting a degree of preservation at depth potentially due to the increased input of guaiacyl lignin coupled with the horizon inversion.

No Γ_S can be calculated for the two SS soils, due to the total absence of S14/15 in the soil. This is not unusual as the current dominant land cover does not contain syringyl lignin and therefore any presence of syringyl lignin would be from a previous land cover which would have be heavily oxidised and the side chains subsequently lost.

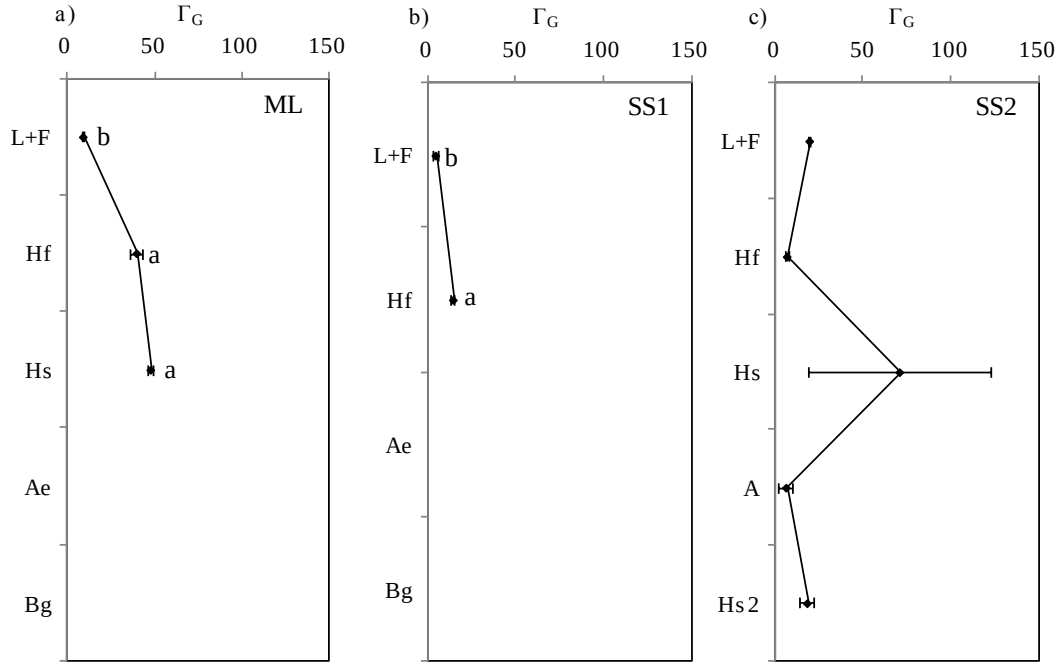

Fig. 3.11: The depth profile showing changes in the Γ_G in (a) Coalburn ML, (b) Coalburn SS1 and (c) Harwood SS2 soil. The error bars indicate the standard error from three analytical replicates. Lettering indicates significant differences from the Tukey's test.

The Γ_S at the ML significantly decreases with increasing depth, from 15.9 ± 1.0 in the L and F horizons to 4.8 ± 1.9 in the deeper H horizon ($p<0.05$) (data not shown), this is the opposite trend to what is observed with Γ_G at the ML, further indication of anoxic conditions at this site.

3.3.2.4 Non-Lignin Phenols

1,2,4-trimethoxybenzene (1,2,4-TMB) was observed in the THM products from the thermochemolysis of all the samples, a compound with two known sources; tannin and polysaccharide (Fabbri and Helleur, 1999; Nierop et al., 2005). The 1,2,4-TMB yield decreases with increasing depth in the ML and SS1 sites. Within the SS2 profile, there was a maximum concentration of 1,2,4-TMB in the mineral A horizon (Fig. 3.12). The yield of 1,2,4-TMB is significantly lower in the SS1 compared to SS2, with the ML displaying an intermediate yield. This suggests that this water-soluble polyphenol is lost during site drainage and preparation for planting. However with increasing time after the land-use change, the sources of 1,2,4-TMB begins to build up again to levels exceeding the original yield, preferentially in the mineral horizon.

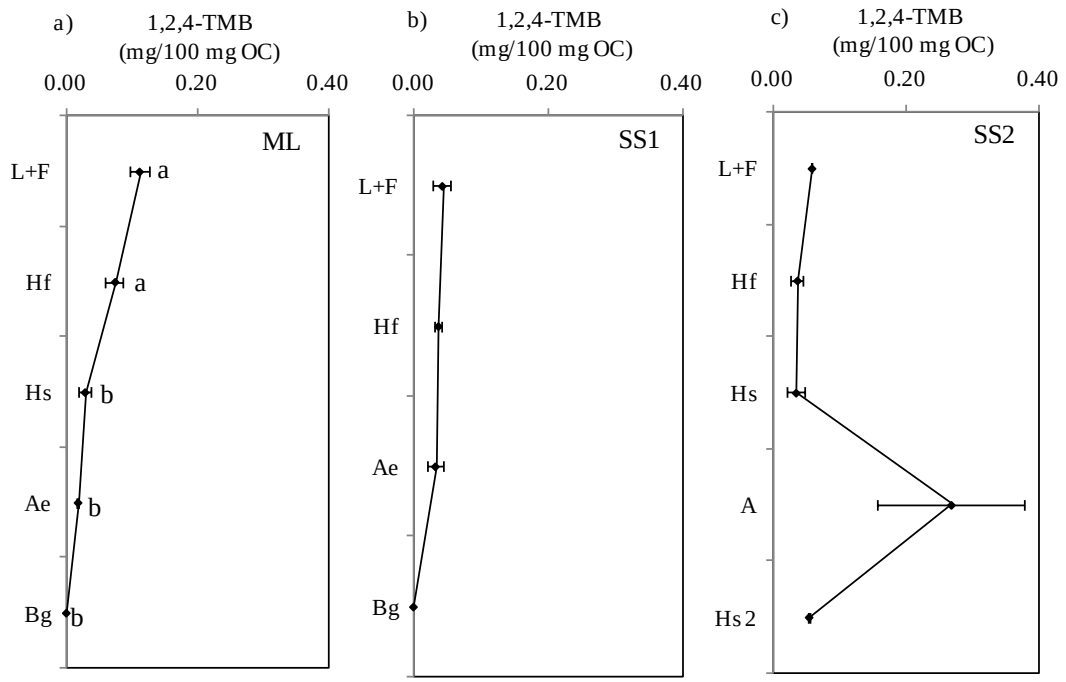

Fig. 3.12: The depth profile showing changes in the 1,2,4-TMB (mg/100 mg OC) in (a) Coalburn ML, (b) Coalburn SS1 and (c) Harwood SS2 soil. The error bars indicate the standard error from three/two analytical replicates. Lettering indicates significant differences from the Tukey's test.

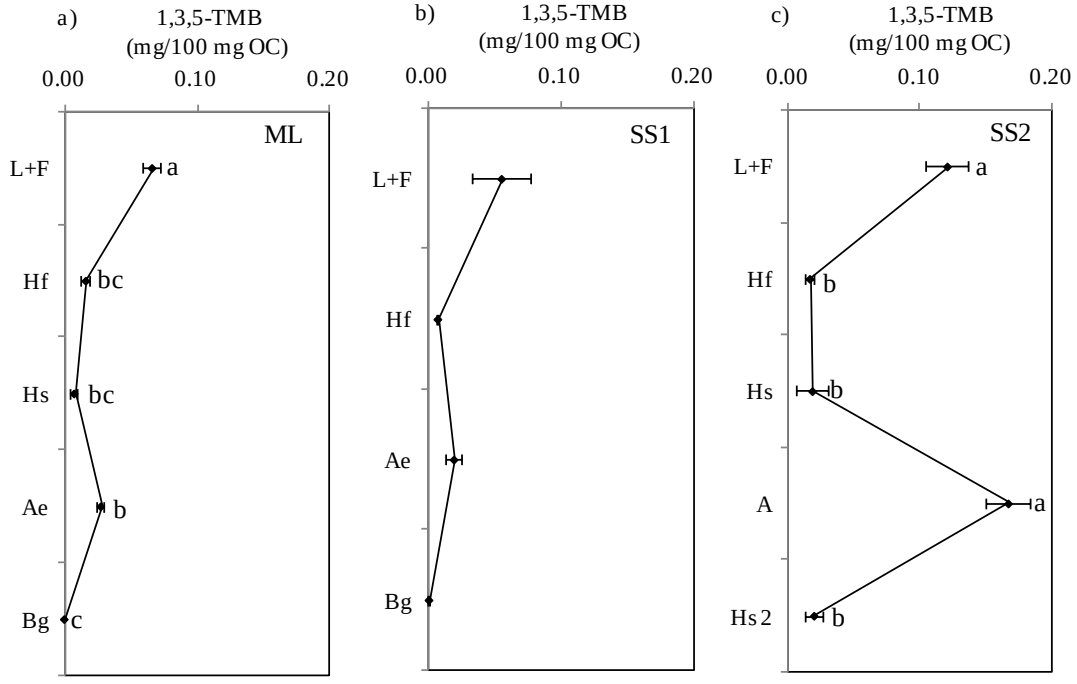

Fig. 3.13: The depth profile showing changes in the 1,3,5-TMB (mg/100 mg OC) in (a) Coalburn ML, (b) Coalburn SS1 and (c) Harwood SS2 soil. The error bars indicate the standard error from three/two analytical replicates. Lettering indicates significant differences from the from Tukey's test.

The ML and SS1 display similar trends of 1,3,5-TMB yield, decreasing with increasing depth. The SS2 profile however displays two maximum concentrations of 1,3,5-TMB; in the litter horizon and the mineral A horizon (Fig. 3.13).

Small increases are observed in the mineral horizons of both the ML and SS1, although they are not significant. The yield of 1,3,5-TMB significantly increases from ML to SS2, with the SS1 similar to both, suggesting that the land cover of Sitka spruce releases more 1,3,5-TMB to the soil which builds up in the litter horizon. The SS roots yielded low quantities of 1,3,5-TMB (0.06 mg/100 mg OC), which could explain the low yield observed in the deeper horizons of SS1 and SS2. Alternatively, this decrease with increasing depth could indicate a rapid loss of CTs in the upper soil profile. As with 1,2,4-TMB and Λ, there is a recovery of 1,3,5-TMB in the A horizon of SS2. 1,2,4-TMB is discussed in further detail in Chapter 7.

3.4 Conclusions

The establishment of Sitka spruce (*Picea sitchensis*) forests on a previous moorland had a significant effect of the soil carbon stocks and phenol contents in these Northumberland peaty gley soils. The depth-related profiles of the lignin phenols and proxies changed after the afforestation of the moorland and again during the second rotation of Sitka spruce.

The establishment of Sitka spruce forests on a moorland habitat led to a decrease in soil carbon during the first rotation but also a net increase of soil carbon during the second rotation, accumulating the soil OC stock to levels above that of the former unplanted moorland. This recovery is, in part, due to the increased bulk density of the soil due to the increased compression caused by the growing trees, coupled with the increasing depth of the ectorganic horizons. The absence of a buried organic horizon at SS1, confirms that the horizon inversion, as identified by the buried Hs horizon, occurred after the clearfelling of the first stand to prepare the land for the second rotation (Mason et al., 2009), and therefore is only observed in SS2. This shows that both Sitka spruce stands experienced land disturbance prior to planting, but displayed very different carbon storage capacities. This is attributed to the initial land-use change including the change of vegetation and the introduction of drainage systems and site preparation for planting that cause increased degradation and loss of OC in the first rotation stand only.

Therefore despite major land disturbance occurring at the SS2 site, large quantities of carbon are able to accumulate.

Progressive decreases in Λ with increasing burial depth were observed across the soil profiles, with the second rotation showing a maximum peak at the mineral horizon which is located above an organic horizon, further evidence of the horizon inversion that occurred prior to planting the second stand. After afforestation, the lignin yield is greatly reduced, however it shows a recovery in the second rotation, increasing to quantities larger than at the ML. The depth-related profiles indicate progressive lignin degradation at the ML, whereas the soil beneath the two Sitka spruce stands record changes in vegetation input, land preparation and land disturbance. The increase of lignin and non-lignin phenols in the overturned mineral A horizon of the second rotation SS suggests that mineral horizons have the potential to store vast quantities of phenols despite low levels of TOC and OC.

The prevailing paradigm has been that drainage of peat will increase carbon losses to the atmosphere. However it appears that the afforestation on peaty gley soils, has the potential to increase carbon storage and stabilise lignin yields, however only once the new vegetation has become established and the soils processes have settled and allowed soil carbon equilibrium and accumulation again (i.e. 80 years). Analysis of self seeded Sitka spruce (Chapter 6) will help further assess the degradation and turnover of lignin with respect to vegetation source, with the absence of land preparation.

It is important to note that soil temperature has not been considered in this study, which will ultimately increase reaction rates within soils. Increased soil temperature can stimulate microbial activity and release carbon from the soil into the atmosphere. Meteorological measurements for the last 20-30 years suggest that there has been an annual increase in soil temperature of 1-2 °C average at 30 cm soil depth, which could have also stimulated a release of organic carbon from topsoil to soil solution (Vanguelova et al., 2010). However, the changes likely to occur due to temperature change will be much smaller than changes expected from land-use change, so it is believed that the change observed in this study are realistic.

Chapter 4:

Sphagnum Biomarkers from a Typical Northern Latitude Peatland: Ryggmossen, Sweden

4 *Sphagnum* Biomarkers from a Typical Northern Latitude Peatland: Ryggmossen, Sweden

4.1 Introduction

In order to understand the processes that occur within soil after the afforestation of peaty soils, it is vital to have a thorough understanding of the processes occurring prior to afforestation; including those that control the stabilisation and release at both the bulk soil organic carbon (SOC) level, and at the molecular level (lignin, non-lignin phenolics and other organic compounds).

The dominant peat forming species, *Sphagnum* mosses, are considered to be important in regulating the environment to their advantage at the expense of other vegetation (Clymo, 1970; van Breemen, 1995). *Sphagnum* mosses are believed to store more carbon in both dead and living biomass, than any other genus of plant (Clymo and Hayward, 1982), despite being completely devoid of lignin phenols (Weng and Chapple, 2010). Instead, *Sphagnum* mosses biosynthesize other phenylpropanoids including *trans*-sphagnum acid (Rasmussen et al., 1995) (Chapter 1, Fig. 1.1). Similar to lignin phenols observed in vascular species, these *Sphagnum* phenolics act both as structural support components and as inhibitors of microbial decomposition of the organic matter (Verhoeven and Liefveld, 1997; Freeman et al., 2001a). The vascular plants associated with peatlands will contribute lignin and other polyphenols to the peat litter, including non-*Sphagnum* mosses (e.g. *Polytrichum commune, Pleurozium schreberi*), heather (*Calluna vulgaris*) and grasses (e.g. *Eriophorum vaginatum, Festuca ovina, and Deschampsia flexuosa*).

The different assemblages of peatland species (Coulson and Butterfield, 1978; Johnson and Damman, 1991; van der Heijden, 1994; van der Heijden and Boon, 1994; Turetsky et al., 2008) have been shown to affect the degree of peat degradation (Yeloff and Mauquoy, 2006). Therefore, there are species-specific rates and degrees of degradation, which can mean that any humification measurements of bulk peat can be misleading (Yeloff and Mauquoy, 2006). As a result, the omission of *Sphagnum* vegetation in many of the global models of ecosystem response to climate change may be erroneous when applied to *Sphagnum*-dominated peatlands (Limpens et al., 2008).

Within peatlands, the phenol oxidase producing microorganisms that degrade lignin phenols are limited, primarily due to the acidic and low molecular oxygen conditions (Freeman et al., 2001b; Thormann et al., 2002). In addition, the activities of other degrading enzymes such as hydrolases (β-glucosidase, phosphatase, sulphatase, xylosidase, and chitinase), which do not normally require molecular oxygen, are also depleted in peatlands (Freeman et al., 2004), providing ideal conditions for phenol and carbon accumulation.

In a study carried out by Williams et al. (1998), the alkaline cupric oxide (CuO) oxidation of 15 species of *Sphagnum* moss released large quantities of unsubstituted *p*-hydroxyl phenolic compounds as well as sphagnum acid, although in minor quantities, in contrast to the large quantities of lignin oxidation products released by 14 species of vascular plants. The analysis of lignin in vascular species with CuO oxidation (Hedges and Parker, 1976; Hedges and Mann, 1979a; Hedges et al., 1982; Kögel, 1986) has shown that lignin phenols with a C3 side chain are lost during the CuO treatment, whereas these side chains are retained when thermally assisted hydrolysis and methylation (THM) in the presence of tetramethylammonium hydroxide (TMAH) is used (Hatcher et al., 1995; Filley et al., 2000). Wysocki et al. (2008) found that CuO oxidation was best suited to lignin-rich, but carbon poor systems, such as marine systems, indicating that CuO oxidation is not best suited for the analysis of *Sphagnum* species and carbon-rich *Sphagnum* peat.

THM in the presence of TMAH, otherwise known as TMAH thermochemolysis, was first introduced as an analytical pyrolysis technique because highly polar pyrolysis products from biopolymers are either difficult or impossible to detect using conventional pyrolysis with combined gas chromatography – mass spectrometry (Py GC-MS) (Challinor, 1989; Kaal and Janssen, 2008). TMAH thermochemolysis has therefore been widely used to characterize substituted phenolic compounds from lignin and tannins in soil organic carbon (e.g. Chapter 3; Mason et al., 2012). In order to make the distinction between lignin, altered lignin and non-lignin phenols including tannins, THM in the presence of ^{13}C-labelled TMAH is used (Filley et al., 1999). This technique has been successfully used to analyse both litter and SOM (Filley et al., 2000; Filley et al., 2002; Filley et al., 2006; Nierop and Filley, 2007; Mason et al., 2012).

The application of flash pyrolysis on peat samples led to the identification of a compound with the $M^{+\cdot}$ (molecular ion) at *m/z* 134, termed 4-isopropenyl phenol (van Smeerdijk and Boon, 1987; van der Heijden et al., 1997). This compound is derived from sphagnum acid, and is considered specific to *Sphagnum* mosses (van Smeerdijk and Boon, 1987; van der Heijden et al., 1997). The single product from the flash pyrolysis of sphagnum acid at 610 °C; 4-isopropenyl phenol reveals complete decarboxylation $[-2CO_2]^+$ of sphagnum acid under elevated temperatures (van der Heijden et al., 1997). Furthermore, van der Heijden et al., (1997) identified six thermochemolysis products of sphagnum acid, including phenolic acids with C3 side chains, during THM treatment of a limited set of *Sphagnum* samples including living *S. fallax*, recent *S. capillifolium* and peatified *Sphagnum* from the Holocene, however no vascular plants were analysed for comparison (van der Heijden et al., 1997).

Several studies have investigated the molecular biomarkers of the *Sphagnum* mosses in peat vegetation (e.g. van der Heijden et al., 1997; McClymont et al., 2011), although none have demonstrated the exclusivity of sphagnum acid to *Sphagnum* species using THM in the presence of TMAH. Considering *Sphagnum* tissue is regarded as recalcitrant due in part to the high content of sphagnum acid and phenolics in the cell walls (Rudolph and Samland, 1985), it is imperative to understand the distinctive biochemistry of *Sphagnum* and its degradation pathways in order to elucidate the dynamics of organic carbon degradation in peat.

McClymont et al. (2011) have recently postulated a proxy for the total input of *Sphagnum* into peat archives using flash pyrolysis, however due to the technique employed, the data available for use in this proxy is rather limited and therefore potentially missing the added detail that comes with TMAH thermochemolysis. For example, the acid and aldehydes lignin sub-units are not observed with pyrolysis, therefore the $[Ad/Al]_{G/S}$ vascular species degradation proxy cannot be utilised alongside the *Sphagnum* proxy. The main advantage of THM is the possibility to analyse the individual sphagnum acid products which could add further detail of the *Sphagnum* litter degradation dynamics due to the natural and TMAH induced decarboxylation (van der Heijden et al., 1997).

In this Chapter, the behaviour of sphagnum acid under unlabelled and ^{13}C-labelled THM conditions is assessed, in order to identify and confirm the presence of the characteristic biomarkers specific to *Sphagnum* mosses as identified by van der Heijden (1994). Second, the THM products from the capitula of peat-forming *Sphagnum* plants from Ryggmossen peatland are investigated, together with typical peat-forming vascular species that will allow an index to be developed that would quantify the proportion of *Sphagnum* phenols in the total phenols measured in the litter and peat samples and thus provide a measure of the botanical composition in the peat cores (Chapter 5). Lastly, a range of peat substrates from Ryggmossen bog will be analysed which will allow the proxy to be tested on the litter and thus provide a measure of the botanical composition across the peat.

Ryggmossen bog, in the boreonemoral zone of central Sweden, is an ideal sample site due to the pristine nature of the peatland, which otherwise has the potential to be particularly sensitive to climate change including changing temperature, precipitation and nitrogen deposition patterns which could result in changes in the dominant plant communities (Gorham, 1991), that could switch the role of peatlands from carbon sinks to carbon sources (Knorr et al., 2005). Over 95% of the total global peatlands are found in the temperate belt of the Northern Hemisphere (Olenin, 1980), therefore this chapter and the following chapter will provide an unprecedented database for inferring the processes of physical and chemical digenesis of peat SOM that is broadly representative of that for a wide class of peatlands in the boreal zone.

4. 2 Overview of Sites and Methods

4.2.1 Sphagnum Acid Standard

An authentic sample of Sphagnum acid was purchased from Exclusive Chemistry Ltd (Russia; 95% purity). The compound was analysed at a ratio of 0.1 mg IS/5 μg TMAH.

4.2.2 Taxon Sampling

Living plant matter and freshly-deposited litter were collected for a range of *Sphagnum* and other species across the micro- and macro-topographic gradients of Ryggmossen (60° 3`N, 17° 20`E; 60 m AOD) by Dr. Lisa Belyea, Dr. Kathryn Allton and Dr. Chris

Laing (Queen Mary, University of London) (Fig. 2.10). The four stages included the bog plateau (BP), bog margin (BM), fen lagg (FL) and swamp forest (SF) (see Table 2.1 for detailed stage descriptions).

Living material was collected from the capitulum (i.e. the cluster of leaves at the top of the plant) of six different *Sphagnum* spp. across the peatland ecotone; *S. angustifolium* (BM, FL), *S. balticum* (BP), *S. fallax* (FL), *S. fuscum* (BP, BM), *S. magellanicum* (BM) and *S. papillosum* (FL). Living material was also collected from two non-*Sphagnum* moss species (*Polytrichum commune* (SF), *Pleurozium schreberi* (FL)), one species of sedge (*Eriophorum vaginatum* (FL)), and several dwarf shrubs (*Andromeda polifolia, Empetrum nigrum, Rhododendron tomentosum*, *Vaccinium microcarpum* (from BM), and *Calluna vulgaris* (from BP)). Nine litter samples (i.e. a section of stem just below the photosynthesising part), all dominated by *Sphagnum*, were also collected; for these samples, an attempt was made to separate out the *Sphagnum*, but small quantities of fungi, vascular plant roots and non-*Sphagnum* bryophytes are likely to be present (*S. angustifolium* from BM and SF; *S. balticum* from BP; *S. fallax* from FL; *S. fuscum* from BP, BM and FL; *S. magellanicum* from BM and; *S. papillosum* from FL). See Chapter 2, Section 2.7.6 for detailed site description.

The freeze-dried plant material (300-500 mg) was extracted by repeated sonication using a mixture of DCM/MeOH (1:1, v/v) by Dr. Aminu Muhammad (Newcastle University) (Chapter 2, Section 2.8). The insoluble residues were then analysed using on-line THM in the presence of either unlabelled or ^{13}C-labelled TMAH. The capitula were analysed in triplicate with unlabelled TMAH. One species; *S. fallax* was also analysed with ^{13}C-labelled TMAH. The non-*Sphagnum* living samples and the *Sphagnum*-dominated litter samples were analysed in duplicate with unlabelled and ^{13}C-labelled TMAH.

4.2.3 THM in the Presence of Unlabelled and ^{13}C-Labelled TMAH

On-line THM in the presence of unlabelled and ^{13}C-labelled TMAH was performed at 610 °C for 10 s (20 °C/ms temperature ramp) using the method set out in Chapter 2 (Section 2.2). The total organic carbon (TOC) contents of the plants and litter, used to normalise yield calculations per 100 mg of organic carbon, were provided by Dr. Greg Cowie (University of Edinburgh, UK) (Hedges and Mann, 1979b; Hedges et al., 1982;

Kögel, 1986). Percent aromatic hydroxyl content was determined with ^{13}C-labelled TMAH using previously established equations and mass spectral methods (Filley et al., 1999; Filley et al., 2006; Mason et al., 2009) (Chapter 2, Section 2.2.1; Appendix A1). Unlabelled TMAH thermochemolysis of samples allowed the structures of products to be identified and determine the appropriate baseline fragment ion ratios needed to accurately calculate % ^{13}C addition when the ^{13}C-labelled TMAH was used.

4. 3 Results and Discussion

4.3.1 THM in the Presence of TMAH of Authentic Sphagnum Acid

Pyrolysis cleaves the bonds of biomacromolecules under elevated temperatures in the absence of oxygen (Chapter 1, Section 1.2.8), however van der Heijden (1997) demonstrated the complete decarboxylation which occurs to sphagnum acid during pyrolysis, which was attributed to its thermal lability. THM employs the additional use of a methylating agent (i.e. TMAH), which permits the cleavage of chemical bonds (including the β-O-4 link in lignin), together with preventing decarboxylation, which lends itself to the analysis of sphagnum acid. A partial trace for the TIC of the thermochemolysis products from sphagnum acid is presented in Fig. 4.1.

The chromatogram contained a mix of partially decarboxylated and methylated sphagnum acid dissociation products including; methylated 4-isopropenylphenol (IUPAC name: 1-methoxy-4-(prop-1-en-2-yl)benzene) (*m/z* 133, <u>148</u>) (**I**), methylated (*E*) and (*Z*)- 3-(4'-hydroxyphen-1-yl)but-2-enoic acid (IUPAC names: (*E*/*Z*)-methyl 3-(4-methoxyphenyl)but-2-enoate) (*m/z* <u>175</u>, 206) (**IIa/b**), as well as methylated 3-(4'-hydroxyphen-1-yl)but-3-enoic acid (IUPAC name: methyl 3-(4-methoxyphenyl)but-3-enoate) (*m/z* 133, <u>148</u>, 206) (**III**) in major quantities (van der Heijden, 1994). Methylated (*E*) and (*Z*)- 2-methyl-3-(4'-hydroxy-phen-1-yl)but-2-enoic acid (**ia/b**) (*m/z* 160, 188, <u>220</u>) and methylated 3-(4'-hydroxyphen-1-yl)pent-3-enoic acid (**ii**) (*m/z* 133, 160, <u>220</u>) were also present in the thermochemolysate in significant amounts (van der Heijden, 1994). The underlined ions represent the base peak. The absence of intact sphagnum acid highlights the thermal instability of the compound. The structures and mass spectra for the sphagnum acid THM products are shown in Fig. 4.2.

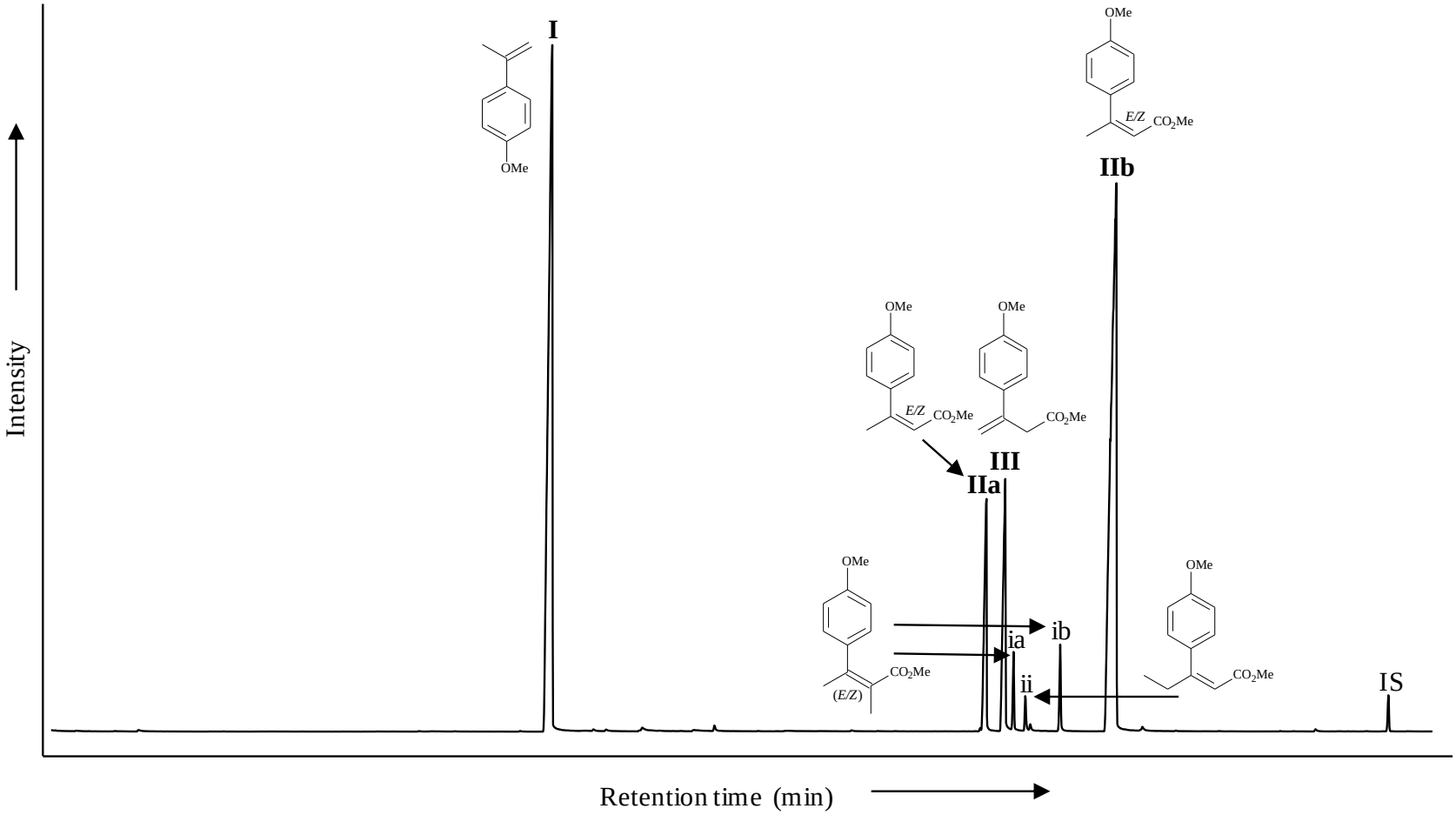

Fig. 4.1: The TIC of the pyrolysed authentic sphagnum acid with unlabelled TMAH. IS denotes internal standard

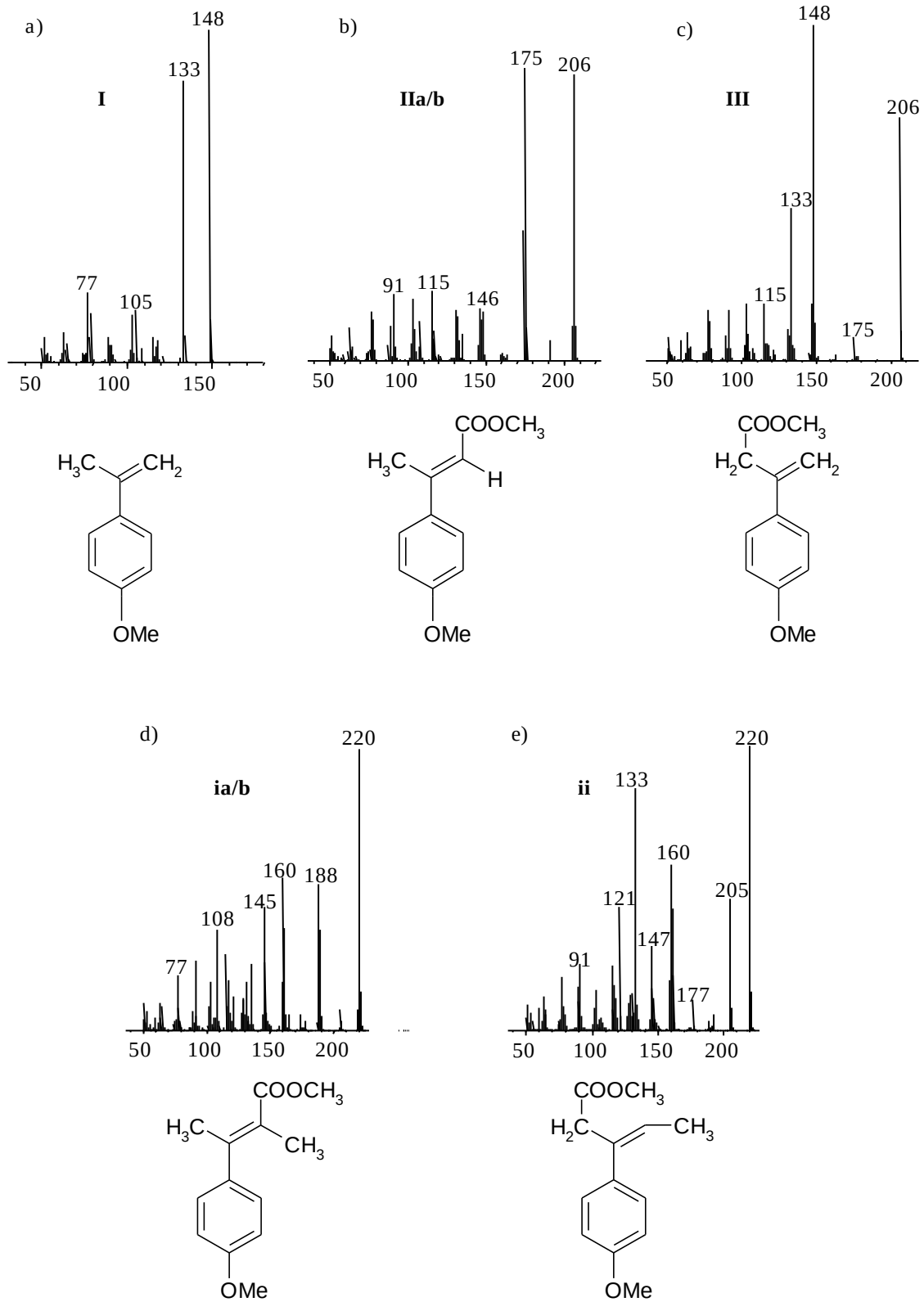

Fig. 4.2: The structure and mass spectra of the sphagnum acid products formed during TMAH treatment: (a) **I;** methylated 4-isopropenylphenol, (b) **IIa** and **IIb;** (*E*) and (*Z*)- methylated 3-(4'-hydroxyphen-1-yl)but-2-enoic acid, (c) **III;** methylated 3-(4'-hydroxyphen-1-yl)but-3-enoic acid, (d) **ia** and **ib;** methylated (*E*) and (*Z*)- 2-methyl-3-(4'-hydroxyphen-1-yl)but-2-enoic acid and (e) **ii;** methylated 3-(4'-hydroxyphen-1-yl)pent-3-enoic acid (van der Heijden, 1994).

4.3.2 THM in the Presence of ^{13}C-TMAH of Authentic Sphagnum Acid

This chapter reports the data from the analyses of *Sphagnum* litter and sphagnum acid with ^{13}C-labelled TMAH, whereby a ^{13}C-labelled methyl group is used as the methylating agent, to test the yield of phenolic groups (i.e. determine the purity of input of the known sphagnum acid products to the TIC).^{13}C-labelled TMAH has been previously used to distinguish between lignin, altered lignin and non-lignin phenolic input (Filley et al., 1999; Filley et al., 2000; Filley, 2003), and will be used for the first time on authentic sphagnum acid.

The five sphagnum acid THM products were identified (Fig. 4.3), however compounds **ia/b** and **ii** were present in low abundances therefore the ^{13}C enrichment equation was performed on the four major peaks only; **I**, **IIa/b** and **III**. Structural mass spectrometry was used to determine ^{13}C-enrichment levels (% ^{13}C) of the individual monomers, using a modification of the equations outlined in Filley et al. 1999 (Eq. 4.1). The ^{13}C-labelled mass spectrum of these dominant products (**I**, **IIa/b** and **III**) are illustrated in Fig. 4.4.

% Hydroxyl (**I**, **IIa/b**, **III**)

$$= 100 \text{ x } \left[\frac{(M_{L+1} - (M_{L+1})_{calc})}{M_L + M_{L+1} - (M_{L+1})_{calc}}\right]$$

Where Eq. 4.1

$$(M_{L+1})_{calc} = M_L \text{ x } \left(\frac{M_{UL+1}}{M_{UL}}\right) \text{ x } \left(\frac{N_L}{N_{UL}}\right)$$

Where M_L is the molecular ion of the mono labelled product, M is the molecular ion of the unlabelled product, and $(M_L+1)_{calc}$ is the calculated intensity of the molecular ion or appropriate fragment ion which is +1 mass unit higher than M_L. The value for $(M_{L+1})_{calc}$ is determined by multiplication of (M_L) by the ratio $(M_{UL+1})/M$ of the same compound obtained from unlabelled TMAH thermochemolysis (Filley et al., 1999). The terms N_L and N_{UL} represent the number of carbon atoms in a labelled product that are not ^{13}C atoms, and the number of carbon atoms in an unlabelled product, respectively.

For example, 4-isopropenyl phenol (**I**) has a M_{UL} of 148 as shown in Fig. 4.2, and a M_L of 149 as shown in Fig 4.4. This shift in one mass unit reflects the contribution of one labelled methoxyl group.

In the ^{13}C-labelled TMAH experiment, the acidic oxygen functional groups on the sphagnum acid products are methylated with the ^{13}C-labelled methyl groups. Therefore, the number of ^{13}C-labelled methyl groups added to the TMAH thermochemolysis reaction products as shown in Fig. 4.4, should be equivalent to the number of acidic oxygen functional groups on the molecule. Figs. 4.2 and 4.4 show the molecular ion for each of the unlabelled and ^{13}C-labelled THM products respectively and the number of ^{13}C-labelled methyl groups added to each compound as determined by GC-MS. The increase in molecular weight upon ^{13}C-TMAH thermochemolysis corresponds to the number of available sites for methylation for all compounds (Appendix A2); one for **I**, and two for **IIa/b** and **III**. Based upon these measurements it is determined that there are no other contributing compounds to the observed peaks, unlike lignin phenols, whereby non-lignin phenols produce the same mass spectra under THM conditions.

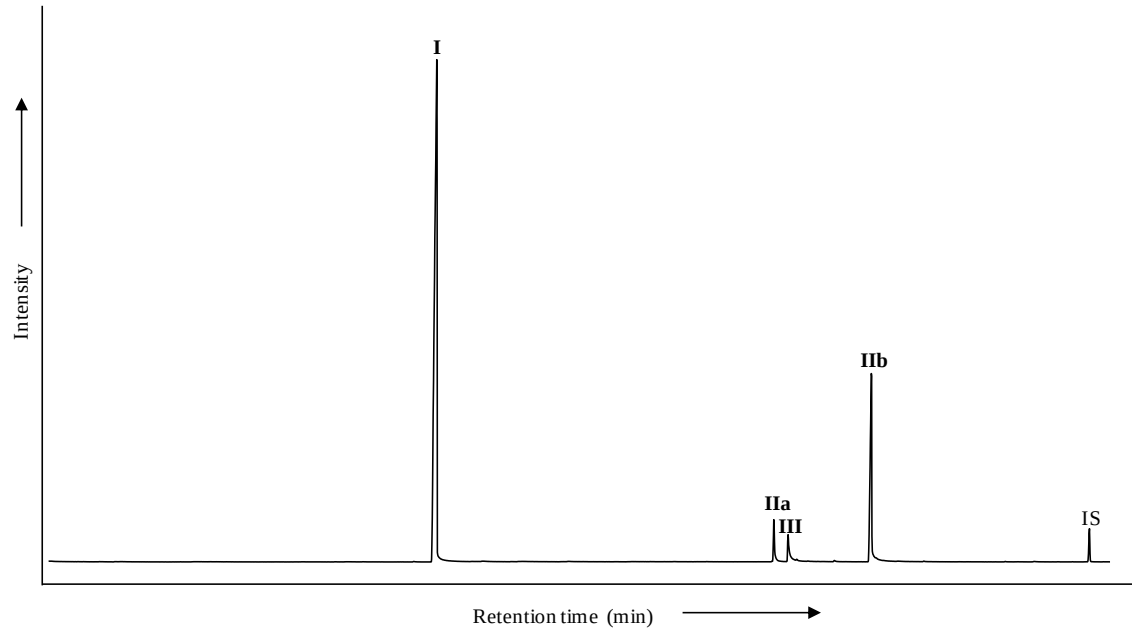

Fig. 4.3: The TIC of the pyrolysed authentic sphagnum acid with ^{13}C-labelled TMAH. IS denotes internal standard.

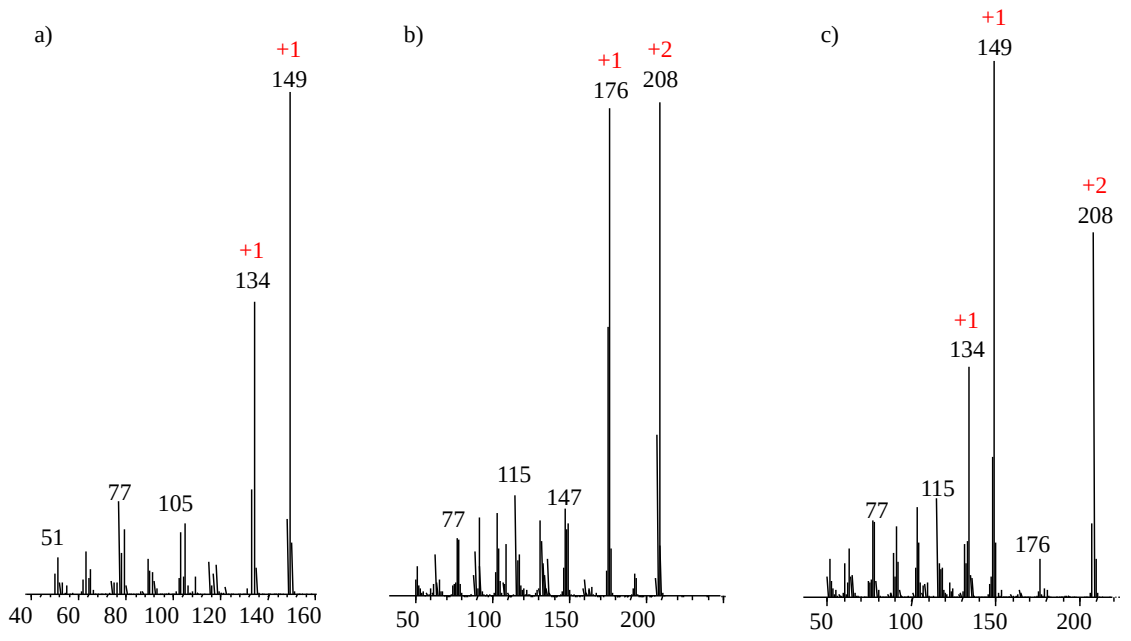

Fig. 4.4: The mass spectra of the dominant sphagnum acid products formed during ^{13}C-TMAH treatment. Numbers in red with a plus prefix reflect the change in M_L from Fig. 4.2.

4.3.3 Sphagnum Acid in Sphagnum capitula

THM in the presence of TMAH of extracted powdered capitulum of *Sphagnum fallax* yielded a range of methylated phenolic and other oxygenated aromatic products (Fig. 4.5) which are consistent with those found by van der Heijden & Boon (1994). The four dominant sphagnum acid pyrolysis products were observed in *S. fallax*; **I**, **IIa/b** and **III** (see Fig. 4.2 for structures). The sphagnum acid THM products **ia/b** and **ii** are not observed in the capitula trace, which could be due to their small abundance as observed in Fig. 4.1.

Together with the sphagnum acid products, there were also large quantities of unsubstituted *p*-hydroxy phenols as first confirmed by Lindberg and Theander (1952), including; methoxybenzene (P1), 4-methoxytoluene (P2), 1-ethyl-4-methoxybenzene, 1-ethenyl-4-methoxybenzene (P3), 4-methoxyacetophenone (P5), and 4-methoxybenzoic acid methyl ester (P6). Compounds 1, 2, 3, 4 and 1,2,4-trimethoxybenzene (1,2,4-TMB) were also identified as major THM products during the thermochemolysis of an authentic standard of cellulose (Chapter 7). The relative abundance of peaks 1-4 and 1,2,4-TMB in Fig. 4.5 reflects significant amounts of cellulose in *S. fallax*. These THM products are discussed in detail in Chapter 7.

There were also smaller amounts of vascular plant-derived phenols produced during the thermochemolysis of *S. fallax*, including the methylated guaiacyl (G) lignin phenols; G1 (1,2-dimethoxybenzene), G4 (3,4-dimethoxybenzaldehyde), G5 (3,4-dimethoxyacetophenone) and G6 (3,4-dimethoxybenzoic acid methyl ester) (Fig. 4.5 and Table 4.1). However, these phenols were not derived solely from undegraded lignin (e.g. Filley et al., 2006; Mason et al., 2009), given that the thermochemolysis of *S. fallax* with ^{13}C-labelled TMAH revealed that only 13.7, 22.0 and 19.2% (± 2.7, 2.3 and 1.6%, respectively, n = 4) of G4, G5 and G6 respectively are sourced from methoxylated phenolic sub-units. Therefore, there are only trace quantities of phenols derived from intact guaiacyl lignin. Guaiacyl and syringyl derivatives that have been detected previously in sub-fossil *Sphagnum* was attributed to contamination from the rootlets of *Ericaceae* (van Smeerdijk and Boon, 1987).

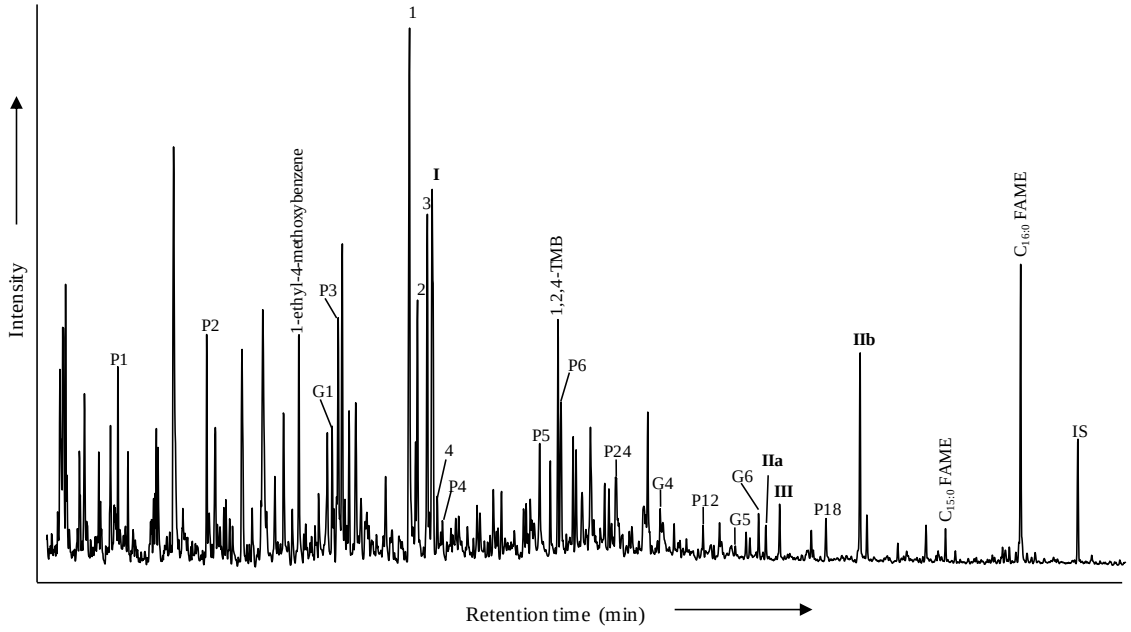

Fig. 4.5: Partial chromatogram for the total ion current (TIC) of the thermochemolysis products from *S. fallax* capitula. Numbers **I**, **IIa/b** and **III** correspond to structures in Fig. 4.2. IS denotes internal standard.

Whilst vascular plants were observed across Ryggmossen bog (see Chapter 5, Table 5.1), *Sphagnum* capitula can be discretely sampled with no physical input from rootlets or other vascular plant tissue. However, it has also been shown that water from the surface of the peatland is used by the living *Sphagnum* (Nichols et al., 2010), where it is held in intercellular spaces known as hyaline cells (Hayward and Clymo, 1982). Given the large water holding capacity of *Sphagnum* species (van Breemen, 1995), coupled with the solubility of vascular plant-derived phenols in water (e.g. Hernes and Benner, 2003) as well as possibly being sourced by root material (van Smeerdijk and Boon, 1987), it is likely that the vascular plant-derived phenols have been mobilized into the *Sphagnum* capitula from dissolved organic carbon (DOC) in the peat water, and have become physically bound and/or protected to the *Sphagnum*, and therefore remain detectable despite the samples undergoing solvent extraction.

Combined THM in the presence of TMAH of the extracted S. *fallax* capitula mixed with the authentic sphagnum acid confirmed the presence of **I** and **IIb**, together with smaller amounts of **IIa** and **III**, in the *Sphagnum*. TMAH thermochemolysis also revealed significant amounts of the sphagnum acid products (**I-III**) in the capitula from harvested specimens of five other species of extant *Sphagnum* (*S. fuscum, S. balticum, S. magellanicum, S. angustifolium,* and *S. papillosum*), which were growing in one or other of the FL, BM and BP stages at the Ryggmossen site (Table 4.1). The four cellulose-derived products (1-4) were also significant thermochemolysis products for all of the *Sphagnum* capitula studied. The average individual yields for **I**, **IIa**, **III** and **IIb** across the eight *Sphagnum* samples were 0.09, 0.02, 0.03 and 0.09 mg/100 mg OC respectively (± 0.01, 0.002, 0.003, 0.01 mg/100 mg OC) (Table 4.1). The relative proportion of the individual phenols to the sum of *Sphagnum* phenols are 39.7, 7.9, 11.1 and 41.3 % (± 2.3, 0.4, 0.4, 2.4%) for **I**, **IIa**, **III** and **IIb** respectively.

The presence of **I** after thermochemolysis indicates a degree of decarboxylation brought on by thermal decomposition, despite the use of TMAH. However, the presence of **II** and **III** indicate incomplete decarboxylation of the sphagnum acid. The formation pathways of **II** and **III** from sphagnum acid as identified by Dallinga et al. (1984) and van der Heijden et al. (1997), involve 1,3-H and 1,5-H shifts and the loss of CO_2 from the sphagnum acid respectively. These elimination steps can be repeated to form **I**, however THM suppresses this second step via transesterification processes, resulting in

Table 4.1. The yield (mg/100 mg OC) of the dominant lignin-phenol products, cellulose derived products (1-4) and sphagnum acid derived products (**I-III**) within the 8 *Sphagnum* capitula samples. Values are an average taken from three replicates, stated to 2 significant figures (s.f.)

Stage	Species	P1	P2	P3	P5	P6	P18	G1	G4	G5	G6	G18	S6	1	2	3	4	**I**	**IIa**	**III**	**IIb**
											(mg/100mg OC)										
BM	*S. angustifolium*	0.033	0.061	0.068	0.027	0.018	0.008	0.020	0.0069	0.0019	0.012	n.d	0.0026	0.11	0.12	0.056	0.031	0.14	0.023	0.033	0.14
BM	*S. fuscum*	0.036	0.071	0.074	0.014	0.031	0.020	0.018	0.013	0.0044	0.026	0.015	0.0040	0.13	0.042	0.031	0.018	0.10	0.016	0.024	0.078
BM	*S. magellanicum*	0.077	0.095	0.11	0.005	0.016	0.024	0.025	0.011	0.0028	0.024	n.d	0.0061	0.12	0.063	0.044	0.019	0.11	0.030	0.031	0.12
BP	*S. balticum*	0.030	0.062	0.050	0.032	n.d	0.011	0.024	0.0049	0.00084	0.013	0.0029	0.0024	0.10	0.069	0.075	0.016	0.042	0.0071	0.013	0.037
BP	*S. fuscum*	0.069	0.13	0.12	0.010	0.014	0.021	0.022	0.021	0.0028	0.044	0.013	0.0045	0.22	0.069	0.072	0.027	0.12	0.022	0.034	0.11
FL	*S. angustifolium*	0.021	0.036	0.050	0.015	0.034	0.013	0.0088	0.0014	0.0011	0.0050	n.d	0.0010	0.089	0.040	0.027	0.020	0.080	0.014	0.023	0.073
FL	*S. papillosum*	0.035	0.076	0.069	0.015	0.044	0.018	0.016	0.0058	0.0017	0.019	0.015	0.0042	0.11	0.06	0.051	0.026	0.080	0.014	0.022	0.080
FL	*S. fallax**	0.061	0.078	0.040	0.010	0.087	0.017	0.080	0.0012	0.00070	0.0033	n.d	n.d	0.18	0.059	0.078	0.044	0.078	0.018	0.024	0.080
	Mean	**0.045**	**0.076**	**0.072**	**0.016**	**0.030**	**0.016**	**0.027**	**0.008**	**0.002**	**0.018**	**0.006**	**0.003**	**0.12**	**0.08**	**0.05**	**0.03**	**0.09**	**0.02**	**0.03**	**0.09**
	SE	**±0.01**	**±0.01**	**±0.01**	**±0.003**	**±0.01**	**±0.002**	**±0.01**	**±0.002**	**±0.0004**	**±0.005**	**±0.003**	**±0.001**	**±0.02**	**±0.01**	**±0.01**	**±0.01**	**±0.01**	**±0.002**	**±0.003**	**±0.01**

n.d = none detected. * ^{13}C-labelled, and therefore the lignin phenols (G 4, G5, G6; S4, S5, S6 and G18) are corrected for non-lignin phenols

the stabilisation of the remaining carboxylic acid methyl esters **II** and **III** (van der Heijden et al., 1997). Therefore, any increase in **I**, beyond that observed in fresh *Sphagnum*-dominated peat, may be assumed to derive from sphagnum acid decarboxylated in situ. Hence, the individual analysis of the four sphagnum acid THM products, rather than the one product from the flash pyrolysis in the absence of TMAH, may be able to reveal the degree of decarboxylation that occurs to the sphagnum acid in the peat. The remainder of this chapter extends this hypothesis to cover vascular species and *Sphagnum* litter to confirm the exclusivity of sphagnum acid pyrolysis products to *Sphagnum* species.

4.3.4 Sphagnum Acid in Non-Sphagnum Plants

Analysis of non-*Sphagnum* species has shown that the four sphagnum acid thermochemolysis products were absent from both the two species of living bryophytes (*Polytrichum commune* and *Pleurozium schreberi*) as well as from six vascular species (*Calluna vulgaris, Andromeda polifolia, Vaccinium microcarpum, Eriophorum vaginatum, , Rhododendron tomentosum and Empetrum nigrum*) (Fig. 4.6).

The phenolic distribution released during THM of the sampled vascular species were dominated by the cinnamyl phenol; P18, and the guaiacyl phenol; G6 (Table 4.2). The non-*Sphagnum* moss species show very specific compound distributions; *Polytrichum commune* is dominated by one compound; G12, 3-(3,4-dimethoxyphenyl)-propanoic acid methyl ester (Fig. 4.6a), whereas *Pleurozium schreberi* is dominated by the guaiacyl ketone (G5) and acid (G6) (Fig. 4.6b). However ^{13}C-TMAH revealed that only 4.7 and 8.5% (± 0.26 and 0.09) of G5 and G6 are sourced from methoxylated phenolic subunits. The high yields of poly-hydroxylated compounds in *Pl. schreberi* most likely originate from non-lignin phenols (Filley et al., 2006) rather than microbially demethylated lignin, due to the fresh nature of the living specimen. However, hydrolysable and condensed tannins are not observed in non-vascular species, therefore these non-lignin phenols display a third source (i.e. phlorotannin, a third type of tannin found in brown algae) (Ragan and Glombitza, 1986). The non-*Sphagnum* mosses display a low lignin yield (Λ) after correction for non-lignin phenols (0.016 and 0.096 mg/100 mg OC; Table 4.2), with *Sphagnum* markers completely absent.

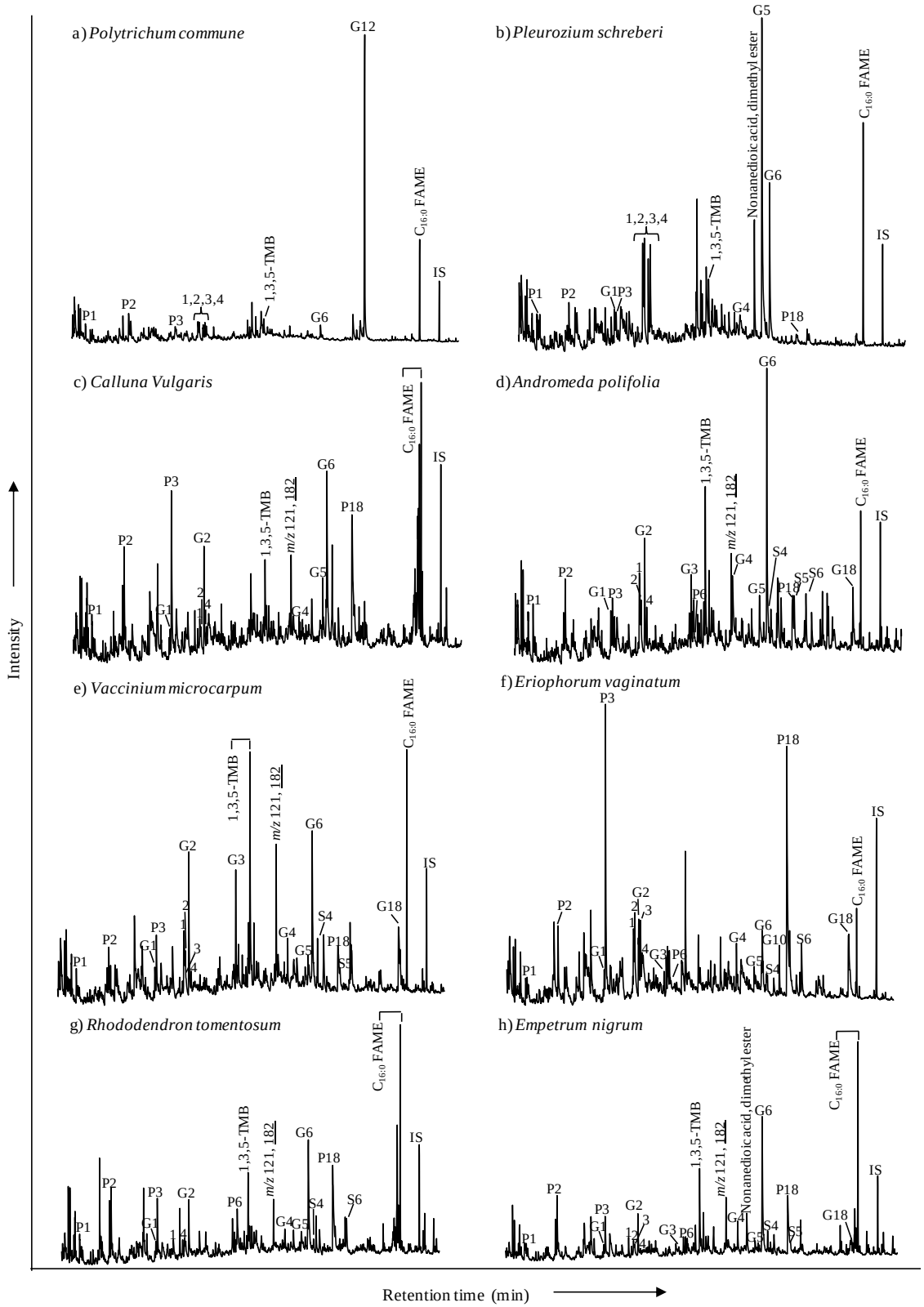

Fig. 4.6: Partial chromatogram for the total ion current (TIC) of the thermochemolysis products from non-*Sphagnum* peat forming plants; (a) *Polytrichum commune*, (b) *Pleurozium schreberi*, (c) *Calluna vulgaris*, (d) *Andromeda polifolia*, (e) *Vaccinium microcarpum*, (f) *Eriophorum vaginatum*, (g) *Rhododendron tometosum*, and (h) *Empetrum nigrum*. IS denotes internal standard.

Table 4.2: The yield (mg/100 mg OC) of the dominant lignin-phenol products, and cellulose derived products (1-4), and the corrected $[Ad/Al]_G$ ratio (uncorrected value in brackets) within the 8 non-*Sphagnum* samples. All samples have been analysed with ^{13}C-labelled TMAH, and therefore are corrected for non-lignin phenols. Yields in brackets state the percent (%) of intact lignin. Yields stated to 2 s.f. (n.d = not detected)

Stage and Species	P1	P2	P3	P6	P18	G1	G2	G3	G4	G5	G6	G12	G18	S4	S5	S6	1	2	3	4	$[Ad/Al]_G$
											mg/100mg OC										
SF Polytrichum commune	0.020	0.061	0.014	n.d	n.d	n.d	n.d	n.d	n.d	n.d	0.016 (16.2)	0.98	n.d	n.d	n.d	n.d	0.044	0.012	0.012	0.010	n.d
FL Pleurozium schreberi	0.028	0.051	0.028	n.d	0.03	0.031	n.d	n.d	0.0077 (21.2)	0.034 (4.7)	0.024 (8.5)	n.d	n.d	n.d	n.d	n.d	0.16	0.089	0.076	0.10	3.09 (7.70)
FL Eriophorum vaginatum	0.019	0.067	0.32	0.015	0.41	0.024	0.018	0.025	0.022 (72.2)	0.012 (60.3)	0.018 (36.1)	n.d	0.13 (87.6)	0.0045 (30.6)	n.d	0.016 (79.2)	0.042	0.043	0.025	0.032	0.83 (1.65)
BP Calluna vulgaris	0.025	0.13	0.29	n.d	0.59	0.032	0.092	n.d	0.0072 (23.6)	0.013 (28.6)	0.028 (8.0)	n.d	n.d	n.d	n.d	n.d	0.030	0.018	n.d	0.022	3.93 (11.6)
BM Rhododendron tomentosum	0.019	0.11	0.11	0.048	0.44	0.045	0.12	n.d	0.031 (48.6)	0.032 (41.7)	0.061 (16.0)	n.d	n.d	0.010 (34.3)	n.d	0.022 (26.5)	0.053	n.d	n.d	0.011	1.96 (5.93)
BM Andromeda polifolia	0.016	0.077	0.048	0.0039	0.12	0.047	0.14	0.034	0.12 (71.8)	0.075 (70.2)	0.083 (28.6)	n.d	0.050 (81.9)	0.021 (42.4)	0.027 (87.2)	0.049 (83.9)	0.094	0.029	n.d	0.029	0.70 (1.75)
BM Empetrum nigrum	0.023	0.14	0.10	0.013	0.37	0.039	0.11	0.037	0.042 (37.3)	0.033 (36.6)	0.098 (17.1)	n.d	0.028 (40.8)	0.0038 (31.3)	0.0063 (80.1)	n.d	0.031	0.014	0.0069	0.012	2.32 (5.06)
BM Vaccinium microcarpum	0.016	0.055	0.065	n.d	0.15	0.034	0.17	0.18	0.042 (47.6)	0.020 (52.3)	0.053 (23.5)	n.d	0.056 (33.8)	0.0031 (18.1)	0.0060 (59.4)	n.d	0.11	0.031	0.015	0.012	1.26 (2.56)

The vascular plants show similar traces to one another with a range of P, S and G-type lignin phenolics and an average corrected lignin yield of 0.55 ± 0.046 mg/100 mg OC. But as with the non-*Sphagnum* mosses, are completely devoid of the *Sphagnum* specific markers (**I**, **IIa**/**b** and **III**). Unlike the *Sphagnum* species, whereby their large water holding capacity has been attributed to the presence of vascular-plant derived phenols in the plant tissue (Section 4.3.3), the vascular species have a much lower water holding capacity. Vascular species have a developed a water transport system consisting primarily of roots and xylem (Boyer, 1985), therefore any soluble sphagnum acid within the DOM will not be held in the vascular tissue, and therefore is not observed in the thermochemolysate of the extracted vascular species.

4.3.5 Sphagnum Parameters

The presence of four sphagnum acid pyrolysis products has been confirmed in all of the dominant Ryggmossen peatland *Sphagnum* species, and are absent in the non-*Sphagnum* species (Sections 4.3.3 and 4.3.4). **I**, **IIa/b** and **III** are therefore putative biomarkers for inputs of *Sphagnum* moss, and these products can be utilised in the same way that lignin phenols are used for vascular vegetation source proxies. Hedges and Parker (1976) proposed a parameter for the total amount of lignin in a sediment (Λ) by summing the concentrations of syringyl and guaiacyl moieties (Hedges and Mann, 1979b). We propose a *Sphagnum* yield represented by sigma (σ) that is equal to the sum of the individual amounts of the *Sphagnum*-derived phenols (**I** + **IIa** + **IIb** + **III**) normalised to 100 mg of organic carbon (OC), Eq. 4.2.

$$\sigma \text{ (mg/100 mg TOC)} = \mathbf{I} + \mathbf{IIa} + \mathbf{IIb} + \mathbf{III} \qquad \text{Eq. 4.2}$$

McClymont et al. (2011) have recently proposed a proxy for the input of *Sphagnum* into peat archives, using a ratio between flash pyrolysis products; 4-isopropenylphenol and two lignin derivatives (2-methoxyphenol and 2,6-methoxyphenol). However, the ratio does not contain all lignin and sphagnum acid sub-units that can be observed after THM, and therefore may not provide information that is as detailed as information obtained from thermochemolysis data.

In order to overcome the differing eluting compounds from pyrolysis and thermochemolysis, the ratio of σ to the sum of itself and the total OC-normalised yield of lignin phenols (Λ = [G4+G5+G6] + [S4+S5+S6] + [P18+G18]), represented as a percentage, will give a measure of the relative contributions of *Sphagnum*- and lignin-derived phenols present in litter or peat. This is termed the *Sphagnum* ratio (SR%).

$$SR\% = [\sigma /(\sigma + \Lambda)]*100 \qquad \text{Eq. 4.3}$$

The *Sphagnum* ratio provides a parameter to assess the relative amounts of *Sphagnum* derived and vascular-plant derived phenols after thermochemolysis, or *Sphagnum* derived and lignin derived phenols after ^{13}C-labelled thermochemolysis.

4.3.6 Sphagnum Markers in Ryggmossen Peat Litter

The major compounds in the thermochemolysate of the litter sample dominated by *S. fallax* are consistent with the products derived from the *S. fallax* capitula; P1, P2, 1-ethyl-4-methoxybenzene (P3), **I**, **IIb** and the cellulose derived products (1-4 and 1,2,4-TMB) (Fig. 4.7 and Table 4.3).

The presence of the four dominant *Sphagnum* markers was observed in all the *Sphagnum* litter species with an average σ yield of 0.70 ± 0.08 mg/100 mg OC. The average individual yields for **I**, **IIa**, **III** and **IIb** across the nine *Sphagnum* litter samples were 0.26, 0.06, 0.08 and 0.30 mg/100 mg OC respectively (± 0.03, 0.01, 0.012, 0.04), with a relative percent contribution to the total yield of 37.0, 8.8, 11.6 and 42.6 % (± 2.2, 0.4, 0.6, 1.6%) for **I**, **IIa**, **III** and **IIb** respectively (Table 4.3).

Sphagnum-dominated litter also yielded small amounts of lignin sourced phenols which are attributed to both to the large water-holding capacity in the living *Sphagnum* as well as the possibility of macromolecular organic carbon input from vascular plant material (van Smeerdijk and Boon, 1987). Thermochemolysis with ^{13}C-labelled TMAH of the *Sphagnum* dominated litter from all of the species shown in Table 4.3 revealed that on average only 17.3, 24.5 and 22.5% (± 2.0, 2.2 and 2.7% respectively from 4 analytical replicates from each species) of G4, G5 and G6 respectively are composed of intact lignin phenols. This correction for non-lignin phenols indicated that the guaiacyl lignin phenols released from all of the *Sphagnum* dominated litter samples were present only

in trace amounts and G18 was absent in all but two litter-types (*S. fuscum*, BM and FL; *S. fallax*, FL) where it is present in only trace amounts (Table 4.3). Phenols from intact syringyl lignin were absent in all but two of the litter samples (*S. magellanicum* and *S. fuscum*; both BM) and in these exceptions the only component detected was S6 which was also only present in trace amounts (Table 4.3). Following the correction for the contribution of non-lignin phenols and altered lignin phenols, it was found that the averaged Λ for the *Sphagnum* dominated litter is 0.12 mg/100 mg OC compared to a σ of 0.70 mg/100 mg OC (± 0.12 and 0.08, respectively), resulting in an average SR of 85% (± 1.1%;Table 4.3).

The percent of sphagnum acid products relative to vascular phenolics ranges from 80-88% across the peatland litter (Table 4.3). This is consistent with the concept of *Sphagnum* mosses as engineering species, therefore dominating the litter biomass (van Breemen, 1995), with the peatlands also often inhabited to a small degree by different species of heathers, non-*Sphagnum* mosses and other vascular species, which will contribute lignin phenols to the bulk peat (e.g. Fig. 4.6) (van Smeerdijk and Boon, 1987; Turetsky, 2003).

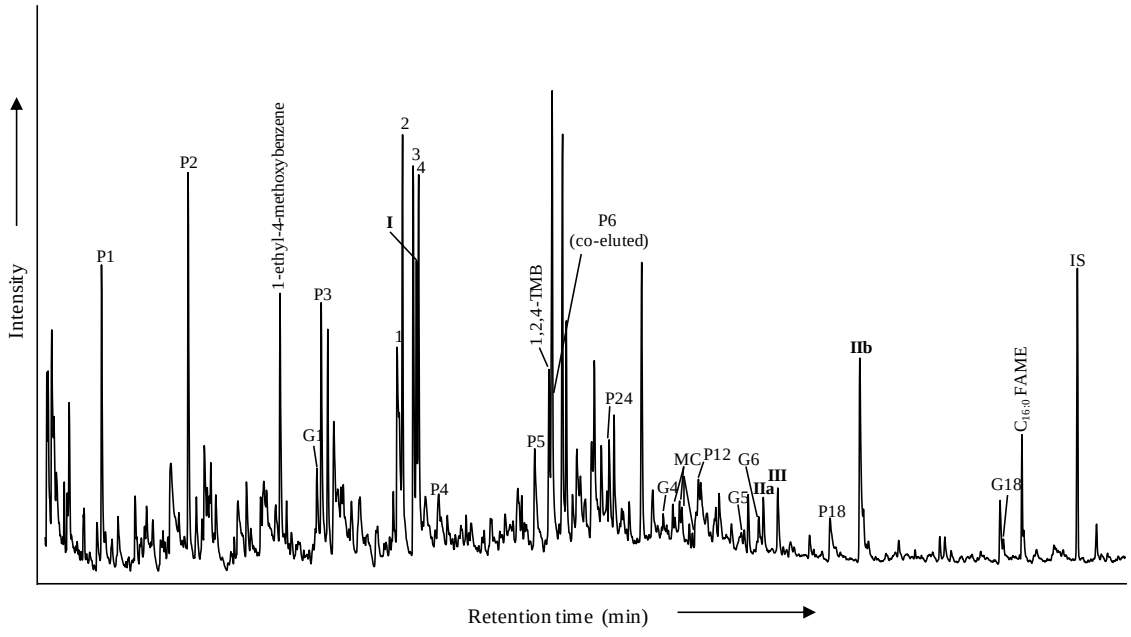

Fig. 4.7: Partial chromatogram for the total ion current (TIC) of the thermochemolysis products from *S. fallax* litter. Numbers **I**, **IIa**/**b** and **III** correspond to structures in Fig. 4.2. IS denotes internal standard.

Table 4.3: The yield (mg/100 mg OC) of (a) the dominant *p*-hydroxy lignin-phenol products, (b) G, S and C lignin-phenol products and corrected $[Ad/Al]_G$ ratio (uncorrected value in brackets), and (c) cellulose derived products (1-4) and sphagnum acid derived products (**I-III**), together with the newly proposed SR% in the nine *Sphagnum* litter samples.

a) Stage	Species	P1	P2	P3	P4	P5	P6	P12	P24
		mg/100 mg OC							
SF	*S. angustifolium*	0.20	0.18	0.12	0.079	0.047	0.040	0.023	0.044
FL	*S. fuscum*	0.18	0.19	0.13	0.053	0.051	0.034	0.034	0.052
FL	*S. fallax*	0.15	0.24	0.17	0.032	0.092	0.067	0.025	0.047
FL	*S. papillosum*	0.26	0.21	0.14	0.033	0.063	0.077	0.028	0.044
BP	*S. fuscum*	0.26	0.24	0.19	0.022	0.038	0.058	0.014	0.023
BP	*S. balticum*	0.26	0.21	0.16	0.021	0.043	0.064	0.014	0.023
BM	*S. magellanicum*	0.22	0.20	0.17	0.019	0.023	0.021	0.013	0.015
BM	*S. angustifolium*	0.23	0.26	0.20	0.029	0.038	0.040	0.018	0.030
BM	*S. fuscum*	0.27	0.23	0.19	0.025	0.019	0.062	0.016	0.026

b) Stage	Species	G1	G4	G5	G6	G18	P18	S6	$[Ad/Al]_G$
		mg/100 mg OC							
SF	*S. angustifolium*	0.044	0.021	0.0061	0.024	n.d	0.12	n.d	1.14 (0.70)
FL	*S. fuscum*	0.038	0.020	0.0062	0.023	0.0039	0.10	n.d	1.17 (0.52)
FL	*S. fallax*	0.057	0.0030	0.0022	0.0076	0.0086	0.064	n.d	2.53 (2.00)
FL	*S. papillosum*	0.034	0.0057	0.0035	0.012	n.d	0.091	n.d	2.05 (1.37)
BP	*S. fuscum*	0.042	0.0085	0.0052	0.012	n.d	0.10	n.d	1.45 (1.15)
BP	*S. balticum*	0.035	0.0032	0.0020	0.0071	n.d	0.070	n.d	2.22 (1.89)
BM	*S. magellanicum*	0.056	0.014	0.0028	0.018	n.d	0.087	0.0013	1.33 (1.68)
BM	*S. angustifolium*	0.066	0.015	0.0057	0.028	n.d	0.12	n.d	1.82 (1.11)
BM	*S. fuscum*	0.062	0.0028	0.0015	0.013	0.00093	0.085	0.00047	4.59 (2.44)

c) Stage	Species	1	2	3	4	**I**	**IIa**	**III**	**IIb**	**SR%**
		mg/100 mg OC								
SF	*S. angustifolium*	0.15	0.022	0.065	0.029	0.40	0.10	0.14	0.48	87
FL	*S. fuscum*	0.24	0.083	0.12	0.056	0.27	0.035	0.044	0.16	77
FL	*S. fallax*	0.17	0.19	0.21	0.14	0.12	0.034	0.050	0.19	84
FL	*S. papillosum*	0.10	0.091	0.085	0.078	0.18	0.049	0.064	0.26	83
BP	*S. fuscum*	0.063	0.048	0.047	0.029	0.24	0.067	0.076	0.31	85
BP	*S. balticum*	0.090	0.11	0.080	0.068	0.20	0.045	0.073	0.21	87
BM	*S. magellanicum*	0.085	0.075	0.074	0.044	0.28	0.061	0.072	0.33	86
BM	*S. angustifolium*	0.22	0.13	0.12	0.068	0.37	0.12	0.15	0.46	87
BM	*S. fuscum*	0.063	0.031	0.037	0.025	0.26	0.061	0.074	0.30	87

All eight non-*Sphagnum* species display a higher proportion of intact G4 relative to G6, this is due to the increased input of non-lignin acids (i.e. protocatechuic acid) (Table 4.2). The *Sphagnum* samples however display the opposite trend, with the proportion of intact G6 elevated with respect to G4 (Table 4.3). As a result, after correction for non-lignin phenols, the $[Ad/Al]_G$ ratio for *Sphagnum* litter samples displays an increase from an average of 1.43 ± 0.21 across the nine samples to 2.03 ± 0.36 (Table 4.3). Opposite to the *Sphagnum* trend, the $[Ad/Al]_G$ ratio is decreased for the vascular plants after correction from 5.17 ± 1.37 to 2.01 ± 0.45, which is the usual trend seen after the use of ^{13}C-TMAH (Mason et al., 2009) (Table 4.2).

Many studies have displayed elevated [Ad/Al] ratios in DOM relative to the POM, particularly in riverine case studies (Ertel et al., 1986), however Hernes et al. (2007) suggested the elevated [Ad/Al] ratio was due to the preferential transfer of acidic phenols from the process of leaching from the POM into the DOM, i.e. lignin fractionation. There appears to be minimal fractionation of the intact lignin phenols (G6 and G4) mobilized into the *Sphagnum*, as after correction for non-lignin phenols, the $[Ad/Al]_G$ ratio for both the *Sphagnum* litter and vascular species produces a similar value of 2.0. This oxidation ratio value represents the oxidation state of the vascular phenols, whereby the vascular species and assumed vascular phenols within the *Sphagnum* would be alike. Therefore it appears that the fractionation of OM during leaching and sorption is not unique to lignin. In fact, it suggests that the fractionation is occurring predominantly in the non-lignin phenols that are quantified prior to the correction applied by ^{13}C-labelled TMAH. It appears that the non-lignin acid phenols are preferentially removed from the POM and solubilised in the DOM, which are subsequently mobilized into the *Sphagnum*, resulting in elevated levels of these non-lignin acids within the *Sphagnum*.

4.4 Conclusions

Methylated 4-isopropenylphenol (**I**), methylated (*E*) and (*Z*)- 3-(4'-hydroxyphen-1-yl)but-2-enoic acid (**II a/b**), and methylated 3-(4'-hydroxyphen-1-yl)but-3-enoic acid (**III**) (van der Heijden et al., 1997) are confirmed as TMAH thermochemolysis products of sphagnum acid and also as being specific to *Sphagnum* mosses. The ^{13}C-labelled TMAH thermochemolysis products of the sphagnum acid demonstrated that the four

products are derived entirely from the sphagnum acid discounting the possibility of any other source of these compounds. The identification of the sphagnum acid pyrolysis products in a range of *Sphagnum* species has confirmed the presence of sphagnum acid in *Sphagnum* species.

Two proxies have been suggested to assess the relative amounts of *Sphagnum* derived and vascular-plant derived phenols after thermochemolysis. The parameter σ is defined as the total amount of these four molecules normalised to 100 mg of TOC; (σ = [**I**] + [**IIa**] + [**III**] + [**IIb**]). The ratio of σ to Λ gives an index (SR%) that provides a measure of the relative amount of sphagnum acid to the vascular plant phenols in peat moss.

The presence of **I** after thermochemolysis indicates a degree of decarboxylation brought on by thermal decomposition, despite the use of the methylating agent; TMAH. However the presence of **II** and **III** indicate incomplete decarboxylation of the intact sphagnum acid. Thermochemolysis limits the further breakdown of **II** and **III** into **I**, therefore, in fresh *Sphagnum* litter, the presence of **I** reflects the complete decarboxylation of the sphagnum acid due to thermal decomposition. However, in more mature samples, any increase in **I**, beyond that observed in fresh peat, may be assumed to derive from sphagnum acid decarboxylated in situ. Whereby the degraded sphagnum acid remains bound to the cell wall as isopropenyl phenol, and remains amenable to THM. The individual analysis of the four sphagnum acid THM products, rather than the one product from the flash pyrolysis in the absence of TMAH, may be able to reveal the degree of decarboxylation that occurs to the sphagnum acid in the peat. This is investigated in more detail in the peat core study described in Chapter 5.

The lignin phenols present in the *Sphagnum*-dominated litter are attributed to the large water-holding capacity in the living *Sphagnum*, whereby lignin phenols in the DOM become entrapped in the *Sphagnum*. The fractionation of the vascular (lignin and non-lignin) phenols during leaching and subsequent sorption into the *Sphagnum* may explain the opposite shift in the $[Ad/Al]_G$ for *Sphagnum* after correction for non-lignin phenols compared to what is normally observed for non-*Sphagnum* litter. The corrected results suggest minimal fractionation of the intact lignin phenols between the vascular species and the entrapped lignin phenols within *Sphagnum*, resulting in similar corrected $[Ad/Al]_G$ values between the vascular and *Sphagnum* species. However, it would appear that the non-lignin acid phenols are preferentially removed from the POM (i.e. vascular

plant material) and solubilised in the DOM, which are subsequently mobilized into the *Sphagnum*, resulting in elevated levels of these non-lignin acids within the *Sphagnum*. These results highlight the need for further research in to the mechanisms involved during phenol fractionation, and the effect this will inevitably have on the traditional lignin proxies.

Chapter 5:

Geochemical Records of *Sphagnum* Peat Cores Spanning the Range of Environmental Conditions from Ryggmossen

5 Geochemical Records of *Sphagnum* Peat Cores Spanning the Range of Environmental Conditions from Ryggmossen

5.1 Introduction

Northern peatlands cover an area of around 4 x 10^6 km^2, and currently store around 547 Gt of organic carbon as waterlogged peat (Yu et al., 2010), amounting to over one-third of global soil organic carbon (Gorham, 1991). Northern peatlands represent the greatest concentration of stored carbon in terrestrial ecosystems (Gorham, 1991), however this pool could become a carbon source under future land-use change and/or climate change (Belyea, 2009). The dominant controls on carbon cycles are often the plant communities, the temperature and precipitation regimes, the water table and the soil chemistry (Holden et al., 2007), which are likely to have complex and non-linear effects on peatland carbon cycling (Davidson and Janssens, 2006; Belyea, 2009).

Water level is a key control on carbon sequestration because it determines the exposure of near-surface, unsaturated peat to rapid aerobic decomposition and, conversely, the stabilisation of deeper, permanently saturated peat (Zaccone et al., 2008). Water level also influences vegetation distribution, which in turn affects both the decomposition rate and biogeochemistry of plant litter inputs. The close association between water level and vegetation is evident along gradients at two distinct spatial scales; micro-topographic microforms at a scale of 1-10 m (i.e. hummocks and hollows) and macro-topographic stages at a scale of 10-1000 m (i.e. bog plateau, BP; bog margin, BM; fen lagg, FL; swamp forest, SF) (Bridgham et al., 1996; Okland et al., 2001). Furthermore, individual *Sphagnum* species inhabit different peat habitats, for example, *S. fuscum* is most suited to hummock habitats, whereas *S. cuspidatum* and *S. angustifolium* are more suited to hollows (Rochefort et al., 1990; Johnson and Damman, 1991). If climate change leads to shifts in the composition and relative abundance of microforms (i.e. hummocks and hollows) and/or shifts in the boundaries between macrotopographic stages (i.e. bog plateau, bog margin, fen lagg and swamp forest), rates of carbon sequestration will change (Belyea 2009). Indeed from experimental warming in a *Sphagnum*-dominated mire in France we can infer that spatial variability of moisture is critical to the deeper understanding of the effects of a changing climate on the fate of organic matter in northern peatlands (Delarue et al., 2011).

The dominant peat-forming moss, *Sphagnum*, outcompetes vascular plants by creating acidic, nutrient-poor and water-saturated conditions (van Breemen, 1995). Vascular plants associated with peatlands contribute lignin and polyphenols including tannins, whereas *Sphagnum* moss contribute phenylpropanoids including *trans*-sphagnum acid (Rasmussen et al., 1995) (see Chapter 4). *Sphagnum* tissue is regarded as extremely recalcitrant due to the high content of sphagnum acid in the cell walls (Rudolph and Samland, 1985), however in a recent carbon mineralisation study, Hájek et al. (2011) have suggested that the cell-wall polysaccharides are the dominant *Sphagnum* decay-inhibitors, with the polysaccharides displaying decay-inhibiting properties traditionally associated with lignin phenols. Therefore it is imperative to understand the distinctive biochemistry of *Sphagnum* and its degradation pathways in order to elucidate the dynamics of organic carbon degradation in peat. This is important because this could help further improve the resolution of process-based simulations (e.g. Ise et al., 2008) that model the decomposition of peat with changing climate.

Thermally assisted hydrolysis and methylation (THM) in the presence of tetramethylammonium hydroxide (TMAH), has frequently been used to characterise lignin in soil organic carbon (e.g. Nierop and Filley, 2007), but has also shown the ability to characterise sphagnum acid within peat archives (van der Heijden, 1994; van der Heijden et al., 1997). So far, however, this method has received little discussion as a tool to analyse *Sphagnum* and peat samples alongside the traditional soil thermochemolysates, i.e. lignin.

In this study, we attempted to address this gap in the research using several indicators of organic matter decomposition (i.e. C/N ratios of organic matter, and the content of stable ^{13}C and ^{15}N isotopes in the peat) coupled with the molecular characterisation of the peat archives. Stable carbon isotope compositions and C, N abundances, have been commonly used as indicators for the degree of decomposition of peat, as these indicators gradually evolve during degradation as different biochemical constituents are preferentially consumed, produced or sequestered (Malmer and Holm, 1984; Benner et al., 1987; Novák et al., 1999). However, changes in the vegetation, microhabitat or climate can affect the signals from these proxies, therefore their interpretation with respect to decomposition may not be straightforward when used independently (Broder et al., 2011).

Polysaccharides represent the main form of photosynthetically assimilated carbon in the biosphere and have also been quantified due to their major contribution to terrestrial vegetation including *Sphagnum* mosses (Jones et al., 1994; Jia et al., 2008). Although a potentially powerful tool for elucidating the sources, process and diagenetic pathways of biologically important organic materials in peatland environments, polysaccharides have rarely been utilised in the past (Comont et al., 2006). Recently however, several polysaccharide indicators and proxies have been proposed for the reconstruction of past peatland vegetation. Comont et al. (2006) illustrated the use of individual sugars as specific peatland vegetation source indicators; xylose and arabinose indicated sedges including *Eriophorum*; rhamnose, galactose and mannose indicated mosses; and ribose (and to a lesser extent, hemicellulosic glucose) was identified as a possible indicator for microbial synthesis.

The aim of this chapter was thus to elucidate organic matter decomposition patterns across a typical pristine peatland using a combination of decomposition indices and biomarkers as outlined above. Eight cores of near-surface peat from locations spanning the micro- and macro-topographic gradients of a raised bog in the boreonemoral zone of central Sweden, Ryggmossen peatland, have been selected for analysis. By targeting hummocks and hollows in four macrotopographic stages (BP, BM, FL and SF), we ensured that our analyses covered a range of plant type sources and contrasting hydrological and chemical conditions.

The specific objectives were (i) to characterize the geochemical profile of each core; and (ii) to analyse down-core changes in THM product composition, in particular to apply the *Sphagnum* proxies; σ and SR%, as introduced in Chapter 4, to test for persistence of the *Sphagnum* markers and to infer their extent of degradation relative to vascular plant-derived phenols as a function of distance from the water table.

5.2 Overview of Methods and Sites

5.2.1 Study Site

Eight peat cores were collected from Ryggmossen, a raised bog in the boreonemoral zone of central Sweden (60° 3’N, 17° 20’E; 60 m AOD) by Dr. Lisa Belyea, Dr. Kathryn Allton and Dr. Chris Laing (Queen Mary, University of London).

Proceeding from the centre to the edge, the macrotopographic gradient comprises four stages: the bog plateau (BP), the bog margin (BM), the fen lagg (FL), and the swamp forest (SF). A detailed site description for Ryggmossen is presented in Chapter 2, Section 2.7.6.

5.2.2 Sample Collection and Preparation

The eight peat cores were taken from both the hollow and hummock microforms in each of the four stages, providing a total of eight cores spanning the range of environmental conditions along the BP–to–SF gradient at Ryggmossen. Ground vegetation was analysed at each coring site by Dr. Kathryn Allton. Freeze-dried core material was extracted as described in Chapter 2, Section 2.8. A sample of the residue was then analysed using on-line THM in the presence of TMAH.

Bulk density measurements were analysed by Dr. Lisa Belyea and Dr. Chris Laing. Owing to the number of samples, the BP samples were analysed in duplicate, whilst the BM, FL and SF samples were analysed once only (Chapter 2, Section 2.7.6). Therefore the OC standard error can only be calculated for the BP site only. The organic carbon stock has been calculated using the bulk density values and the TOC values using equation 2.2 (Chapter 2, Section 2.6).

5.2.3 Water Table and Temperature Dynamics

Water table fluctuations and temperature (°C) at each coring station were monitored at hourly intervals for one year prior to core extraction, using self-logging pressure transducers (Solinst Leveloggers), set up by Dr. Lisa Belyea and Dr. Kathryn Allton (Fig. 5.1). The data were summarised by calculating the annual mean, minimum and maximum water table depths by Dr. Greg Cowie. The data were interpolated at the jumps observed at FL2, BM1 and BM2, so that the record was relative to the same datum. Over the course of measurement (Sept 2007 - Sept 2008), the annual temperature at Ryggmossen ranged from 0.2 °C in the winter to 19.6 °C in the summer, with an annual average temperature across the peatland of 6.5 °C. Temperatures throughout the winter are similar at both the hummock and the hollow cores at the BP, BM and FL.

Deviations occur in the summer months, whereby the hollow cores in the BP and BM display higher temperatures (0.7 and 1.0 °C. respectively). The SF hummock displays a smaller annual variation compared to the hollow core, reflected in the warmer temperatures in the winter and cooler temperatures in the winter with respect to the hollow. The observed thermal regime across Ryggmossen bog will not only be influenced by the ecology of the species present but is also a result of the microtopography formed by the same species, creating a feedback (van der Molen and Wijmstra, 1994). Therefore any change in the vegetation cover could ultimately alter the microclimate at that site.

The Ryggmossen water table depths at all core locations were positively skewed (i.e. a short distance from the surface of peat) throughout most of the year, and fell deeper (i.e. a large distance from the surface of peat) only during summer dry periods (June/July) (Fig. 5.1). In addition, there are short-term fluctuations in the water table due to rain showers (Kettunen et al., 1999). This pattern is observed frequently in peatlands, and indicates self-regulating behaviour that arises from depth-dependent changes in hydraulic properties (Belyea, 2009).

The water table level fluctuates *ca* 18 cm in the BM, whereas larger fluctuations of up to 44 cm are observed across the BP, FL and SF. The mean water table (mwt) depths are consistently lower from the peat surface in the hummock cores compared to the hollow cores, with an average difference of 15 cm. As the water table rises during wet periods, water is stored and/or discharged rapidly through porous peat; as the water table falls into denser peat during dry periods, discharge occurs more slowly (due to lower hydraulic conductivity) and a unit loss of water has a smaller effect on water table position (due to the lower specific yield).

As a consequence, the water table tends to be maintained within a narrow range of peat depths, as observed for the BM. Reducing and ultimately anoxic conditions develop in water-saturated peat, because oxygen consumed by aerobic microorganisms is replenished very slowly by diffusion (Clymo, 1983; Haraguchi, 1991). Hence, oxic conditions are expected to dominate in the unsaturated layer (i.e. acrotelm); anoxic conditions to predominate in the permanently saturated layer (i.e. catotelm) and; alternating oxic/anoxic conditions to occur during drainage and recharge of the seasonally-saturated layer (i.e. mesotelm) (Clymo and Bryant, 2008).

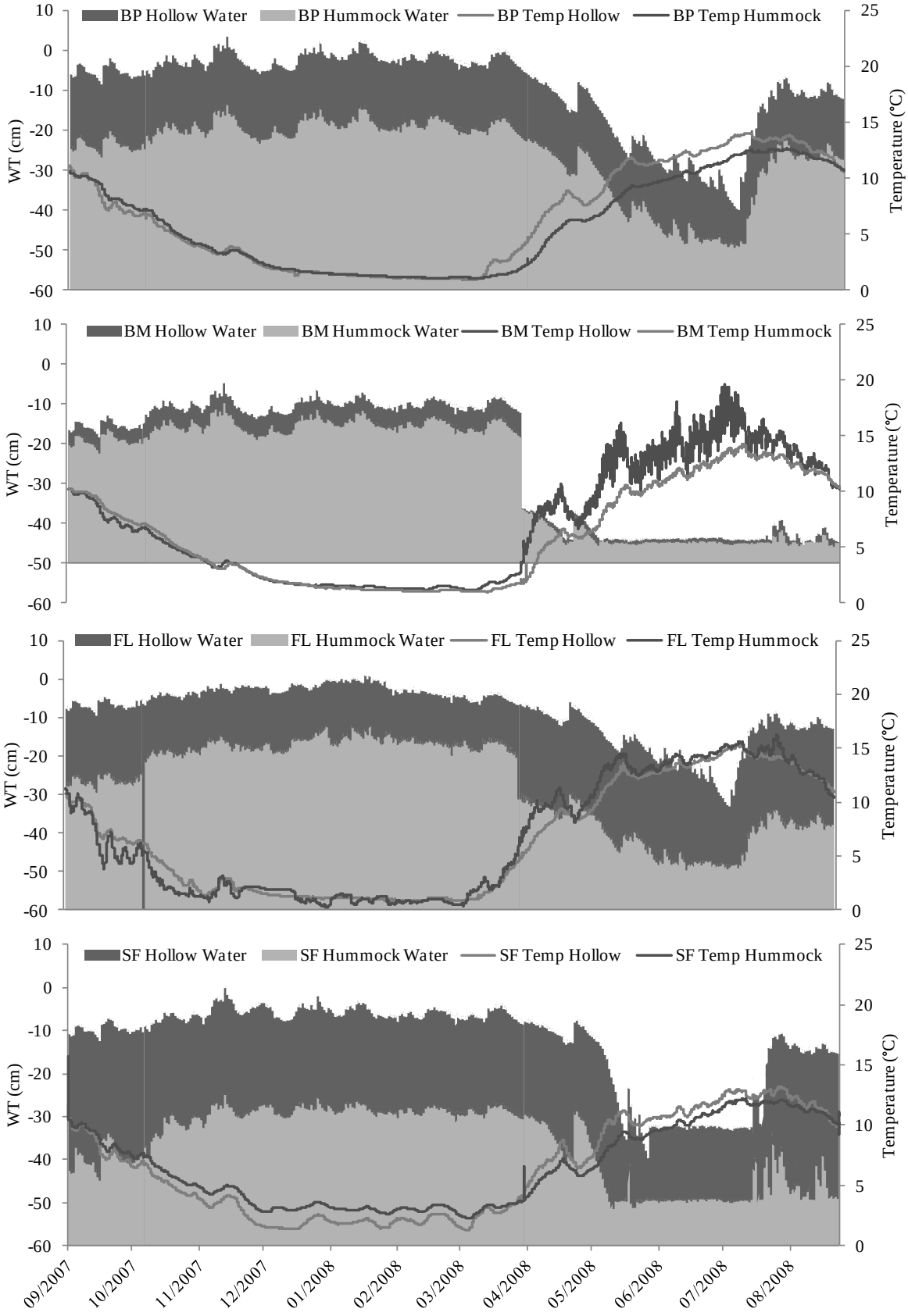

Fig. 5.1: The water table (WT) fluctuation and temperature changes across one year (mm/yyyy) at Ryggmossen bog (a) BP, (b) BM, (c) FL, and (d) SF. WT relative to peat surface. Loggers for FL2, BM1 and BM2 show a suspicious jump in levels on 23 April 2008, which corresponds to a site visit. Loggers for BM have been positioned too high for the lowest water levels.

5.2.4 THM in the Presence of TMAH

On-line THM in the presence of unlabelled TMAH was performed using a shorter GC oven programme than was used in the rest of the thesis, although THM was carried out at 610 ℃ for 10 s, consistent with the other chapters. The GC oven programme began at 40 ℃ where it was held for 4 minutes, then the temperature was increased from 40 ℃ to 90 ℃ at a rate of 4 ℃ /min, then at 2 ℃/min to 150 ℃ and finally at 4.5 ℃/min to 320 ℃ where it was held for 6 minutes.

5.2.5 Carbohydrate and Elemental Analyses

The carbohydrates were analysed by the method of Cowie and Hedges (1984) by GC-flame ionization detector (FID) of trimethylsilane (TMS) derivatives. Total organic carbon (TOC) and total organic nitrogen (TON) were determined, along with stable isotopic compositions ($\delta^{13}C$ and $\delta^{15}N$), by elemental analyzer-isotopic ratio mass spectrometer (EA-IRMS) following HCl vapour treatment to remove any inorganic residue. Acetanilide was used as calibration standard for elemental composition. Stable isotopic signatures were calibrated on the basis of air (N_2) and a suite of in-house standards.

Carbohydrate and elemental analyses were carried out by Dr. Greg Cowie (University of Edinburgh, UK).

5.2.6 Sphagnum Proxies

Sphagnum proxies were used as described in Chapter 4, with all compound masses normalised to 100 mg of organic carbon. Sigma (σ) is the sum of the amounts of the four dominant sphagnum acid derived phenols ([**I**] + [**IIa**] + [**IIb**] + [**III**]) normalised to 100 mg of OC. The ratio of σ to the sum of itself and the total OC-normalised yield of lignin phenols (Λ), represented as a percentage, provides a measure of the relative contributions of *Sphagnum*- and lignin-derived phenols present in litter or peat. This is termed the *Sphagnum* ratio (SR%).

5.3 Results and Discussion

5.3.1 Surface Vegetation

Ground layer vegetation analyses at the coring sites (Table 5.1), reflect differences in species composition. Hummocks in BP, BM and FL stages were all dominated by *S. fuscum*, a well documented hummock-forming *Sphagnum* species (Rochefort et al., 1990; Johnson and Damman, 1991), although vascular plants covered at least 30% of the ground layer. Hollows in these stages were dominated by different *Sphagnum* species (BP – *S. balticum*; BM – *S. angustifolium*; FL – *S. fallax*); coverage of vascular plants was highest in BM (45%) and lowest (12%) in FL. The understory vegetation in the SF sites was almost completely dominated by mosses, *P. commune* in the hummock and *S. angustifolium* in the hollow. Increased species diversity is observed in the hummock core of the BP, BM and FL compared to the hollow core.

To assess whether depth-dependent changes in phenolic composition were due to past vegetation shifts or to diagenesis, the present-day vegetation (Table 5.1) was compared with results from a detailed study of the botanical composition of Ryggmossen conducted *ca* 90 years ago (Du Rietz and Nannfeldt, 1925). Overall, the composition of *Sphagnum* mosses and vascular plants has remained relatively constant over the last 90 years. Based on lead-210 dating of the cores (L. Belyea. *pers. comm.*), this period covers most of the record for the BP, BM and FL cores (i.e. to depths of *ca* 30 cm below the peat surface in hollows and *ca* 40 to 50 cm in hummocks), and much of the record for SF cores (i.e. to depths of 16-18 cm below the peat surface). The cores showed no major changes in stratigraphy, other than in the SF hollow, where moss remains disappeared at *ca*12 cm below the peat surface (Section 5.3.6, Fig. 5.9), however the peat depth at the SF site was much shallower, with a mineral soil occurring at *ca* 20 cm below the peat surface (Section 5.3.2, Table 5.2). Hence, we are confident that any depth-dependent changes in the phenolic composition of the cores can be attributed to diagenetic changes, except perhaps in the SF hollow core, where the rapid decrease in *Sphagnum* biomarkers below the mean water table may reflect a past shift in vegetation.

Table 5.1: Ground vegetation cover at each core site.

Species	%	Species	%
BP Hummock		**BP Hollow**	
S. fuscum	57	*S. balticum*	71
Calluna vulgaris	30	*Eriophorum vaginatum*	25
Rubus chamaemorus	5	*Andromeda polifolia*	3
Vaccinium microcarpum	5	*Vaccinium microcarpum*	1
Andromeda polifolia	2		
Empetrum nigrum	1		
BM Hummock		**BM Hollow**	
S. fuscum	67	*S. angustifolium*	65
Calluna vulgaris	25	*Rubus chamaemorus*	25
Empetrum nigrum	2	*Calluna vulgaris*	20
Vaccinium microcarpum	3		
S. magellanicum	3		
FL Hummock		**FL Hollow**	
S. fuscum	47	*S. fallax*	88
Empetrum nigrum	30	*Andromeda polifolia*	10
Polytrichum strictum	15	*Vaccinium microcarpum*	1
Andromeda polifolia	3	*Eriophorum vaginatum*	1
Calluna vulgaris	2		
Drosera rotundifolia	1		
Vaccinium microcarpum	1		
Polytrichum commune	1		
SF Hummock		**SF Hollow**	
Polytrichum commune	91	*S. angustifolium*	95
S. angustifolium	6	*Vaccinium uliginosum*	4
Vaccinium uliginosum	3	*Carex limosa*	1

5.3.2 Down Core Variation in Elemental and Isotope Parameters

The TOC, TON and C/N values for the peat cores are presented in Table 5.2. The BP, BM and FL display similar carbon contents down core (mean = 43.4 ± 0.3%); however the deeper core section of the SF contains a lower TOC, evidence of the mineral soil at this site. The SF cores also exhibit a much smaller range of C/N ratios (21.1 - 57.4) compared to the BP, BM and FL cores (41.8 - 178.9), consistent with SF environments having higher rates of decay and nutrient turnover (e.g. Thormann et al., 1999). The high C/N ratios determined for the BP, BM and FL are similar to values reported for other peatlands (~26 - 183; Damman, 1988; Hornibrook et al., 2000). This is likely a result of the high C/N found in *Sphagnum* litter (>50) (van Breemen, 1995).

The TON shows elevated levels of up to 1.5% observed at 19.5 cm above the mean water table and 2.3cm below the mean water table in the SF hummock and hollow cores that corresponds to a core depth of *ca* 16 cm. These results are significantly elevated compared to the average of 0.56 ± 0.34% in the BP, BM and FL cores ($p<0.005$). These results are consistent with the low abundance of N in peat-forming *Sphagnum* species (Berendse et al., 2001). However, this is somewhat contradictory to the vegetation cover results for the SF hollow, whereby 95% was considered *S. angustifolium* (Table 5.1). However, it is known that pine trees (*Pinus sylvestris*) cover the SF site which will contribute to the surface litter via leaf litter. Additionally, the shift in TON suggests that the vegetation cover has recently altered from a previous vegetation cover of N-rich species that is now reflected in a high TON at depth, to N-poor *Sphagnum* species near the surface. The SF was the only habitat that displayed a gradual decrease of the C/N ratio with increasing depth, a reflection of the microbial consumption of the labile C- and H-rich compounds down the core (e.g. carbohydrates; Section 5.3.4) and/or a vegetation change, resulting in a decreased abundance of C relative to N (Hornibrook et al., 2000). In the hummock cores only, the C/N ratio can be identified as three different layers, as observed by Malmer and Holm (1984). The surface samples have a relatively low C/N ratio, whereby new carbon is incorporated through the growth of mosses. The C/N ratio then increases into the second layer which occurs above the mean water table, this peat is only weakly decomposed and humified, however OM is being deposited as litter and carbon losses occur. The third layer is characterised by a decrease in the C/N ratio, which is more humified and decomposed (Malmer and Holm, 1984).

Table 5.2: The TOC, TON and C:N values for (a) hummock and (b) hollow cores across bog plateau (BP), bog margin (BM), fen lagg (FL) and swamp forest (SF) stages.

Core	*Depth relative to mwt (cm)*	TOC %	TON %	C/N	*Depth relative to mwt (cm)*	TOC %	TON %	C/N
		a) Hummock				***b) Hollow***		
BP	24.5	42.0	0.70	59.7	8.4	40.6	0.52	77.4
	22.5	43.6	0.53	81.6	6.4	40.2	0.41	98.7
	18.5	44.3	0.37	119.3	2.4	41.7	0.49	84.4
	14.5	43.6	0.43	101.5	-1.6	40.6	0.41	99.4
	8.5	44.0	0.49	89.3	-5.6	42.5	0.37	115.5
	0.5	44.2	0.73	60.7	-19.6	42.8	0.60	70.9
	-11.5	43.9	0.67	65.6	-25.6	43.1	0.79	54.9
	-23.5	45.6	0.47	96.1	-33.6	44.1	1.06	41.8
	mean	**43.9**	**0.55**	**84.2**	-39.6	44.8	0.76	58.8
					mean	**42.3**	**0.60**	**78.0**
BM	16.9	37.3	0.37	101.0	13.2	42.6	0.60	71.6
	14.9	43.1	0.45	96.7	11.2	42.7	0.53	80.2
	10.9	43.0	0.45	95.3	9.2	43.0	0.61	70.4
	0.9	42.8	0.45	96.1	5.2	47.7	1.02	46.9
	-3.1	58.0	0.75	77.8	1.2	44.2	0.94	47.1
	-5.1	43.6	0.62	70.4	-4.8	43.6	0.75	58.1
	-9.1	44.8	0.80	55.7	-10.8	44.5	0.72	61.8
	-15.1	43.2	0.46	93.6	-16.8	45.0	0.92	49.1
	-19.1	43.9	0.67	65.3	-24.8	44.7	0.63	71.5
	-25.1	41.3	0.42	99.3	-30.8	42.1	0.45	93.6
	-33.1	44.5	0.36	123.1	-34.8	42.2	0.58	72.3
	-41.1	43.4	0.36	120.6	mean	**43.8**	**0.70**	**65.7**
	mean	**44.1**	**0.51**	**91.2**				
FL	20.2	44.9	0.44	101.3	7.6	39.5	0.66	60.0
	18.2	42.9	0.44	98.6	5.6	42.3	0.80	52.9
	14.2	42.4	0.31	136.0	1.6	40.9	0.35	115.9
	6.2	43.2	0.38	114.5	-4.4	43.4	0.45	97.5
	0.2	42.1	0.24	178.9	-10.4	41.2	0.43	95.2
	-3.8	43.4	0.35	122.9	-14.4	43.3	0.44	99.4
	-5.8	43.1	0.41	105.4	-24.4	42.5	0.46	91.9
	-9.8	42.4	0.45	93.4	-34.4	42.8	0.47	90.6
	-21.8	43.3	0.70	62.1	mean	**42.0**	**0.51**	**87.9**
	-35.8	44.2	0.89	49.9				
	mean	**43.2**	**0.46**	**106.3**				
SF	35.5	36.2	0.63	57.4	11.7	42.8	0.91	47.2
	33.5	46.4	1.25	37.1	9.7	44.4	1.18	37.5
	29.5	44.3	1.19	37.2	7.7	44.7	1.07	41.6
	25.5	43.0	1.39	31.0	5.7	45.1	1.37	33.0
	19.5	41.0	1.46	28.1	-2.3	34.4	1.45	23.8
	9.5	14.0	0.58	24.1	-4.3	23.9	1.13	21.1
	mean	**37.5**	**1.08**	**35.8**	-6.3	22.9	1.08	21.2
					mean	**43.0**	**1.37**	**37.6**

mwt: mean water table

Changes with depth in $\delta^{13}C$ and $\delta^{15}N$ are illustrated in Fig. 5.2; displaying a sequence of ever higher isotope ratios with an increasing depth (a positive isotope signal) for each of the two elements. Carbon isotope signatures at all sites were *ca* -28.1 ± 1.4‰ with exception of the SF hollow and one lower value in the BP hummock (Fig. 5.2). This average value is consistent with previous studies of isotopic signatures in peat (e.g. Macko et al., 1991; Wieder and Yavitt, 1994; Broder et al., 2011).

The subtle but progressive decrease of $\delta^{13}C$ values from the core bottom to the core top (Δ4.5‰), indicates the light carbon fractions are steadily removed from the OM, resulting in $\delta^{13}C$ enrichment with increasing depth (Hornibrook et al., 2000). However these signals can also reflect temporal changes in the composition of original C and N sources (Novák et al., 1999), although this is disregarded for the BP, BM and FL due to consistent vegetation observations from the botanical composition of Ryggmossen conducted 90 years ago (Du Rietz and Nannfeldt, 1925). Historic atmospheric $\delta^{13}CO_2$ values have shown a progressive decrease from -6.45‰ in 1850 to -8.08‰ in 2002, which will have contributed to the decrease observed in the bulk peat, however changes are larger in the peat than the changes in the atmospheric $\delta^{13}CO_2$, consistent with findings from Esmeijer-Liu et al. (2012). These results indicate that the changing atmospheric CO_2 $\delta^{13}C$ and changing vegetation source alone are not the primary peat isotope forcings.

The $\delta^{13}C$ values were more negative in the SF hollow (-31.1‰) compared to the other three hollow sites (-23.3, -26.8 and -25.6‰; BP, BM and FL, respectively). The $\delta^{13}C$ values suggest increased degradation with depth and from the bog centre (BP) to bog forest margin (BM, SF). However, the correlation between $\delta^{13}C$ and C/N as observed by Hornibrook et al. (2000) was not observed in these samples. This is likely due to the variable N-input (Table 5.2), a result of either a varying input of N-rich species or changing N deposition.

The $\delta^{15}N$ signatures in the peat cores increased from a low of -7.8‰ in the BP hummock to a maximum of +2.2‰ in the SF hollow (Fig. 5.2), consistent with previous values for *Sphagnum* mosses (-8 to +2.5‰) (Nordbakken et al., 2003; Asada et al., 2005; Bragazza et al., 2005). Previous studies have also reported an increasing $\delta^{15}N$ with depth; -3‰ to 0‰ within a pristine *Sphagnum* bog in the Czech Republic (Novák et al., 1999); and -7.5‰ to 0‰ within a northern Finland bog (Esmeijer-Liu et al., 2012). The

consistently high value of 0‰ in the deep peat throughout the literature, could be a reflection of pre-anthropogenic N input of *ca* 0‰ (Bedard-Haughn et al., 2003), with the lower $\delta^{15}N$ isotope ratio an indication of N deposition. This increased N deposition can occur despite a steady N concentration in *Sphagnum* mosses. This is due to the N-filter in *Sphagnum* mosses, which under typical N deposition rates in northern Europe, would remain unsaturated and therefore N concentrations would be determined by productivity and not deposition (Lamers et al., 2000; Berendse et al., 2001), however this is not always the case as shown by Bragazza et al. (2005).

As with $\delta^{13}C$ values, $\delta^{15}N$ values can be affected by many processes. The change in species composition has been ruled out for all of the sites bar the SF hollow, whilst other processes including decomposition, nitrification, denitrification and microbial incorporation of N (Esmeijer-Liu et al., 2012), may explain the enrichment of $\delta^{15}N$ in to the deeper peat cores. ANOVA showed that the $\delta^{15}N$ values are significantly similar across the hummock and hollow cores ($p=0.130$), however, the $\delta^{15}N$ displayed an increase from the bog centre (BP), which will have a tendency to absorb rain water depleted in nitrogen, through the FL to the bog-forest margin (BM/SF), which are more likely to absorb groundwater which is enriched in nitrogen (Kendall, 1998). The site-specific enrichment of isotopically light $\delta^{15}N$ with increasing depth may be caused by the preferential loss of N during aerobic decomposition (Natelhoffer and Fry, 1988), which is further suggested by the increase at the marginal peat sites; BM and SF. Natelhoffer and Fry (1988) found that litter inputs decreased $\delta^{13}C$ and $\delta^{15}N$ values, whilst decomposition increased $\delta^{13}C$ and $\delta^{15}N$ values, which can largely explain the positive isotope signal observed at the cores at Ryggmossen.

5.3.3 Bulk Density and Carbon Storage

The BP, BM and FL cores all show a progressive increase in the bulk density from *ca* 0.03 g cm^{-3} up to 0.1 g cm^{-3}, consistent with the values cited by Clymo (1992) (0.03 g cm^{-3} in the acrotelm and 0.12 g cm^{-3} in the catotelm) (Fig. 5.3). The SF bulk density plot displays a clear increase from 0.12 g cm^{-3} to *ca* 0.4 and *ca* 0.6 g cm^{-3} in the hummock and hollow core respectively (Fig. 5.3; note the different scale used for the SF). This increase occurs at 18 cm at the hummock and 14 cm at the hollow core, corresponding to the decrease in TOC, further evidence of a mineral substrate at the SF (Table 5.2).

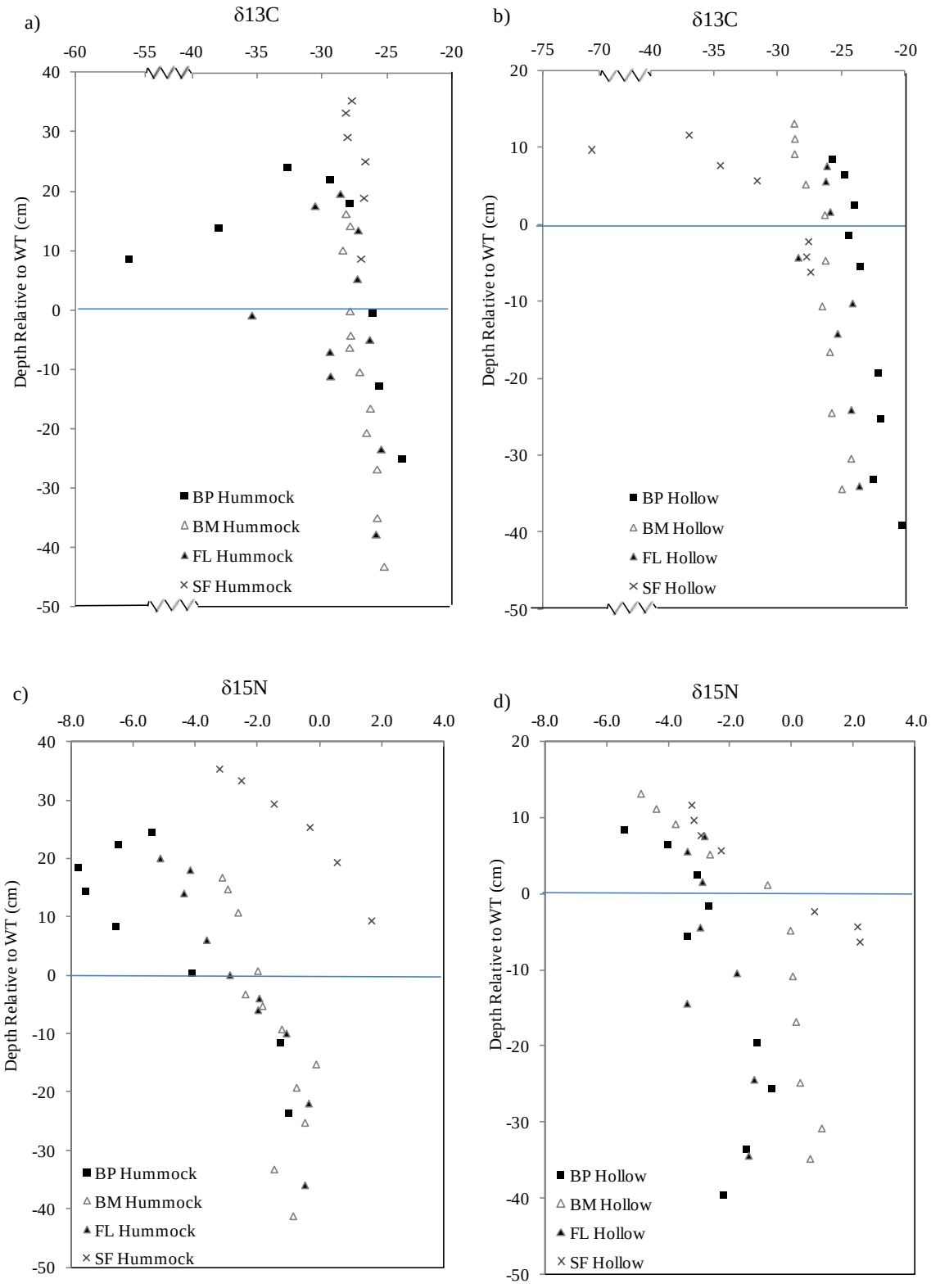

Fig. 5.2: The $\delta^{13}C$ and $\delta^{15}N$ values for (a,c) hummock and (b,d) hollow cores across the BP (filled squares), BM (open triangles), FL (closed triangles) and SF (cross) stages. Depths are relative to the mean water table, indicated by the solid horizontal line.

The carbon storage (t C ha^{-1}) of each 2 cm peat core slice increases with increasing depth, with the exception of the SF hummock core (Fig. 5.4; again note the different scale used for the SF carbon storage). This increase is a direct result of the increasing bulk density down core, i.e. an increasing compaction down core (Novák et al., 1999), as shown in Fig. 5.3. At the SF, there is evidence of a mineral subsoil, hence we expect the carbon storage to be limited, as observed in the hummock core. However due to the relatively high TOC for mineral soils (24.6%) coupled with the elevated bulk density, the SF hollow displays a large carbon storage particularly in the deep seasonally saturated mineral soil. These results indicate that the mineral-fed marginal peats that are saturated for at least part of the year may have the highest capacity for carbon storage.

The average carbon storage across Ryggmossen bog can be calculated at 3.4 t C ha^{-1} per centimetre thickness, however this value includes the mineral SF cores. Excluding the SF mineral core section, the average declines to 2.79 t C ha^{-1} per cm. The carbon storage of the hollow cores exceeds that of the hummock cores at all four habitats, which can be attributed to the elevated bulk densities within the hollow cores (Fig. 5.4).

Swedish peats cover an area of 4.7 x 10^4 km^2 and have an average depth of 1.1 m (Eriksson, 1991; Gorham, 1991). Coupled with the calculated average TOC of 52.5%, and bulk density of 0.09 g cm^3 across Swedish peats (Eriksson, 1991), the average carbon storage per centimetre thickness of Swedish peats can be calculated as 4.86 t C ha^{-1}, consistent with Cannell's estimation for British peats; 4.7 t C ha^{-1}(Cannell et al., 1993).

However, these carbon storage values are somewhat higher than those calculated from Ryggmossen, this could be due to the average taken over a short core depth of up to 60 cm, whereas the Swedish average is taken over 1.1 m, and the British average is taken over 2.43 m, whereby further increases in bulk density are expected, thereby producing a high carbon storage.

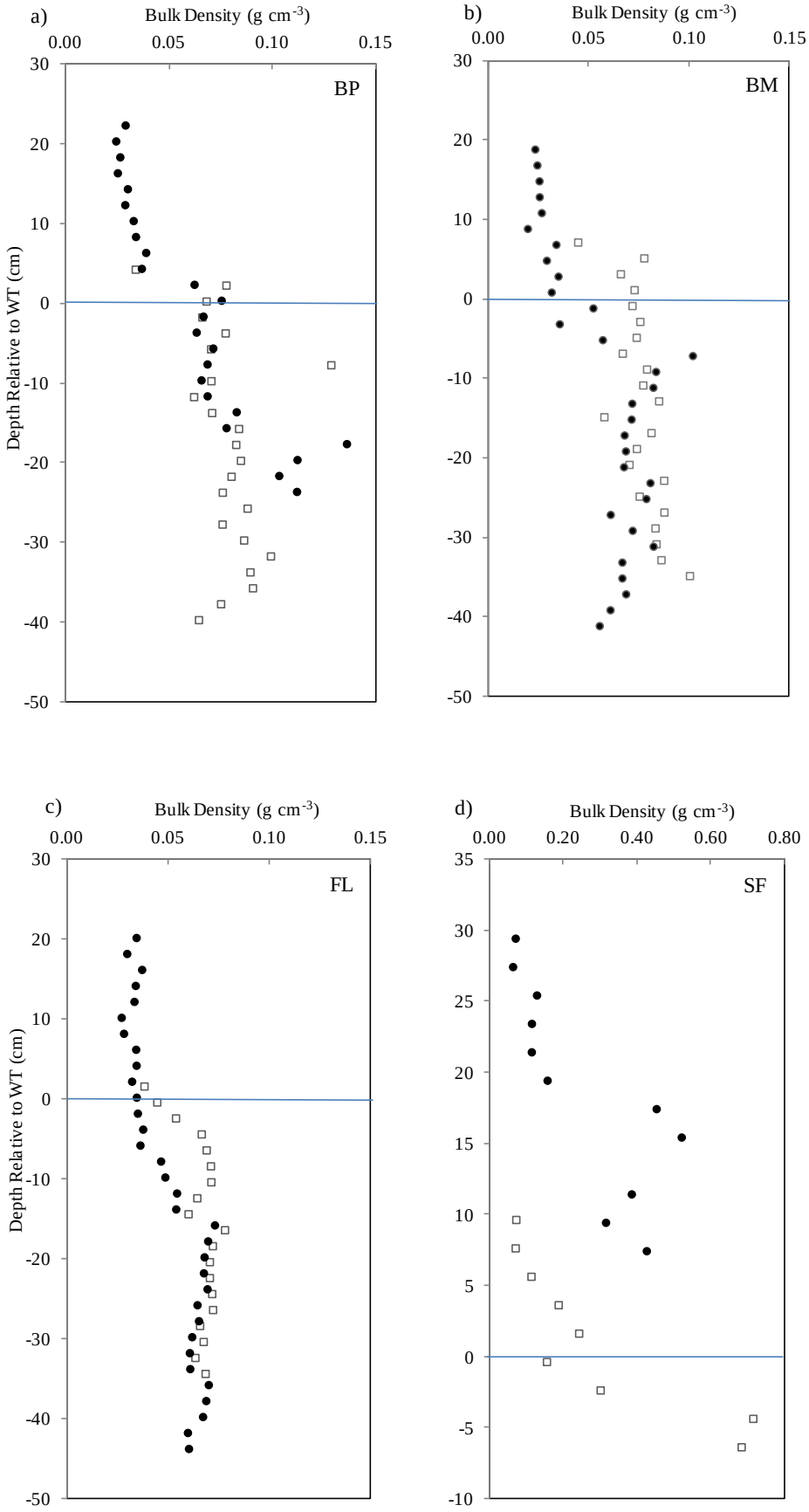

Fig. 5.3: Depth profiles of bulk density (g cm^{-3}) values for the (a) BP, (b) BM, (c) FL and (d) SF stages across the hummock (filled circles) and hollow cores (open squares). Depths are relative to the mean water table, indicated by the solid horizontal line. Note the different scale used for the SF.

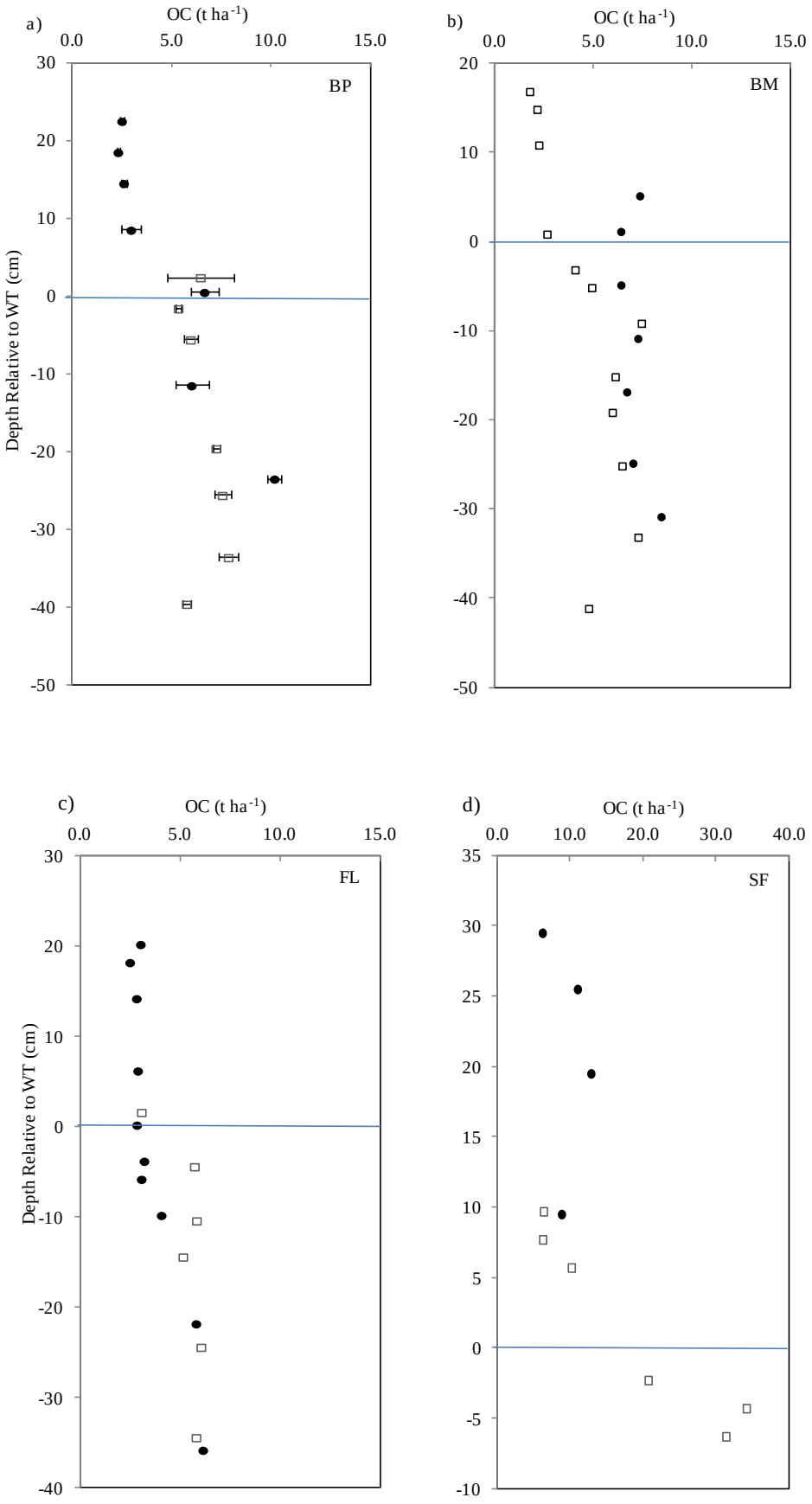

Fig. 5.4: The OC values (t C ha^{-1}) for the (a) BP, (b) BM, (c) FL and (d) SF stages across the hummock (filled circles) and hollow cores (open squares). Depths are relative to the mean water table, indicated by the solid horizontal line. Note the different scale used for the SF.

5.3.4 Carbohydrates

The total carbohydrate yield (TCHO; mg/100 mg OC) for the eight peat cores was calculated (Fig. 5.5) using the quantities of eight neutral monosaccharides; arabinose, rhamnose, ribose, xylose, fucose, mannose, galactose and glucose (Fig. 5.6). The TCHO was highest in the BP hollow core, increasing from 107.3 mg/100 mg OC at the surface to 114.4 mg/100 mg OC at the base of the core. The SF hollow and hummock cores displayed the lowest carbohydrate yields, decreasing from 71.9 to 13.7 mg/100 mg OC and from 85.4 to 35.5 mg/100 mg OC in the hollow and hummock cores, respectively. This could be a direct result of the increased degradation at the SF reflected in the low C/N ratio at the SF cores (Section 5.3.2). The remaining profiles displayed a TCHO yield ranging between 61.2 and 111.9 mg/100 mg OC (Fig. 5.5). ANOVA revealed a gradient of decreasing carbohydrate yield from the bog centre out to the bog-forest margin (BP=FL>BM>SF) ($p<0.001$).

These relatively high yields of carbohydrates down core are consistent with previous studies of carbohydrates in peats (e.g. Comont et al., 2006). Recent research has suggested the cell-wall polysaccharides abundant in *Sphagnum* mosses have a major role in the resistance to decay of *Sphagnum* mosses (Hájek et al., 2011), however Verhoeven and Liefveld (1997) have suggested that the sphagnum acid inhibits the microbial decomposition of the cell wall polysaccharides. Although it is uncertain which process is occurring to resist the degradation of *Sphagnum* mosses, both theories contradict the paradigm of the rapid consumption of carbohydrates in peats (e.g. Pancost et al., 2002).

Glucose displayed the largest yield of the eight sugars throughout the eight cores, accounting for up to 70% of the TCHO (Fig. 5.6). The proportion of glucose in the BP, BM and FL cores relative to the other sugars increases with depth. However the SF shows a decrease in TCHO, at the expense of primarily glucose (Fig. 5.6). As reported in Chapter 4 (Section 4.3.3), the *Sphagnum* mosses analysed with TMAH were found to contain significant quantities of cellulose derived products (products 1-4 and 1,2,4-TMB). Cellulose is derived from glucose units, therefore the increasing proportion of glucose with depth suggests the stabilisation of *Sphagnum* derived sugars (i.e. glucose units) (Section 5.3.6).

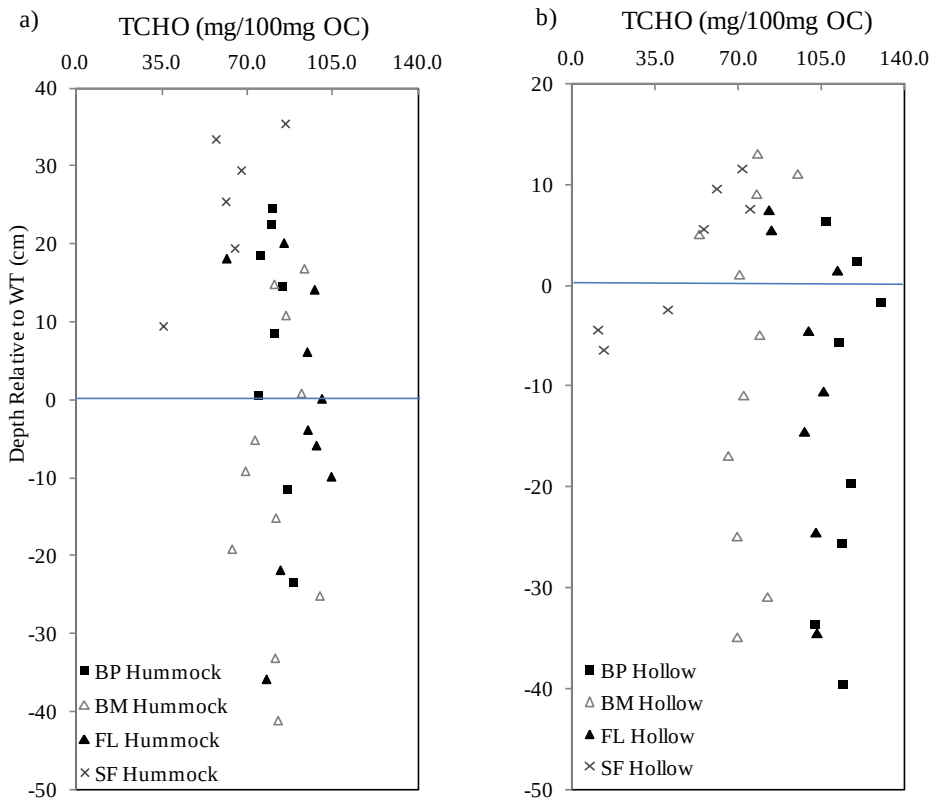

Fig. 5.5: The TCHO (mg/100 mg OC) values for (a) hummock and (b) hollow cores across BP (closed squares), BM (open triangles), FL (closed triangles) and SF (cross) stages. Depths are relative to the mean water table, indicated by the solid horizontal line.

The BP has a significantly higher yield of glucose compared to the BM and SF ($p<0.001$), indicating glucose is the chief monosaccharide affecting the gradient of decreasing TCHO from the bog centre out to the bog-forest margin (Fig. 5.6), consistent with the decrease of cellulose rich *Sphagnum* mosses.

Galactose, the second most abundant sugar within these peat cores (5.8-18.1%), shows a gradual decrease in both weight and proportion relative to TCHO down the profiles, with the exception of the FL hollow where the yield remains constant. As for galactose, the concentration of mannose is higher in the acrotelm and lower in the mesotelm. In the catotelm of the hollow cores of the BP and BM, the yield of rhamnose, mannose, galactose and glucose increases. The same sugars remain constant in the FL catotelm, and decrease in the SF hollow. The sum of these sugars (Gal+Man+Rha) are significantly higher in the BP, BM and FL compared to the SF ($p<0.001$), confirming these sugars as indicators of moss (Comont et al., 2006).

The SF hummock core displays a high yield of mannose at the surface, however this is reduced below the surface, reflecting the presence of *Polytrichum* moss at the surface of this site (Table 5.1; Fig. 5.6) (Comont et al., 2006). The contribution of arabinose and to a lesser degree fucose to the total carbohydrate yield in the SF is elevated in comparison to the other three sites. The SF cores display a decrease in the yield of the aldopentoses (arabinose, xylose, fucose) at 16-18 cm depth, although the relative input of these sugars to the total carbohydrate yield increases. The decrease of arabinose and fucose with depth in the BP, BM and FL, is occurring at a faster rate than the other sugars, indicating the selective preservation of the moss monosaccharides.

The proportion of xylose increases down the profile of the BP and BM hummock cores, but decreases in the catotelm of the hollow cores (Fig. 5.6). These aldopentoses are considered sedge indicators (Comont et al., 2006). Assuming that the litter input to the peat has remained relatively constant over the course of humification (Du Rietz and Nannfeldt, 1925), these results indicate that in the anoxic zone of the peat core, the sedge litter is preferentially degraded over the moss litter, despite smaller quantities of sedge sugars.

The profiles of the four sites display a relatively stable carbohydrate yield, reflecting the high preservation of these biopolymers. The peatland gradient shows a decrease of TCHO from the BP to the SF, confirming the large abundance and preservation of carbohydrates in peatlands (Comont et al., 2006).

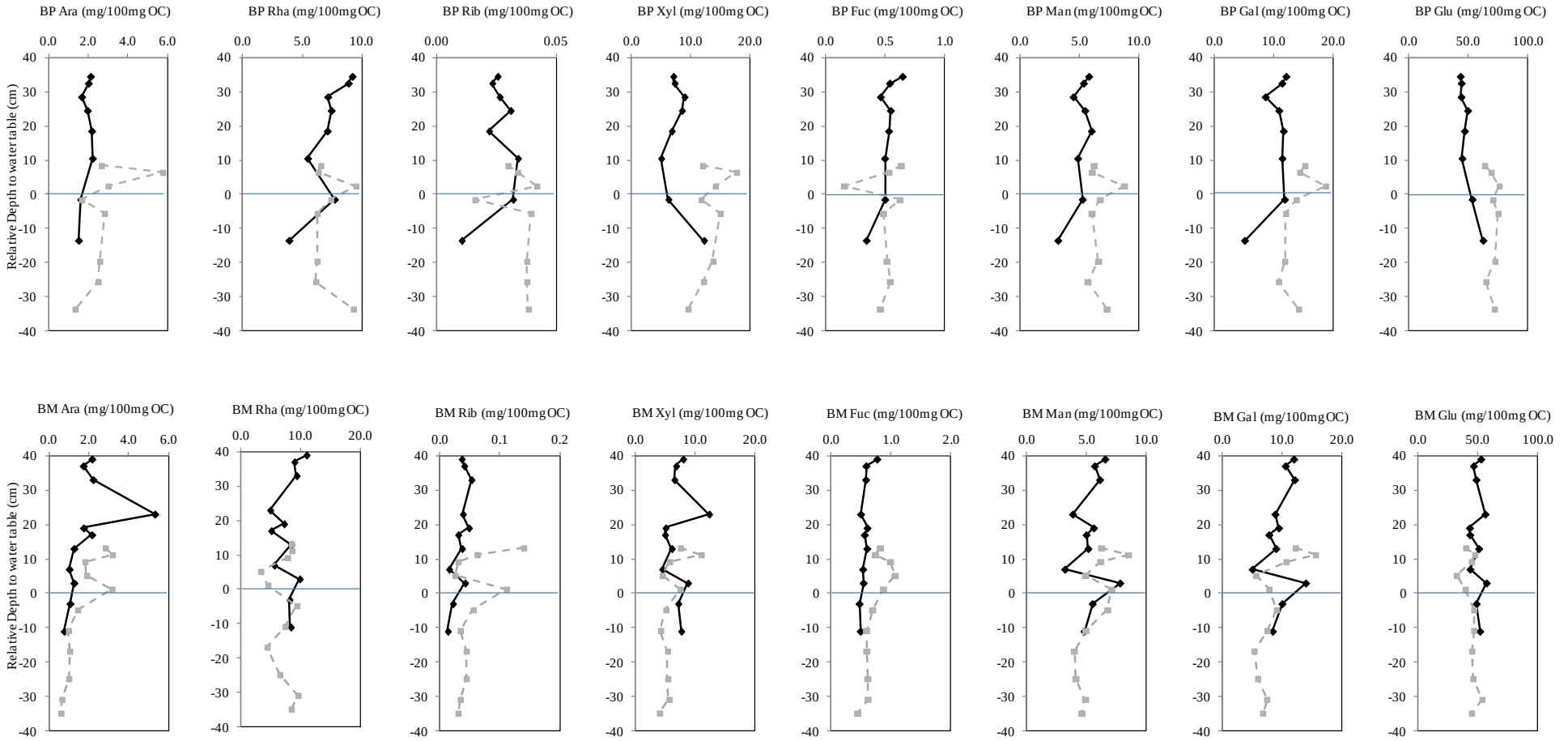

Fig. 5.6: Depth distribution of individual carbohydrate concentrations (ara, rha, rib, xyl, fuc, man, gal and glu) within the hummock core (black line) or hollow (grey line) within the BP and BM peat cores, released after H_2SO_4 hydrolysis. Depths are relative to the mean water table, indicated by the solid horizontal line.

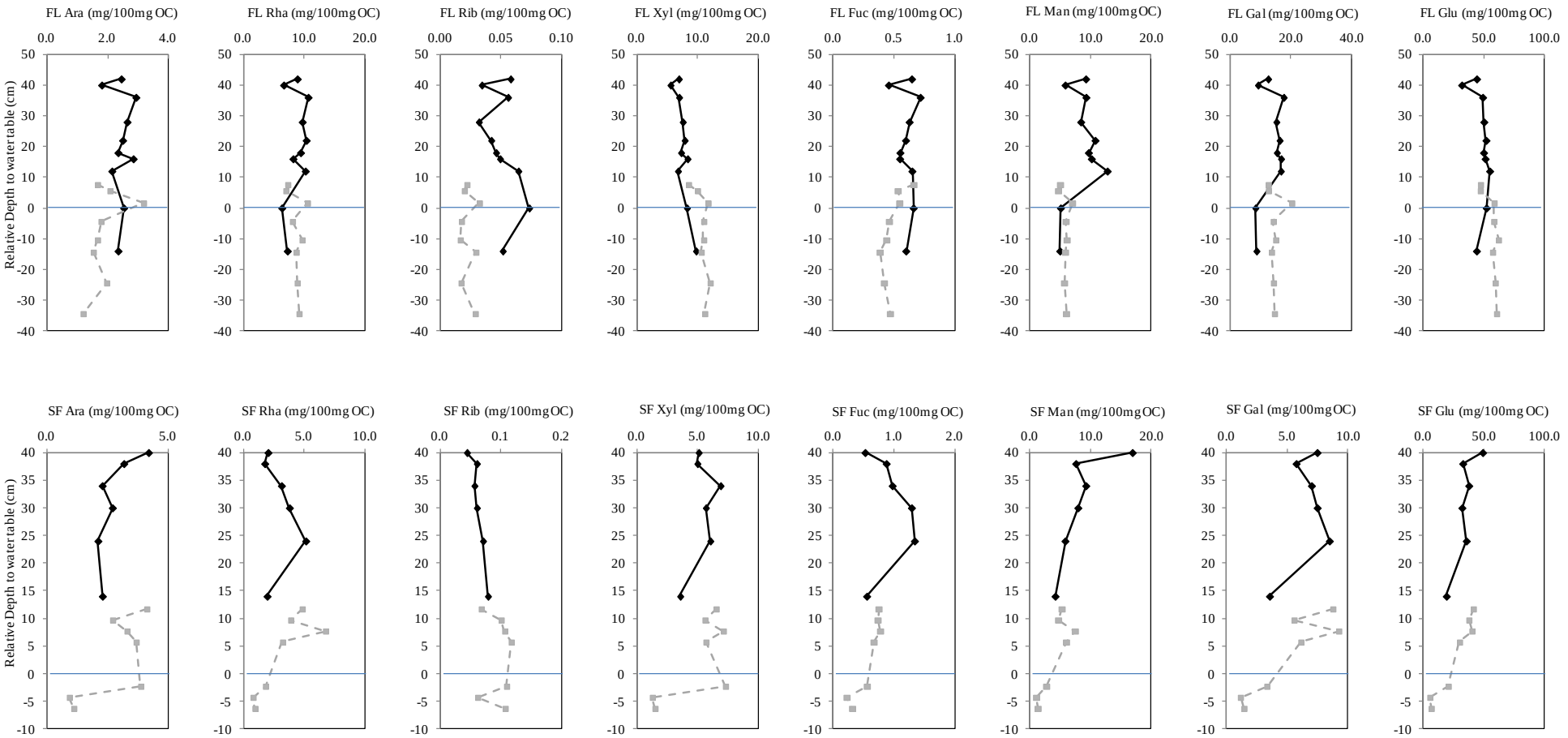

Fig. 5.6.CONT: Depth distribution of individual carbohydrate concentrations (ara, rha, rib, xyl, fuc, man, gal and glu) within the hummock core (black line) or hollow (grey line) within the FL and SF peat cores, released after H_2SO_4 hydrolysis. Depths are relative to the mean water table, indicated by the solid horizontal line.

5.3.5 THM in the Presence of TMAH

The TMAH thermochemolysis products in the surficial peat (0-2 cm; Fig. 5.7a) in the BP hollow core included the sphagnum acid pyrolysis products: **I**, **IIa** and **b**, and **III** together with a range of methylated phenolic and other oxygenated aromatic products as listed in Table 5.3. The most abundant of the non-*Sphagnum* components included the *p*-hydroxyl phenols; methoxybenzene (P1), methoxytoluene (P2), 1-ethyl-4-methoxy-benzene, and 1-ethenyl-4-methoxybenzene (P3). There were also smaller amounts of other vascular plant-derived phenols produced during the thermochemolysis of the peat cores, including the methylated guaiacyl lignin phenols; 3,4-dimethoxybenzaldehyde (G4) and 3,4-dimethoxybenzoic acid methyl ester (G6) and the cinnamyl lignin phenols; *p*-coumaric acid (P18) and ferulic acid (G18). However, these phenols were not derived solely from undegraded lignin (e.g. Filley et al., 2006; Mason et al., 2009) given that the thermochemolysis of *S. fallax* capitula with ^{13}C-labelled TMAH revealed that only 13.7, 22.0 and 19.2% (± 2.7, 2.3 and 1.6%, respectively, n = 4) of G4, G5 and G6, respectively are sourced from methoxylated phenolic sub-units (Chapter 4, Section 4.3.3).

Fig. 5.7b shows that the THM products; **I-III** persisted into the deepest horizon (48-50 cm) sampled from the same BP core. Similar product distributions were also observed during the TMAH thermochemolysis of the peat horizons sampled in the BM and FL stages. Therefore these *Sphagnum* bioindicators (**I**, **IIa/b**, and **III**) are relatively stable under both oxic and anoxic conditions where the integrity of the *Sphagnum* plants is being gradually lost with increasing burial.

THM in the presence of TMAH of the surficial horizon (0-2 cm) in the SF hollow core yielded smaller amounts of the sphagnum acid phenols (**I**, **IIa**/**b**, **III**) relative to the lignin phenols (Fig. 5.8a). From field observations, it is known that pine trees (*Pinus sylvestris*) cover the SF site which will contribute to the surface litter via leaf litter. The presence of gymnosperms at the SF hollow site is reflected in the high abundance of methylated guaiacyl phenols; 3,4-dimethoxybenzaldehyde (G4), 3,4-dimethoxy-acetophenone (G5), 3,4-dimethoxybenzoic acid methyl ester (G6), (*E*/*Z*)- 1-(3,4-dimethoxyphenyl)-2-methoxyethylene (G8), 3,4-dimethoxybenzeneacetic acid methyl ester (G24), and *threo/erythro* 1-(3,4-dimethoxyphenyl)-1,2,3-trimethoxypropane (G14/15).

Table 5.3: The main thermochemolysis products

Peak Label	Compound
P1	methoxybenzene
P2	4-methoxytoluene
G1	1,2-dimethoxybenzene
P3	4-methoxybenzeneethylene
1	cellulose derivative
2	cellulose derivative
3	cellulose derivative
G2	3,4-dimethoxytoluene
I	4-isopropenylphenol
4	cellulose derivative
P4	4-methoxybenzaldehyde
P5	4-methoxyacetophenone
G3	3,4-dimethoxybenzeneethylene
1,2,4-TMB	1,2,4-trimethoxybenzene
P6	4-methoxybenzoic acid methyl ester
1,3,5-TMB	1,3,5-trimethoxybenzene
P24	4-methoxybenzene acetic acid methyl ester
G4	3,4-dimethoxybenzaldehyde
G5	3,4-dimethoxyacetophenone
G6	3,4-dimethoxybenzoic acid methyl ester
S4	3,4,5-trimethoxybenzaldehyde
IIa	(*E*/*Z*)- 3-(4'hydroxyphen-1-yl)-but-2-enoic acid methyl ester
III	3-(4'hydroxyphen-1-yl)-but-3-enoic acid methyl ester
G24	3,4-dimethoxybenzeneacetic acid methyl ester
G8	(*E*)- 1-(3,4-dimethoxyphenyl)-2-methoxyethylene
G10	(*Z*)- 1-(3,4-dimethoxyphenyl)-methoxyprop-1-ene
P18	(*E*)- 3-(4-methoxyphenyl)-3-propenoic acid methyl ester
S5	3,4,5-trimethoxyacetophenone
G24	3,4-dimethoxybenzene acetic acid methyl ester
G12	3,4-dimethoxybenzenepropanoic acid methyl ester
G11	(*E*)- 1-(3,4-dimethoxyphenyl)-methoxyprop-1-ene
5	cellulose derivative
IIb	(*E*/*Z*)- 3-(4'hydroxyphen-1-yl)-but-2-enoic acid methyl ester
S6	3,4,5-trimethoxybenzoic acid methyl ester
S7	(*Z*)- 1-(3,4,5-trimethoxyphenyl)-2-methoxyethylene
S8	(*E*)- 1-(3,4,5-trimethoxyphenyl)-2-methoxyethylene
G14	*threo/erythro* 1-(3,4-dimethoxyphenyl)-1,2,3-trimethoxypropane
G15	*threo/erythro* 1-(3,4-dimethoxyphenyl)-1,2,3-trimethoxypropane
G18	(*E*)- 3-(3,4-dimethoxyphenyl)-3-propenoic acid methyl ester
S14	threo/erythro 1-(3,4,5-trimethoxyphenyl)-1,2,3-trimethoxybenzene
FA	C_{16} fatty acid methyl ester
S15	threo/erythro 1-(3,4,5-trimethoxyphenyl)-1,2,3-trimethoxybenzene
IS	5α-androstane

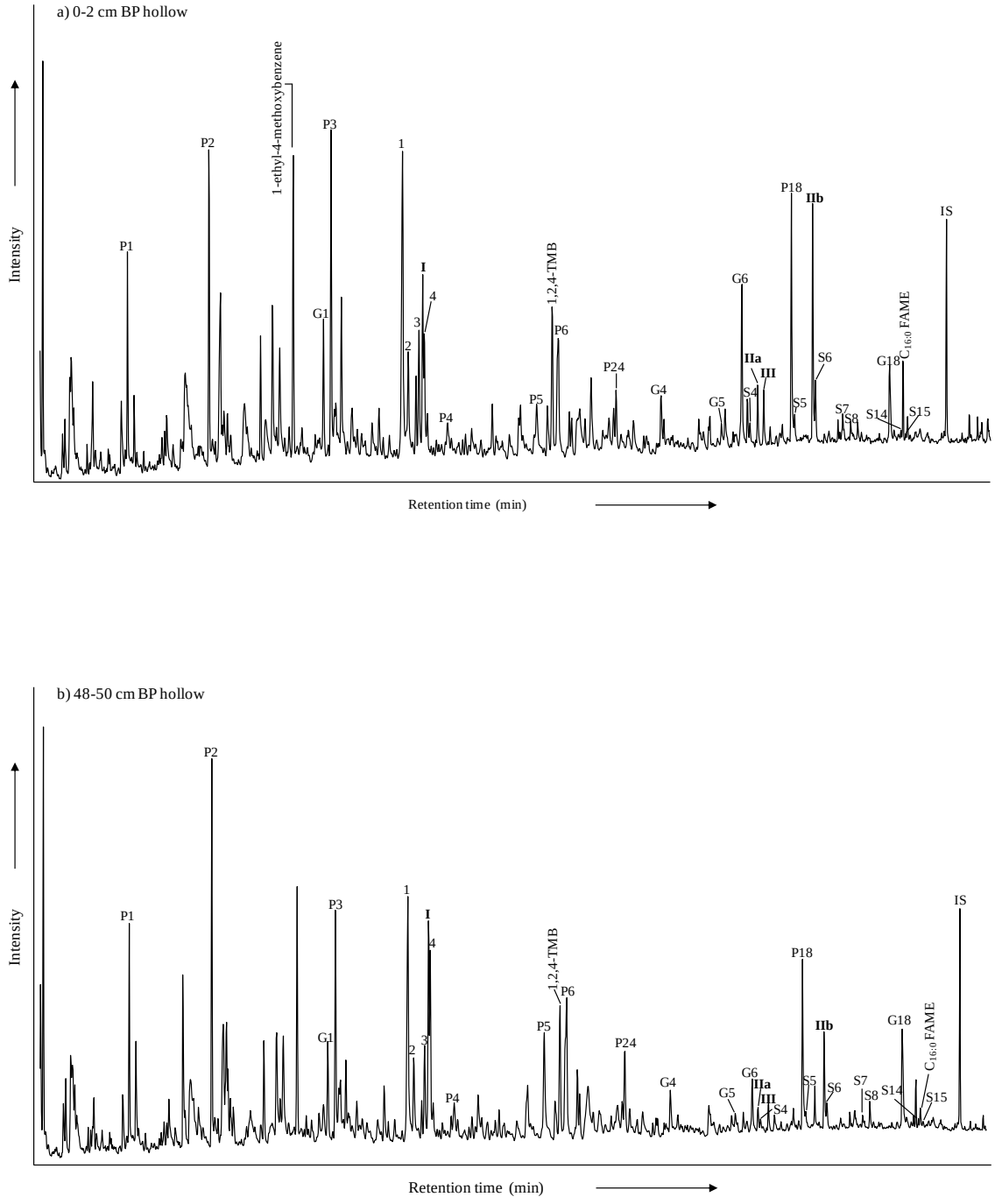

Fig. 5.7: Partial chromatogram for the total ion current (TIC) of the thermochemolysis products from the BP hollow core at the depth interval (a) 0-2 cm and (b) 48-50 cm. **I, IIa, IIb** and **III** correspond to structures in Fig. 4.2 (Chapter 4). Peak identities and symbols are listed in Table 5.3.

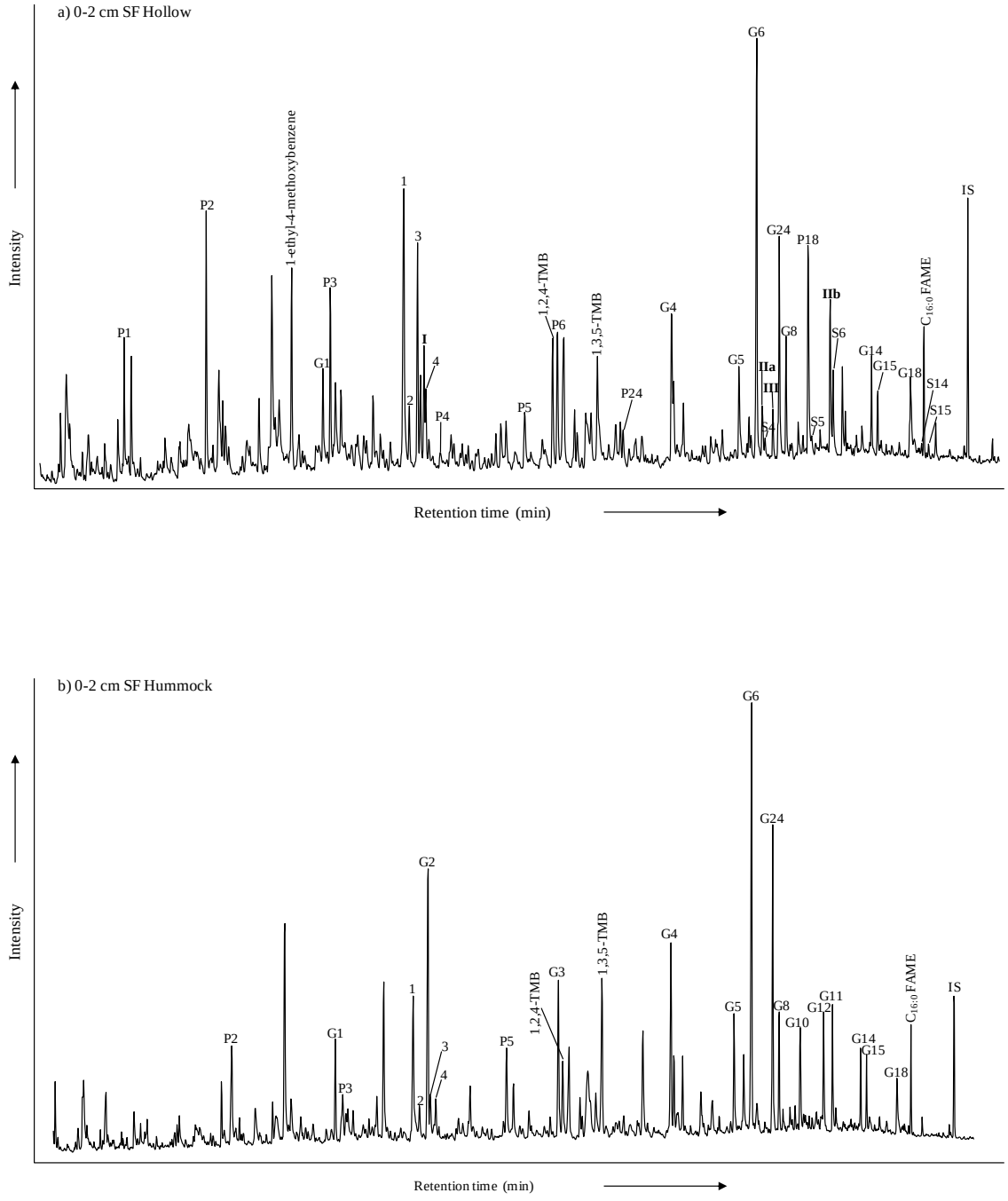

Fig. 5.8: Partial chromatogram for the total ion current (TIC) of the thermochemolysis products from the SF (a) hollow and (b) hummock cores at the depth interval 0-2 cm. Peak identities and symbols are listed in Table 5.3.

The presence of gymnosperms can also be observed at the SF hummock site, displaying a high abundance of methylated guaiacyl phenols; 3,4-dimethoxytoluene (G2), 3,4-dimethoxybenzeneethylene (G3), 3,4-dimethoxybenzaldehyde (G4), 3,4-dimethoxy-acetophenone (G5), 3,4-dimethoxybenzoic acid methyl ester (G6), (E/*Z*)- 1-(3,4-dimethoxyphenyl)-2-methoxyethylene (G8), (E/*Z*)- 1-(3,4-dimethoxyphenyl)-methoxyprop-1-ene (G10/11), 3,4-dimethoxybenzeneacetic acid methyl ester (G24), *threo/erythro* 1-(3,4-dimethoxyphenyl)-1,2,3-trimethoxypropane (G14/15), and 3-(3,4-dimethoxyphenyl)-propanoic acid methyl ester (G12) (Fig. 5.8b). The later of these compounds; G12, has been shown to be a dominant product in the THM of *Polytrichum commune* litter (Chapter 4, Section 4.3.4). From Table 5.1, it is clear that *P. commune* is the dominant species in the surface vegetation at this site. The relatively high abundance of lignin phenols indicates the additional input of pine tree litter to the SF floor, whilst the absence of compounds **I-III** indicates the complete absence of *Sphagnum* mosses.

5.3.6 Characterisation of Peat Archives

As discussed in Chapter 4, McClymont et al. (2011) proposed a biomarker proxy using 4-isopropenyl phenol (**I**) from the flash pyrolysis products of peat litter, which can be used as a rapid tool to reconstruct past peatland vegetation (Section 4.3.5). However, results from Chapter 4 revealed the formation of four sphagnum acid THM products, with their relative abundances potentially providing information on the oxic conditions of the peat. Therefore, the proxy provided by McClymont et al. (2011) may provide limited information compared to proxies that encompass all four sphagnum acid THM products (Chapter 4, Section 4.3.3).

Fig. 5.9 displays the yield of **I** and the *Sphagnum* proxy, I% as proposed by McClymont et al. (2011) (a ratio between 4-isopropenylphenol and two lignin derivatives 2-methoxyphenol and 2,6-methoxyphenol) for each of the eight peat cores. Although the presence of methoxybenzyl alcohol methyl ether products have been identified in the THM products of wheat straw (Robertson, 2008), these methylated alcohols are not present in the peat cores. Therefore the ratio has been modified to allow for differences occurring between pyrolysis and thermochemolysis products: using G4, G5 and G6, and S4, S5 and S6 as opposed to 2-methoxyphenol and 2,6-dimethoxyphenol.

The profiles of 4-isopropenyl phenol yield (**I**) and I% for BP, BM and FL cores showed broadly similar patterns in relation to water-table dynamics (Fig. 5.9; interannual water fluctuations denoted by the dashed and dotted lines for the hollow and hummock cores, respectively). In all cases, **I** decreased from the surface through the unsaturated and seasonally-saturated layers, reaching a minimum near the transition to permanently-saturated peat, with the exception of the SF, where the presence of *Sphagnum* is low. This decrease was most pronounced in the BP hummock core (decreasing from 0.66 ± 0.05 to 0.14 ± 0.02 mg/100 mg OC), with the decrease in this core occurring above the mean water table. In cores that extended deep enough, **I** tended to increase through the permanently-saturated layer. The proxy I% profiles largely corroborated these depth-dependent changes, although the profiles were more noisy than for **I**. The depth profile of the I% values for the FL stage however, differed from those in the BP and BM stages in that it oscillated between *ca* 55 and 92% down both hummock and hollow cores and did not exhibit the deep minima in the I% depth functions.

For the SF stage, the **I** and I% profiles (Figs. 5.9d) were different to those of the BP, BM and FL stages. The entire lengths of the SF cores were unsaturated for at least part of the year, because the summer water tables fell into the underlying mineral substrate (Fig. 5.1). The increased abundance of vascular plant phenols (Λ) in the SF hummock (Fig. 5.10) relative to the other stages indicates the dominance of non-*Sphagnum* inputs. There were small amounts of **I** in the hummock core, the maximum yield being 0.040 ± 0.002 mg/100 mg OC, considerably lower than the yields observed in the BP, BM and FL stages, corresponding to the low *Sphagnum* cover (<6%) observed from the vegetation survey at the SF hummock site (Table 5.1). The surficial layer in the hollow core had greater amounts of **I** than the hummock horizons, owing to the differing ground vegetation at each of these sites (Table 5.1): *S. angustifolium* had a 95% coverage in the SF hollow whereas the hummock was dominated by a non-*Sphagnum* moss namely that of *P. commune*. There was a dramatic decrease in **I** in the hollow core from 0.03 ± 0.003 at the base of the unsaturated layer to 0.002 ± 0.001 mg/100 mg OC just below the mean water table (Fig. 5.9d), suggesting a previous non-*Sphagnum* vegetation cover. The changes in **I** were mirrored in the I% profile shown in Fig. 5.9. The SF cores yielded largely dissimilar pyrolysis products to the previously mentioned cores, owing to the increased abundance of guaiacyl lignin phenols and a significantly reduced abundance of **I** ($p<0.005$) (Fig. 5.8).

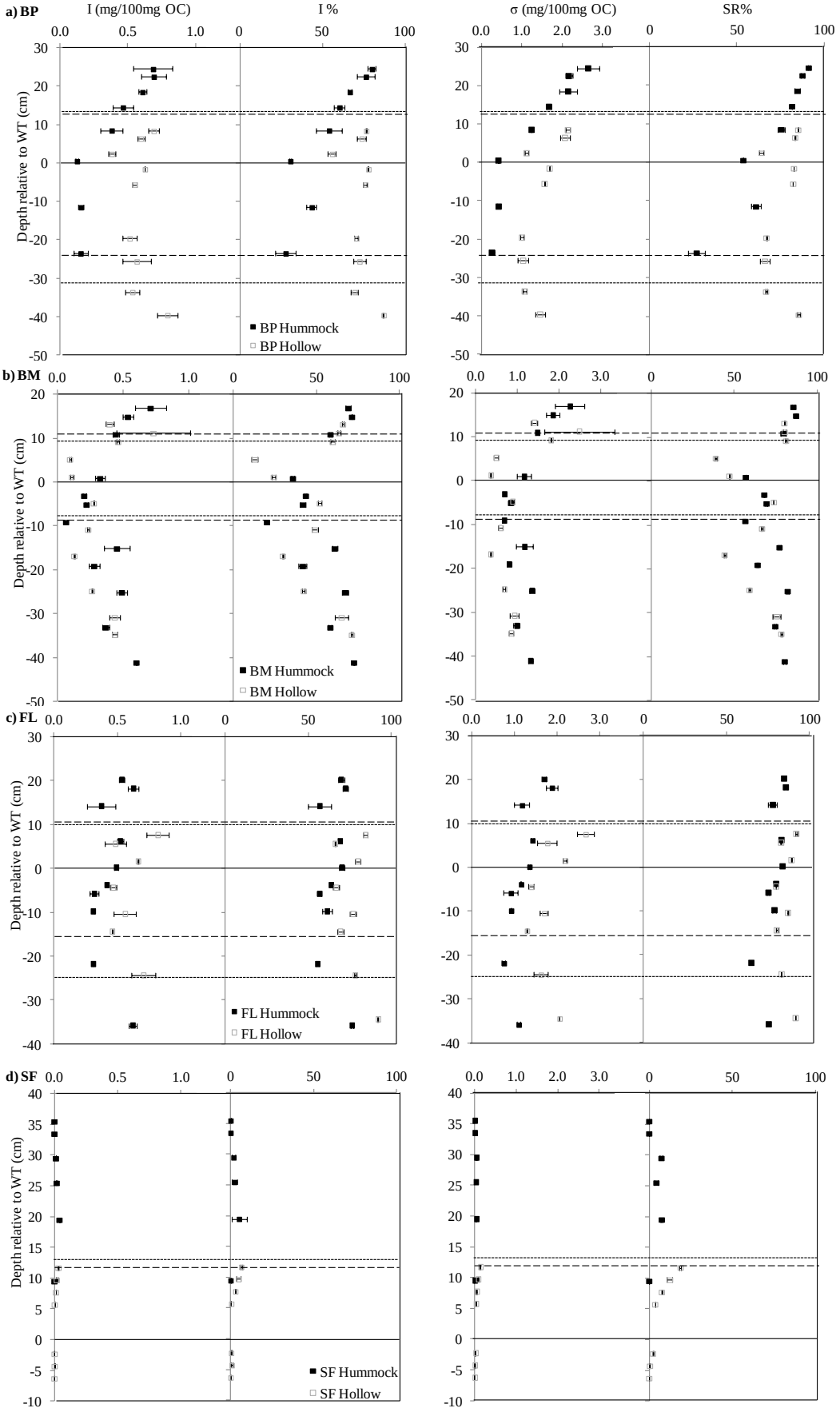

Fig. 5.9: Depth profiles of **I** (mg/100 mg OC), I%, σ (mg/100 mg OC) and SR% for cores from the hummock (filled squares) or hollow (open squares) from (a) BP, (b) BM) (c) FL and (d) SF stages. Error bars represent the standard error from two analytical replicates. *Mean water table indicated by the solid horizontal line, interannual water fluctuations denoted by the dashed/dotted lines for the hollow/hummock cores, respectively.

The profiles of *Sphagnum* yield (σ) and *Sphagnum* ratio (SR%) showed broadly similar patterns in relation to **I** and I % (Figs. 5.9, showing σ and SR% plotted as a function of depth), however the error bars are decreased when using all four biomarkers.
As with **I**, σ in the BP and BM decreased from 2.11 ± 0.07 mg/100 mg OC at the surface through the unsaturated and seasonally-saturated layers, reaching a minimum of 0.57 ± 0.01 mg/100 mg OC near the transition to permanently-saturated peat, however unlike **I**, the *Sphagnum* phenols showed no accumulation in the permanently-saturated peat. The BP hummock core displayed a progressive decrease of SR% with depth, from 91.2% at the peat surface to 28.9% at the core base (50 cm below surface). The BP hollow core and the two BM cores displayed a more stable SR%, decreasing from ~85% at the surface to 40-60% in the seasonally-saturated peat, before increasing to 85% at the base of the peat core (50 cm below surface).

As with I%, the associated SR% values in the FL stage oscillated between 64 and 92%. This contrasts with the four BP and BM profiles where SR% passed through a minimum at the mean water table (55.5 ± 0.28%), although the SR% recovered to 81.5 ± 2.1% at the base of the BP hollow and both BM peat cores. The BP hummock core displayed a continuous decrease in the SR% to 26.9%. Although these observations suggest that not all the peatland habitats will respond in a similar way to climate-induced changes (Jassey et al., 2011), they reveal the sensitivity of *Sphagnum* peat to fluctuations in the water-table that could be caused by a changing climate.

The SF hollow σ decreases from 0.14 mg/100 mg OC at the surface to 0.03 mg/100 mg OC above the mean water table, below the mean water table σ decreases to 0, indicating the recent introduction of *S. angustifolium* at the predominantly vascular site. Within the SF hummock, the σ is zero at the surface, as illustrated in Fig. 5.8b, but increases to 0.04 mg/100 mg OC within the acrotelm. These low yields of the *Sphagnum* biomarkers are reflected in the SR%. The SF hollow SR% decreases from 19.8% at the surface to 3.6% above the mean water table, below the mean water table the SR decreases further to 0. Within the SF hummock, the SR% is zero at the surface, but increases to 7.4% within the acrotelm. Literature has described *Sphagnum* as a paludifier, due to its ability to expand from the bog centre into surrounding forest (Heinselman, 1970). This process appears to be occurring within the SF hollow core, whereby THM products and yields indicate the relatively recent introduction of *Sphagnum* mosses to this site. The input of *Sphagnum* phenols relative to vascular phenols increased on average 21% from the I% proxy to the SR% proxy at the four stages, with the SR% providing a more

accurate indication of the plant input due to the use of all available lignin and *Sphagnum* markers.

The yield of carbohydrates (TCHO) (Section 5.3.4) display a positive correlation with the *Sphagnum* yield (σ) (Pearsons correlation = 0.546; $p<0.001$). These results indicate that both carbohydrates and sphagnum acid products have roles in the decay resistance of *Sphagnum* peat. Whereby the cellulose products can only be degraded once the sphagnum acid has been degraded, thereby removing the mask protecting the carbohydrates (Verhoeven and Liefveld, 1997).

The summed amounts of lignin phenols (Λ) in the BM, LF and SF cores (Fig. 5.10) remains relatively constant down the profile; 0.41, 0.30, and 0.68 mg/100 mg OC, respectively. However in the BP hummock core, Λ shows an initial increase from 0.25 to 0.38 mg/100 mg OC before decreasing slightly in the mesotelm, whilst the hollow core oscillates around a mean Λ of 0.43 mg/100 mg OC. These values are relatively consistent both across the bog and down the cores, which could be due to the low lignin concentration that has been shown to limit lignin degradation (Berg and Staaf, 1980), and therefore it is the *Sphagnum* yield that is dominating and thus controlling the SR%.

The $[Ad/Al]_G$ ratio can serve as a proxy for the oxidative stress experienced by the vascular phenols within the peat (Fig. 5.10). Within all four stages $[Ad/Al]_G$ increases down core from the peat surface to the base of the acrotelm. The ratio then decreases with further burial in the mesotelm and catotelm of the BP, BM and FL stages (Fig. 5.10a-c). A different type of profile is observed for the soil horizons underlying the boreal forest surrounding the mire (SF). Here there is a continuous down core increase in the lignin oxidation proxy $[Ad/Al]_G$ for both the hummock and the hollow (Fig. 5.10d). The Mann Whitney test shows that the BM and SF have significantly higher $[Ad/Al]_G$ ratios with respect to the BP and LF cores ($p<0.005$), indicating that from the bog-forest margin (BM/SF) to the bog centre and fen lagg (BP/LF), the oxidative stress decreases, limiting the degree of decomposition occurring at these two sites. The use of unlabelled TMAH for the THM analysis of the peat core samples means that the lignin phenols are uncorrected for non-lignin phenols, therefore Λ displays the total vascular phenol yield, as opposed to the lignin phenol yield.

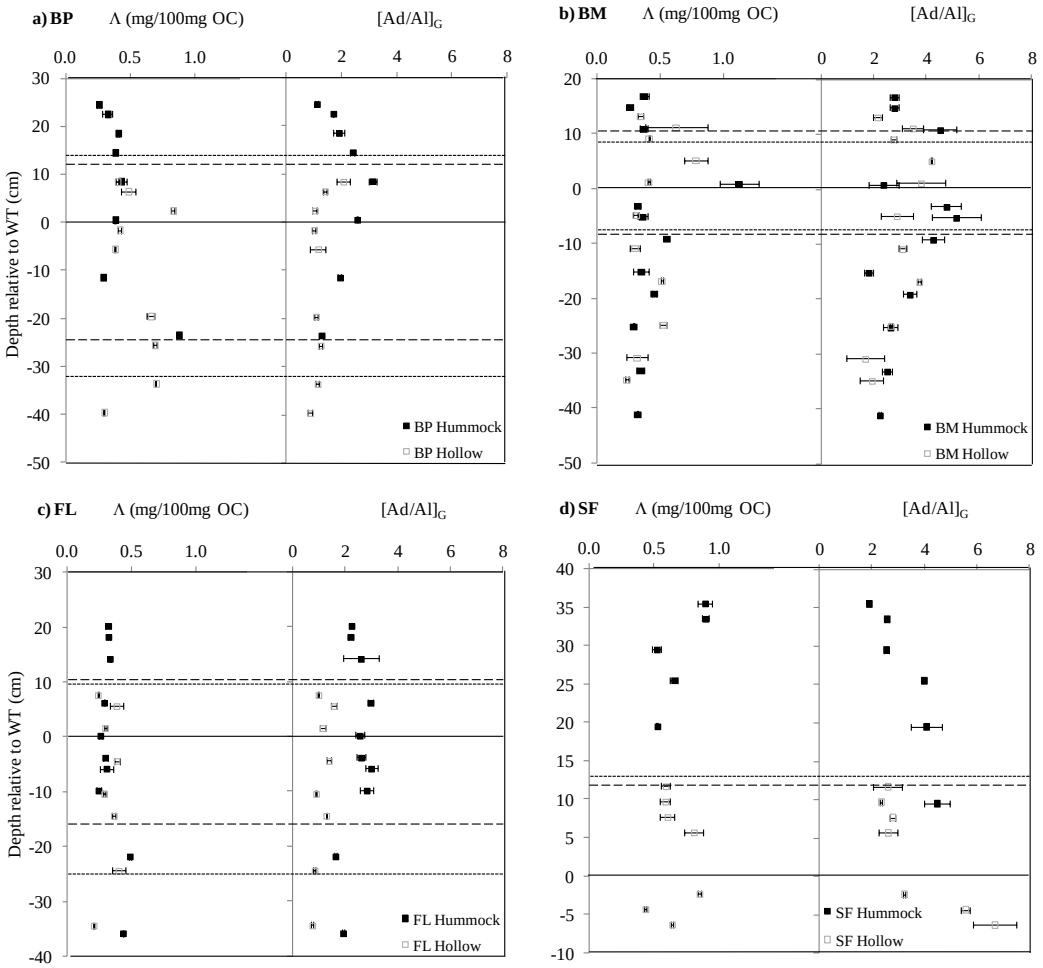

Fig. 5.10: Depth profiles of Λ (mg/100 mg OC) and $[Ad/Al]_G$ for cores from either hummock (filled squares) or hollow (open squares) from the (a) BP, (b) BM, (c) FL and (d) SF stages. Error bars represent the standard error from two analytical replicates.

*Mean water table indicated by the solid horizontal line, interannual water fluctuations denoted by the dashed/dotted lines for the hollow/hummock cores, respectively.

Furthermore, the $[Ad/Al]_G$ values may underestimate the state of oxidation, as the degree of fractionation of the phenols, and input of non-lignin phenols has not been taken into account (Chapter 4, Section 4.3.6). However, the input of non-lignin phenols and the subsequent degree of underestimation should be consistent down core, therefore the trends can still be assessed.

The yield of each of the four *Sphagnum* marker compounds **I**, **IIa/b** and **III** ($\sigma_{\mathbf{I}}$, $\sigma_{\mathbf{IIa/b}}$ and $\sigma_{\mathbf{III}}$) are shown in Fig. 5.11. Trends were similar to the σ depth profiles in the unsaturated and seasonally-saturated layers, with the four sphagnum acid products decreasing simultaneously. However in the cores that extended deep enough, the amount of **I** tended to increase through the permanently-saturated layer, whilst the yield of **IIa/b** and **III** remained relatively constant below the mean water table.

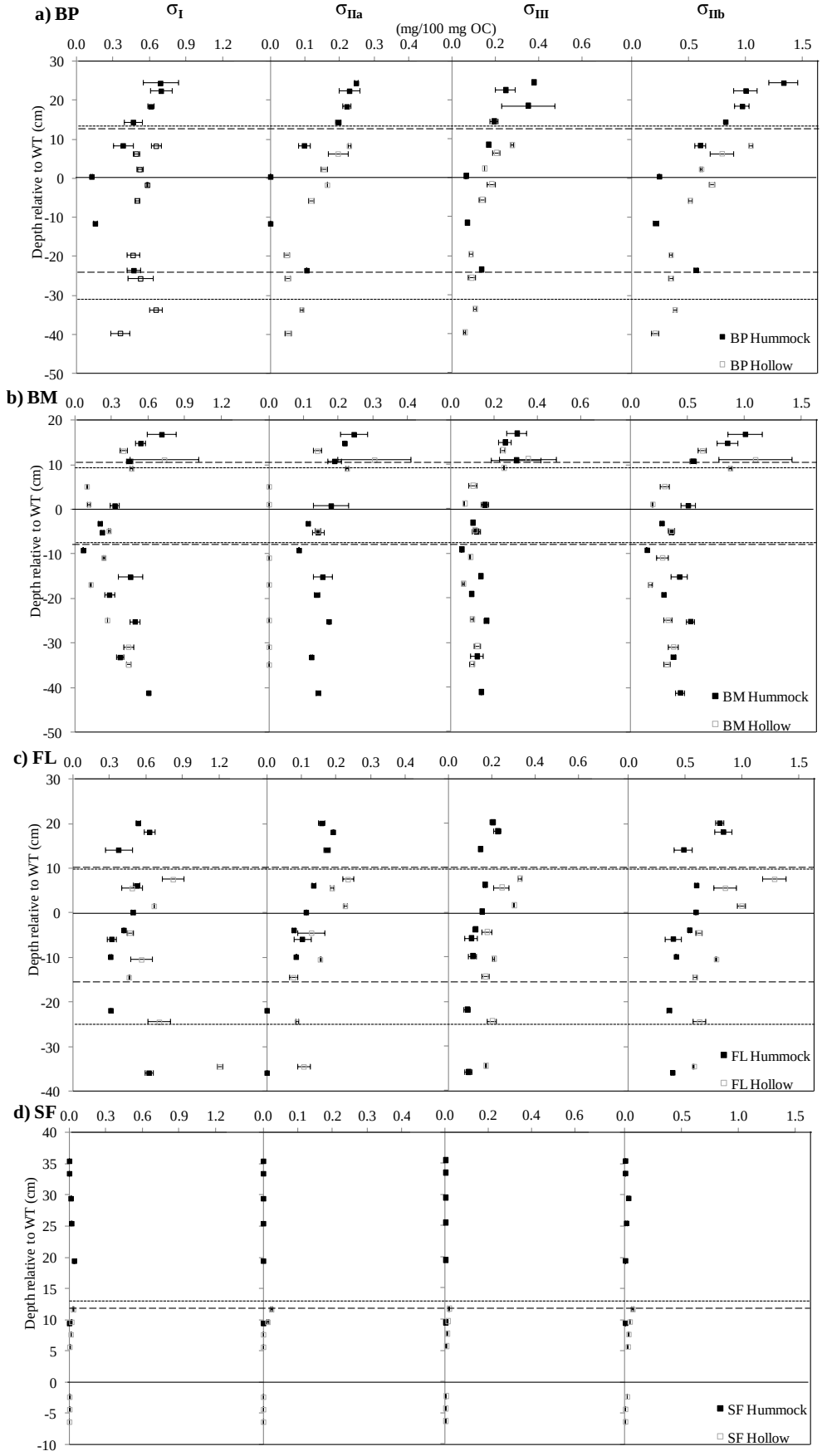

Fig. 5.11: Depth profiles of individual σ component yields; **I**, **IIa**, **III**, **IIb** (mg/100 mg OC) from either hummock (filled squares) or hollow (open squares) from the (a) BP, (b) BM, (c) FL and (d) SF stages. Error bars represent SE from two analytical replicates. *Mean water table indicated by the solid horizontal line, interannual water fluctuations denoted by the dashed/dotted lines for the hollow/hummock cores, respectively.

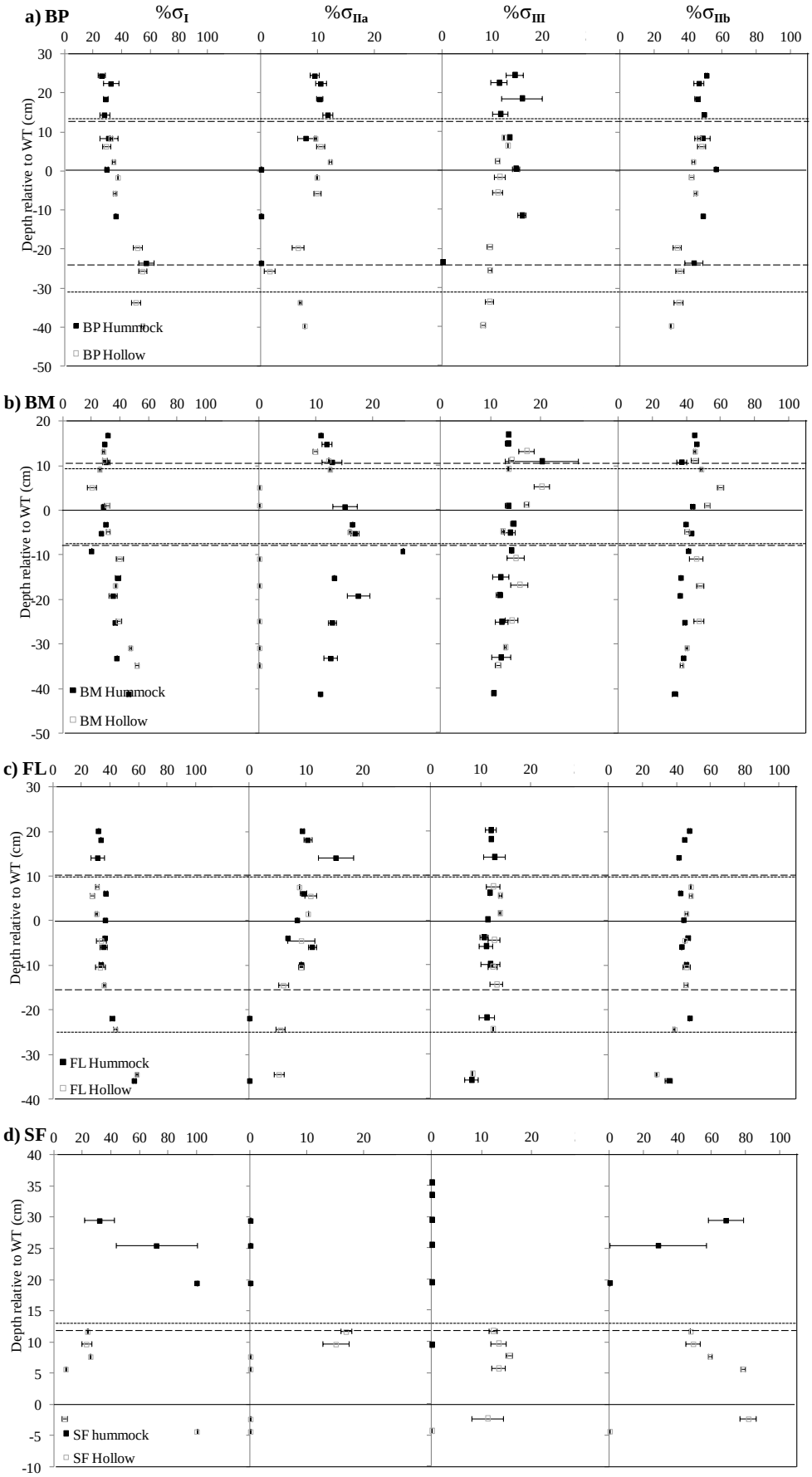

Fig. 5.12: Depth profiles of individual σ components relative to total σ (%) from either hummock (filled squares) or hollow (open squares) from the (a) BP, (b) BM, (c) FL and (d) SF stages. Error bars represent the standard error from two analytical replicates. *Mean water table indicated by the solid horizontal line, interannual water fluctuations denoted by the dashed/dotted lines for the hollow/hummock cores, respectively.

For the SF stage, there were small amounts of **I** and **IIb** in the hummock core (< 0.04 ± 0.01 mg/100 mg OC), however **IIa** and **III** were not present, corresponding to the low *Sphagnum* cover (< 6%) observed at the site. The surficial layer in the hollow core contained **IIa** and **III**, and had greater amounts of **I** and **IIb** than the hummock core, owing to the increased *Sphagnum* vegetation cover at this site. There was a dramatic decrease in the total *Sphagnum* yield in the hollow core from 0.14 ± 0.14 at the base of the unsaturated layer to 0.02 ± 0.009 mg/100 mg OC just below the mean water table.

The proportion of each of the four *Sphagnum* marker compounds to the total *Sphagnum* yield was calculated to determine the specific degradation profiles of the four sphagnum acid thermochemolysis products across the peat. Where: $\left[\sigma_{\mathbf{I}}\% = \left(\frac{\sigma_{\mathbf{I}}}{\sigma}\right) \text{ x } 100\right]$; $\left[\sigma_{\mathbf{IIa}}\% = \sigma\mathbf{IIa}\sigma \text{ x } \textit{100}; \sigma_{\mathbf{III}}\% = \sigma\mathbf{III}\sigma \text{ x } \textit{100}; \text{and } \sigma_{\mathbf{IIb}}\% = \sigma\mathbf{IIb}\sigma \text{ x } \textit{100}\right.$ (Fig. 5.12).

As for the $\sigma_{\mathbf{I}}$, $\sigma_{\mathbf{IIa/b}}$ and $\sigma_{\mathbf{III}}$ amount-depth profiles for the BP, BM and FL cores, the percent of **I**, **IIa/b** and **III** relative to total *Sphagnum* yield showed similar patterns in relation to water table fluctuations (Fig. 5.12a-c).

Compounds **I** and **IIb** are the dominant *Sphagnum* markers, contributing an average 80.5 ± 0.7% of total *Sphagnum* yield across the four bog stages. In the BP, BM and FL, the contribution of **I** to the total *Sphagnum* yield remained constant in the unsaturated and seasonally-saturated peat (30.7 ± 1.2%), increasing to 46.7 ± 2.1% in the permanently-saturated peat. The percent of **IIa/b** and **III** also remain stable in the unsaturated peat, however display a decrease in the seasonally-saturated and permanently-saturated peat. For the SF stage, the $\%\sigma_{\mathbf{(I,\ IIa/b\ and\ III)}}$ depth profiles (Fig. 5.12d) were markedly different to those of the BP, BM and FL stages. The hummock core displays a rapid increase in the proportion of **I** at the expense of **IIb**, however individual yields of these products are very small, and therefore lead to rather high standard errors. The SF hollow core displayed an increase in $\%\sigma_{\mathbf{IIb}}$ above the mean water table, however once below, the proportion of **I** increases at the expense of **IIb**.

Within the unsaturated peat the yield of **I**, **IIa/b** and **III** decrease simultaneously in the oxic peat (Fig. 5.11). With further increase in burial depth to the seasonally-saturated layer, total *Sphagnum* yield remains stable, as $\%\sigma_{\mathbf{I}}$ increases relative to $\%\sigma_{\mathbf{(IIa/b\ and\ III)}}$, indicating additional decarboxylation of **II** and **III**. In the cores that extend into the permanently saturated peat, the yield of **I** increases, as $\%\sigma_{\mathbf{I}}$ continues to increases

relative to $\%\sigma_{(\mathbf{IIa/b}\text{ and }\mathbf{III})}$ (Figs. 5.9 and 5.12). It appears that at the peat surface where the *Sphagnum* litter is relatively fresh, **I** is present in the thermochemolysate due to the in situ decarboxylation of sphagnum acid brought on by TMAH, and accounts for approximately 31% of the *Sphagnum* yield (van der Heijden et al., 1997). Throughout the unsaturated peat, the sphagnum acid is degraded resulting in a consistent proportion of the four products. However with increasing depth the yield of **I** increases relative to **IIa/b** and **III**. As previously established by van der Heijden et al. (1997), **II** and **III** are stabilised via transesterification processes, preventing the further formation of **I** beyond that observed via the decarboxylation of the sphagnum acid (van der Heijden et al., 1997).Therefore the increase in the yield of **I** relative to **II** and **III** at depth suggests further decarboxylation of sphagnum acid within the peat (Fig. 5.12). The increase occurs at the bottom seasonally-saturated peat, and into the permanently-saturated peat, and occurs alongside a stabilisation in the total *Sphagnum* yield, suggesting that **I** remains stable within the anoxic zone of peat.

Due to the ultrasonic extraction procedure prior to thermochemolysis, the products released from the peat samples are representative of the bound products only. Therefore these results suggest that the sphagnum acid which is ether linked to the cell wall is decarboxylated prior to TMAH analysis, probably by microbial activity in the anoxic peat. It is hypothesised that the decarboxylated product of sphagnum acid (i.e. isopropenyl phenol) remains bound into the polymer via the original ether bonds (van der Heijden et al., 1997), and therefore remains present after solvent extraction. However, the activity of the major biodegradative hydrolyase enzymes are known to be suppressed in peatlands (Kang and Freeman, 1999). The sphagnum acid may also include ester links on the carboxylic acid functional groups, however this would not lend itself to the increase of isopropenyl phenol during degradation. These results clearly indicate that further research into the mechanisms involved during sphagnum acid decarboxylation, and the linkages involved within sphagnum acid is required.

The loss of sphagnum acid occurs primarily in the aerated and seasonally aerated peat, whilst deeper saturated peat displays the stabilisation of sphagnum acid primarily as **I**, where anoxic decomposition occurs about 50 times slower than aerobic decomposition (Clymo, 1983). If drawdown of the water table were to occur in any of these stages, previously stabilised *Sphagnum* phenols may become susceptible to degradation. The breakdown of phenols more than likely results from the stimulation of phenol oxidase

activity, which intensifies during drought conditions (Fenner and Freeman, 2011). The removal of sphagnum acid during water table drawdown may explain why rates of decomposition in peatlands are highest in the seasonally saturated layer (Belyea, 1996). Furthermore, Schouwenaars (1988) showed that the aeration and subsequent decomposition of *Sphagnum* peat after drainage irreversibly increased the permeability of peat, which made the peat substrate unsuitable for the re-growth of *Sphagnum*.

If climate change leads to intensification of the hydrological cycle with more frequent and more extreme drying and rewetting, previously stabilised peat may become subject to rapid decomposition (Fenner and Freeman, 2011). Projected increases in evapotranspiration are likely to lead to drier summers in continental regions (IPCC, 2007), including those with large expanses of peatland. As a consequence of such climatic change, lawns and hummocks may expand laterally and thicken vertically, becoming drier; conversely, hollows may shrink in lateral extent but deepen, becoming wetter (Belyea, 2009). At the peatland-forest ecotone, local topography and successional history may determine whether projected climate change will lead to expansion or shrinkage of the peatland extent (Peregon et al., 2007). This further supports the view that although peatlands are adaptive systems they may be shifting to new states at higher levels of disturbance (Dise, 2009).

5.4 Conclusions

Consistent vegetation cover since 1925 has shown that the depth-dependent changes in phenolic composition of the cores can be primarily attributed to diagenetic changes, except perhaps in the SF hollow core, where the rapid decrease in *Sphagnum* phenols below the mean water table coupled with a high TON, reflects a vegetation change. Therefore the decomposition of OM in the surficial peat appears to be isotopically selective process for carbon, with the preferential release of lighter molecules resulting in the enrichment of more positive isotope shifts in the residual solid peat matrix.

The BP, BM and FL cores all show a progressive increase in the bulk density from the acrotelm into the catotelm consistent with the values cited by Clymo (1992), which subsequently leads to the progressively increasing carbon storage with depth. The SF hollow displays a large carbon storage particularly in the deep mineral soil, indicating that the mineral-fed marginal peats undergoing paludification may have the highest

capacity for carbon storage due to the high bulk density combined with the relatively high TOC for mineral soil.

The peat cores revealed large quantities of carbohydrates, indicating a relatively slow degradation of these compounds, with the carbohydrate yield decreasing from the bog centre to the bog-forest margin. The dominant monosaccharide, glucose, reflected the large cellulose content in *Sphagnum* mosses. Individual sugar profiles confirmed vegetation source; with high levels of the aldopentoses (specifically arabinose and fucose) in the SF indicative of sedges, and high levels of galactose, mannose and rhamnose in the BP, BM and FL indicative of mosses. These moss indicators increased in the catotelm of the BP, BM and FL, whereas sedge indicators showed decreases in the catotelm, indicating the selective preservation of the moss monosaccharides in the anoxic zone. Within the acrotelm of the BP, BM and FL cores, *Sphagnum* phenols are lost then become stabilised in the catotelm. The carbohydrates however remain relatively stable down core. From these results we can infer that the cell-wall carbohydrates of the *Sphagnum* mosses are the primary microbial inhibitors resulting in a high decay resistance regardless of the oxic conditions, whereas *Sphagnum* phenols only become resistant to degradation in the anoxic conditions.

The individual sphagnum acid biomarkers; **I**, **IIa/b**, **III** persist into the peat archives and provide information on the extent of the oxic conditions of a site. The SR% across the BP, BM and FL stages in the Ryggmossen bog indicates that *Sphagnum* phenols are oxidised preferentially over vascular plant phenols in the acrotelm and mesotelm, with all four sphagnum acid THM products decreasing simultaneously. The stabilisation of *Sphagnum*-derived phenols relative to other phenols occurs within the permanently saturated layer, however the distribution of the four sphagnum acid THM products has shifted, so that **I** accounts for a larger proportion of the *Sphagnum* yield. The increase of **I** relative to **IIa/b** and **III**, indicates the additional decarboxylation beyond that caused by thermochemolysis. Therefore these four products could potentially be used as a proxy for the degree of oxidation in peatlands, and provide direct information on the degradation of *Sphagnum* mosses in peat. Further work could utilise deeper cores to establish whether sphagnum acid is completely decarboxylated with increasing depth.

The new biomarkers and indices reported here provide tools for tracking the input, accumulation and degradation of *Sphagnum* phenols in peat profiles. From these results we can infer that the water table dynamics play an important role in the degradation of

Sphagnum phenols, with the seasonally and permanently saturated layers favouring the stability and accumulation of *Sphagnum* phenols. However when exposed to oxic conditions above the mean water table, the *Sphagnum* markers are rapidly lost. This suggests that sphagnum acid is stripped away from the bryophyte cell walls under oxic conditions such that any rewetting of the peat could potentially lead to anaerobic hydrolysis and fermentation of the newly exposed carbohydrates thereby further increasing the vulnerability of the peat to further decomposition whereas *Sphagnum* phenols will be preferentially stabilized in peatlands shifting to a wetter regime. These results highlight the sensitivity of *Sphagnum* litter and peat exposed to oxic conditions, which would be affected by a lowered water table brought on by climate change. Further studies on peat profiles from different climate regions, as well as mechanistic studies on processes of *Sphagnum* phenol degradation, are required.

Chapter 6:

The Edge Effect of a Sitka Spruce Plantation on the Carbon Storage and Phenolic Distribution in an Adjacent Peatland

6 The Edge Effect of a Sitka Spruce Plantation on the Carbon Storage and Phenolic Distribution in an Adjacent Peatland

6.1 Introduction

Peatland soils are by definition, soils with more than 40 cm organic material, or more than 30 cm if directly overlying bedrock, and lacking overlying non-humose mineral horizons extending below 30 cm (Avery, 1980). The high carbon storage of peatlands (547 Gt OC) makes them very valuable habitats (Yu et al., 2010), however the rates of carbon sequestration on peatlands are a complex balance between carbon inputs and carbon outputs (Post et al., 1982), with minor changes in surface vegetation or water table depth, amongst other variables, potentially having a significant effect on the carbon storage dynamics (Belyea and Malmer, 2004).

Between the 1950s and 1980s approximately 190,000 ha of deep peats and 315,000 ha of shallow peats in Britain alone were drained, ploughed and planted with coniferous forest, the largest recent land-use change seen in Britain (Cannell et al., 1993). The afforestation of deep peats is no longer supported in the UK, owing to the adverse effects on the wetland habitat including its capacity as a carbon sink (Morison et al., 2010). Pockets of unplanted moorland have remained at many plantation sites across the UK including Kielder Forest, due to their unsuitability for timber production, many of which are now considered conservation areas (Robinson et al., 1998). The effect of afforestation on moorlands has been explored in Chapter 3, however there has been concern that the impact of afforestation of moorlands is not restricted to the planted area alone (Holden et al., 2007). For example, the vegetation cover of an unplanted moorland site at Wark Forest shifted from a *Sphagnum* dominated vegetation cover in the late 1950s to a mixed cotton grass, heather and grass vegetation cover in the late 1980s (Chapman and Rose, 1991). These changes have been attributed to the drying and shrinkage of the organic soils, which can occur at some distance away from the afforested site depending on local topography and drainage (Chapman and Rose, 1991; Holden et al., 2007). Together with a change in vegetation cover, the spreading of Sitka spruce (*Picea sitchensis* (Bong.) *Carr.*) from forest plantations and onto areas of open bog and moorland has been seen to have a significant negative impact upon the habitat by further reducing the area of natural habitat (Farmer, 2011). For example, recent management of open moorland to restore the original habitat of blanket bog in Wales,

included the removal of over 11,000 self-seeded trees on 6000 ha of moorland in Vyrnwy (Farmer, 2011).

The effects of afforestation on the phenolic distributions of soil organic matter from peaty gley soils have been presented in Chapter 3 and by Mason et al. (2009; 2012) at Coalburn and Harwood Forest; sites within close proximity to Wark Forest explored in this study. It was found that the afforestation had a significant effect on the degradation of lignin; identifying a change in the vegetation input and investigating the effect of land preparation undertaken prior to the afforestation. A maximum of lignin products were found at depth in both studies and was chiefly attributed to the horizon inversion that occurred between stands. So far, however, there has been no research carried out on the effect of the establishment and growth of self seeded Sitka spruce adjacent to the plantation site on the carbon storage and phenolic dynamics of blanket bog habitats.

The contribution of lignin and tannin to soil organic matter (SOM) and their role in the global carbon cycle is significant, as they are the second most abundant biopolymers on Earth after cellulose and hemicellulose (Hernes and Hedges, 2000). Lignin, a complex aromatic polymer, provides mechanical strength to vascular plants and is essential to water transport (Nierop and Filley, 2008). Whereas tannin, a water soluble polyphenol, can inhibit the growth of a number of micro-organisms, resisting microbial attack, and therefore are recalcitrant to biodegradation (Bate-Smith and Swain, 1962; Bhat et al., 1998). Lignin can be divided into three main groups based on their structural monomer units; gymnosperm, angiosperm and grass lignin (non-woody) (Higuchi, 1980) (Section 1.2.7). Tannin can be divided into two main groups; hydrolysable tannins and condensed tannins (Section 1.2.11).

Tannin can exceed lignin concentrations in plant litter (leaves, roots, needles), accounting for up to 40% dry weight (Kraus et al., 2003), however the fate of tannin within soils remains largely unknown (Nierop et al., 2005). This is a direct result of the principal shortcoming of unlabelled thermochemolysis, making it impossible to differentiate between the intact lignin, demethylated lignin (from fungal degradation) and non-lignin phenols (e.g. tannin) (Filley et al., 2000). However the introduction of ^{13}C-labelled TMAH in 1999, methylating phenolic acids and phenols using ^{13}C-labelled methyl groups, allows the true lignin input, or at least lignin bound by the dominant β-O-4 linkage (Section 1.2.10) (Filley et al., 1999; Filley et al., 2006), to be ascertained.

This technique has been successfully used to analyse a variety of biopolymers, SOM and DOM (Filley et al., 2000; Filley et al., 2002; Frazier et al., 2005; Filley et al., 2006; Nierop and Filley, 2007; Mason et al., 2012). As a result, it is important to accurately determine the concentration and input of these groups of products within soils to provide a better understanding of the importance of lignin and tannin to ecosystem processes.

This chapter reports on a chronosequence of carbon rich peat soils. A chronosequence is defined as a sequence of related soils that differ from one another in certain properties primarily as a result of time as a soil forming factor, and the phenolic distribution both down the profile and across the chronosequence (Soil Science Society of America, 2001) . The peat profiles were sampled from Wark Forest, an afforested moorland site in northeast England, part of the larger Kielder Forest, and analysed with ^{13}C-labelled TMAH. The site includes two soil profiles in an undisturbed open peat and four profiles in the forest-margin peat, where self seeded Sitka spruce have encroached from the plantation site on to the undisturbed moorland. The assessment of the forest-margin peat comprised two pits amongst self seeded area of Sitka spruce but not situated underneath the canopy, and two pits located directly under the canopy of Sitka spruce. This site has not experienced any land preparation such as drainage or mounding which is often seen prior to afforestation. This is the first study to investigate the potential edge effect of Sitka spruce plantations on the adjacent moorland including self seeding Sitka spruce, on the soil carbon storage and phenolic dynamics.

The objectives of this study are to (i) identify key vegetation biomarkers and evaluate the changes of the chemical characteristics as a function of depth down the litter (L), and histic horizons (Hf and Hs), (ii) compare and evaluate the changes across the three sites within Wark Forest to explore whether the adjacent forest and self seeded Sitka spruce affect the phenolic and SOC dynamics down core and (iii) further explore the potential of ^{13}C-TMAH thermochemolysis as a screening method for the rapid characterisation of biomacromolecules in SOM as a function of depth.

6.2 Overview of Methods and Sites

6.2.1 Site Background

Peat profiles were sampled from Wark Forest, an afforested moorland site in northeast England (55°04`N, 2°18`W), which is located within Kielder Forest, a plantation forest colonised primarily with Sitka spruce since the 1930s (Fig. 2.7). A detailed site description of Wark Forest is presented in Chapter 2, Section 2.7.4.

A chronosequence of six peat profiles extending from the open peat to the forest-peat ecotone (forest-margin; FM) experiencing the growth of self seeded Sitka spruce (SS) from the adjacent plantation site were identified (Fig. 6.1). The profiles comprised two soil profiles in an undisturbed open peat and four profiles in the forest-margin peat, where the adjacent Sitka spruce plantation has begun to encroach on to the unprepared open moorland via self seeding.

In March 2010, soil pits were dug at each site to a depth of 50 cm, soil samples taken from the centre of each identified soil horizon. The soil profiles were entirely organic, with samples taken from the three ectorganic layers; the litter (L) horizon, the fabric histic (Hf) horizon and the sapric histic (Hs) horizon, identified according to the EU humus classification system (Zanella et al., 2011). Profile details are described in Section 2.7.4.

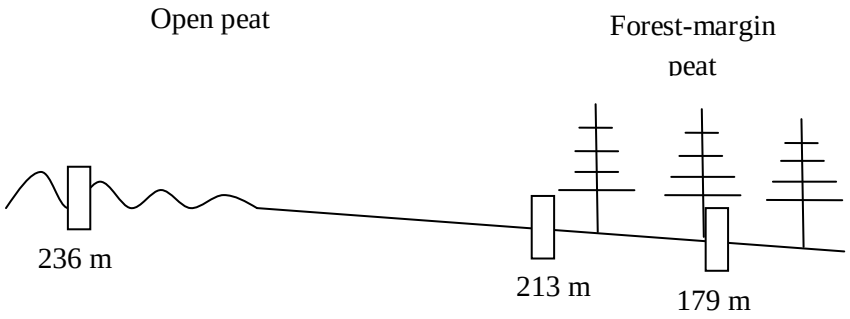

Fig. 6.1: Diagrammatic representation of the Wark Forest chronosequence. The site locations located along the transect moving from the open peat towards self seeded Sitka spruce on forest-margin peat with their respective mean elevations (AOD) for two pits.

6.2.2 TOC, Bulk Density & Carbon Storage

Peat bulk density (D_b) was determined in duplicate for each peat horizon (H) within each pit using 100 cm^3 soil cores, and the total organic carbon (TOC) content was measured in duplicate for each horizon. The organic carbon storage (OC t C ha^{-1}) in each horizon is calculated using the bulk density values and the horizon depths using Equation 2.2 (Chapter 2, Section 2.6).

6.2.3 ^{13}C-TMAH Thermochemolysis

On-line THM in the presence of ^{13}C-labelled and unlabelled TMAH was performed at 610 °C for 10 s (20 °C/ms temperature ramp) using the method set out in Section 2.2. Percent aromatic hydroxyl content was determined using equations and mass spectral methods set out in previous work (Filley et al., 1999; Filley et al., 2006; Mason et al., 2009) (Appendix A1). Duplicate samples of each solvent extracted soil were analysed from each horizon using both unlabelled and ^{13}C-labelled TMAH. THM in the presence of ^{13}C-labelled TMAH and aromatic hydroxyl contents are discussed in further detail in Section 2.2.

6.2.4 Lignin & Sphagnum Parameters

Lignin proxies were used as described in Chapter 2 (Section 2.2.2), with all phenol yields normalised to 100 mg of organic carbon (see Fig. 1.5, for compound structures) (Hedges and Mann, 1979b; Hedges et al., 1982; Kögel, 1986). Sphagnum proxies were used as described in Chapter 4 (Section 4.3.5).

6.3 Results and Discussion

6.3.1 Carbon Storage

The TOC and organic carbon storage (OC t C ha^{-1}) for each horizon of the three sites are presented in Table 6.1 and Fig. 6.2. The TOC (wt%) across the three sites does not vary significantly (p=0.398), and with a total average TOC across the sites of 43.0% ± 0.45 down to 50 cm, these soils are classified as peats. In the forest-margin peat under Sitka spruce (SS) and the open peat, the TOC significantly increases down core by 5.7

and 7.1%, respectively ($p<0.001$ and 0.020), suggesting either an accumulation of TOC at depth and/or the loss of TOC at the surface due to increased decomposition or reduced input (Table 6.1).

The bulk density increases from 0.13 g cm^{-3} in the forest-margin peat under the SS through to 0.18 g cm^{-3} in the open peat, although changes are not significant ($p=0.711$), indicating that neither the edge effect from the adjacent drained plantation nor the compaction from the increased loading as observed in Chapter 3, has yet had a significant effect on the bulk density of the forest-margin peat. However Braekke (1987) also found no significant difference in the bulk density of the peat soil after afforestation, which was attributed to an increased density of roots, coupled with the subsequent decrease in the density of the original peat, resulting in no discernible differences.

The open peat has a significantly higher carbon storage of 409.2 t ha^{-1} compared to the forest-margin peat sites 284.1 and 297.3 t ha^{-1} respectively ($p=0.006$) (Table.6.1), which is comparable to the moorland (ML) soil carbon storage at Coalburn Forest (431.9 t ha^{-1} in 45 cm; Chapter 3), a site which is in close proximity to Wark Forest with peaty gley soils with mineral soil horizons and higher bulk densities. Despite no significant changes in the bulk density across the Wark chronosequence, the carbon storage decrease at the forest-margin peat could be due to enhanced aeration from the preliminary drying occurring at the site, which has not yet affected the bulk density; a result of the adjacent ditched and drained plantation site.

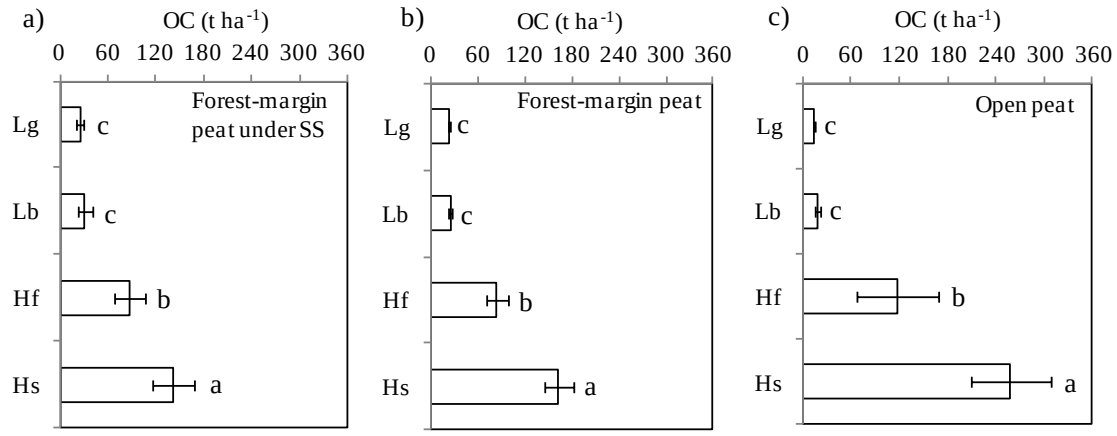

Fig. 6.2: Soil carbon storage contents (t C ha^{-1}) in (a) FM peat under Sitka spruce, (b) the FM peat and (c) the open peat. Error bars represent the standard error of the mean for the two pit replicates. Means with different letters are significantly different (Tukey's HSD, $p<0.05$).

Table 6.1: The TOC (%), bulk density (g cm^{-3}), soil organic carbon storage (t C ha^{-1} and %) for each horizon of the Wark Forest chronosequence.

	TOC[1] (wt %)	D_b[2] (g cm^{-3})	OC[1] (t ha^{-1})	OC (% total)
Forest-margin peat under Sitka spruce				
L (Green)	38.1 b ± 0.26	0.130 ± 0.006	24.7 c ± 4.8	8.7
L (Brown)	42.5 a ± 1.14	0.130 ± 0.006	30.7 c ± 9.2	10.8
H (fibric)	45.5 a ± 1.31	0.130 ± 0.006	86.5 b ± 18.9	30.4
H (sapric)	43.8 a ± 0.69	0.130 ± 0.006	142.1 a ± 25.9	49.9
			284.1 b	100
Forest-margin peat				
L (Green)	43.2 ± 1.27	0.138 ± 0.015	23.8 c ± 0.49	8.0
L (Brown)	40.8 ± 1.92	0.138 ± 0.015	25.3 c ± 2.44	8.5
H (fibric)	43.7 ± 0.87	0.138 ± 0.015	84.7 b ± 14.18	28.5
H (sapric)	43.0 ± 0.69	0.138 ± 0.015	163.5 a ± 18.72	55.0
			297.3 b	100
Open peat				
L (Green)	40.6 b ± 1.66	0.179 ± 0.064	14.5 c ± 0.30	3.5
L (Brown)	42.7 ab ± 0.40	0.179 ± 0.064	19.1 c ± 3.66	4.7
H (fibric)	44.5 ab ± 1.52	0.179 ± 0.064	117.0 b ± 50.46	28.6
H (sapric)	47.7 a ± 0.91	0.179 ± 0.064	258.6 a ± 49.11	63.2
			409.2 a	100

[1]SE=4; [2] Bulk density measurement taken in H horizon, SE=2.

Means followed by the same letter are not significantly different.

Carbon storage in each horizon down to 50 cm depth at each site is presented in Fig. 6.2, displaying a significant increase in the carbon storage from the Litter (Lg and Lb) into the Hf horizon and again into the Hs horizon at all three sites ($p<0.001$). Carbon storage in the litter horizon (LOC) of the open peat (33.6 t C ha^{-1}), was significantly smaller than that of the litter in the forest-margin peat under SS (55.4 t C ha^{-1}) ($p=0.03$) (Fig. 6.3). The forest-margin peat away from the SS canopy had an intermediate litter carbon storage of 49.1 t C ha^{-1}. The increased LOC across the chronosequence suggests an increased litterfall at the forest-margin peat under SS, reflected in the thicker litter horizon of the forest-margin peat under SS, which decreases with increasing distance from the tree canopy.

The carbon storage of the Hf horizon is significantly similar across the three sites (96.1 t C ha^{-1}) ($p=0.059$), whereas the carbon storage in the Hs horizon is significantly higher in the open peat (258.6 t C ha^{-1}) than the two forest-margin peats (142.1 and 163.5 t C ha^{-1}) ($p=0.005$). The distribution of carbon down the cores shifts from the forest-margin peats having a higher LOC than the open peat, to the open peat having a higher Hs OC compared to the forest-margin peats (Fig. 6.3). Data reported in Chapter 3, together with literature also display an elevated carbon content in the Hs horizon (Zerva and Mencuccini, 2005; Mason et al., 2009) where an elevated Hs OC in the moorland site relative to the first rotation Sitka spruce stand was observed. The forest-margin peats are behaving similarly to the first rotation SS stand (SS1; Coalburn Forest), displaying an elevated LOC, constant Hf OC and reduced Hs OC relative to the natural undisturbed habitat (Chapter 3, Section 3.3.1.3), indicating that the OC trends are strongly governed by the introduction and early stages of tree growth, whether it be human-induced or natural. This increased carbon storage at depth in the open peat is likely a result of the stabilisation of carbon in SOM, due to the prevalent anaerobic conditions in the open peat (Freeman et al., 2001a), coupled with the destabilisation of carbon stocks in the forest-margin peat due to increased aeration, potentially as a result of the introduction of Sitka spruce as seen in Chapter 3 and by Zerva et al. (2005) and Hargreaves et al. (2003).

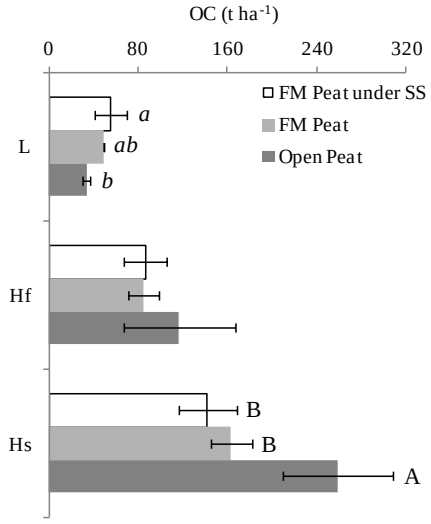

Fig. 6.3: Soil carbon storage (t C ha^{-1}) in litter the (L), weakly degraded humic (Hf) and degraded humic (Hs) horizons of the peat under the Wark chronosequence. Error bars represent the standard error of the mean for the two pit replicates. Means with different letters are significantly different (Tukey's HSD, $p<0.05$).

6.3.2 Thermochemolysis Products

THM in the presence of TMAH of the solvent-extracted powdered soil samples yielded mainly four sets of methylated phenolic and other oxygenated aromatic products (Table 6.2). The first set includes methylated phenols with guaiacyl (G), syringyl (S), and *p*-hydroxyphenyl (P) structures together with the methyl esters of the cinnamyl phenols, ferulic acid (G18), and *p*-coumaric acid (P18). ^{13}C-labelled TMAH allowed the distinction between lignin- and non-lignin-derived (particularly tannin) phenols and enabled each group to be analysed separately. The second set comprises four sphagnum acid pyrolysis products (**I**, **IIa/b** and **III**); methylated 4-isopropenylphenol, methylated (E) and (*Z*)- 3-(4-hydroxyphen-1-yl)but-2-enoic acid, and methylated 3-(4-hydroxyphen-1-yl)but-3-enoic acid, derived from the *Sphagnum* specific, sphagnum acid (Chapter 4) (van der Heijden, 1994; van der Heijden et al., 1997). The third set comprises non-lignin aromatic compounds including 1,2,4-trimethoxybenzene (1,2,4-TMB) and 1,3,5-trimethoxybenzene (1,3,5-TMB). The aromatic hydroxyl content of 1,2,4-TMB and 1,3,5-TMB were determined using equations and mass spectral methods set out in previous work (Filley et al., 1999; Mason et al., 2009); whereby 100% of the identified peak could be assigned to 1 hydroxyl (i.e. one contributing compound). The fourth set of THM products contains four methylated carbohydrates (MC1-4) with *m/z* 101, 129, and five cellulose derived products (1-5). These are discussed in further detail in Chapter 7.

Table 6.2: The main thermochemolysis products

Peak Label	Compound
P1	methoxybenzene
P2	4-methoxytoluene
G1	1,2-dimethoxybenzene
P3	4-methoxybenzeneethylene
1-4	cellulose derivatives 1 - 4
G2	3,4-dimethoxytoluene
I	4-isopropenylphenol
P4	4-methoxybenzaldehyde
P5	4-methoxyacetophenone
G3	3,4-dimethoxybenzeneethylene
1,2,4-TMB	1,2,4-trimethoxybenzene
P6	4-methoxybenzoic acid methyl ester
1,3,5-TMB	1,3,5-trimethoxybenzene
P24	4-methoxybenzeneacetic acid methyl ester
MC1- MC4	methylated carbohydrate derivatives 1 - 4
G4	3,4-dimethoxybenzaldehyde
	(3-hydroxy-4-methoxybenzaldehyde)
P12	4-methoxybenzenepropanoic acid methyl ester
G5	3,4-dimethoxyacetophenone
	(3-hydroxy-4-methoxyacetophenone)
P17	(*Z*)- 3-(4-methoxyphenyl)-3-propenoic acid methyl ester
G6	3,4-dimethoxybenzoic acid methyl ester
	(3-hydroxy-4-methoxybenzoic acid methyl ester)
IIa	(E/*Z*)- 3-(4'hydroxyphen-1-yl)-but-2-enoic acid methyl ester
S4	3,4,5-trimethoxybenzaldehyde
	(3,5-dimethoxy-4-hydroxybenzaldehyde)
III	3-(4'hydroxyphen-1-yl)-but-3-enoic acid methyl ester
G7	(*Z*)- 1-(3,4-dimethoxyphenyl)-2-methoxyethylene
G24	3,4-dimethoxybenzene acetic acid methyl ester
G8	(*E*)- 1-(3,4-dimethoxyphenyl)-2-methoxyethylene
P18	(*E*)- 3-(4-methoxyphenyl)-3-propenoic acid methyl ester
S5	3,4,5-trimethoxyacetophenone
	(3,5-dimethoxy-4-hydroxyacetophenone)
5	cellulose derivative 5
IIb	(E/*Z*)- 3-(4'hydroxyphen-1-yl)-but-2-enoic acid methyl ester
G12	3,4-dimethoxybenzenepropanoic acid methyl ester
S6	3,4,5-trimethoxybenzoic acid methyl ester
	(3,5-dimethoxy-4-hydroxybenzoic acid methyl ester)
S7	(*Z*)- 1-(3,4,5-trimethoxyphenyl)-2-methoxyethylene
S8	(*Z*)- 1-(3,4,5-trimethoxyphenyl)-2-methoxyethylene
G18	(*E*)- 3-(3,4-dimethoxyphenyl)-3-propenoic acid methyl ester
	((*E*)-3-(3-methoxy, 4-hydroxyphenyl) 3-propenoic acid methyl ester)
S14	*threo/erythro* 1-(3,4,5-trimethoxyphenyl)-1,2,3-trimethoxybenzene
FA	C_{16} fatty acid methyl ester
S15	*threo/erythro* 1-(3,4,5-trimethoxyphenyl)-1,2,3-trimethoxybenzene
IS	5α-androstane

* Compounds in red brackets indicate intact lignin products prior to methylation most likely to be affected by non-lignin phenolic input

6.3.2.1 Green litter

Fig. 6.4 depicts the THM results from the Lg horizon across all profiles. The abundance of a wide range of phenolics highlights the different surface vegetation inputs across the relatively short chronosequence. The occurrence of all four *Sphagnum* markers (**I**, **IIa**, **III**, **IIb**) in the forest-margin peat pits under SS and the forest-margin peat pits indicates a vegetation cover consisting of *Sphagnum* moss. 3,4-dimethoxybenzenepropanoic acid methyl ester (G12) is also observed in the forest-margin peat pit one, indicating a vegetation cover of the non-*Sphagnum* moss *Polytrichum commune* (Chapter 4, Section 4.3.4) together with *Sphagnum* moss biomarkers. The forest-margin peat pit two is dominated by 3,4-dimethoxybenzoic acid methyl ester (G6) an indication of gymnosperm input, however only 23.5% is intact lignin, see Section 6.3.3 for further discussion on mass yields. The open peat pits display a different TIC, dominated by G12 in pit one; supported by the identification of *P. commune* within this sample prior to milling (Taylor, 1960). Pit two shows the presence of two unidentified compounds, and despite this litter appearing visually similar to *Sphagnum* moss, contains no *Sphagnum* biomarkers and has therefore been tentatively identified as a common clubmoss (*Lycopodium clavatum*) (Taylor, 1960). This moss-like plant is distinguished from mosses due to the presence of a well developed vascular system, and is often found in well-drained heaths and moors (Taylor, 1960), suggesting the presence of lignin phenols in this species. Further work is evidently required to assess this vegetation with atypical moss characteristics.

The small quantities of *threo/erythro* 1-(3,4,5-trimethoxyphenyl)-1,2,3-trimethoxybenzene (S14/15); true lignin phenols derived solely from lignin (Filley et al., 1999; Nierop and Filley, 2007), in the forest-margin peat samples suggest that the extent of lignin oxidation is advanced even at the surface of the forest-margin peats. The complete absence of these intact lignin phenols in the open bog, further suggests a dominant non-vascular input to the green litter.

6.*3.2.2 Brown litter*

The Lb traces shown in Fig. 6.5, display an increased proportion of lignin phenol G6 across all the sites, although <60% can be attributed to intact lignin (Section 6.3.3). The previously dominating *Sphagnum* markers have decreased in abundance, instead large

abundances of 1,2,4-TMB, 4-methoxybenzoic acid methyl ester (P6), 1,3,5-TMB are observed across the four forest-margin peats. The open peat TICs are still dominated by G12 and two unidentified compounds, however cinnamyl lignin phenols (*p*-coumaric acid, P18 and ferulic acid, G18) are now also dominating, which are indicative of a graminaceous input (Hedges and Mann, 1979a).

6.*3.2.3* *Fibric humic material*

Fig. 6.6 depicts the THM results from the Hf horizon across all profiles. The *Sphagnum* markers have decreased to trace levels, whereas the lignin phenols including the guaiacyl and syringyl acids (G6, S6), and cinnamyl phenols (P18 and G18) are now dominating all six pits. The presence of G18 and P18 highlights a non-woody input (Hedges and Mann, 1979a) across the chronosequence, which is likely to be a combination of grass and heather leaf input. G12 and the 2 unidentified compounds are no longer present in the open peats.

6.3.2.4 *Sapric humic material*

Fig. 6.7 depicts similar Hs horizon traces across the chronosequence, dominated by 3,4-dimethoxybenzeneethylene (G3), 4-methoxybenzoic acid methyl ester (P6), guaiacyl acid (~60% intact G6), the two cinnamyl phenols (~90% intact G18) and 1,2,4-TMB. The humified horizon also shows an increase of methylated carbohydrates in relation to the other compounds. Small quantities of S14 and S15 (lignin phenols with an intact glycerol side chain) remain present down the six peat cores, suggesting that despite advanced oxidation at the surface, there is no further side-chain oxidation down core.

6.3.2.5 *Characterisation of peat profiles*

The green litter strongly reflects the current vegetation growing at each site, however there is no clear indication of the growth of Sitka spruce at the forest-margin peats, but rather a growth of *Sphagnum* and non-*Sphagnum* mosses, with the exception of the forest-margin peat pit two. Therefore it is likely that these traces reflect the ground vegetation, rather than the leaf litter from the Sitka spruce. This is not unexpected, as due to the natural growth of Sitka spruce at this site, the previous vegetation cover of

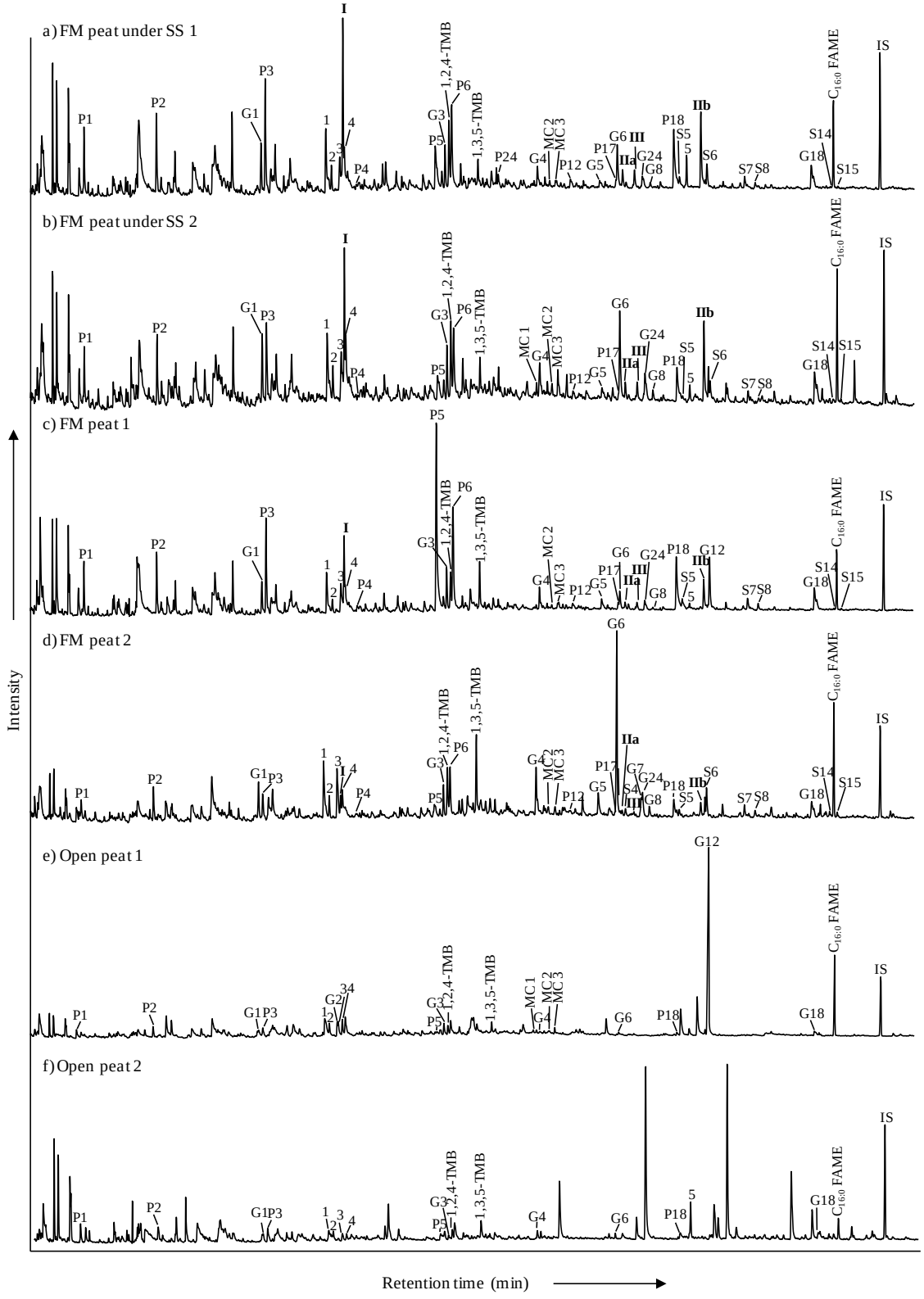

Fig. 6.4: Partial chromatogram for the total ion current (TIC) of the thermochemolysis products from the green litter across all profiles (a) FM peat under SS 1 (b) FM peat under SS 2 (c) FM peat 1 (d) FM peat 2 (e) Open peat 1 and (f) Open peat 2. Peak identities and symbols are listed in Table 6.2.

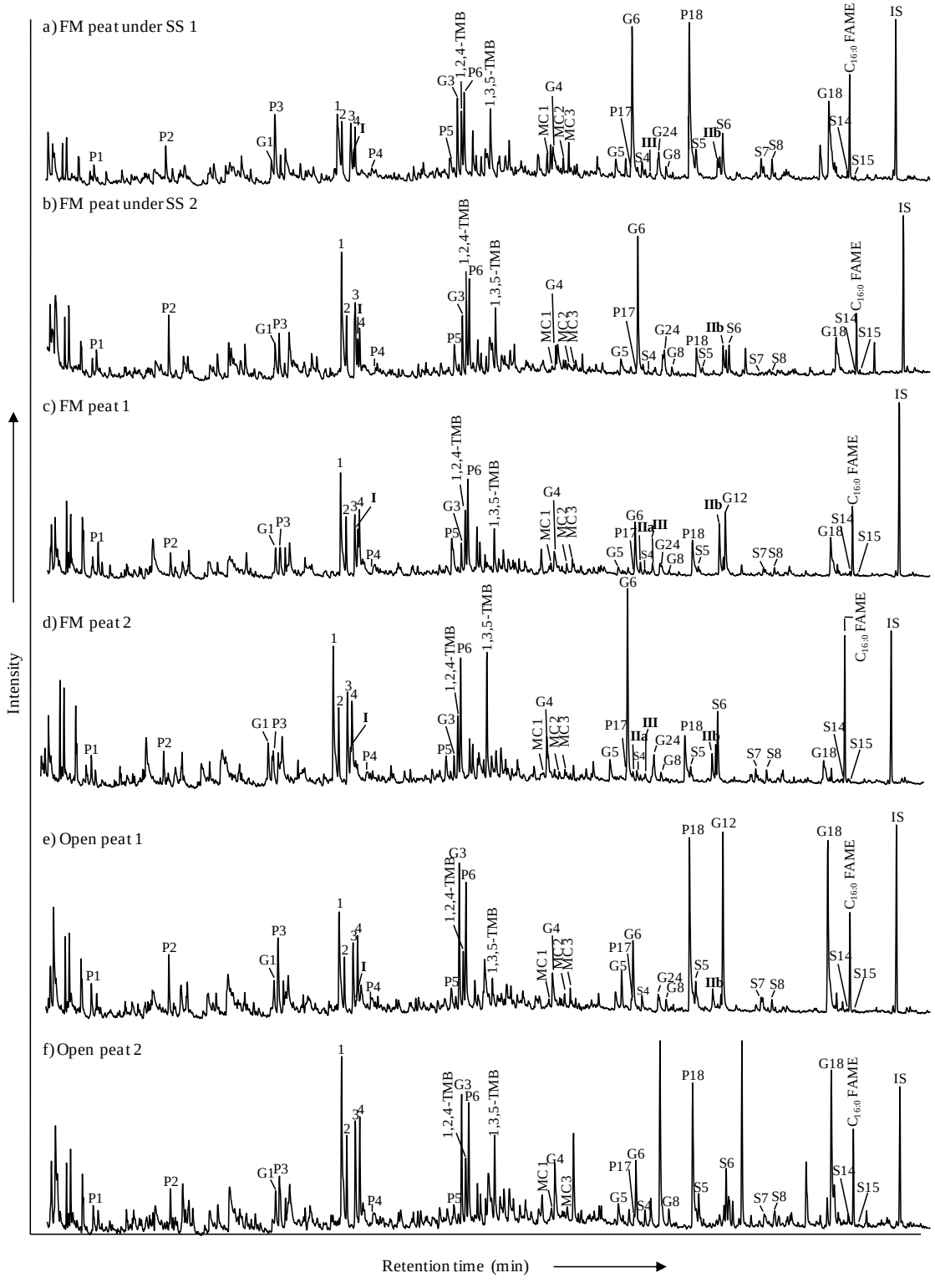

Fig. 6.5: Partial chromatogram for the total ion current (TIC) of the thermochemolysis products from the brown litter across all profiles (a) FM peat under SS 1 (b) FM peat under SS 2 (c) FM peat 1 (d) FM peat 2 (e) Open peat 1 and (f) Open peat 2. Peak identities and symbols are listed in Table 6.2.

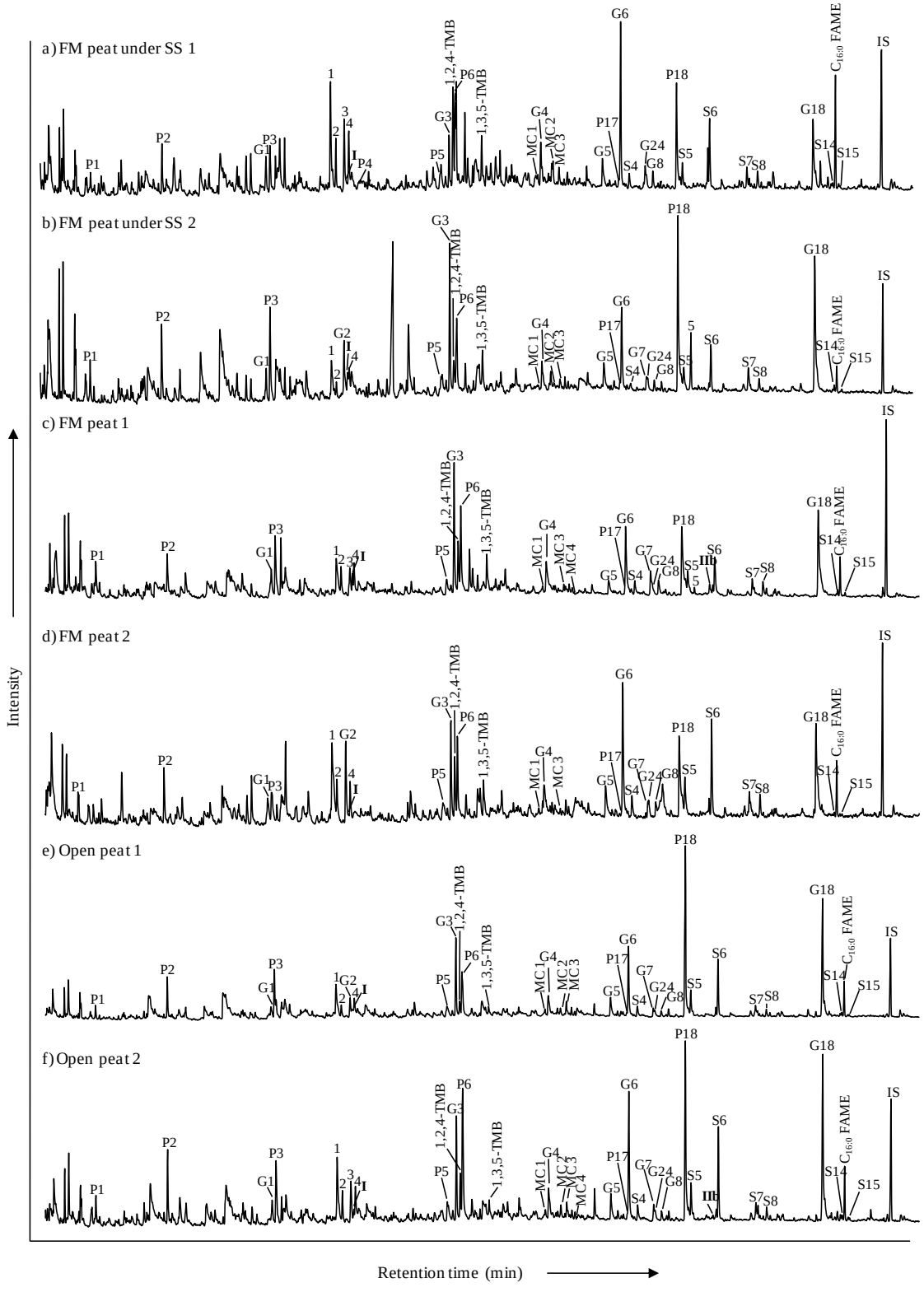

Fig. 6.6: Partial chromatogram for the total ion current (TIC) of the thermochemolysis products from the Hf horizon across all profiles (a) FM peat under SS 1 (b) FM peat under SS 2 (c) FM peat 1 (d) FM peat 2 (e) Open peat 1 and (f) Open peat 2. Peak identities and symbols are listed in Table 6.2.

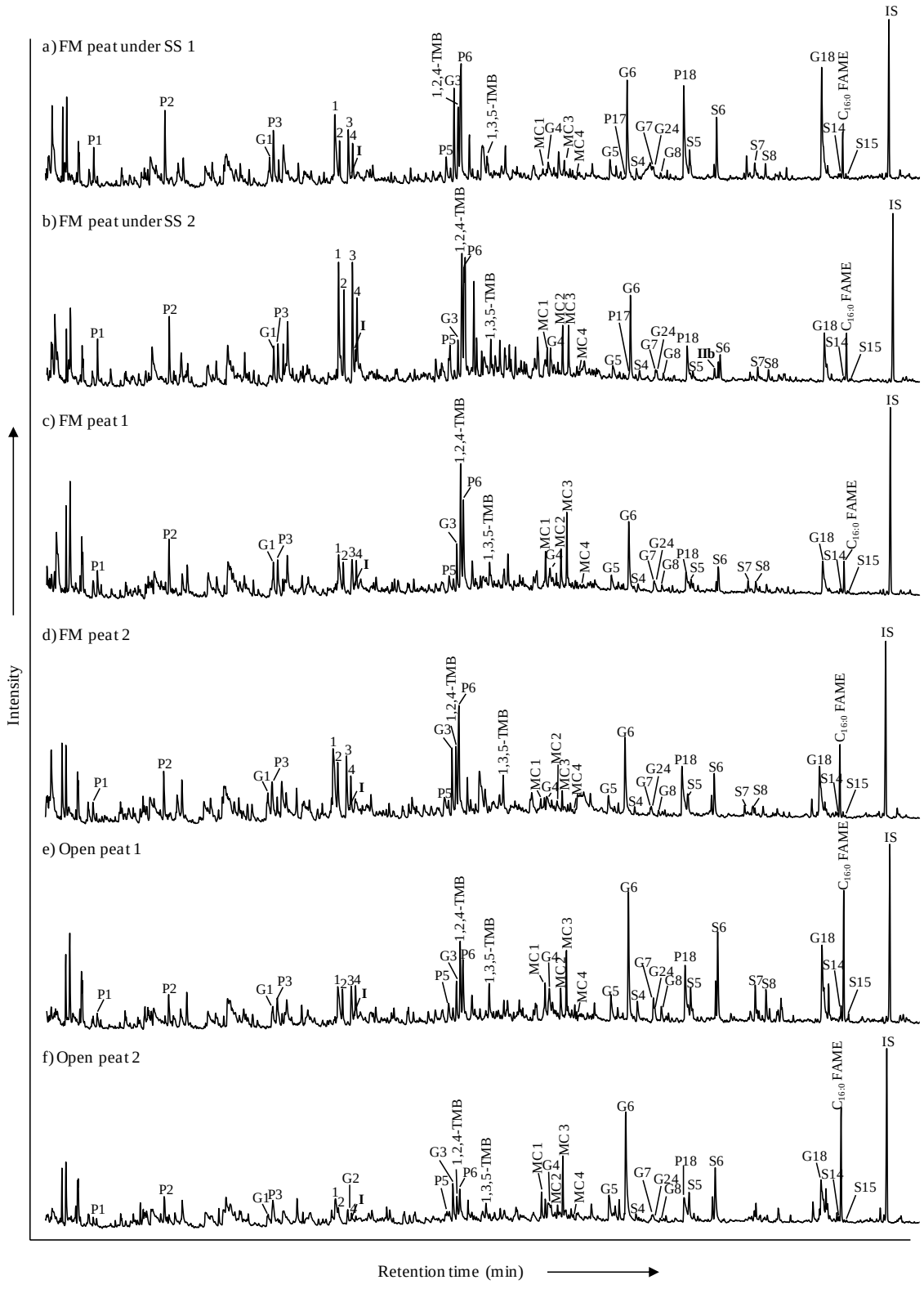

Fig. 6.7: Partial chromatogram for the total ion current (TIC) of the thermochemolysis products from the Hs horizon across all profiles (a) FM peat under SS 1 (b) FM peat under SS 2 (c) FM peat 1 (d) FM peat 2 (e) Open peat 1 and (f) Open peat 2. Peak identities and symbols are listed in Table 6.2.

grasses and mosses will not have been disturbed or outcompeted as the tree canopy is sparse. Only when canopy closure is achieved, will the natural and understory vegetation be shaded out (Mounsey, 2000).

The open peat pits show a dominance of *P. commune* and unidentified litter (potentially clubmoss) or contaminant, with very small abundances of lignin and *Sphagnum* compounds. The forest-margin peats show the presence of the four *Sphagnum* markers, however there are also large abundances of lignin phenols. This indicates that the open peat is colonised by primarily non-*Sphagnum* mosses, whilst the forest-margin peats display an increased species diversity, including *Sphagnum* moss, non-*Sphagnum* moss and vascular species. The distinctive *Sphagnum* and *P. commune* markers are rapidly lost down the profiles indicating either a recent change in the vegetation or the rapid loss of these diagnostic markers relative to the vascular species markers (i.e. lignin).

The Hf horizons begin to show similar distribution of compounds with a slight variance of the abundance of compounds, with the humified horizons showing very similar distribution and abundance of compounds across the chronosequence. This consistent suite of compounds in the humified horizon suggests that either the vegetation across the three sites used to be the same, or that certain compounds preferentially degrade over others (e.g. Kirk and Farrell, 1987) resulting in a consistent suite of phenols. The high abundance of P18 and G18 in the Hf and Hs horizons across the chronosequence highlights the input of non-woody vascular litter. Furthermore, P3 and G3 are also major lignin-derived phenols throughout the samples, indicative of a non-woody graminaceous input (Clifford et al., 1995; Chefetz et al., 2000). These four non-woody input indicator compounds are present in all of the samples and abundant in the deeper Hf and Hs horizons of the samples analysed, indicating the previously dominating grass input at the three sites.

The profile traces draw attention to a shift in the vegetation from grassy non-woody species in the deeper peat, to a current vegetation cover of primarily *Sphagnum* and non-*Sphagnum* mosses. *Sphagnum* moss is known to create conditions favourable to its growth, as discussed in Chapter 4 (van Breemen, 1995), however, studies have shown that *Sphagnum* peatlands can become susceptible to vascular species invasion, which could reduce the carbon store capacity of the peat (Tomassen et al., 2003; Tomassen et al., 2004). For example, a study of vegetation in an open peat area within Wark Forest between 1958 and 1986 observed an increase of grasses at the expense of *Sphagnum*

mosses, which was attributed to the adjacent afforestated habitat altering the local hydrology (Chapman and Rose, 1991). Therefore the changes observed in this study could be due to a natural vegetation shift, or a result of changing hydrological trends (i.e. from changing precipitation patterns and/or changing ground water patterns from the adjacent forest drainage (edge effect)). *Sphagnum* moss inputs are likely to cease once canopy closure has occurred, and thereby likely to further affect the carbon and phenol dynamics under the self seeded Sitka spruce.

6.3.3 Aromatic Hydroxyl Content of THM Products of Lignin

The % 3-methoxy, 4-hydroxy (intact lignin) content of G18, G4 and G6 (Figs. 6.8, 6.10 and 6.11) and % 1, 2 and 3-hydroxyl (intact lignin, altered lignin and non-lignin phenols) content of S6 (Fig. 6.12) are presented for the three sites. These are the products most likely to be affected by non-lignin phenolic input, and the percentages reflect the relative contribution of tannins, lignin, and the breakdown products of lignin phenols to the THM products. The percent hydroxyl content is explained in detail in Section 2.2.1.

6.3.3.1 Cinnamyl derivatives

G18 exhibits a consistently high level (70-100%) of 3-(3-methoxy, 4-hydroxyphenyl) 3-propenoic acid methyl ester (1% OH) (i.e. intact lignin derived ferulic acid) with a mean value of 88.6 ± 1.35%, indicating the consistent proportion of ferulic acid to caffeic acid across the chronosequence and down the profiles (Fig. 6.8) ($p=0.061$). The mass of P18 and intact G18 at each horizon are significantly similar across the chronosequence (Fig. 6.9) ($p=0.151, 0.114$), with an increasing yield into the Lb and Hf horizons; further indication of a previous grassy vegetation cover across the chronosequence (Section 6.3.2.5). The cinnamyl phenols dominate the lignin input to these samples (59.8 ± 2.8%) (Table 6.3), however the cinnamyl phenol yield decrease in the Hs horizon indicates a loss of lignin phenols in the deeper peat, further evidence that lignin phenols are not as recalcitrant as historically considered (Kiem and Kögel-Knabner, 2003; Kalbitz et al., 2006).

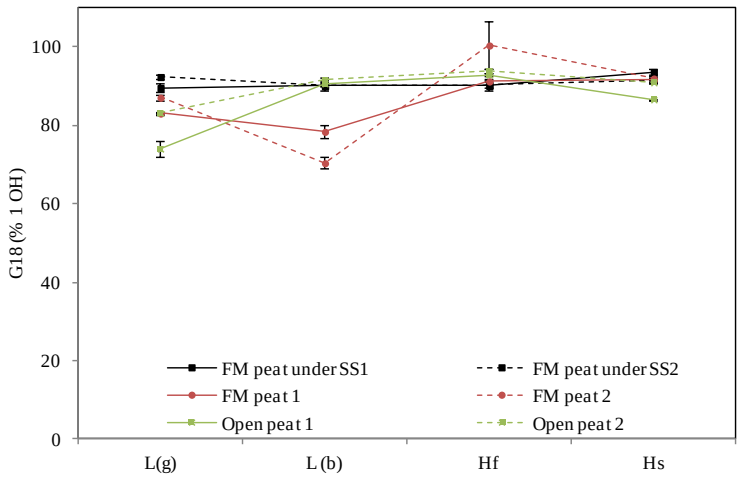

Fig. 6.8: 1 %OH extents of G18 from the (a) FM peat under Sitka spruce (black lines) (b) FM peat (red lines) and (c) open peat (green lines). Error bars show standard error of two analytical replicates. Pit one denoted by solid line, pit two denoted by slashed line.

6.*3.3.2* *Guaiacyl derivatives*

With the exception of the forest-margin peat under Sitka spruce pit two, the percent of intact G4 (3-hydroxy-4-methoxybenzaldehyde) and G6 (3-hydroxy-4-methoxybenzoic acid methyl ester) increase down core across the chronosequence (Figs. 6.10 and 6.11), consistent with the increased input of vascular phenols in the Hf and Hs horizons (Section 6.3.2.5).

Discounting the forest-margin peat under Sitka spruce pit two, the low yield of intact G4 and G6 (0.018 mg/100 mg OC) in the green litter represents *ca* 50% of the total uncorrected G4/6 yield, therefore the yield of polyhydroxylated compounds originating from non-lignin phenols (e.g. hydrolysable tannins (Filley et al., 2006)) and/or microbially demethylated lignin at the surface is equivalent to the intact lignin yield. The intact guaiacyl yield increases down core alongside an increased contribution of these compounds relative to the polyhydroxylated and demethylated lignin compounds. However in the Hs horizon, the yield decreases, further evidence of the lability of these lignin phenols, assuming a similar lignin input in the H horizons as revealed in Section 6.3.2.5 (Figs. 6.10 and 6.11).

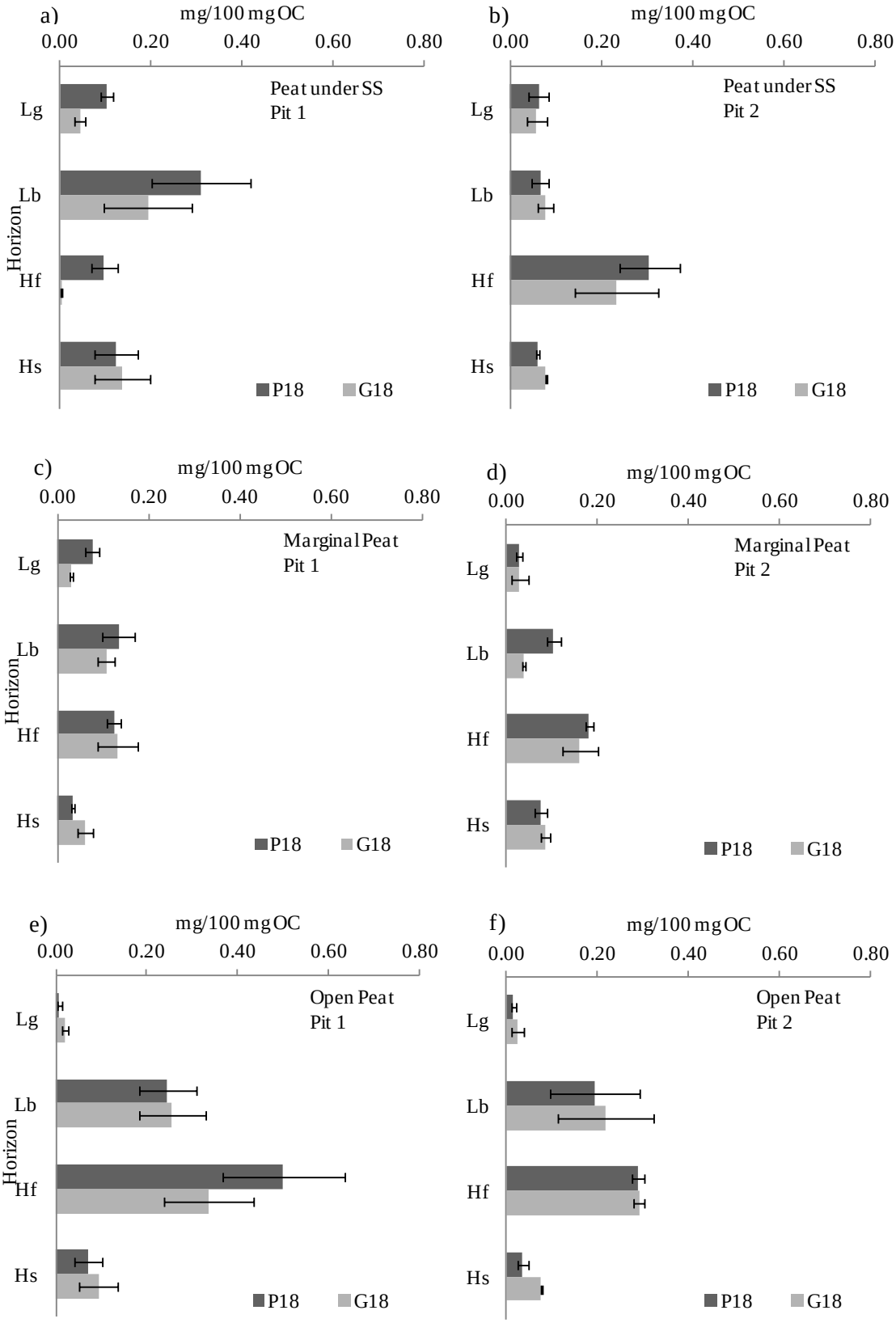

Fig. 6.9: Depth profile showing changes in yield of cinnamyl lignin phenols, P18 and G18 in; (a and b) FM peat under Sitka spruce pit 1 and 2, (c and d) FM peat pit 1 and 2 and (e and f) open peat pit 1 and 2. Error bars show standard error of two analytical replicates.

Table 6.3: The proportion of lignin phenols (%) to the total lignin yield (Λ) in each soil horizons taken from the three sites; Guaiacyl (%G), syringyl (%S) and cinnamyl (%C).

	%G	%S	%C
Forest-margin peat under Sitka spruce 1			
L (green)	12.6	14.0	73.5
L (brown)	17.5	8.0	74.5
H (fibric)	45.3	20.2	34.5
H (sapric)	25.8	13.5	60.6
Forest-margin peat under Sitka spruce 2			
L (green)	49.5	4.8	45.7
L (brown)	48.9	5.6	45.4
H (fibric)	16.6	8.7	74.6
H (sapric)	30.8	12.7	56.5
Forest-margin peat 1			
L (green)	13.0	6.0	81.0
L (brown)	23.4	3.1	73.5
H (fibric)	22.8	11.2	65.9
H (sapric)	41.8	17.0	41.2
Forest-margin peat 2			
L (green)	36.0	10.0	54.0
L (brown)	31.0	18.9	50.1
H (fibric)	27.8	18.2	54.0
H (sapric)	25.3	13.7	61.0
Open peat 1			
L (green)	28.5	0.0	71.5
L (brown)	22.2	7.4	70.5
H (fibric)	19.6	11.5	68.9
H (sapric)	39.4	16.0	44.6
Open peat 2			
L (green)	19.6	6.8	73.6
L (brown)	22.1	12.1	65.8
H (fibric)	24.7	15.0	60.3
H (sapric)	48.5	16.6	35.0

Filley et al. (2006) reported a decrease in the proportion of non-lignin phenols with depth, which was attributed to the selective metabolism of ortho-hydroxy substituted rings resulting in an apparent enrichment in undegraded lignin, which could explain the decreased content of polyhydroxylated compounds. Alternatively the change could be a result of the shifting vegetation input that occurred, with Section 6.3.2.5 highlighting the shift from lignin-rich grassy species in the deeper peat, to a current vegetation cover of primarily lignin-devoid *Sphagnum* and non-*Sphagnum* mosses.

The forest-margin peat under Sitka spruce pit two displays a high yield of intact G4 (0.035 mg/100 mg OC) and G6 (0.087 mg/100 mg OC) in the green litter (compared to <0.06 and <0.03 mg/100 mg OC for G4 and G6 respectively at the remaining sites). A progressive decrease of intact G4 occurs with increasing burial depth, whilst intact G6 and non-lignin G6 remain relatively constant (due to the 50:50 distribution) (Figs. 6.10 and 6.11). These results suggest that the G6 di-hydroxy content is coupled with intact G6, therefore potentially reflecting the microbially demethylated lignin rather than protocatechuic acid. The loss of easily leached tannin phenols could explain the increased percent of di-hydroxyl G4 with depth (Nierop and Filley, 2007). On the other hand, the presence of the hydroxyl phenols could also derive from the adjacent Sitka spruce plantation, however further research into the dynamics of leaching phenols is required.

The relative input of guaiacyl phenols into the litter (L) is less than a quarter of the total lignin yield (Λ) with the exception of forest-margin peat under Sitka spruce pit 2, which displays an input of almost 50% (Table 6.3). Assuming a constant vegetation input into the H horizons (Sections 6.3.2), the increased proportion of guaiacyl lignin phenols from 26.1% in the Hf horizon to 35.3% in the Hs horizon coupled with the decreased proportion of cinnamyl phenols from 59.7 to 49.8% across the same horizons indicates the selective preservation of guaiacyl phenols relative to the cinnamyl phenols as stated by Sarkanen (1971) (Table 6.3) (the relative proportion of syringyl phenols remains relatively constant in the H horizons; 14.1 and 14.9% respectively).

The intact guaiacyl lignin contents at the litter horizons of these samples support a greater non-lignin phenolic contribution (e.g. *Sphagnum* and non-*Sphagnum* mosses), with the exception of the forest-margin peat under Sitka spruce pit 2, whereby the proportion of intact G4 coupled with the high yield of intact G4 and G6 provides evidence of the growth of guaiacyl rich Sitka spruce.

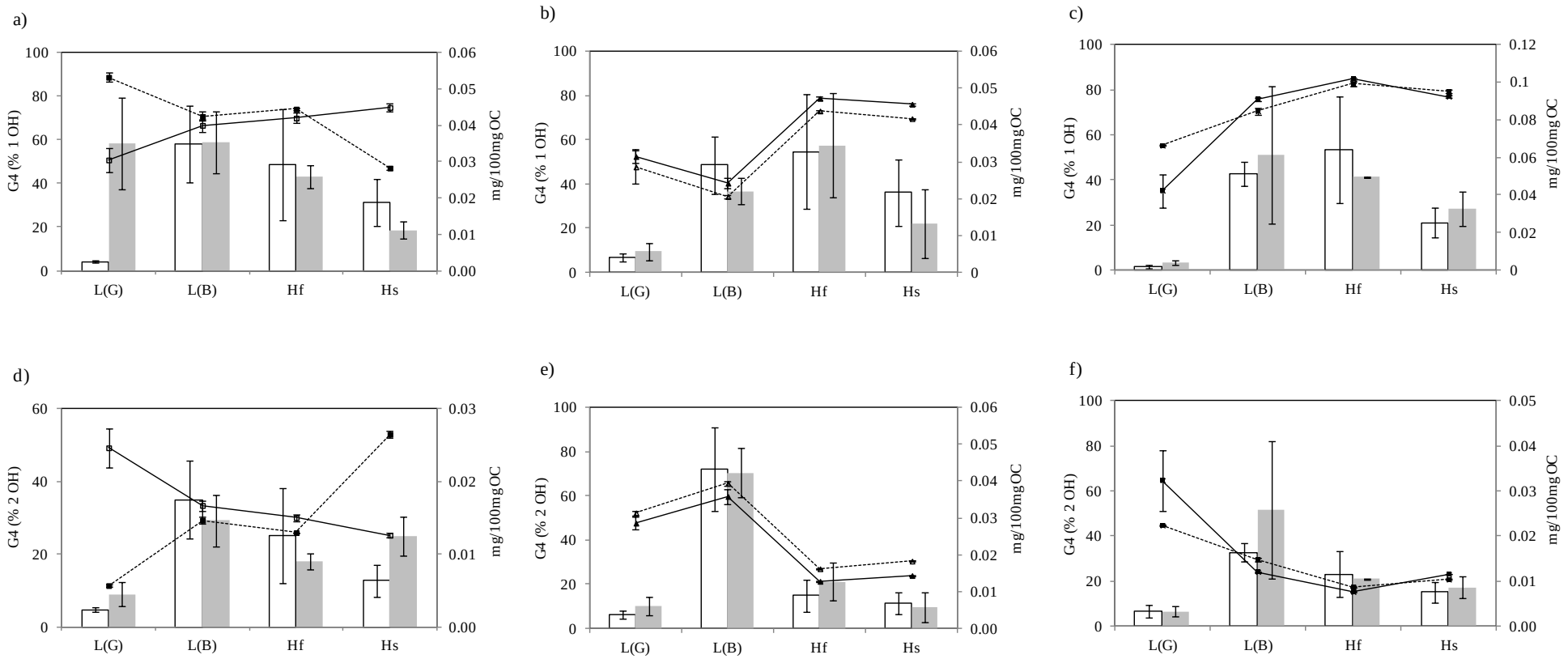

Fig. 6.10: 1 %OH (a-c) and 2 %OH (d-f) extents (lines) and yield (mg/100 mg OC) (bars) of G4 from either pit one (open bars; solid lines) or pit two (grey bars; dashed lines) from the (a, d) FM peat under Sitka spruce (b, e) FM peat and (c, f) open peat. Error bars show standard error of two analytical replicates.

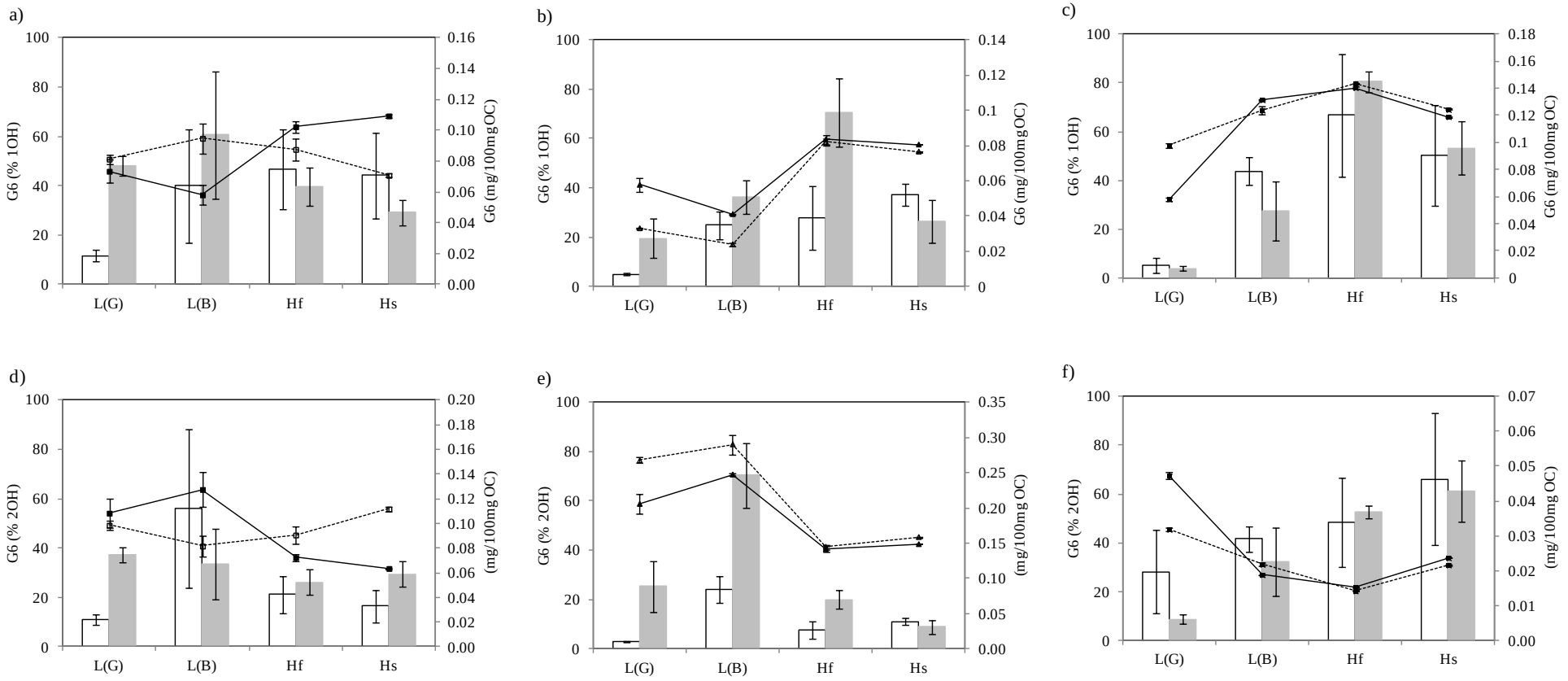

Fig. 6.11: 1 %OH (a-c) and 2 %OH (d-f) extents (lines) and yield (mg/100 mg OC) (bars) of G6 from either pit one (open bars; solid lines) or pit two (grey bars; dashed lines) from the (a, d) FM peat under Sitka spruce (b, e) FM peat and (c, f) open peat. Error bars show standard error of two analytical replicates.

6.3.3.3 Syringyl derivatives

In all of the samples that contained S6 (with the exception of the Lb in the forest-margin peat under Sitka spruce pit 2), the majority of S6 originates from an intact lignin source (>50%) (Fig. 6.12). The tri-hydroxy content of S6 (i.e. 3% OH) has been identified as gallic acid (tannin input), therefore the 'true' demethylation extent of S6 is calculated by quantifying only the 3,4-dihydroxy-5-methoxybenzoics acids (2% OH) in relation to the intact S6 monomers thus removing the contribution from trihydroxy gallic acid, however fully demethylated lignin (microbially demethylated syringic acid) cannot be distinguished from gallic acid (Nierop and Filley, 2007). The demethylation degree (2% OH) varied between 4.4 and 20.7% across the three sites (Fig. 6.12).

The percent of intact S6 contribution remains significantly similar across the sites and down the profiles ($p=0.315, 0.161$), with an average of 76%, however the mass of intact S6 increases into the Hf horizon from which is associated with a small increase in the proportion of S phenols to Λ; 8.1 to 14.1% (Fig. 6.12).

The trihydroxy content of S6 in the four forest-margin peat pits display a range between 5 and 40%, whereas the open peat profiles showed a much smaller contribution of gallic acid to S6 (5-13%). This indicated that there was a large input of gallic acid to the brown litter horizons of the three forest-margin peat pits with respect to intact S6, particularly the forest-margin peat pit two where the yield exceeds 0.02 mg/100 mg OC (Fig. 6.12h). This is potentially due to the increased tannin input from the Sitka spruce needles deposited as litter (Hernes and Hedges, 2004), which have laterally leached across the chronosequence and down to the brown litter (Nierop and Filley, 2007).

The chronosequence displays low levels of guaiacyl, syringyl and cinnamyl phenols (i.e. Λ) in the surface litter (Lg), however the yields increase into the Lb and Hf horizons, indicating the previous input of vascular derived phenols. The subsequent decrease of phenols, in particular G4 into the deepest Hs horizon is a direct result of the oxidation of the lignin phenols, this is shown in Table 6.4, whereby once below the green litter the $[Ad/Al]_G$ ratio progressively increases down core (Section 6.3.4.1).

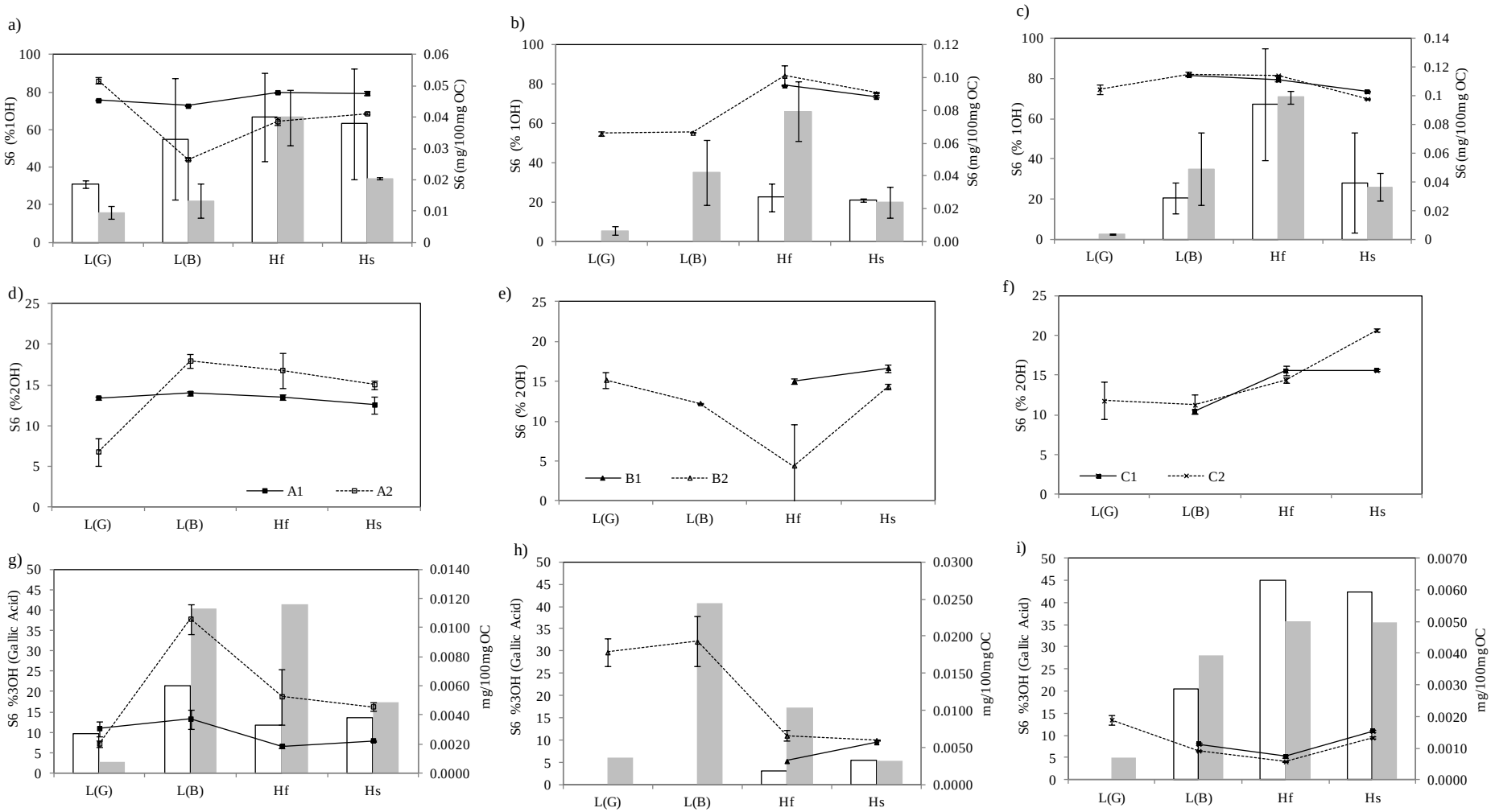

Fig. 6.12: 1 %OH (a-c), 2 %OH (d-f) and tri-hydroxy (g-i) extents (lines) of S6 and yield (mg/100 mg OC) (bars) from either pit one (open bars; solid lines) or pit two (grey bars; dashed lines) from (a, d, g) FM peat under SS (b, e, h) FM peat and (c, f, i) open peat. Error bars show standard error of two analytical replicates.

6.3.4 Lignin Products

6.3.4.1 Lambda & $[Ad/Al]_G$

Table 6.4 shows the uncorrected (Λ*) and corrected lambda (Λ) values. The aromatic hydroxyl contents were determined so that the corrected mass yields and lignin parameters could be calculated (Chapter 2, Section 2.2.1; Section 6.3.3). It was found that the total lignin yield was reduced by up to 50% after correction for tannin, poly-hydroxy compounds, and demethylated lignin. This decrease is a result of changes primarily to S6, G6 and G18, but all lignin monomers showed that they comprise some hydroxyl species (Section 6.3.3).

Fig. 6.13 displays the corrected Λ down the profile of the six pits, allowing a visual representation of the lignin yield changes occurring across the chronosequence and down core. A maximum in the depth profile of the lignin phenols was observed in the Hf horizon of each profile, with the exception of pit one of the forest-margin peat under Sitka spruce where the maximum was observed in the Lb horizon. However across the entire site, the lignin maximum corresponds to a depth of approximately 20 cm despite changes in the current vegetation cover, as observed from the chromatograms (Section 6.3.2). It is unusual to see the lignin yield increase down the profile despite linearly deposited soils (Fig. 6.13), however this could be due to a recent vegetation shift from lignin-rich vascular species to lignin-devoid non-vascular species (i.e. *Sphagnum* and non-*Sphagnum* mosses), reducing the input of lignin phenols to the upper litter horizons across the entire chronosequence (Section 6.3.2).

This lignin maximum at depth has also been observed in Chapter 3, and Mason et al. (2009; 2012), and was ascribed to the preservation of lignin due to horizon inversion as a result of land preparation prior to planting. However this site has not experienced any land preparation, although the forest-margin peat may be experiencing changes due to the natural growth of the Sitka spruce. Rumpel et al. (2002) also observed an increase of soil carbon in the form of lignin in the subsoil of forest soils, this was partly attributed to root input, however, Zerva et al. (2005), indicated that root input alone cannot explain the lignin maximum, and owing to the fact that there are no trees in the open peat (Fig. 2.8b), Sitka spruce roots are not likely to be the cause for the maximum.

Table 6.4: Lignin parameters in each soil horizon taken from the three Wark Forest sites. The corrected, intact values are displayed without a *, whilst uncorrected values are displayed with a *.

	Λ*	Λ	S/G*	S/G	C/G*	C/G	$[Ad/Al]_G$*	$[Ad/Al]_G$	Tannin/ lignin
Forest-margin peat under Sitka spruce 1									
L (green)	0.24	0.20	0.80	1.18	3.11	6.34	8.47	7.65	0.05
L (brown)	0.86	0.67	0.29	0.42	2.12	4.34	3.05	1.66	0.04
H (fibric)	0.37	0.28	0.41	0.45	0.54	0.78	3.16	2.89	0.02
H (sapric)	0.50	0.43	0.45	0.49	1.71	2.30	4.04	3.68	0.02
Forest-margin peat under Sitka spruce 2									
L (green)	0.33	0.26	0.10	0.10	0.66	0.90	3.14	2.44	0.01
L (brown)	0.43	0.31	0.15	0.11	0.66	0.99	3.13	2.62	0.07
H (fibric)	0.85	0.72	0.51	0.52	2.87	4.39	3.44	2.54	0.06
H (sapric)	0.35	0.24	0.33	0.41	0.94	1.84	4.49	4.22	0.05
Forest-margin peat 1									
L (green)	0.16	0.13	0.28	0.44	2.85	6.19	2.32	1.83	0.00
L (brown)	0.51	0.32	0.10	0.14	1.22	3.17	1.65	1.20	0.00
H (fibric)	0.45	0.39	0.49	0.51	2.35	3.22	1.57	1.19	0.01
H (sapric)	0.29	0.22	0.38	0.42	0.67	0.98	3.63	2.75	0.03
Forest-margin peat 2									
L (green)	0.22	0.11	0.15	0.28	0.50	1.70	9.65	4.76	0.07
L (brown)	0.39	0.29	0.30	0.59	1.03	1.62	3.33	2.28	0.17
H (fibric)	0.76	0.64	0.55	0.67	1.35	2.07	3.94	3.16	0.04
H (sapric)	0.33	0.26	0.46	0.55	1.68	2.60	5.31	4.18	0.03
Open peat 1									
L (green)	0.07	0.04	0.00	0.00	1.48	3.58	5.16	4.75	0.00
L (brown)	0.81	0.71	0.37	0.34	2.46	3.12	1.60	1.54	0.01
H (fibric)	1.34	1.21	0.65	0.58	3.14	3.74	2.09	1.93	0.02
H (sapric)	0.48	0.37	0.38	0.34	0.85	1.10	4.02	3.46	0.03
Open peat 1									
L (green)	0.07	0.06	0.26	0.35	2.32	3.77	2.21	2.18	0.05
L (brown)	0.72	0.63	0.54	0.56	2.30	3.07	0.95	0.93	0.02
H (fibric)	1.09	0.97	0.65	0.61	2.05	2.45	3.03	2.92	0.01
H (sapric)	0.44	0.33	0.52	0.34	0.58	0.74	3.42	2.98	0.02

* uncorrected lignin values (intact lignin, altered lignin and non-lignin phenolics)

The build up of lignins at depth has also been linked to the leaching of phenolics (Cerli et al., 2008). The maximum could also be a result of the selective preservation of lignin phenols with respect to *Sphagnum* and moss phenols or a recent vegetation change from lignin containing vascular species to non-lignin containing non-vascular plants. This latter point could be further explained by the consistent composition of phenols observed in the H horizons of the six peat cores (Section 6.3.2).

The lignin yield of the green litter is significantly lower in the open peat compared to the forest-margin peat under Sitka spruce, highlighting a decrease in vascular species from the forest-margin peat under the Sitka spruce to the open peat ($p=0.048$). The deeper horizons (Lb, Hf and Hs) showed no differences in the lignin yield between the sites, suggesting a previous similar vegetation cover across the chronosequence ($p>0.05$), most likely dominated by non-woody (i.e. grassy) vascular species. It appears that the open peat has naturally shifted from a typical moorland grassland to a non-*Sphagnum* moss peat, which is not observed in the forest-margin peats.

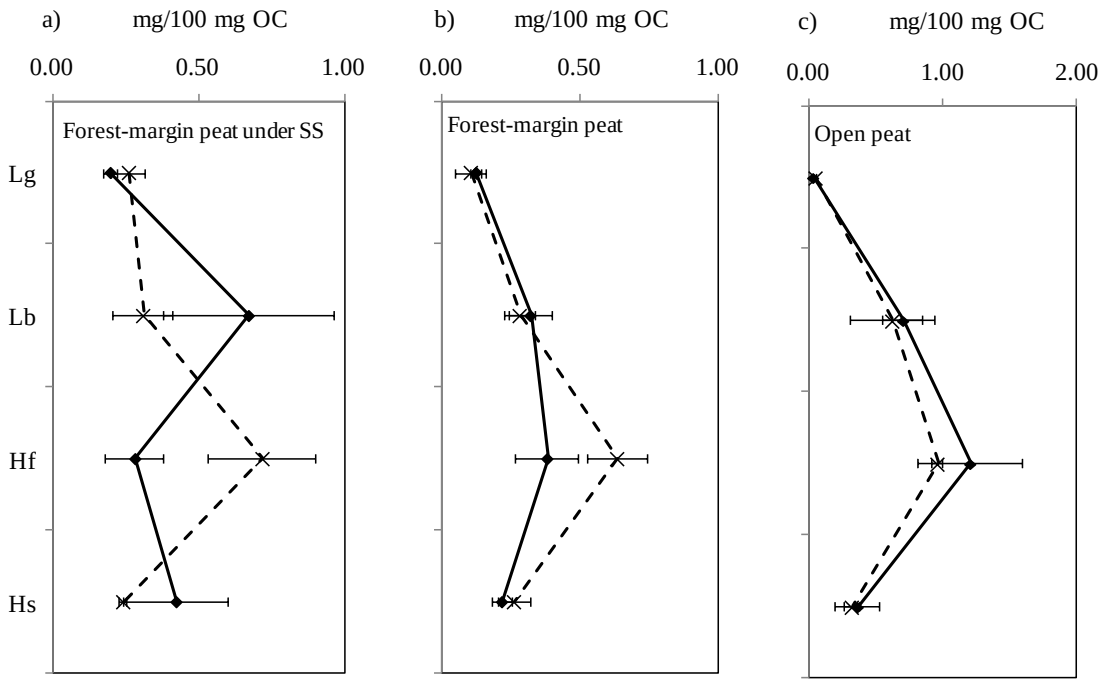

Fig. 6.13: The lignin content, Λ (mg/100 mg OC) at (a) FM peat under Sitka spruce (b) FM peat and (c) open peat. Pit one denoted by solid black line, pit 2 denoted by slashed black line. Error bars show standard error of two analytical replicates.

Across the chronosequence, the corrected decay proxy $[Ad/Al]_G$ initially decreased into the Lb before increasing into the H horizons (with the exception of the forest-margin peat under Sitka spruce pit 2), indicating a progressive oxidation of lignin with increasing depth once below the green litter (Table 6.4) (Vane et al., 2001; Nierop and Filley, 2008). Differences down core were only significant in the forest-margin peat under pit one, where the green litter was significantly higher (7.65) than the deeper horizons (1.66, 2.89 and 3.68) ($p=0.012$). The ratio decreases after correction for the non-lignin phenols due to the relatively high concentrations of dihydroxyl G6 (Fig. 6.12; Section 6.3.3).

6.3.4.2 Lignin proxies (S/G, C/G)

Table 6.4 summarises the values for plant source proxies applied to these peat profiles. In the majority of samples after correction, the S/G ratio increases, whereas for the C/G ratio, all of the samples show an increase, reflecting the larger proportion of intact G18 and S6 relative to intact G6 (Section 6.3.5). The S/G ratio decreases after correction for the H horizons in the open peat cores reflecting a larger proportion of intact guaiacyl lignin compared to syringyl lignin.

In profiles where no vegetation change has occurred, it can be assumed that the S/G ratio will progressively decrease down the soil profile as syringyl moieties are preferentially degraded over guaiacyl moieties, as observed in the ML soil in Coalburn Forest (Chapter 3) (Chefetz et al., 2000). However this is not the case for these sites, indicating a recent change of vegetation input to these peats including the open peat.

The peat profiles display an increase in S/G with depth due to a decreasing guaiacyl and increasing syringyl contribution, reflecting the input from grasses into the H horizon, with the exception of the forest-margin peat under Sitka spruce pit 1, which displays a decrease from 1.2 in the Lg to a constant ~0.4 down the profile, however changes are not significant ($p=0.076$) (Tables 6.3 and 6.4). The high average S/G ratio of 0.49 in the Hf and Hs horizons across the chronosequence is comparable to the surface litter of the ML in Chapter 3, further suggesting a previous vegetation of a relatively uniform cover of grassy species, whereas vegetation cover now is more patchy, consisting of vascular species, *Sphagnum* mosses and non-*Sphagnum* mosses, reflected in the wide range of S/G values observed across the green litter (0-1.18).

The C/G ratio is variable across the chronosequence and down the cores, ranging from 0.74 in the Hs horizon of the open peat to 6.34 in the green litter of the forest-margin peat under Sitka spruce. This is caused by the large but highly variable yield of cinnamyl lignin phenols (Fig. 6.9). The introduction of Sitka spruce would expect to reduce the C/G and S/G ratio in the litter due to the litterfall of guaiacyl-rich Sitka spruce litter, however this is only observed in the second pit of the forest-margin peat under Sitka spruce, which is consistent with the high abundance of G6 observed in the green litter at this site (Fig. 6.11a). The C/G (uncorrected) for Sitka spruce roots has been calculated and exhibits a low ratio of 0.09 (Section 3.3.2.3). The uncorrected C/G ratio across the sites is relatively high, with no evidence of a reduced C/G in the Sitka spruce forest-margin peat pit where the roots would be expected. Additionally, as with the Coalburn site, the THM product distribution and abundance from the Sitka spruce roots (Fig. 3.5) does not match the TICs from the forest-margin peats under Sitka spruce, suggesting that the root input cannot be observed above the bulk peat SOC. These two proxies are good indicators of vascular plant source; however they do not take into consideration the non-vascular plants including mosses which are the prevailing vegetation type on these soils.

A third proxy was introduced by Nierop and Filley (2007), which provides an indication of the input of woody and non-woody tissue based on the tannin (gallic acid)/lignin (Λ_{S+G}) ratio, based on the high yield of tannins in leaves, bark and needles (Kraus et al., 2003). The tannin/lignin ratio was elevated (0.17 compared to 0.03 ± 0.004 in the rest of the site) in the forest-margin peat pit 2 (Lb), consistent with the elevated G6 dihydroxy yield (Table 6.4; Fig. 6.5). The non-uniformity across the site reflects the relatively young Sitka spruce, and therefore limited input of Sitka spruce-derived tannin phenols into the soils (Paul et al., 2002).

6.3.5 Non-Lignin Products

6.3.5.1 Tannin input

Tannin phenols are split into two groups, hydrolysable (HT) and condensed (CT) tannins. Gallic acid can derive from both CTs and HTs, and has been discussed in Section 6.3.3.3.

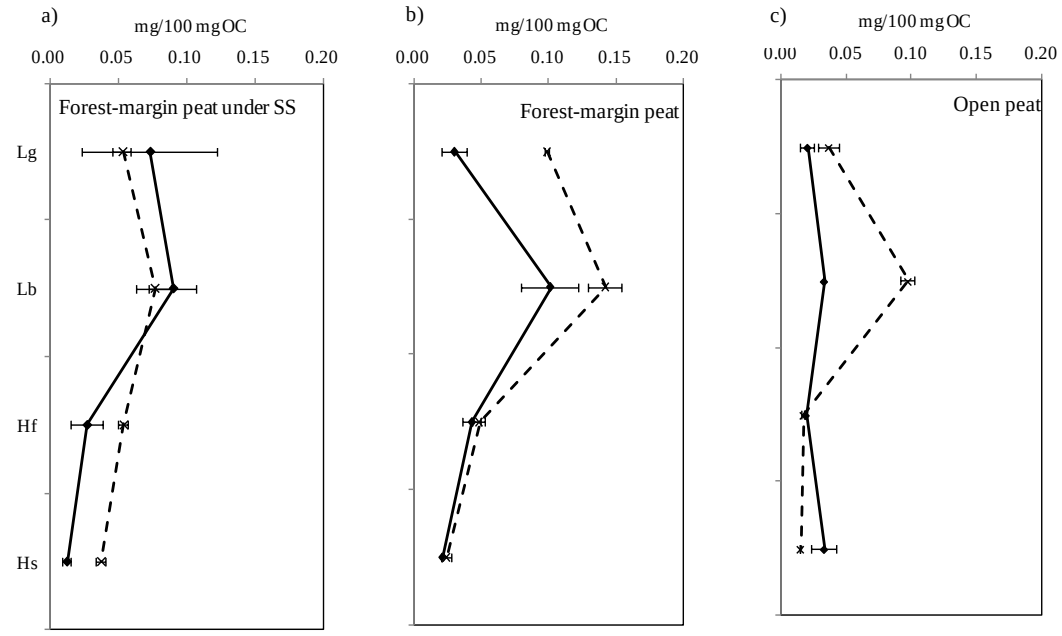

Fig.6.14: Depth profile showing changes in the amount of 1,3,5-trimethoxybenzene (mg/100 mg OC) at (a) FM peat under Sitka spruce, (b) FM peat and (c) the open peat. Error bars show standard error of two analytical replicates. Pit one denoted by solid line, pit two denoted by slashed black line.

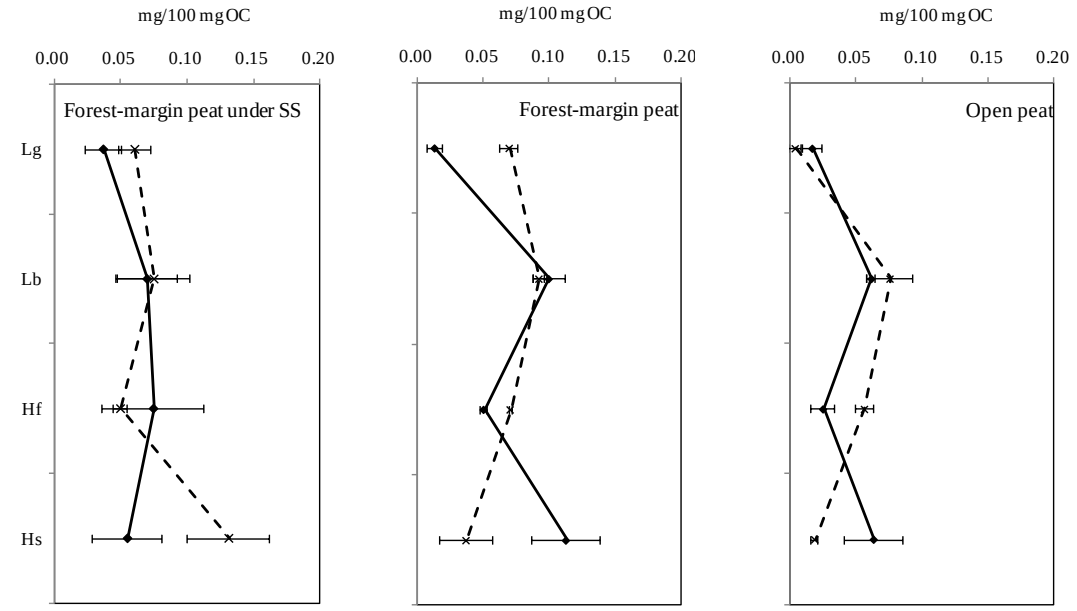

Fig. 6.15: Depth profile showing changes in the amount of 1,2,4-trimethoxybenzene (mg/100 mg OC) at (a) FM peat under Sitka spruce, (b) FM peat and (c) the open peat. Error bars show standard error of two analytical replicates. Pit one denoted by solid line, pit two denoted by slashed black line.

The elevated thermochemolysis temperature of 610 °C allows for CTs and HTs to be cleaved and amenable to GC-MS analysis (Nierop and Filley, 2007), therefore the relative input of gallic acid from HTs and CTs cannot be established.
1,3,5-TMB is derived from the A rings of CTs, which have previously been recorded as the dominant tannin products (Nierop et al., 2005) and therefore can be used as an unequivocal CT marker in these samples (Hernes and Hedges, 2004).

Fig. 6.14 displays a significant maximum of 1,3,5-TMB in the Lb horizon across the chronosequence, which could be a reflection of the shallow input of fresh root material containing high levels of tannins (Gallet and Lebreton, 1995), or the leaching from tannin-rich Sitka spruce needles (Kraus et al., 2003), however these trends do not fully match those from gallic acid (Fig 6.12) ($p<0.001$). The Tukey's significantly different test revealed that the open peat has a significantly lower yield than the forest-margin peat, with the forest-margin peat under Sitka spruce having a significantly similar yield to both (Fig. 6.14) ($p=0.04$). This is expected as the open peat is furthest away from the tannin rich Sitka spruce needles and roots, also the topography means that the gradient slopes down from the open peat to the forest-margin peat (Fig. 6.1), and therefore is less likely to be affected by leaching.

1,2,4-TMB can be derived from the B ring of CT, however it can also be derived from polysaccharides, therefore the relative input of 1,2,4-TMB from tannin and polysaccharides cannot be established. The open peat displays a significantly lower 1,2,4-TMB yield than the two forest-margin peat sites (Fig. 6.15) ($p=0.015$). Tukey's significantly different test shows the Lb and Hs horizons have a significantly higher 1,2,4-TMB yield that then the Lg horizon, however the Hf horizon was statistically similar to all the other horizons ($p=0.004$). This compound and associated yield profiles are discussed in further detail in Chapter 7, whereby a attempt to differentiate between the two potential sources is carried out (Section 7.3.5).

6.3.5.2 Sphagnum biomarkers

The individual yields of the four sphagnum acid THM products are shown in Fig. 6.16. The compounds are shown from left to right in order of compound elution; i.e. the dark grey bars are **I** (methylated 4-isopropenylphenol), white bars are **IIa (**methylated (E/Z)-

3-(4-hydroxyphen-1-yl)-but-2-enoic acid), the light grey bars are **III (**methylated 3-(4-hydroxyphen-1-yl)-but-3-enoic acid) and the black bars are **IIb** (methylated (E/Z)- 3-(4-hydroxyphen-1-yl)-but-2-enoic acid). Across all six pits, the *Sphagnum* markers **IIa** and **III** are absent from the H horizons, whilst **I** and **IIb** are the dominant *Sphagnum* compounds down the profile of all the sites, suggesting the reduced input of *Sphagnum* mosses with depth. The discussion in Section 5.3.6, postulated that any increase in **I**, beyond that observed in fresh peat, may be assumed to derive from decarboxylated sphagnum acid in-situ. However from Fig. 6.16 and the traces discussed in Section 6.3.2 it is clear that *Sphagnum* mosses have only recently started to grow at the forest-margin peat, therefore the yields below the litter are low and, consequently, are unlikely to yield any useful information regarding the degradation of *Sphagnum* at this site.

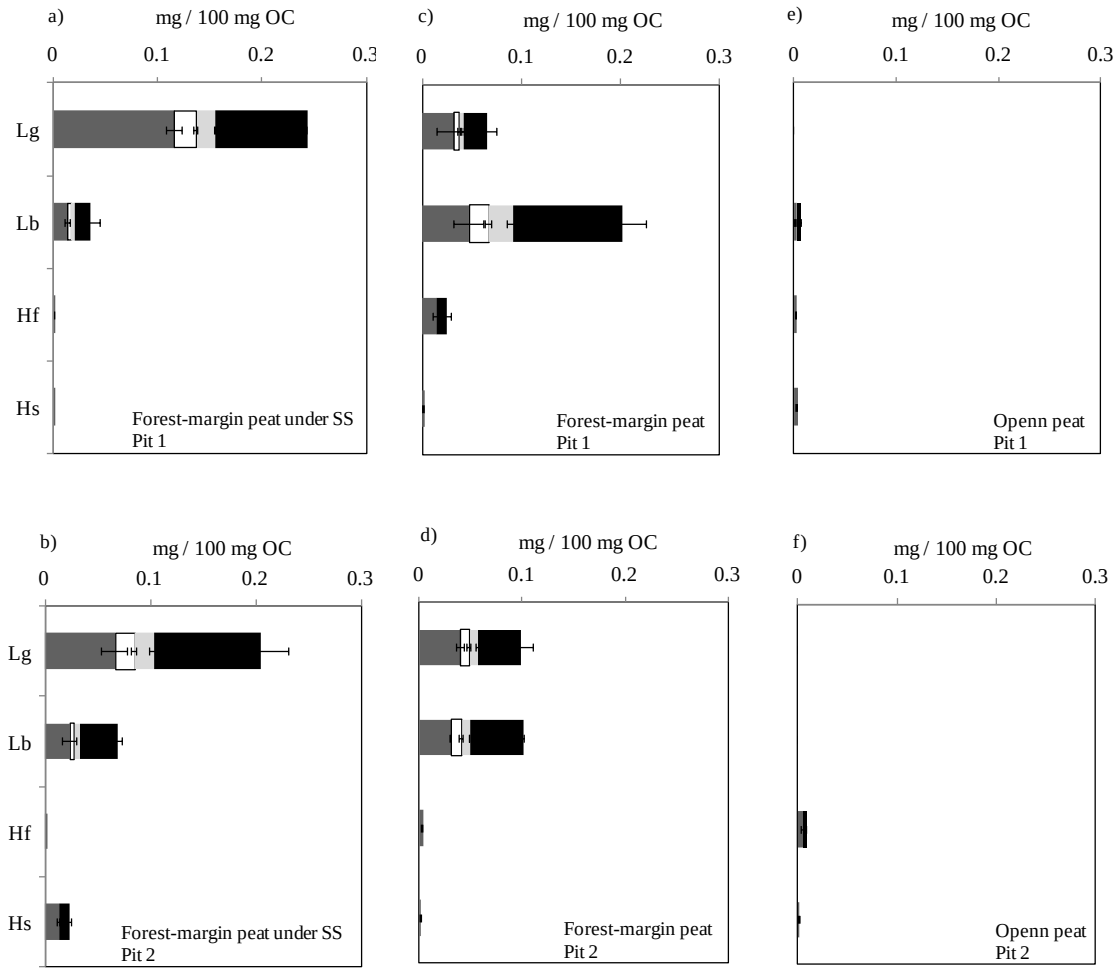

Fig. 6.16: The total *Sphagnum* content (mg/100 mg OC) at (a) and (b) FM peat under Sitka spruce, (c) and (d) FM peat and (e) and (f) the open peat. Error bars show standard error of two analytical replicates.

This is reflected in the progressive and significant decrease of the *Sphagnum* yield from the litter down the four forest-margin peat profiles into the H horizons (Fig. 6.16) ($p<0.05$). The open peat shows a *Sphagnum* yield a factor of ten smaller than the forest-margin peats where **I** is the dominant *Sphagnum* marker (Fig. 6.16). As observed from the green litter TIC traces (Fig. 6.4) the open peat pit one is dominated by *Polytrichum* litter.

6.*3.5.3* *Polytrichum commune*

Although G12 has been identified in other plants, e.g. *Pseudotsuga menziesii* (Douglas fir) and *Sida cordifoilia* (Flannel weed) (Hatcher et al., 1995; Martínez et al., 2011), the THM of *Polytrichum commune* releases large abundances of 3,4-dimethoxybenzene propanoic acid methyl ester (G12) (*m/z* 151, 224) (Chapter 4, Section 4.3.4). G12 was absent from all but two samples; the litter (green and brown) of the forest-margin peat pit 1 (0.075 mg/100 mg OC) and the open peat pit 1 (0.38 mg/100 mg OC). Their presence coincides with low yields of *Sphagnum* (Fig. 6.16), together with the visual identification of *P. commune* litter at the open peat pit 1 (Section 6.3.2.1).

6.3.5.4 *Relative vegetation input*

A ratio was proposed in Chapter 4 to determine the relative input of *Sphagnum* litter to vascular litter in peats and soils (SR%). However non-*Sphagnum* mosses such as *Polytrichum commune* are not accounted for using this ratio. *Polytrichum commune* does not contain any *Sphagnum* phenols, and only trace quantities of lignin phenols (Chapter 4), and therefore is not accounted for in any previous vegetation proxies used in this study. Using the following equations, the relative input of vascular, *Sphagnum* and non-*Sphagnum* mosses can be ascertained:

$$\% \text{ Vascular} = [\Lambda / (\Lambda + \sigma + p)]*100$$

$$\% \textit{ Sphagnum} = [\sigma / (\Lambda + \sigma + p)]*100$$

$$\% \textit{ Polytrichum} = [p / (\Lambda + \sigma + p)]*100$$

Where Λ is the vascular lignin phenol yield, σ is the sphagnum yield and p is the *Polytrichum* yield. These proxies provide a quick and effective first measure of the

dominant vegetation at a site, particularly when displayed in a ternary diagram (Fig. 6.17). The ternary plot shows that the majority of the Wark Forest samples are devoid of *Polytrichum commune* markers, owing to their position along the 0 mg/100mg OC *P. commune* axis. These samples display an increasing contribution of vascular compounds alongside a decreasing contribution of *Sphagnum* markers, with the histic and fibric peat displaying a high input of vascular markers (where Λ>99%) compared to the litter. The litter of the marginal peat pit1 displays a 21.6 and 15.4 % input of *P. commune*, whilst the green litter of the open peat pit1 displays a *P. commune* input of 92.3%. It is important to note that the unknown peaks in the open peat pit 2 have not been accounted for in this section. The potential presence of the common moss at this site needs to be investigated further.

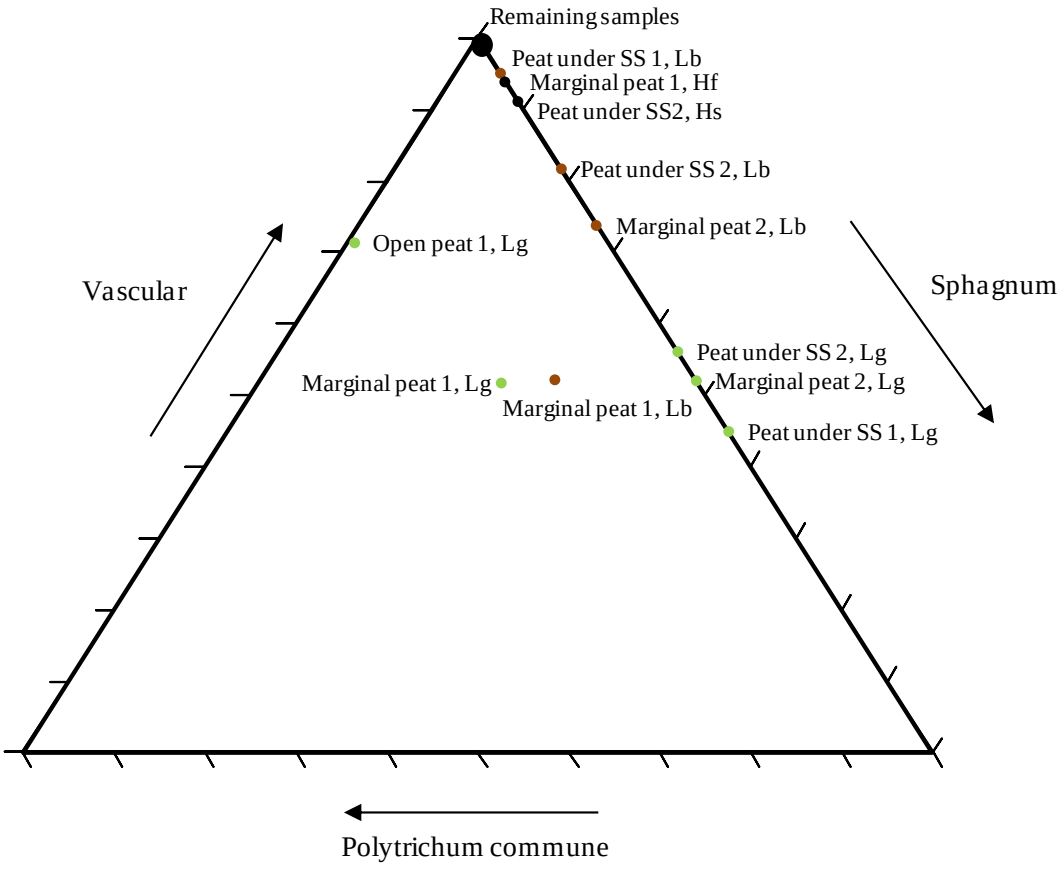

Fig. 6.17: The relative proportion of vascular, *Sphagnum* and non-*Sphagnum* mosses to the Wark Forest soils. Where SS: Sitka spruce, Lg: green litter, Lb: brown litter, Hf: histic peat, and Hs: sapric peat.

6.4 Conclusions

The encroachment of self seeded Sitka spruce onto the adjacent undisturbed moorland has been observed at Wark Forest, and has had an impact on both the carbon and phenol dynamics. The OC stocks decrease from the open bog to the forest-margin peats, with the distribution of OC shifting from high stocks in the Hs horizon of the open peat to higher stocks in the litter of the forest-margin peat, reflecting increased litterfall at the forest-margin peat.

Although the forest-margin peats have not been artificially disturbed, the growth of the self seeded trees will have caused some disturbance to the soil, coupled with the beginning of drying and shrinkage of soils caused by the adjacent Sitka spruce plantation which could be the primary mechanism decreasing OC values down the forest-margin peat profiles (Holden et al., 2007). These mechanisms suggest that a natural stabilisation of SOM in the open peat is occurring alongside the destabilisation of SOM in the forest-margin peats. However, similar oxidation rates across the site reflected in the $[Ad/Al]_G$ ratio indicates that the forest-margin peat is not experiencing increased oxidation due to the growth of the Sitka spruce or the edge effect. Therefore the changing carbon storage can be primarily attributed to the decreasing bulk density from the open peat to the forest-margin peats, reducing the carbon storage capacity in the marginal peats.

The lignin yield parameter (Λ), lignin proxies (S/G and C/G) and dominating THM products (P3, G3, P18 and G18) in the deeper horizons indicate that the vegetation across the three sites was previously non-woody vascular dominated, and is reflected in a cinnamyl-dominated lignin maximum at depth. The present vegetation, reflected in the green litter, suggests a gradual shift from a dominating single non-*Sphagnum* moss, to high species diversity from the open peat to the forest-margin peat under the Sitka spruce. Therefore the lignin maximum at depth at this site is not due to land disturbance as was the case in the afforested Sitka spruce stand (Chapter 3), but rather a change in vegetation.

The intact lignin contents at the litter horizons of these samples support a greater non-lignin phenolic contribution (e.g. *Sphagnum* and non-*Sphagnum* mosses), with the exception of forest-margin peat under Sitka spruce pit two, where there is evidence of the introduction of the self seeded Sitka spruce in the way of the high proportion of

intact G4 coupled with the high yield of intact G6 and demethylated lignin, increased litterfall, and low S/G and C/G ratios.

The maximum of tannins, specifically 1,3,5-TMB in the brown litter, suggests the translocation of these phenolics from the deeper horizons. These tannins, as with lignins, do not occur in non-vascular species, and therefore are most likely to have either originated alongside the lignin maximum or originated from vascular roots.

These results indicate that the presence of the self seeded Sitka spruce has not had a major effect on the phenolic composition and distribution. However there has been a notable change in surface vegetation across the entire chronosequence, which has brought about changes in the phenolic yields. However, the introduction of Sitka spruce on the forest-margin peat has appears to have destabilised the SOC at depth, reducing the carbon storage at these sites. An extended study at the site through canopy closure would be required to provide a more complete evaluation of the effect of self seeded Sitka spruce and the edge-effect occurring due to the adjacent plantation site.

This work highlights the importance of ^{13}C-labelled TMAH in lignin analytical studies of peat samples where tannin input is likely and has the potential to significantly mask the lignin signal. The factors controlling the accumulation of lignin in the deeper horizons needs to be investigated further, including water table and DOC measurements which will reflect the leaching of phenolics down core.

Chapter 7:

The TMAH Thermochemolysis of Carbohydrates in Peat and Soils

7 The TMAH Thermochemolysis of Carbohydrates in Peat and Soils

7.1 Introduction

Carbohydrates are ubiquitous and abundant in soils, and therefore are potentially useful in elucidating sources, processes and pathways of organic matter in soils (Jia et al., 2008). However, carbohydrates have been used relatively infrequently for organic matter source discrimination and degradation patterns in carbon-rich soils (van Smeerdijk and Boon, 1987; Moers et al., 1989; Jia et al., 2008). Currently, acid hydrolysis is the most common method used to liberate almost the entire carbohydrate pool from soils (e.g. Amelung et al., 1996; Jia et al., 2008). The method involves acid hydrolysis using either sulfuric acid (H_2SO_4), hydrochloric acid (HCl) or trifluoroacetic acid (TFA), which cleaves the glycosidic (1→4) bonds of the polysaccharides yielding sugar monomers, and the subsequent purification prior to the analysis via liquid chromatography (LC) or gas chromatography (GC) after derivatisation (Amelung et al., 1996).

Chapter 5 utilised acid hydrolysis data from the Ryggmossen peat samples, revealing large quantities of carbohydrates. The persistence of these products down the peat profiles indicated a relatively slow consumption of these compounds, with the carbohydrate yield decreasing from the bog centre to the bog-forest margin (Chapter 5; Section 5.3.4). The use of individual sugars as specific peatland source indicators as proposed by Comont et al. (2006), was confirmed in Chapter 5 for both the moss indicators (rhamnose, galactose and mannose) and sedge indicators (xylose and arabinose). Ribose (and to a lesser extent, hemicellulosic glucose) as also identified by Comont et al. (2006) as possible indicators for microbial synthesis. Building on this information Jia et al. (2008) used neutral monosaccharides as proxies for peat forming plants; [(Mannose+Galactose)/(Arabinose+Xylose)] and % (Rhamnose+Fucose), were proposed as tools to differentiate between lichens, *Sphagnum*, and vascular species.

This study for the most part however, utilised tetramethylammonium hydroxide (TMAH) thermochemolysis. The capability of TMAH to cleave ether and ester bonds and to methylate acidic functional groups of macromolecular structures in soil organic matter (SOM), including lignin (Challinor, 1995; Hatcher et al., 1995; Wysocki et al., 2008), allows the analyses of compounds entrapped in the macromolecular network

(Grasset and Amblès, 1998) including carbohydrates (Fabbri and Helleur, 1999; Schwarzinger, 2003; Tanczos et al., 2003; Estournel-Pelardy et al., 2011). However, the carbohydrates released by thermochemolysis does not represent the entire carbohydrate pool as seen in the acid hydrolysis method (Estournel-Pelardy et al., 2011).

Fabbri and Helleur (1999) discovered that reducing monosaccharides (i.e. sugars that have an aldehyde group; e.g. aldoses (Rose, 1994)) form methylated metasaccharinic acid (3-deoxyaldonic acid) methyl esters under thermally assisted hydrolysis and methylation (THM) conditions. This is a result of isomerisation of the C-2 position (Lobry de Bruyn-Alberda van Ekenstein rearrangement) followed by the dehydration of the C-3 position and a benzylic acid rearrangement (Fig. 7.1), first established in the early1900s by Nef et al., (1907; 1910; 1917) (See Knill and Kennedy, 2003, and references therein). These methylated metasaccharinic acids have a mass spectra with *m/z* 129 as a base peak (Fabbri and Helleur, 1999). The mechanism for the formation of methylated metasaccharinic acids and 1,2,4-trimethoxybenzene from the TMAH thermochemolysis of glucose is shown in Fig. 7.1.

The THM of the polysaccharide cellulose, has been shown to produce a specific epimeric pair of methylated isosaccharinic acids forming specific ions in EI mass spectroscopy (*m/z* 173) (Estournel-Pelardy et al., 2011). Cellulose is known to degrade under alkaline conditions due to an endwise depolymerisation reaction (peeling), leading to the formation of carboxylic acid products (Knill and Kennedy, 2003). The peeled end can then go through similar reactions as those observed by the monosaccharides, however instead of producing a hexonic acid which would methylate to form metasaccharinic acids, cellulose produces a 2-hydroxymethyl pentonic isomer (isosaccharinic acid (Fabbri & Helleur, 1999).

Results from THM at 610 °C presented in the preceding chapters have shown the tentative identification of carbohydrate derivatives in soil and litter samples, however it has been suggested that the presence of these methylated carbohydrates could be derived from the use of cellulose extraction thimbles (Mason, 2009). Described herein are the results of the potential carbohydrate markers as observed throughout the thesis, with the aim to (i) ascertain whether or not the extraction thimbles are a source of the methylated carbohydrates, (ii) identify and explore the behaviour of abundant monosaccharides and polysaccharides in soil; glucose, galactose and cellulose under TMAH thermochemolysis, and (iii) examine the usefulness of the technique of THM-

GC-MS in the analysis of carbohydrates within soil and peat samples. This chapter is not a comprehensive review of carbohydrate analysis by THM in carbon-rich soils, however it does provide insights to the potential of this method for future research.

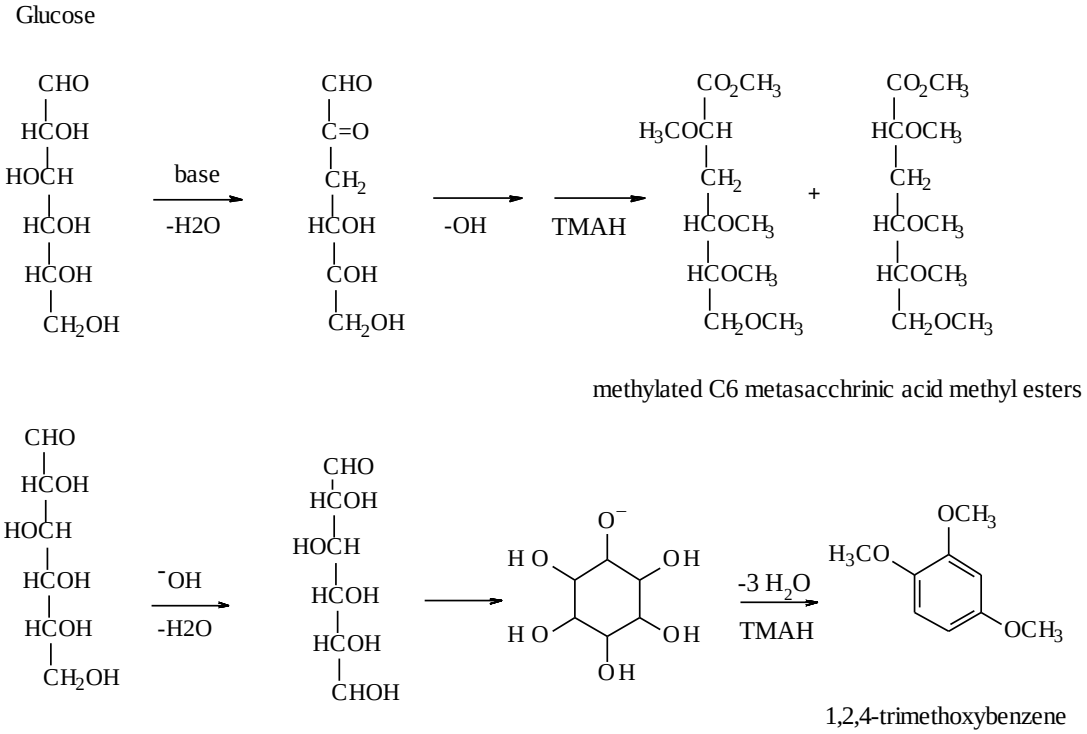

Fig. 7.1: Mechanism proposed by Fabbri & Helleur (1999) and Schwarzinger (2002) for the formation of methylated metasaccharinic acids and 1,2,4-trimethoxybenzene from the TMAH thermochemolysis of glucose.

7.2 Methods

7.2.1 Chemicals

Authentic reference samples of the two abundant monosaccharides in soil (Chapter 5; Section 5.3.4); D-(+)-glucose, D-(+)-galactose, and cellulose were purchased from Sigma. Cellulose and glass fibre extraction thimbles (33 mm x 80 mm) were purchased from Fisher Scientific. Standards were ran at a ratio of 1 uL/100 µg TMAH.

7.2.2 TMAH Thermochemolysis

On-line THM in the presence of ^{13}C-labelled and unlabelled TMAH was performed at 610 °C for 10 s (20 °C/ms temperature ramp) using the method set out in Chapter 2 (Section 2.2). Compound identification was based on the on ion fragmentation patterns

and following the conventions described in other studies, together with the comparison of mass spectra and relative retention times with the literature (Fabbri and Helleur, 1999; Tanczos et al., 2003; Schwarzinger, 2004).

7.2.3 Thimbles

To establish whether the cellulose thimbles are the source of methylated carbohydrate derivatives, two soils (one organic and one mineral soil) from Harwood Forest were split into two parts. Each part was either extracted with a cellulose thimble or a glass fibre thimble, providing four separate samples. The extracted soils were then analysed using THM in the presence of TMAH. Furthermore, small fragments of the cellulose and glass fibre thimbles were pyrolysed directly. Results were statistically interpreted using Minitab 16 statistical software package (Minitab Inc., USA).

7.3 Results and Discussion

The THM of the soil samples discussed throughout this thesis were dominated by oxygenated aromatics; however a range of polysaccharide derived compounds (1-4), methylated carbohydrates (MC1-4) and one of the products of cellulose, namely 1,2,4-trimethoxybenzene (1,2,4-TMB) were also observed. Fig. 7.2 shows the presence of these compounds (listed in Table 7.1) in the humified peat at the Wark Forest marginal peat under Sitka spruce pit two (Chapter 6).

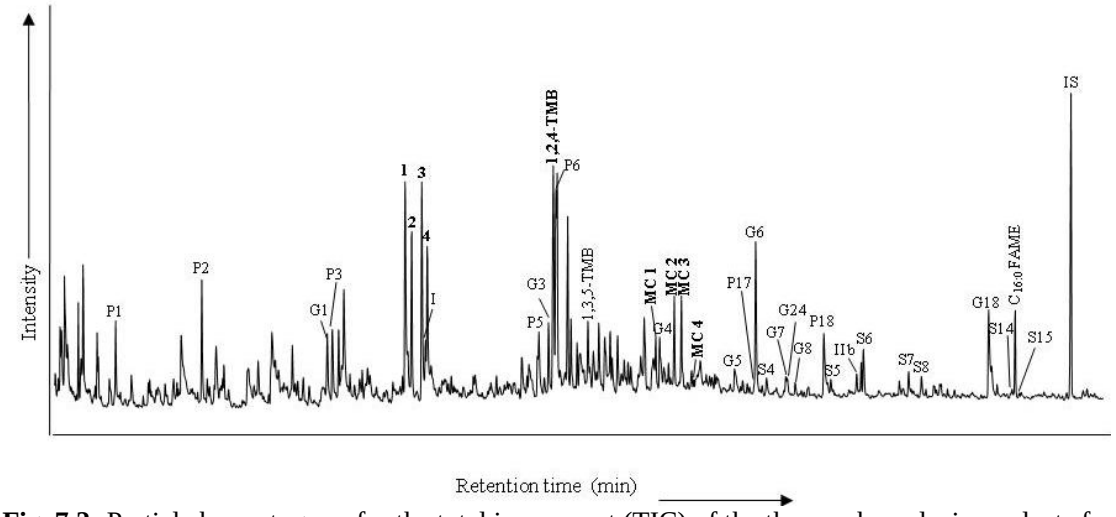

Fig. 7.2: Partial chromatogram for the total ion current (TIC) of the thermochemolysis products from the humified peat (Hs) at the Wark Forest marginal peat under SS, pit 2. Peak identities and symbols are listed in Table 6.2, Chapter 6. Compounds of interest in bold are listed in Table 7.1.

Table 7.1: TMAH thermochemolysis products from cellulose, glucose and galactose reference samples (base peak underlined).

Peak Label	*m/z*	Tentative structural assignment
1	57, 71, 83, 113, 127, <u>142</u>	polysaccharide derived compounds[1]
2	55, 71, 97, 113, 141, <u>156</u>	polysaccharide derived compounds
3	53, 85, 97, 127, 141, <u>156</u>	polysaccharide derived compounds
4	53, 83, 111, 125, 139, <u>154</u>	polysaccharide derived compounds[1]
1,2,4-TMB	69, 95, 110, 125, 153, <u>168</u>	1,2,4-trimethoxybenzene
5	75, 89, 113, 141, <u>173</u>, 191	Partially methylated isosaccharinic acid methyl ester (3-deoxy-2-methoxymethylpentonic) acid methyl ester[1]
6	75, 89, 119, 141, <u>173</u>, 205	Permethylated isosaccharinic acid methyl ester (3-deoxy-2-methoxymethylpentonic) acid methyl ester[1]
MC1	59, 101, <u>129</u>, 147, 177	Partially methylated 3-deoxy-hexonic acid, methyl ester[2]
MC2	75, 101, <u>129</u>, 161, 191	Permethylated 3-deoxy-hexonic acid, methyl ester[2]
MC3	59, 101, <u>129</u>, 147, 177	Partially methylated 3-deoxy-hexonic acid, methyl ester[2]
MC4	75, 101, <u>129</u>, 161, 191	Permethylated 3-deoxy-hexonic acid, methyl ester[2]

[1] Schwarzinger (2002); [2] Schwarzinger (2004)

7.3.1 Preliminary Test on Extraction Thimbles

Preliminary THM tests on the extraction thimbles were performed following the procedure described in the methods section. The GLM indicated that the soils extracted with the glass fibre thimbles yielded significantly similar quantities of 1,2,4-TMB (p=0.832), methylated carbohydrates (p=0.838) and polysaccharide derived compounds (p=0.288) as the soils extracted with cellulose thimbles.

The extraction thimbles themselves were also analysed with TMAH. The THM of the cellulose thimbles indicates the presence of 1,2,4-TMB and the four polysaccharide derived compounds but the methylated carbohydrates we absent (Fig. 7.3). The four polysaccharide derived compounds released during the THM analysis of the cellulose thimbles are observed throughout the soil, peat and litter samples, however are most abundant in the Ryggmossen peat samples, which were not extracted using Soxhlet extraction (Chapters 4 and 5; See Chapter 2, Section 2.8 for methodology).

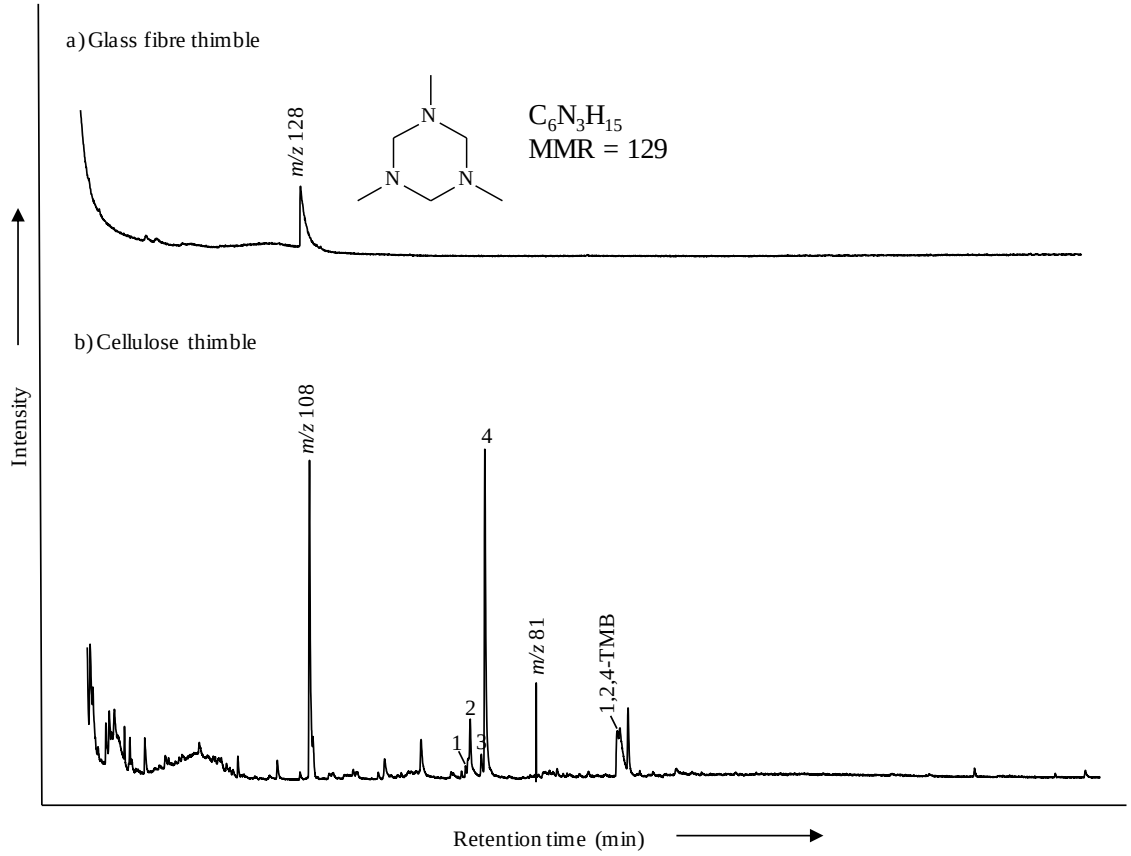

Fig. 7.3: Partial chromatogram for the total ion current (TIC) of the thermochemolysis products from the (a) glass fibre thimble and (b) cellulose thimble. Peak identities and symbols are listed in Table 7.1.

The TIC from the glass fibre thimble released no methylated carbohydrates or cellulose compounds; however it did release one peak with an *m/z* 128. This peak has previously been identified by Templier et al. (2005); Nierop and Buurman (2007), and Bardy et al. (2011), as a TMAH by-product, namely 1,3,5-trimethylhexahydro-1,3,5-triazine.

Due to the presence of polysaccharide derived compounds within samples not extracted using cellulose thimbles, coupled with no significant differences in the yields of these products in cellulose or glass fibre thimbles, the cellulose thimbles as a source of the polysaccharide derived compounds and methylated carbohydrates compounds in this study can be assumed to be negligible. However if future work focused on the analysis of carbohydrates, it is reccommend that glass fibre thimbles or an alternative extraction technique is utilised, to eliminate any chance of contamination.

7.3.2 Analysis of Authentic Reference Samples

When two monosaccharides of hexose (glucose and galactose) are subjected to THM analysis, various methylated products are released. The TIC (Fig. 7.4) shows the major THM products are a series of four methylated metasaccharinic acid methyl esters (MC1-4) (see Fig. 7.1 for the structure of the methylated metasaccharinic acids) (Schwarzinger, 2004). Compounds 1, 2, 3, and 4 were also present, although in higher abundance in the glucose standard. 1,2,4-trimethoxybenzene (1,2,4-TMB) was also a major component detected by GC-MS in both the glucose and galactose standards.

A variety of products are released following the pyrolysis of cellulose in the presence of TMAH (Fig. 7.5). These products included compounds 1- 6, and 1,2,4-TMB. The absence of methylated carbohydrates in the TIC of cellulose displays the lack of hexonic acid as identified by Fabbri and Helleur (1999), instead forming the typical polysaccharide thermochemolysis products; isosaccharinic acids (compounds 5 and 6) (Schwarzinger, 2002). The corresponding mass spectral data are reported in Table 7.1.

It is important to note that a cautious interpretation of these results when compared to the literature is required, due to differences in the experimental conditions (e.g. temperature, ratio of TMAH to sample, solvent choice and contact time between sample and TMAH), which can create large differences in the output (Schwarzinger et al., 2002).

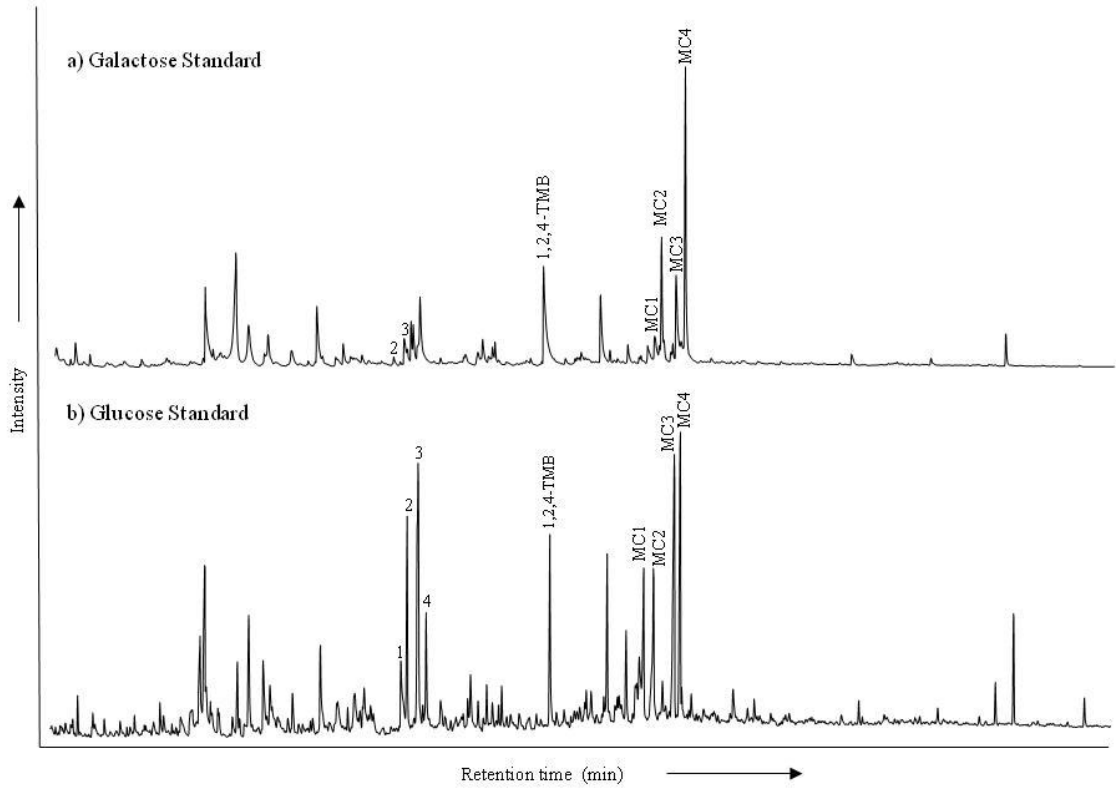

Fig. 7.4: Partial chromatogram for the total ion current (TIC) of the thermochemolysis products from authentic (a) galactose and (b) glucose sample. Peak identities and symbols are listed in Table 7.1.

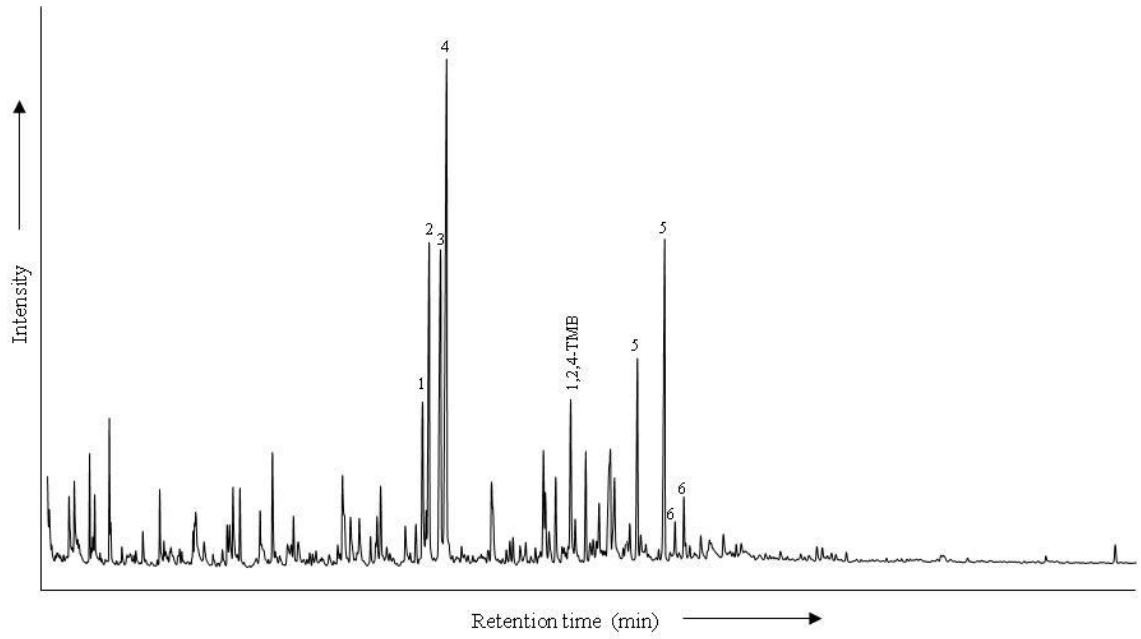

Fig. 7.5: Partial chromatogram for the total ion current (TIC) of the thermochemolysis products from cellulose. Peak identities and symbols are listed in Table 7.1.

7.3.3 Metasaccharinic Acid Methyl Esters

First tentatively assigned as methylated carbohydrates in 1996, the four compounds with prominent ions at *m/z* 101 and *m/z* 129 (MC1-MC4) (Fabbri et al., 1996), have since received much attention to correctly identify and understand their presence (Fabbri and Helleur, 1999; Schwarzinger et al., 2002; Schwarzinger, 2003; Schwarzinger, 2004) in the pyrolysates of soils (Mason et al., 2009), humic matter and plant gums (Riedo et al., 2009).

These methylated carbohydrate derivatives (Fabbri et al., 1996; Fabbri and Helleur, 1999) were tentatively assigned in varying abundances across the majority of the soil samples analysed in this thesis; Chapter 3, Chapter 6 (e.g. Fig. 7.2), due to the identification of the prominent ions (Fabbri et al., 1996). In agreement with other studies (Fabbri et al., 1996; Fabbri and Helleur, 1999) the THM of the monosaccharides lead mainly to a set of two pairs of permethylated metasaccharinic acids (MC1 and MC3; MC2 and MC4), with each pair exhibiting an identical mass spectrum (Fabbri and Helleur, 1999; Chiavari et al., 2007).

For each pair of the methylated carbohydrates, a comparison between the mass spectra from unlabelled and ^{13}C-labelled TMAH are shown (Fig. 7.6). After THM with ^{13}C-labelled TMAH, the acidic oxygen functional groups are methylated by the ^{13}C-labelled methyl groups. Therefore, the number of ^{13}C-labelled methyl groups added to the carbohydrate products should be equivalent to the number of acidic oxygen functional groups on the molecule. Figs. 7.7 and 7.8 show the fractionation patterns of the two pairs of metasaccharinic acids, displaying the molecular ion for each of the ^{13}C-labelled and unlabelled products and the number of ^{13}C-labelled methyl groups added to each compound as determined by GC-MS. The increase in molecular weight upon ^{13}C-TMAH thermochemolysis corresponds to the number of available sites for methylated for MC2 and MC4, but not for MC1 and MC3.

MC2 and MC4 are therefore fully methylated, and will be considered as pair one; the fragmentation scheme of the major *m/z* ions for MC2 and MC4 is interpreted in Fig. 7.7. However, several fragment ions of pair two (MC1 and MC3), indicate a certain level of incomplete methylation (Fig. 7.8). $M^{+\cdot}$ (molecular ion) for these two pairs of products was assumed at *m/z* 250 consistent with published sources (Fabbri and Helleur, 1999), however it is important to note that the reference samples used (i.e. glucose) would need

to be analysed with chemical ionisation (CI) in order to ascertain the molecular weight of the MCs.

Pair one (MC2 and MC4) showed several fragment ions at *m/z* 191, *m/z* 205, *m/z* 161, *m/z* 129 and *m/z* 101 (Fabbri and Helleur, 1999; Tanczos et al., 2003). The labelled mass spectra (Fig. 7.6) displayed a base peak *m/z* 131, indicating the addition of two labelled methyl groups, consistent with complete methylation of this fragment as shown in Fig. 7.7.

The incomplete methylation observed for products MC1 and MC3 has previously been observed when the pyrolysis temperature is reduced, with higher temperatures required for complete methylation (Schwarzinger et al., 2002). Although the pyrolysis temperature used herein (610 °C) was in excess of the maximum pyrolysis temperature used by Schwarzinger et al. (2002) (500 °C) indicating complete methylation may require higher amounts of TMAH. The ions with *m/z* 177 and *m/z* 147 have a molecular weight of 14 less than their respective ions in the fully methylated saccharinic acids (*m/z* 191, 161), suggesting one acidic oxygen functional group has not been methylated, this is confirmed by the shift of only two and three mass units in the mass spectra, for *m/z* 147 and 177 respectively, where there are in fact three and four potential sites for ^{13}C-methylation respectively (Fig. 7.6). Pair two (MC1 and MC3) showed several fragment ions at *m/z* 177 (partially methylated), *m/z* 205, *m/z* 147 (partially methylated), *m/z* 129 and *m/z* 101. The proposed mechanism for the fragmentation of the major ions has been illustrated in Fig. 7.8.

7.3.4 Cellulose Derived Products

The thermochemolysis of cellulose (Fig. 7.4) released 2 compounds that were observed in the THM products of the cellulose standard only: peaks 5 and 6. Peaks 1- 4 were also observed in the THM of cellulose, and have been described throughout this chapter as polysaccharide derived compounds. The corresponding mass spectra of these six products are shown in Figs. 7.9-7.11.

Fig. 7.9 shows that compound 1 has a base peak *m/z* 142 (Fig. 7.9a), and compound 4 has a base peak *m/z* 154 (Fig. 7.9d), these two compounds have been observed by Schwarzinger et al. (2002) in the thermochemolysis of cellulose and cellulose acetate, however only under certain conditions; including under surplus levels of TMAH.

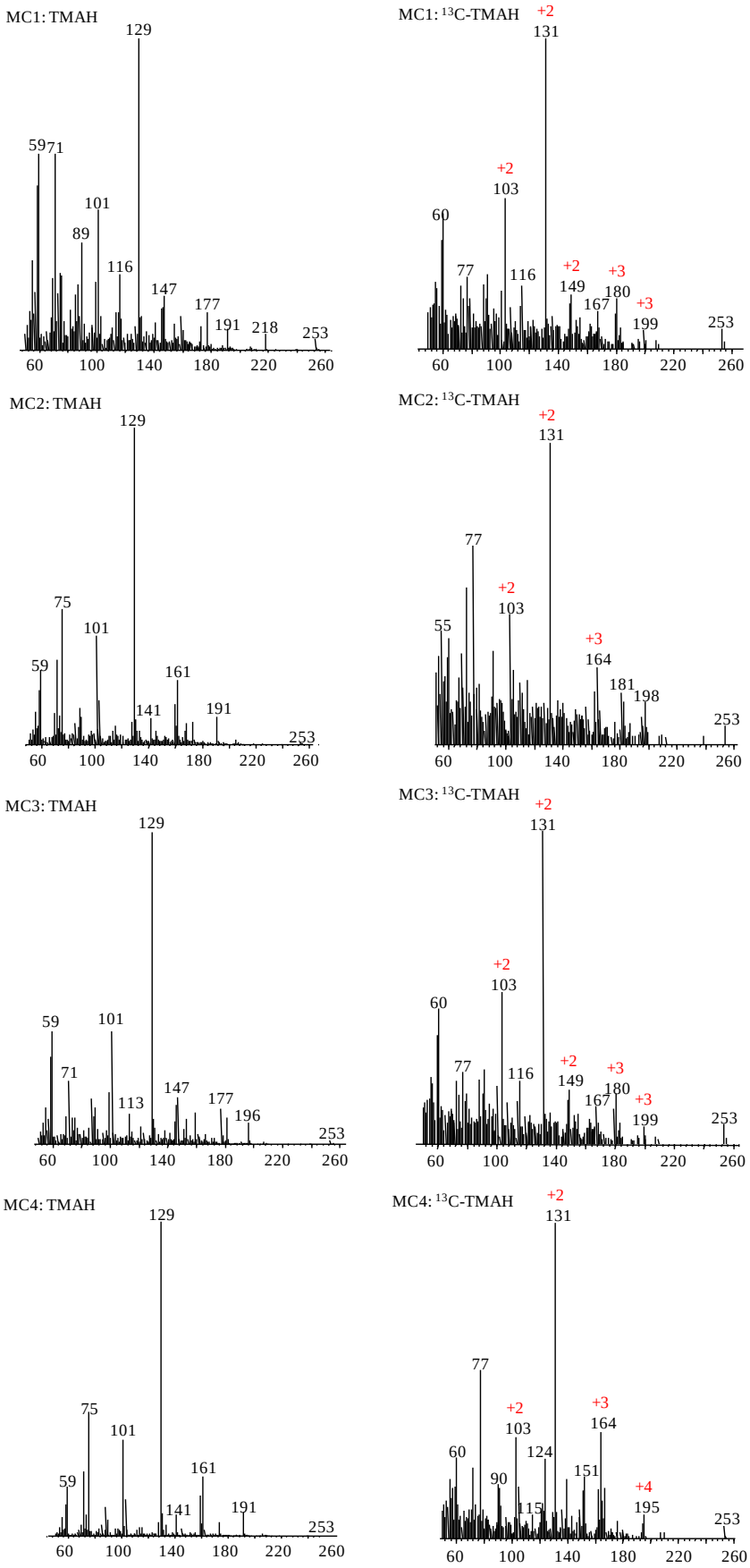

Fig. 7.6: The mass spectra of the unlabelled and associated ^{13}C-labelled monosaccharides: MC1, MC2, MC3 and MC4. Numbers in red with a plus (+) prefix indicate the number of added labelled C atoms, i.e. methyl groups added by ^{13}C-TMAH.

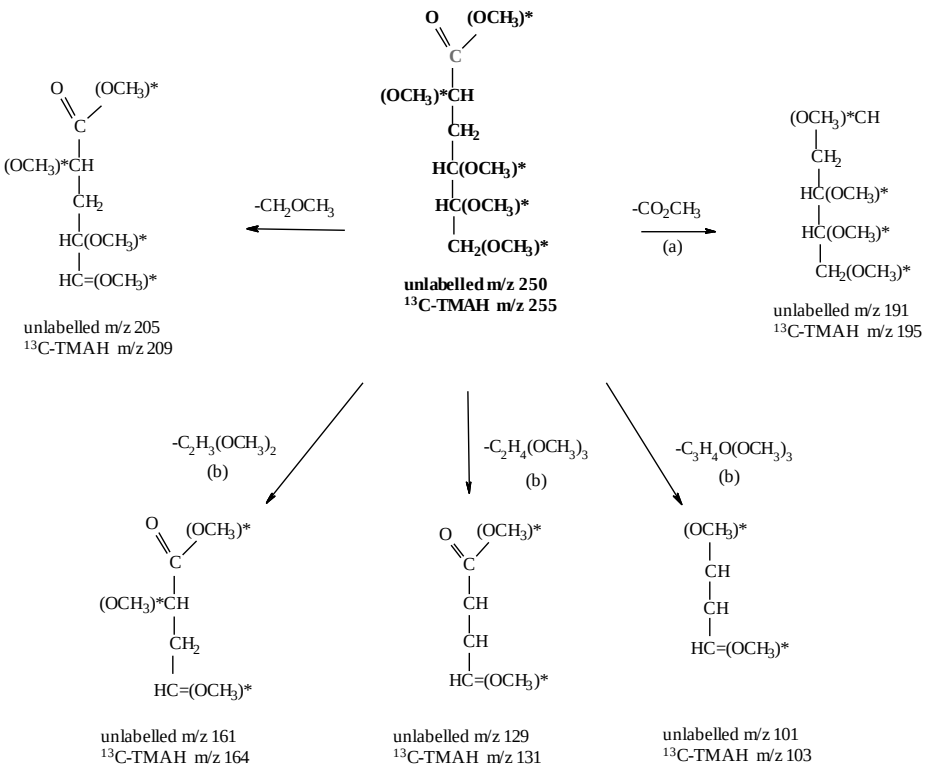

Fig. 7.7: Proposed fragmentation pathway of MC2 + MC4 (permethylated deoxyaldonic acid epimers). Displaying the methyl groups that can increase the molecular weight using ^{13}C-TMAH (OCH_3)*. (a) Fabbri & Helleur (1999), (b) Tanczos et al. (2003).

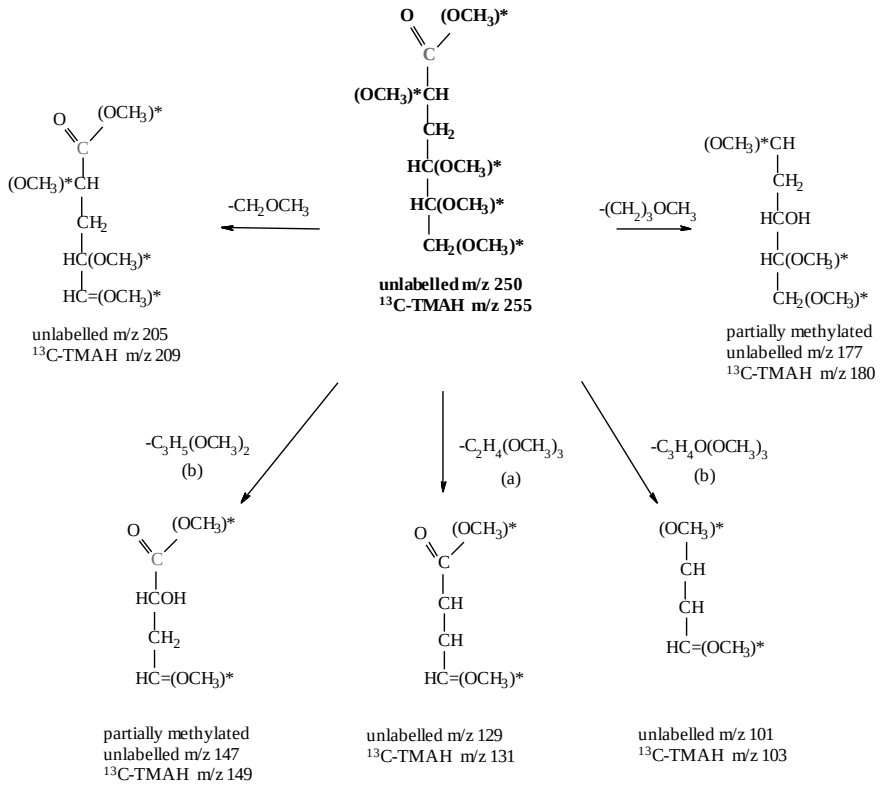

Fig. 7.8: Proposed fragmentation pathway of MC1 + MC3 (partially methylated deoxyaldonic acid epimers). Displaying the methyl groups that can increase the molecular weight using ^{13}C-TMAH (OCH_3)*. (a) Schwarzinger (2004), (b) Tanczos et al. (2003).

More recently, these compounds have been observed in podzol SOM by Bardy et al. (2011). Compound 4 has been assigned 2,4-dimethoxyphenol by Fabbri & Helleur (1999), however Schwarzinger et al. (2002) suggested that the assignment may be incorrect based upon the inconsistent retention times attained from Fabbri and Helleur (1999) and Schwarzinger (2002), and therefore these compounds remain un-assigned. Peaks 2 and 3 have similar mass spectra, suggesting two isomers with a base peat *m/z* 156 (Fig. 7.9b and c). Although these products remain unassigned, all four products displayed an increased molecular weight of two after THM with ^{13}C-labelled TMAH, indicating the presence of two hydroxyl groups on each of these four products.

Fabbri and Helleur (1999) described two isomers of partially methylated isosaccharinic acid methyl ester with *m/z* 173, 141, 127, in the thermochemolysis products of cellulose which would be consistent with the mass spectrum observed for compound 5 (Fig. 7.10). These two products have since been identified as methylated and partially methylated isosaccharinic (3-deoxy-2-hydroxymethylpentonic) acid methyl esters (Schwarzinger, 2002). Fabbri and Helleur (1999) proposed the mechanism for the formation of THM products 5 and 6 from cellulose illustrated in Fig. 7.5. The detailed mechanism proposed for the fragmentation pattern of compounds 5 and 6 are shown in Figs. 7.10 and 7.11 respectively.

Schwarzinger et al. (2002), showed that although the main degradation products are not influenced by drying the samples prior to analysis, products 5 and 6 are encouraged when the water is not removed. This is consistent with the endwise depolymerisation reaction (peeling) of cellulose, which occurs in an aqueous media at elevated temperatures (see section 7.3.2, for a detailed description of this reaction) (Schwarzinger,2002; Knill and Kennedy, 2003).

The molecular ion of compound 5 was assumed at *m/z* 236 (partially methylated) consistent with published sources (Schwarzinger, 2004), with several fragment ions at *m/z* 191 (partially methylated), *m/z* 177, *m/z* 145, *m/z* 141, *m/z* 127 and *m/z* 113. It should be pointed out that the compound structure for ion *m/z* 177 published in Schwarzinger (2004) should display a double bond on the C4 bond.

Compound 6 displayed a similar mass spectrum to compound 5, however displaying the complete methylation of the product, with the partially methylated fragment at *m/z* 191 from compound 5, displaying an increase of 14 mass units to *m/z* 205, indicating the addition of 4 methylated groups, adequate for the complete methylation. The molecular

ion was assumed at *m/z* 250, due to the complete methylation, with several fragment ions at *m/z* 205, *m/z* 173, *m/z* 141, *m/z* 191, and *m/z* 159. The low pyrolysis temperature of 500 °C used by Schwarzinger (2004); was held responsible for the incomplete methylation of the saccharinic acids, causing the OH-group at position 2 to remain un-methylated. The higher pyrolysis temperature in this study (610 °C) has shown a degree of complete methylation concomitant with the presence of partially methylated components.

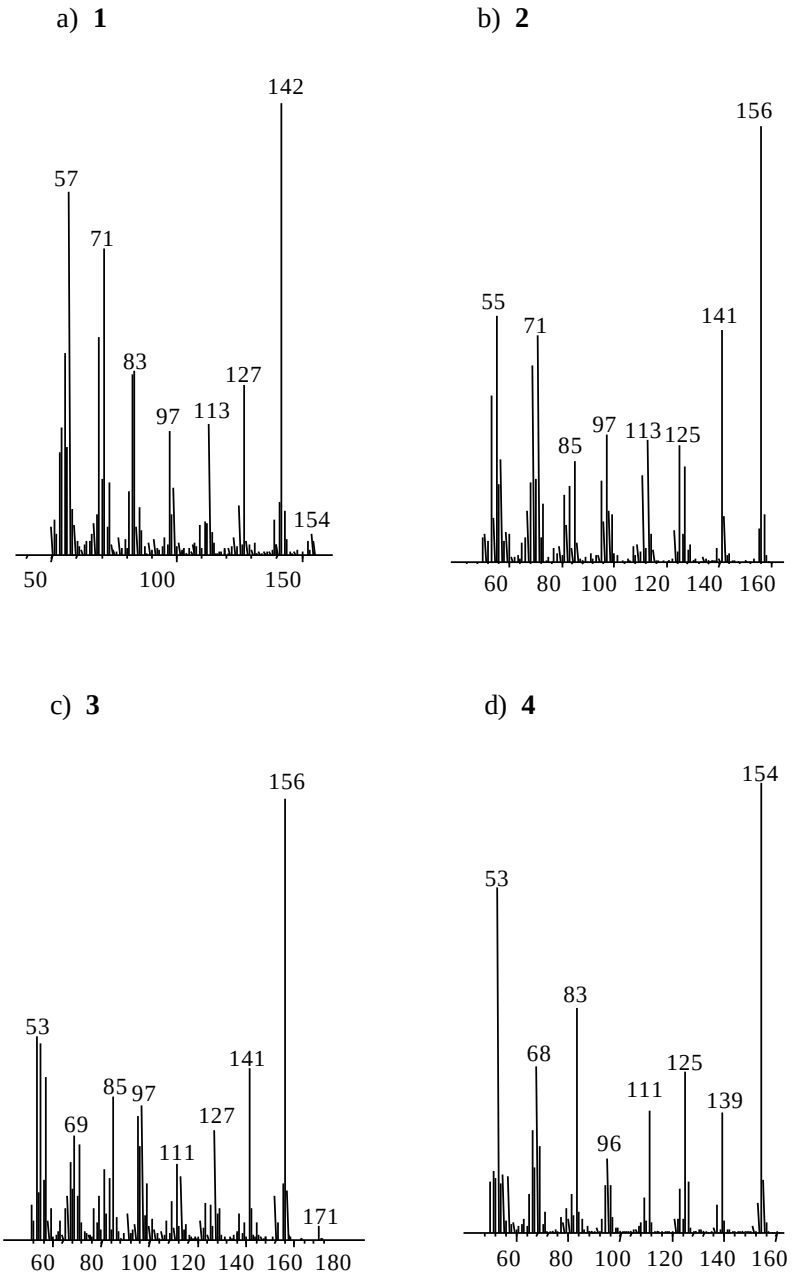

Fig. 7.9: EI mass spectrum of polysaccharide derived products (a) 1, (b) 2, (c) 3 and (d) 4.

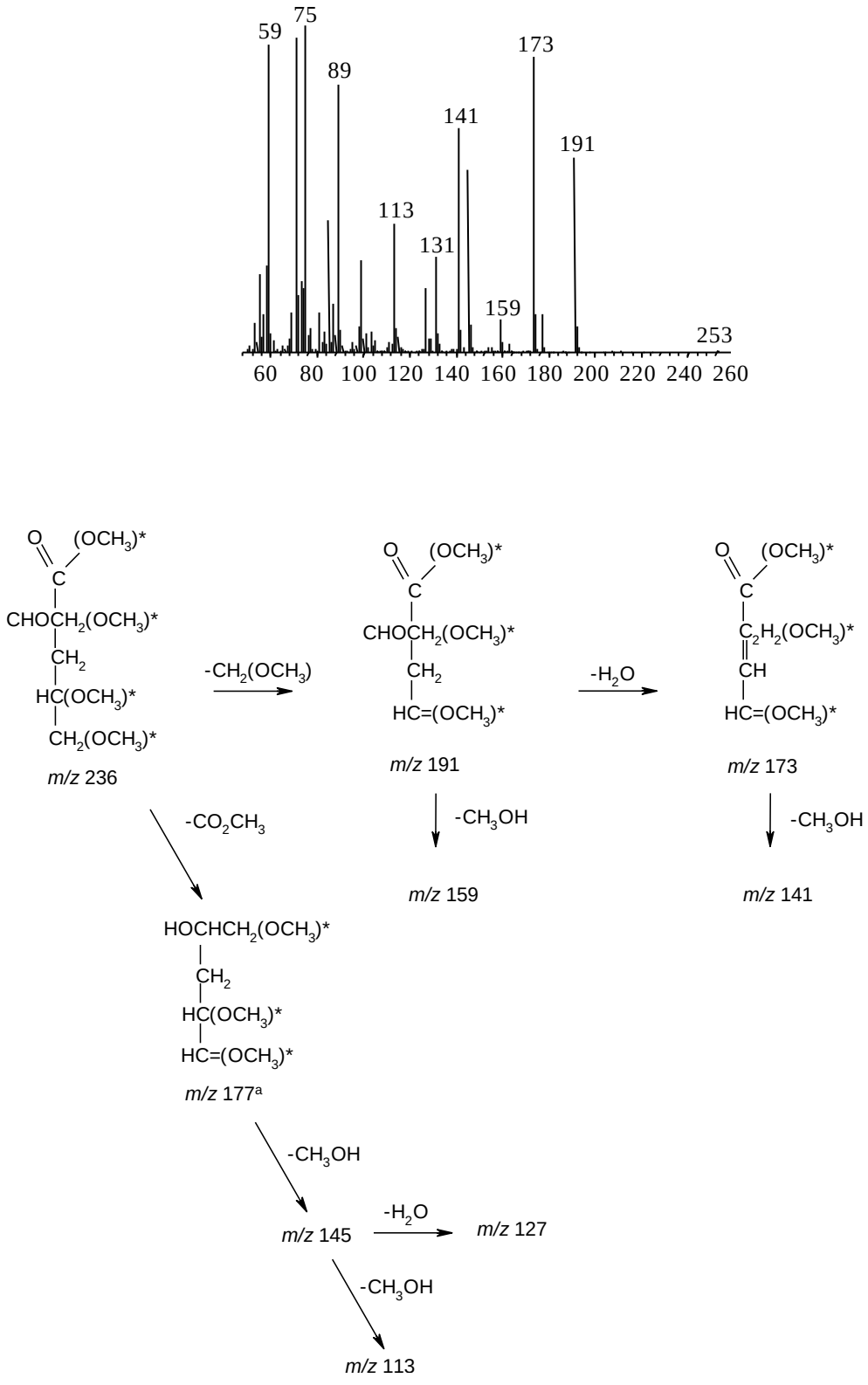

Fig. 7.10: EI mass spectrum and the proposed fragmentation pathway for peak 5: partially methylated isosaccharinic acid: Modified from Schwarzinger (2004).

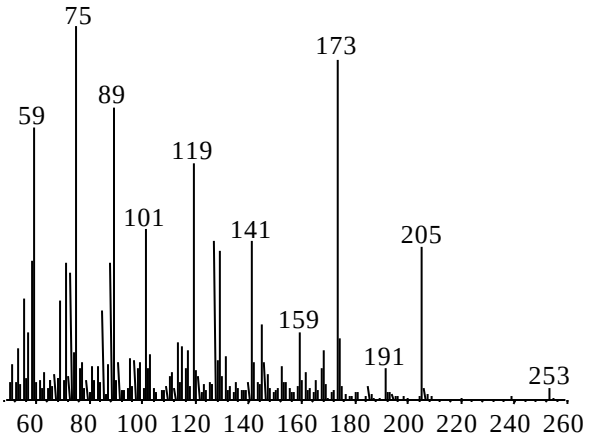

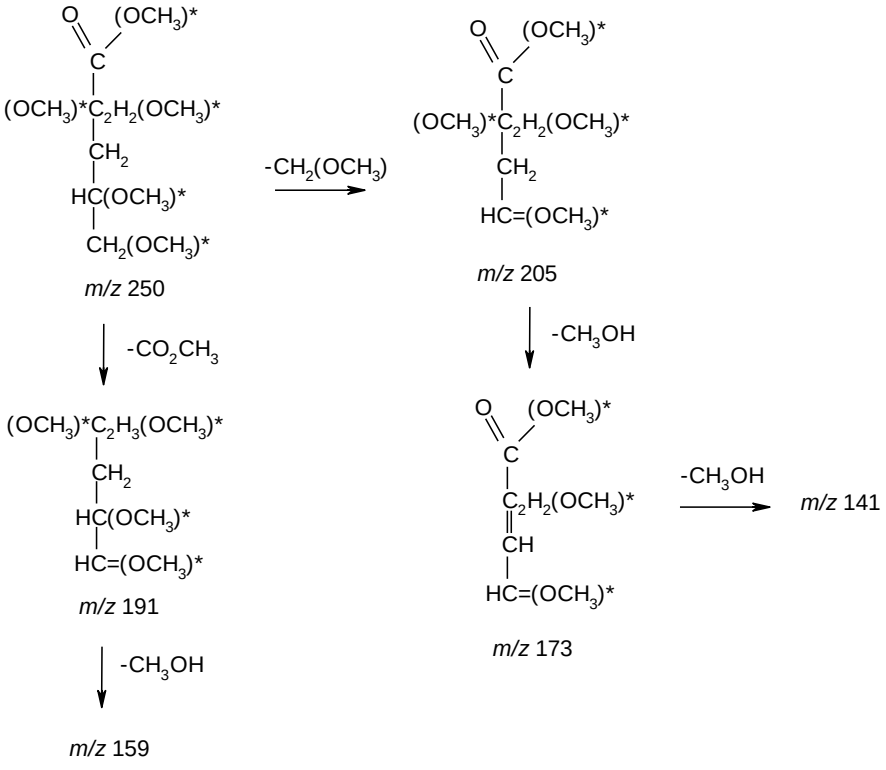

Fig. 7.11: EI mass spectrum and the proposed fragmentation pathway for peak 6**:** permethylated isosaccharinic acid.

7.3.5 1,2,4-trimethoxybenzene

1,2,4-trimethoxybenzene (1,2,4-TMB) was observed in all the samples analysed in this thesis and identified in the thermochemolysis of both the monosaccharides and glycosidically-linked polysaccharides (Figs. 7.3 and 7.4). Fig. 7.12 displays the mass spectrum of 1,2,4-TMB.

Whilst a common product observed in the thermochemolysates of multiple samples (i.e. carbohydrates (Fabbri and Helleur, 1999), soils (Mason, 2009), peats (Chapter 5)), the precise source remains unclear. Although Fabbri and Helleur (1999) observed 1,2,4-TMB in the TMAH thermochemolysis products of carbohydrates, within soils, Chefetz et al. (2000) did not link 1,2,4-TMB to cellulose, due to the perceived reactivity of cellulose within soil. More recently, Nierop et al. (2005), suggested that this compound may be a marker for condensed tannins, derived from a procyanidin (PC) B ring (Fig. 1.7), when there is an absence of polysaccharides. As a result, this compound could derive from two sources; tannin and polysaccharide (Fabbri and Helleur, 1999; Nierop et al., 2005). In order to elucidate the profile trend of 1,2,4-TMB through soil and peat profiles the source needs to be differentiated between input from tannin or polysaccharide.

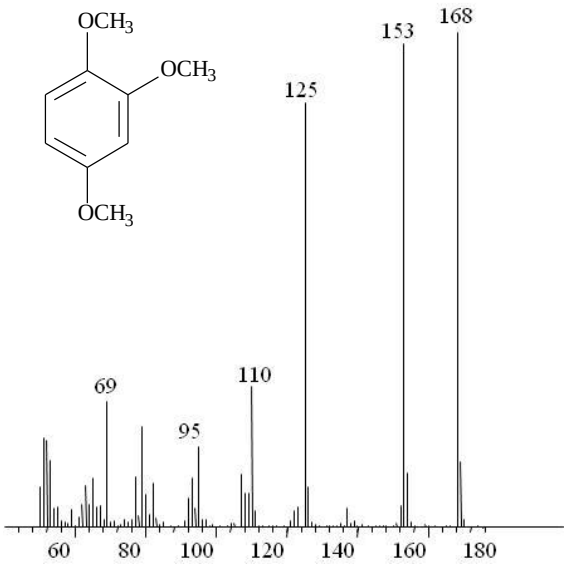

Fig. 7.12: EI mass spectrum and compound structure for 1,2,4-trimethoxybenzene.

The presence of 1,2,4-TMB has been observed in the thermochemolysate of both cellulose and the monosaccharides glucose and galactose (Figs. 7.3 and 7.4). A ratio of this compound to the sum of the total OC-normalised yield of identified carbohydrate compounds: 1,2,4-TMB / ((MC1-MC4) + (1-4)) is proposed, which will provide a measure of the relative amount of 1,2,4-TMB derived from a carbohydrate source. This ratio works on the assumptions that these carbohydrate derived compounds degrade at a similar rate in soil, and that MC1-4 and 1-4 have no other sources.

The three reference compounds (i.e. cellulose, glucose and galactose) provide a ratio of 0.26 ± 0.07. This ratio value can be used as a baseline for carbohydrate input, with values exceeding this ratio an indication of the addition of tannin-derived 1,2,4-TMB.

The ratio for the Coalburn and Harwood Forest results are shown in Table 7.2, and Wark Forest results shown in Table 7.3. The Coalburn Forest moorland (ML) profile suggests that the 1,2,4-TMB is primarily derived from the polysaccharide source due to the consistently low ratio down core. The Coalburn Forest first rotation afforested site (SS1) soil shows a relatively consistent input of both saccharides and tannins down core reflected in the consistent but elevated ratio down core (>0.5), which indicates the additional presence of tannins alongside the polysaccharides. The Harwood Forest second rotation afforested site (SS2) shows an increased tannin input in the A horizon, reflected in the increase in the ratio to 0.83. This is consistent with the maximum of tannin marker 1,3,5-TMB observed in the A horizon (Chapter 3; Fig. 3.13).

The Wark Forest soils show an average of 0.3 ± 0.03, down the six profiles, suggesting a predominant saccharide input to the 1,2,4-TMB yield. The only exception is the green litter of the marginal peat pit two, which shows an elevated ratio (0.89), indicating an increased tannin input. This is further reflected in the elevated yield of 1,2,4-TMB and 1,3,5-TMB in the upper green litter of the marginal peat pit 2 (Chapter 6, Section 6.3.5.1, Figs 6.15b and 6.16b), whereas the polysaccharide inputs at this horizon remain fairly low and consistent with the marginal peat pit 1 (Fig. 7.14). This is consistent with findings in Chapter 6, showing that this profile is displaying signs of the introduction of Sitka spruce, which are known to contain high levels of tannins. The remaining five profiles are predominantly vegetated with grasses and mosses, in which the distribution of tannins are of minor importance (White, 1957).

Table 7.2: The ratio indicating the polysaccharide input to 1,2,4-TMB in the Coalburn (CB) and Harwood (HW) Forest soil profiles using [1,2,4-TMB / ((MC1-MC4) + (1-4))]

CB ML	ratio	CB SS1	ratio	HW SS2	ratio
L+F	0.38	L+F	0.53	L+F	0.40
Hf	0.21	Hf	0.56	Hf	0.37
Hs	0.41	Ae	0.60	Hs	0.27
Ae	0.50	Bg	n.d	A	0.83
Bg	n.d			H	0.21

Table 7.3: The ratio indicating the polysaccharide input to 1,2,4-TMB in the Wark Forest soil profiles using [1,2,4-TMB / ((MC1-MC4) + (1-4))]

	Marginal peat under SS ratio		Marginal peat ratio		Open peat ratio	
Lg	0.21	0.25	0.15	0.89	0.22	0.16
Lb	0.25	0.34	0.19	0.18	0.19	0.18
Hf	0.44	0.29	0.47	0.31	0.14	0.23
Hs	0.59	0.32	0.32	0.29	0.41	0.21

These results indicate that the proposed ratio to determine the source of 1,2,4-TMB provides a quick indication of source, especially when combined with other factors and proxies, such as lignin ratios C/G and S/G. However, care must be used when interpreting the data, due to the potential of other sources; e.g. Mason et al. (2009) suggested that methylated carbohydrates in deeper soils were of microbial origin; indicating further research into the differentiation of 1,2,4-TMB from a tannin and polysaccharide source is required.

7.3.6 Profile Trends

7.3.6.1 Coalburn, Harwood and Wark Forest

THM in the presence of TMAH of solvent-extracted soil from Coalburn, Harwood and Wark Forest yielded methylated carbohydrates and the cellulose derived products. The THM traces for these samples are shown in their respective results chapters (Chapter 3; Figs. 3.2-3.4, and Chapter 6; Figs. 6.4-6.7). The sum of the methylated carbohydrates and the sum of the cellulose derived products are normalised to 100 mg of OC and displayed ion Figs. 7.13 and 7.14.

The total methylated carbohydrates yield for the ML is constant down the profile, decreasing only in the mineral B horizon, however displays an increase with depth in

the two afforested soils. The polysaccharide derived products in the ML and SS1 display a high yield in the litter (*ca* 0.26 and 0.06 mg/100 mg OC respectively), however they are lost with increasing depth. In the SS2 soil, the polysaccharide derived products increase in to the deeper horizons, however changes are not significant ($p>0.05$).The GLM indicated the ML soil had significantly higher yield of polysaccharide derived products compared to the two afforested sites ($p<0.001$). However there were no differences observed between the sites for the MC yield ($p=0.05$).

The polysaccharide derived products exceed the methylated carbohydrate yield throughout the Wark Forest soils (Fig. 7.14). The GLM indicated the three Wark sites all had similar yields of methylated carbohydrates and products 1-4 ($p=0.955$ and 0.382). However, significant differences were observed between the total methylated carbohydrates and 1-4 yield down the core ($p=0.002$ and 0.000). The Tukey's test showed that the Hs horizon had significantly higher yield of methylated carbohydrates than the shallower litter horizons, and Lb had significantly higher yield of products 1-4 than the Lg, Hf and Hs horizons. Quantities of methylated carbohydrates and products 1-4 in the Wark Forest profiles (0.18 and 0.04 mg/100 mg OC) are comparable to the yields in the ML soil of Coalburn Forest (0.11 and 0.04 mg/100 mg OC). However the yield of cellulose products 1-4 decline to 0.06 mg/100 mg OC in the afforested stands, whilst the methylated carbohydrates are elevated to 0.08 mg/100 mg OC.

The yield of the polysaccharide derived compounds exceeds the yield of the methylated carbohydrates in the litter of the Coalburn, Harwood and Wark Forest soils. However with increasing depth, the yield decreases to a similar yield of methylated carbohydrates. The larger contribution of these metasaccharinic acids at depth, which were observed in the two monosaccharides of hexose, but not in the cellulose (Figs. 7.3 and 7.4), could be a reflection of the preferential decomposition of cellulose by white-rot fungi, and the input of microbially synthesised hexose in the deeper soil, especially of fungi (Dijkstra et al., 1998; Huang et al., 1998). Polysaccharides are the principal energy source for heterotrophic microbial communities, so their progressive decrease with depth is expected (Huang et al., 1998). The land use change appears to have increased the loss of compounds 1-4, concomitant with increased lignin oxidation (Chapter 3; Fig. 3.10) (Filley et al., 2002), whilst allowing the accumulation of the microbially synthesised methylated carbohydrates in the deeper soil (Spaccini et al., 2000; Gleixner et al., 2002).

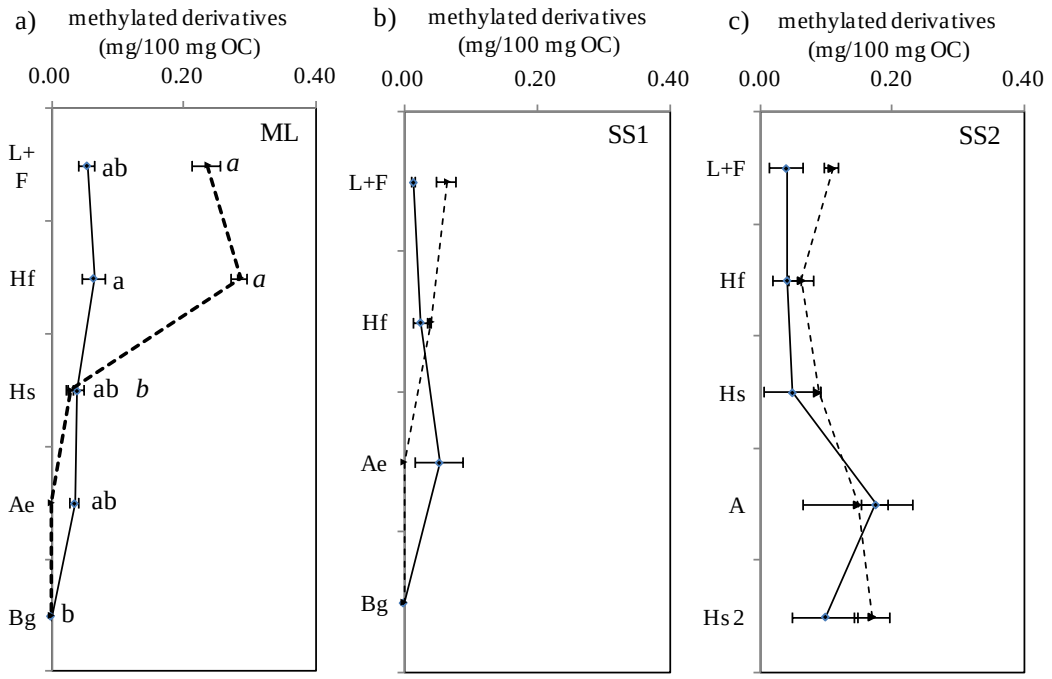

Fig. 7.13: The depth profile showing changes in the methylated carbohydrates (solid lines) and the polysaccharide derived compounds 1-4 (dashed lines) (mg/100 mg OC) in (a) ML, (b) SS1 and (c) SS2 soil. The error bars indicate the standard error from three/two analytical replicates. Means with different letters are significantly different (Tukey's HSD, $p>0.05$).

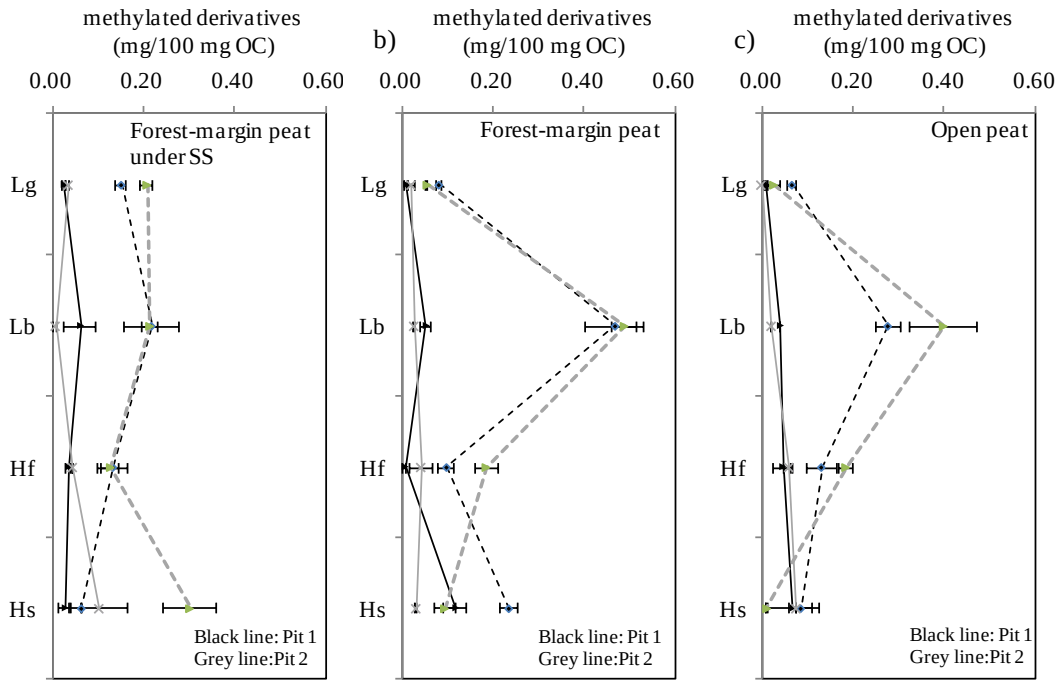

Fig. 7.14: Depth profile showing changes in the amount of methylated carbohydrates (solid lines) and the polysaccharide derived compounds 1-4 (dashed lines) (mg/100 mg OC) in a) FM peat under SS, b) FM peat and c) the open peat. Error bars show standard error of two analytical replicates.

7.3.6.2 Ryggmossen Peatland

The acid hydrolysis carbohydrates from the Ryggmossen peat cores carried out by Dr. Greg Cowie (Edinburgh University), showed consistently higher amounts compared to the THM cellulose products 1-4 (Fig. 7.15) consistent with previous work (Comont et al., 2006; Estournel-Pelardy et al., 2011). Estournel-Pelardy et al. (2011) found a poor agreement between acid hydrolysis carbohydrates and THM carbohydrates; however Estournel-Pelardy used the methylated carbohydrate markers with *m/z* 101, 129 as indicators for carbohydrates. The thermochemolysates of the peat cores released very small quantities of these methylated carbohydrates (average BM hummock = 4.3×10^{-5} mg/100mg OC). Therefore the dominant cellulose markers 1-4 were used. Combined THM in the presence of TMAH of the extracted S. *fallax* capitulum mixed with the authentic cellulose confirmed the presence of compounds 1-4 in the *Sphagnum*.

The Ryggmossen site as a whole displays a positive correlation between the acid hydrolysis carbohydrates and THM products 1-4 (Pearson correlation = 0.674; $p<0.001$).

The acid hydrolysis carbohydrates of the BP and BM hummock cores show a general decrease in the acrotelm, followed by an increase in the mesotelm, whilst the THM compounds 1-4 show a gradual increase down the two profiles. The BP hollow core displays an increase in both acid hydrolysis and THM carbohydrates in the upper mesotelm (i.e. above the mean water table), followed by a decrease and subsequent stabilisation in the lower mesotelm (i.e. below the mean water table). The BM core also displays an increase in the acrotelm, followed by a sharp decrease in the upper mesotelm, however a subsequent increase below the mean water table into the catotelm is observed. The FL and SF hummock cores show a relatively stable carbohydrate yield (acid hydrolysis and THM) in the acrotelm, followed by a decrease in the mesotelm. The FL hollow core displays a general increase in carbohydrate yield, whereas the SF hollow shows a progressive decrease.

These results suggest that the THM yield of compounds 1-4 can provide profile trends which are consistent to the profile trends of the acid hydrolysis carbohydrates. Therefore THM can be used as a tool to analyse both the lignin and carbohydrate pools within peat.

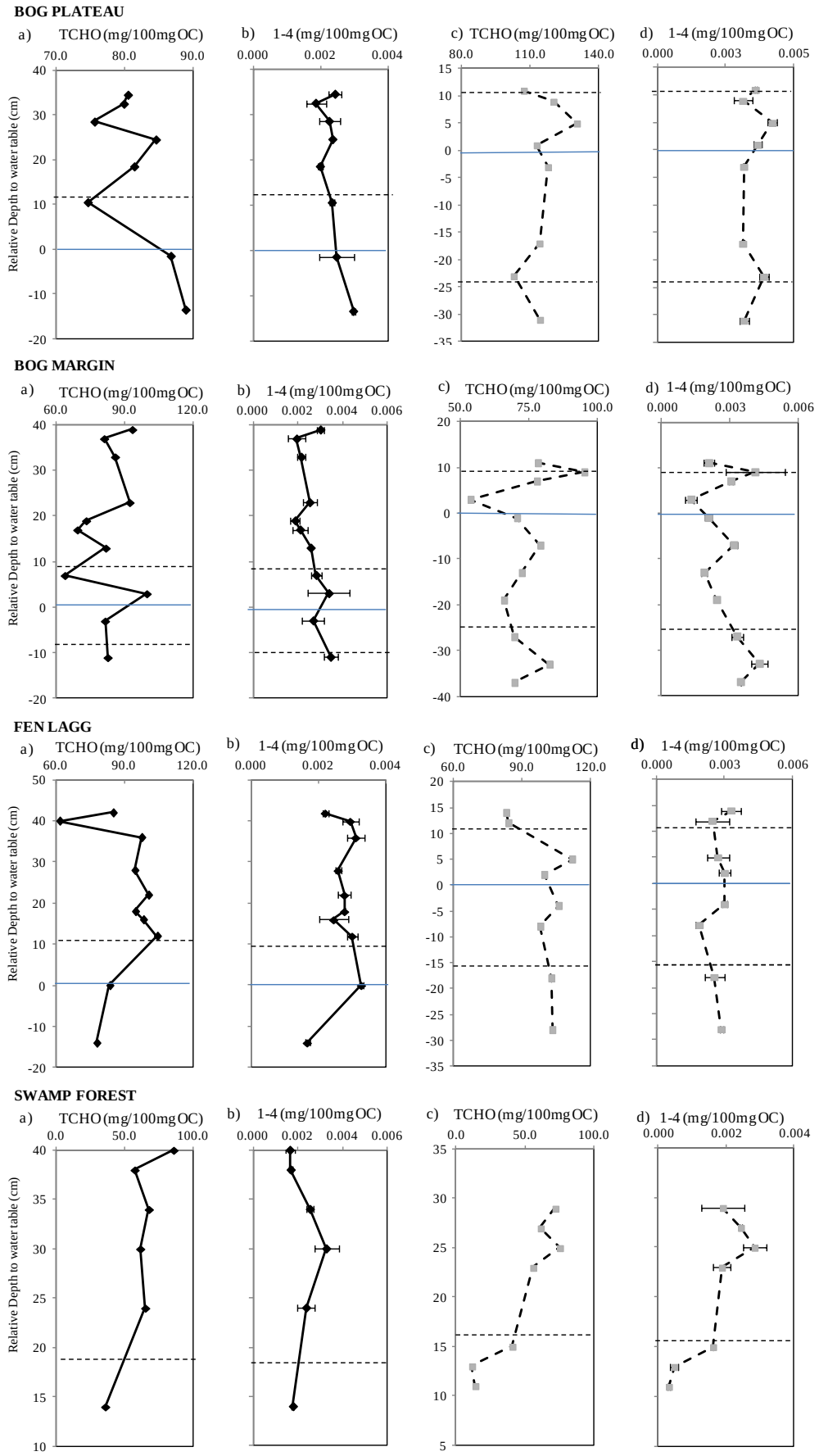

Fig. 7.15: The depth profiles of carbohydrate concentration within Ryggmossen BP, BM, FL and SF released after acid hydrolysis (TCHO) and TMAH thermochemolysis (1-4) (a,b: hummock and c,d: hollow). Solid line is the mean water table, dashed lined indicate upper and lower water table extent.

7.4 Conclusions

Thermochemolysis is a valuable technique in analytical chemistry, and is being increasingly utilised to investigate carbohydrates. However there are still several products that have only been identified tentatively or not at all. Although not comprehensive, the findings from this chapter provide the following insights for future research.

The thermochemolysis of one polysaccharide and two monosaccharide reference samples released a suite of THM products that are considered specific to carbohydrates. The methylated metasaccharinic acids (MC) were derived from the monosaccharide reference samples only, whilst 1,2,4-TMB was released from both the polysaccharide and monosaccharide reference samples. A further 4 products (1-4) were also observed in these reference samples, however their molecular structures still remain unknown. Lastly two isosaccharinic products 5 and 6, were identified in the thermochemolysate of the cellulose reference compound.

1,2,4-TMB was observed in all the samples analysed in this thesis and identified in the thermochemolysis of both the monosaccharides and glycosidically-linked polysaccharides. The preliminary differentiation of 1,2,4-TMB from its carbohydrate and tannin source has been investigated, with results consistent with findings from previous chapters.

The yield of the polysaccharide derived compounds exceeds the yield of the methylated carbohydrates in the litter of the three forest soils. However with increasing depth, the yield decreases to a similar yield of MCs. The selective decrease in the cellulose derived products relative to the sugars, could be a reflection of the breakdown of cellulose coupled with the microbial production of saccharinic acids (Huang et al., 1998). This suggests that the upper horizons are biologically active, with decomposition readily occurring. Microbial polysaccharides that are synthesised in situ are likely to be responsible for the persistent polysaccharides in the mineral horizons of SS1 and SS2, however further research is evidently required.

When compared with the widely used acid hydrolysis, results from the TMAH thermochemolysis results to the Ryggmossen samples, the profile trends are consistent.

Therefore THM can be used as a tool to analyse both the lignin and carbohydrate pools within peat.

This chapter has provids a glimpse into the potential use of carbohydrate and polysaccharide inputs in soil. Future research should therefore focus on the identification of products 1-4 and the further differentiation of the source of 1,2,4-TMB. Additionally, since microbially derived saccharides are known to contribute substantially to carbohydrates, further research to investigate their occurrence and persistence is required.

Chapter 8:

Conclusions and Future Work

8 Conclusions and Future Work

8.1 Conclusions

This study was carried out to assess the carbon and phenolic dynamics occurring after the afforestation of carbon-rich peat and peaty gley soils. Soil and litter were analysed using thermally assisted hydrolysis and methylation (THM) in the presence of ^{13}C-labelled and unlabelled tetramethylammonium hydroxide (TMAH) with the primary interest focused towards the soil organic matter (SOM) dynamics at both the bulk (SOC) and molecular level (lignin, non-lignin phenolics and other organic compounds) in carbon-rich soil profiles. Sites included two afforested peaty gley soils under first and second Sitka spruce rotations, an unforested moorland, and self seeded Sitka spruce on unprepared peat, all of which are located in Kielder Forest, northern England. A pristine peatland in central Sweden was also extensively sampled to observe the phenolic processes occurring prior to afforestation; including the processes that control the stabilisation and release of carbon within soil, and the chemical structure of plant macromolecules, such as lignin and their long-term turnover in soils. Changes in carbon storage were also investigated across the sites to assess the effects afforestation will have on soil organic carbon stocks.

Molecular biomarkers including lignin provide an invaluable measurement in carbon cycling studies due to the unambiguous information that they can provide regarding the source and diagenesis. *Sphagnum* biomarkers have been identified alongside lignin biomarkers in soil and peat using TMAH thermochemolysis to provide detailed structural information on both vascular and non-vascular species simultaneously.

Ideally, ^{13}C-labelled TMAH would have been used throughout the study in order to account for the tannin contribution, however, due to limited supplies it was not possible to use it for all samples investigated.

8.1.1 Afforested Sites

The phenolic changes associated with afforestation on carbon-rich soils have been successfully investigated in a below ground system (Chapter 3). The establishment of coniferous forests on peaty gley soils displayed a net accumulation of soil carbon during the second rotation, surpassing the moorland capacity. Both first rotation and second

rotation Sitka spruce stands experienced land disturbance prior to planting, however the two stands displayed very different carbon storage capacities. This is attributed to the initial land-use change including the change of vegetation and the introduction of drainage systems that cause increased degradation and loss of organic carbon in the first rotation stand only. Therefore despite major land disturbance occurring at the second rotation site, large quantities of carbon are able to accumulate. This recovery of organic carbon storage is, in part, due to the increased bulk density of the soil due to the increased compression caused by the growing trees, coupled with the increasing depth of the ectorganic horizons. The lignin yield largely mirrors the carbon storage trends, decreasing after afforestation, however displaying a recovery in the second rotation, increasing to quantities larger than at the moorland. The depth-related profiles indicate progressive lignin degradation at the moorland, whereas the soil beneath the two Sitka spruce stands record changes in vegetation input, land preparation and land disturbance. The phenol composition of soil horizons presented a lignin maximum at depth across the afforested sites caused primarily by the mounding (horizon inversion) that occurred prior to planting the second rotation. The increase of lignin and non-lignin phenols in the overturned mineral A horizon of the second rotation Sitka spruce suggests that mineral horizons have the potential to store significant quantities of phenols despite low levels of TOC and OC.

In Chapter 3, unlabelled TMAH was used as the methylating agent during thermochemolysis. This may introduce bias into the results, as Sitka spruce systems will have a tannin input as shown in Chapter 6, which has the potential to mask the lignin sample. Ideally ^{13}C-TMAH would have been used in this study to account for this input.

Overall, the impact of afforestation appears to significantly influence both carbon storage capacities and phenolic composition in northern UK peaty gley soils, with mounding after the first rotation increasing the SOC capacity in the second rotation.

The concern of the impact of afforestation is not restricted to the planting area alone; the encroachment of Sitka spruce on to adjacent open peatland via self seeding revealed a decreased carbon stock, with the distribution of OC shifting from high stocks in the deep peat of the open peat to higher stocks in the litter of the forest-margin peat undergoing the Sitka spruce encroachment (Chapter 6). These results indicate that a natural stabilisation of SOC in the open peat is occurring alongside the destabilisation of

SOM in the forest-margin peats. However unlike afforested plantations, the addition of carbon via biomass will be minimal at these marginal peat sites.

The lignin maximum at depth at the self-seeded marginal peat was due to a shift in vegetation cover across the three sites from a continuous non-woody vascular dominated moorland to a higher spatial variation across the chronosequence introducing *Sphagnum* and non-*Sphagnum* mosses. The intact lignin contents at the litter horizons of these samples support a greater non-lignin phenolic contribution (e.g. *Sphagnum* and non-*Sphagnum* mosses), with the exception of forest-margin peat under Sitka spruce pit two, where there is evidence of the introduction of the self-seeded Sitka spruce by way of the high proportion of intact G4 coupled with the high yield of intact G6 and demethylated lignin, increased litterfall, and low S/G and C/G ratios. These results highlight the importance of using ^{13}C-labelled TMAH and the identification and use of *Sphagnum* moss biomarkers in soil archives.

It appears that the presence of the self-seeded Sitka spruce has not had a major effect on the phenolic composition and distribution. However there has been a notable change in surface vegetation across the entire chronosequence, which has brought about changes in the phenolic yields and carbon storage.

8.1.2 Pristine Peatlands

Chapters 4 and 5 are the first major studies of sphagnum acid thermochemolysis products as a tool to assess the degradation of *Sphagnum* mosses within peat.

Methylated 4-isopropenylphenol (**I**), methylated (E) and (*Z*)-3-(4'-hydroxyphen-1-yl)but-2-enoic acid (**II a/b**), and methylated 3-(4'-hydroxyphen-1-yl)but-3-enoic acid (**III**) are confirmed as TMAH thermochemolysis products of sphagnum acid and also as being specific to *Sphagnum* mosses. Equations 4.2 (Sphagnum yield; σ) and 4.3 (SR%) are presented to provide estimates of the relative quantity of *Sphagnum* mosses to vascular plant phenols in peat moss and peat archives.

The sphagnum acid biomarkers (**I**, **IIa/b** and **III)** persist into the peat archives. The SR% across the bog centre indicates that *Sphagnum* phenols are oxidised preferentially over vascular plant phenols in the acrotelm and mesotelm, with σ decreasing in the oxic peat

with all four sphagnum acid THM products decreasing simultaneously. In the anoxic peat σ stabilises, however the distribution of the four sphagnum acid THM products has shifted, so that **I** accounts for a larger proportion of σ. The increase of **I** relative to **IIa/b** and **III**, indicates the sphagnum acid is decarboxylated prior to TMAH analysis probably by microbial activity in the permanently anoxic conditions of the catotelm. Therefore these four products could potentially be used as a proxy for the degree of oxidation in peatlands, and provide direct information on the degradation of *Sphagnum* mosses in peat, whilst avoiding time consuming and costly water level recording within peatlands.

The peat cores revealed large quantities of carbohydrates, indicating a relatively slow consumption of these compounds, with the carbohydrate yield decreased from the bog centre to the bog-forest margin. The moss indicators (Rha+Man+Gal) increased in the catotelm of the BP, BM and FL, whereas sedge indicators (Ara+Xyl+Fuc) showed decreases in the catotelm, further indicating the selective preservation of the moss monosaccharides in the anoxic zone.

The BP, BM and FL cores all show a progressive increase in the bulk density from the acrotelm into the catotelm consistent with the values cited by Clymo (1992), which subsequently leads to the progressivley increasing carbon storage with depth. The SF hollow displays a large carbon storage particularly in the deep mineral soil, indicating that the mineral-fed marginal peats undergoing paludification may have the highest capacity for carbon storage due to the high bulk density combined with the relatively high TOC for mineral soil.

The new biomarkers and indices reported here provide tools for tracking the input, accumulation and degradation of *Sphagnum* phenols in peat profiles. From these results we can infer that the water table dynamics play an important role in the degradation of *Sphagnum* phenols, with the seasonally and permanently saturated layers favouring the stability and accumulation of *Sphagnum* phenols. However when exposed to oxic conditions above the mean water table, the *Sphagnum* markers are rapidly lost.

These results highlight the sensitivity of *Sphagnum* litter and peat exposed to oxic conditions, which would be affected by a lowered water table brought on by climate change.

Furthermore, the intact lignin phenols present in the *Sphagnum* and the *Sphagnum*-dominated litter are attributed to the large water-holding capacity in the living *Sphagnum*, whereby lignin phenols in the DOM are likely to have become entrapped and have become physically bound and/or protected to the *Sphagnum*, and therefore remain detectable despite the samples undergoing solvent extraction. The fractionation of the vascular (lignin and non-lignin) phenols as introduced by Hernes et al. (2007), was identified in the Ryggmossen samples (Chapter 4).

The corrected $[Ad/Al]_G$ ratio produces similar results for both the *Sphagnum* and vascular species, therefore there appears to be minimal fractionation of the intact lignin phenols (G6 and G4) mobilized into the *Sphagnum*. However, the non-lignin phenols contributing to the uncorrected lignin yield appear to be fractionated. These results suggest that the non-lignin acid phenols are preferentially removed from the POM and solubilised in the DOM, which are subsequently mobilized into the *Sphagnum*, resulting in elevated levels of these non-lignin acids within the *Sphagnum*.

8.1.3 Soil Carbohydrates

The soil, peat and litter samples analysed in this thesis released several potential THM saccharinic products; 1,2,4-trimethoxybenzene (1,2,4-TMB), four methylated carbohydrates (MC 1-4), and cellulose derived products (1-6). Their identification was confirmed by the analysis of a range of carbohydrate reference samples. The polysaccharide cellulose and monosaccharides glucose and galactose (Chapter 7).

Although the cellulose thimbles have been suggested as a source of the polysaccharide derived compounds and methylated carbohydrates compounds, results indicate that the thimbles as a source of these compounds can be assumed to be negligible. However if future work focused on the analysis of carbohydrates, it is reccommend that glass fibre thimbles or an alternative extraction technique is utilised, to eliminate any chance of contamination.

The preliminary differentiation of 1,2,4-TMB from its carbohydrate and tannin source has been investigated, with results implying increased tannin inputs to the buried mineral horizon of the second rotation Sitka spruce stand at Harwood Forest, and in the green litter of the marginal peat pit two at Wark Forest. These results are consistent

with the traditional lignin proxies such as C/G and S/G. However, care must be used when interpreting the data, due to the potential of other sources, including the potential microbial origin in deeper soils.

When compared with the widely used acid hydrolysis technique, the yield of carbohydrates obtained from the TMAH thermochemolysis of the Ryggmossen samples revealed similar profile trends as observed with the yield of sugars released from acid hydrolysis. Therefore THM can be used as a tool to simultaneously analyse both the lignin and carbohydrate pools within peat.

The selective decrease in the cellulose derived products (polysaccharides) relative to the monosaccharides (methylated carbohydrates) in the three forest soils, could be a reflection of the concurrent breakdown of cellulose coupled with the microbial production of saccharinic acids (Huang et al., 1998). This suggests that the upper horizons are biologically active, with decomposition readily occurring. Microbial polysaccharides that are synthesised in situ are likely to be responsible for the persistent polysaccharides in the mineral horizons of first and second rotation afforested sites, however further research is evidently required.

8.2 Recommendations for Future Work

The research conducted during this study has raised some issues and questions that could be recommended for future investigations.

The spatial and temporal variability in soil carbon is high, especially in afforested sites (Chapter 3). The preparation and implementation of a detailed experimental design could be employed, such as a factorial or split plot design, complete with blocks and replicates, which would allow the spatial variability to be quantified, whilst carrying out detailed statistical analyses, including multivariate analysis. Samples at multiple time-points throughout the year would take into account any temporal variability. This detailed stratified soil sampling design has recently been adopted by Forest Research in a detailed chronosequence experiment within Kielder Forest, taking into account the heterogeneity of the stands and calculating the difference between soil carbon stocks in mounds compared to undisturbed flat areas between tree mounds (E. Vanguelova, *pers.*

comm.). This research has focussed on the land-use change associated with carbon rich soils (peaty gley and peat soils), however climate change is also an important factor which will have an impact on the soil carbon storage and phenolic dynamics. Therefore it is important to note that soil temperature has not been considered in this study. Soil temperature can stimulate microbial activity and release carbon from the soil into the atmosphere. Therefore future work should consider temperature changes on SOC stocks.

Results at the self-seeded Wark Forest site indicated a minimal effect of the self-seeded Sitka spruce on the phenolic composition and distribution (Chapter 6). An extended study at the site through canopy closure would be required to provide a more complete evaluation of the effect of self-seeded Sitka spruce and the edge-effect occurring due to the adjacent plantation site.

The leaching of highly-oxidised lignin and non-lignin phenolics has not been addressed in this study. The concept of lignin phenol fractionation (Hernes et al., 2007) and the potential for non-lignin phenol fractionation (Chapter 4), whereby the Hernes et al. (2007) reported the preferential removal of specific phenols during the solubilisation of lignin-phenols from litter and subsequent sorption of the resulting leachates to soils. This fractionation highlights the need for the investigation of lignin included within DOM, and the phase changes that occur after afforestation, in order to assess the impact of lignin and non-lignin fractionation on lignin proxies, and provide more information on the fate of lignin from these systems.

^{210}Pb or ^{14}C-radiocarbon dating of the soil profiles would provide an age of the organic matter and provide an indication of the relative stability of the organic matter in soil. This would also allow for kinetic information to be extended from the BP Ryggmossen core in Chapter 5, and determined for the loss of carbon and phenols in the remaining peats and soils with time.

The stabilisation of *Sphagnum*-derived phenols relative to other phenols was identified within the permanently saturated Ryggmossen peat, due to the increase of **I** relative to **IIa/b** and **III**. As previously established by van der Heijden et al. (1997), after THM, **II** and **III** are stabilised via transesterification processes, preventing the further formation of **I** beyond that observed via the decarboxylation of the sphagnum acid (van der Heijden et al., 1997). These results suggested that the sphagnum acid, which is ether-linked to the cell wall, is decarboxylated prior to TMAH analysis, probably by

microbial activity in the anoxic peat. It was hypothesised that the decarboxylated product of sphagnum acid (i.e. isopropenyl phenol) remains bound into the polymer via the original ether bonds, and therefore remains present after solvent extraction. However, the activity of the major biodegradative hydrolyase enzymes are known to be suppressed in peatlands (Kang and Freeman, 1999), therefore the mechanisms involved in the sphagnum acid decarboxylation in-situ require further research. Additionally, further studies on peat profiles from different climate regions, as well as mechanistic studies on the processes of *Sphagnum* phenol degradation, is required, to determine whether the sensitivity of *Sphagnum* litter and peat exposed to oxic conditions, as observed at Ryggmossen, is representative of all northern peatlands.

Chapter 7 is not a comprehensive review of carbohydrate analysis by TMAH thermochemolysis in carbon-rich soils, however it provides insights into the potential of this method for future research. Additionally, since microbially derived saccharides are known to contribute substantially to carbohydrates, especially peat, further research to investigate their occurrence and persistence is required.

References

Adler, E., (1977). Lignin Chemistry - Past, Present and Future. *Wood Science Technology* **11**, 169-218.

Alberti, G., Peressotti, A., Piussi, P., and Zerbi, G., (2008). Forest ecosystem carbon accumulation during a secondary succession in the Eastern Prealps of Italy. *Forestry* **81**, 1-11.

Amelung, W., Cheshire, M. V., and Guggenberger, G., (1996). Determination of neutral and acidic sugars in soil by capillary gas liquid chromatography after trifluoroacetic acid hydrolysis. *Soil Biology and Biochemistry* **28**, 1631-1639.

Andrus, R. E., (1986). Some Aspects of *Sphagnum* Ecology. *Canadian Journal of Botany* **64**, 416-426.

Armentano, T. V. and Menges, E. S., (1986). Patterns of change in the carbon balance of organic soil-wetlands of the temperate zone. *Journal of Ecology* **74**, 755-774.

Asada, T., Warner, B. G., and Aravena, R., (2005). Nitrogen isotope signature variability in plant species from open peatland. *Aquatic Botany* **82**, 297-307.

Atherden, M., 1992. *Upland Britain: a natural history*. Manchester University Press, Manchester, UK. pp 224.

Avery, B. W., 1980. *Soil Classification for England and Wales*. Technical monograph (Soil Survey of England and Wales); no. 14, Harpenden. pp 67.

Bahri, H., Dignac, M. F., Rumpel, C., Rasse, D. P., Chenu, C., and Mariotti, A., (2006). Lignin turnover kinetics in an agricultural soil is monomer specific. *Soil Biology and Biochemistry* **38**, 1977-1988.

Baker, A., Bolton, L., Newson, M., and Spencer, R. G. M., (2008). Spectrophotometric properties of surface water dissolved organic matter in an afforested upland peat catchment. *Hydrological Processes* **22**, 2325-2336.

Ball, T., Smith, K. A., Garnett, M. H., Moncrieff, J. B., and Zerva, A., (2011). An assessment of the effect of Sitka Spruce (*Picea sitchensis Bong. Carr*) plantation forest cover on carbon turnover and storage in a peaty gley soil. *European Journal of Soil Science* **62**, 560-571.

Bardy, M., Derenne, S., Allard, T., Benedetti, M. F., and Fritsch, E., (2011). Podzolisation and exportation of organic matter in black waters of the Rio Negro (upper Amazon basin, Brazil). *Biogeochemistry* **106**, 71-88.

Bashir, F. Z., 1999. Molecular characterization of sedimentary organic matter, PhD Thesis. Newcastle University, Newcastle-Upon-Tyne, UK.

Bate-Smith, E. C., (1977). Astringent tannins of Acer species. *Phytochemistry* **16**, 1421-1426.

Bate-Smith, E. C. and Swain, T., 1962. Flavonoid compounds. In: Mason, H. S. and Florkin, A. M. Eds.), *Comparative Biochemistry*. Academic Press New York. pp 75-809.

Batjes, N. H., (1996). Total carbon and nitrogen in the soils of the world. *European Journal of Soil Science* **47**, 151-163.

Bedard-Haughn, A., van Groenigen, J. W., and van Kessel, C., (2003). Tracing ^{15}N through landscapes: potential uses and precautions. *Journal of Hydrology* **272**, 175-190.

Behrens, A., Maie, N., Knicker, H., and Kogel-Knabner, I., (2003). MALDI-TOF mass spectrometry and PSD fragmentation as means for the analysis of condensed tannins in plant leaves and needles. *Phytochemistry* **62**, 1159-1170.

Bellamy, P. H., Loveland, P. J., Bradley, R. I., Lark, R. M., and Kirk, G. J. D., (2005). Carbon losses from all soils across England and Wales 1978-2003. *Nature* **437**, 245-248.

Belyea, L. R., (1996). Separating the effects of litter quality and microenvironment on decomposition rates in a patterned peatland. *Oikos* **77**, 529-539.

Belyea, L. R., 2009. Nonlinear dynamics of peatlands and potential feedbacks on the climate system. In: (Baird, A. J., Belyea, L. R., Comas, X., Reeve, A. S., and Slater, L. D. Eds.), *Carbon Cycling in Northern Peatlands, Geophys. Monogr. Ser.* American Geophysical Union, Washington, DC. pp 5-18.

Belyea, L. R. and Malmer, N., (2004). Carbon sequestration in peatland: Patterns and mechanisms of response to climate change. *Global Change Biology* **10**, 1043-1052.

Benner, R., Fogel, M. L., Sprague, E. K., and Hodson, R. E., (1987). Depletion of C in lignin and its implications for stable carbon isotope studies. *Nature* **329**, 708-710.

Berendse, F., Van Breemen, N., Rydin, H., Buttler, A., Heijmans, M., Hoosbeek, M. R., Lee, J. A., Mitchell, E., Saarinen, T., Vasander, H., and Wallén, B., (2001). Raised atmospheric CO_2 levels and increased N deposition cause shifts in plant species composition and production in *Sphagnum* bogs. *Global Change Biology* **7**, 591-598.

Berg, B. and Staaf, H., (1980). Decomposition Rate and Chemical Changes of Scots Pine Needle Litter. II. Influence of Chemical Composition. *Ecological Bulletins*, 373-390.

Bhat, T. K., Singh, B., and Sharma, O. P., (1998). Microbial degradation of tannins - A current perspective. *Biodegradation* **9**, 343-357.

Biggs, W. O., 1979. The hydrological impact of afforestation in Great Britain. In: Hollis, G. E. (Ed.), *Man's impact on the hydrological cycle in the United Kingdom*. Geo Books, Norwich. pp 55-69.

Billett, M. F., Charman, D. J., Clark, J. M., Evans, C. D., Evans, M. G., Ostle, N. J., Worrall, F., Burden, A., Dinsmore, K. J., Jones, T., McNamara, N. P., Parry, L., Rowson, J. G., and Rose, R., (2010). Carbon balance of UK peatlands: Current state of knowledge and future research challenges. *Climate Research* **45**, 13-29.

Black, K., Byrne, K. A., Mencuccini, M., Tobin, B., Nieuwenhuis, M., Reidy, B., Bolger, T., Saiz, G., Green, C., Farrell, E. T., and Osborne, B., (2009). Carbon stock and stock changes across a Sitka spruce chronosequence on surface-water gley soils. *Forestry* **82**, 255-272.

Boerjan, W., Ralph, J., and Baucher, M., (2003). Lignin Biosynthesis. *Annual Review of Plant Biology* **54**, 519-546.

Boom, A., Sinninghe Damsté, J. S., and De Leeuw, J. W., (2005). Cutan, a common aliphatic biopolymer in cuticles of drought-adapted plants. *Organic Geochemistry* **36**, 595-601.

Boyer, J., (1985). Water transport. *Annual Review of Plant Physiology* **36**, 473-516.

Braekke, F. H., (1987). Nutrient relationships in forest stands: Effects of drainage and fertilization on surface peat layers. *Forest Ecology and Management* **21**, 269-284.

Bragazza, L., Gerdol, R., and Rydin, H., (2003). Effects of mineral and nutrient input on mire bio-geochemistry in two geographical regions. *Journal of Ecology* **91**, 417-426.

Bragazza, L., Limpens, J., Gerdol, R., Grosvernier, P., Hájek, M., Hájek, T., Hajkova, P., Hansen, I., Iacumin, P., Kutnar, L., Rydin, H., and Tahvanainen, T., (2005). Nitrogen concentration and $\delta^{15}N$ signature of ombrotrophic *Sphagnum* mosses at different N deposition levels in Europe. *Global Change Biology* **11**, 106-114.

Brett, C. T. and Waldron, K. W., 1996. *Physiology and biochemistry of plant cell walls*. Chapman & Hall London. pp 255.

Bridgham, S. D., Pastor, J., Janssens, J. A., Chapin, C., and Malterer, T. J., (1996). Multiple limiting gradients in peatlands: A call for a new paradigm. *Wetlands* **16**, 45-65.

Broder, T., Blodau, C., Biester, H., and Knorr, K. H., (2011). Peat decomposition records in three pristine ombrotrophic bogs in southern Patagonia. *Biogeosciences Discussions* **8**, 10543-10576.

Brown, L. E., Cooper, L., Holden, J., and Ramchunder, S. J., (2010). A comparison of stream water temperature regimes from open and afforested moorland, Yorkshire Dales, northern England. *Hydrological Processes* **24**, 3206-3218.

BS7755-3.8, 1995. *Soil quality. Chemical methods. Determination of organic and total carbon after dry combustion (elementary analysis)* BS 7755-3.8: pp 12.

Byrne, K. A. and Farrell, E. P., (2005). The effect of afforestation on soil carbon dioxide emissions in blanket peatland in Ireland. *Forestry* **78**, 217-227.

Cannell, M. G. R., (1999). Growing trees to sequester carbon in the UK: answers to some common questions. *Forestry* **72**, 237-247.

Cannell, M. G. R., Dewar, R. C., and Pyatt, D. G., (1993). Conifer plantations on drained peatlands in Britain: A net gain or loss of carbon? *Forestry* **66**, 353-369.

Cerli, C., Celi, L., Kaiser, K., Guggenberger, G., Johansson, M. B., Cignetti, A., and Zanini, E., (2008). Changes in humic substances along an age sequence of Norway spruce stands planted on former agricultural land. *Organic Geochemistry* **39**, 1269-1280.

Challinor, J. M., (1989). A pyrolysis-derivatisation-gas chromatography technique for the structural elucidation of some synthetic polymers. *Journal of Analytical and Applied Pyrolysis* **16**, 323-333.

Challinor, J. M., (1995). Characterisation of wood by pyrolysis derivatisation-gas chromatography/mass spectrometry. *Journal of Analytical and Applied Pyrolysis* **35**, 93-107.

Challinor, J. M., (2001). Thermally assisted hydrolysis and methylation (THM) reactions. *Journal of Analytical and Applied Pyrolysis* **61**, 1-2.

Chapman, S. B. and Rose, R. J., (1991). Changes in the Vegetation at Coom Rigg Moss National Nature Reserve within the Period 1958-86. *Journal of Applied Ecology* **28**, 140-153.

Charman, D. J., 2002. *Peatlands and environmental change*. John Wiley & Sons, New York, NY. pp 312.

Chefetz, B., Chen, Y., Clapp, C. E., and Hatcher, P. G., (2000). Characterization of Organic Matter in Soils by Thermochemolysis Using Tetramethylammonium Hydroxide (TMAH). *Soil Sci Soc Am J* **64**, 583-589.

Cheshire, M. V., 1979. *Nature and Origin of Carbohydrates in Soils*. Academic Press, London. pp 224.

Chiavari, G., Montalbani, S., Prati, S., Keheyan, Y., and Baroni, S., (2007). Application of analytical pyrolysis for the characterisation of old inks. *Journal of Analytical and Applied Pyrolysis* **80**, 400-405.

Clark, J. M., Billett, M. F., Coyle, M., Croft, S., Daniels, S., Evans, C. D., Evans, M., Freeman, C., Gallego-Sala, A. V., Heinemeyer, A., House, J. I., Monteith, D. T., Nayak, D., Orr, H. G., Prentice, I. C., Rose, R., Rowson, J., Smith, J. U., Smith, P., Tun, Y. M., Vanguelova, E., Wetterhall, F., and Worrall, F., (2010a). Model inter-comparison between statistical and dynamic model assessments of the long-term stability of blanket PEAT in great britain (1940-2099). *Climate Research* **45**, 227-248.

Clark, J. M., Gallego-Sala, A. V., Allott, T. E. H., Chapman, S. J., Farewell, T., Freeman, C., House, J. I., Orr, H. G., Prentice, I. C., and Smith, P., (2010b). Assessing the vulnerability of blanket peat to climate change using an ensemble of statistical bioclimatic envelope models. *Climate Research* **45**, 131-150.

Clark, J. M., Orr, H. G., Freer, J., House, J. I., Smith, P., and Freeman, C., (2010c). Assessment of projected changes in upland environments using simple climatic indices. *Climate Research* **45**, 87-104.

Clayden, B. and Hollis, J. M., (1984). Criteria for differentiating soil series. *Soil Survey Technical Monograph No.17*. Soil Survey of England and Wales, Harpenden, UK. pp159.

Clifford, D. J., Carson, D. M., McKinney, D. E., Bortiatynski, J. M., and Hatcher, P. G., (1995). A new rapid technique for the characterization of lignin in vascular plants: thermochemolysis with tetramethylammonium hydroxide (TMAH). *Organic Geochemistry* **23**, 169-175.

Clymo, R. S., (1970). The Growth of *Sphagnum*: Methods of Measurement. *Journal of Ecology* **58**, 13-49.

Clymo, R. S., 1983. Peat. In: Gore, A. J. P. (Ed.), *Ecosystems of the World. Mires: Swamp, Bog, Fen and Moor*. Elsevier, Amsterdam. pp 159-224.

Clymo, R. S., (1992). Models of peat growth. *Suo* **43**, 127-136.

Clymo, R. S. and Bryant, C. L., (2008). Diffusion and mass flow of dissolved carbon dioxide, methane, and dissolved organic carbon in a 7-m deep raised peat bog. *Geochimica et Cosmochimica Acta* **72**, 2048-2066.

Clymo, R. S. and Hayward, P. M., 1982. The Ecology of *Sphagnum*. In: Smith, A. J. E. (Ed.), *Bryophyte Ecology*. Chapman and Hall, London. pp 229-289.

Comont, L., Laggoun-Defarge, F., and Disnar, J. R., (2006). Evolution of organic matter indicators in response to major environmental changes: The case of a formerly cut-over peat bog (Le Russey, Jura Mountains, France). *Organic Geochemistry* **37**, 1736-1751.

Coulson, J. C. and Butterfield, J., (1978). An Investigation of the Biotic Factors Determining the Rates of Plant Decomposition on Blanket Bog. *Journal of Ecology* **66**, 631-650.

Cowie, G. L. and Hedges, J. I., (1984). Determination of neutral sugars in plankton, sediments, and wood by capillary gas chromatography of equilibrated isomeric mixtures. *Analytical Chemistry* **56**, 497-504.

Crawford, R. L., 1981. *Lignin biodegradation and transformation*. Wiley, New York. pp 154.

Dallinga, J. W., Nibbering, N. M. M., and Boerboom, A. J. H., (1984). Curie-point pyrolysis of saturated and unsaturated dicarboxylic acids studied by tandem mass spectrometry. *Journal of the Chemical Society, Perkin Transactions 2*, 1065-1076.

Damman, A. W. H., (1988). Regulation of nitrogen removal and retention in *Sphagnum* bogs and other peatlands. *Oikos* **51**, 291-305.

Davidson, E. A. and Janssens, I. A., (2006). Temperature sensitivity of soil carbon decomposition and feedbacks to climate change. *Nature* **440**, 165-173.

Davis, M. R., Allen, R. B., and Clinton, P. W., (2003). Carbon storage along a stand development sequence in a New Zealand Nothofagus forest. *Forest Ecology and Management* **177**, 313-321.

Dawson, J. J. C. and Smith, P., (2007). Carbon losses from soil and its consequences for land-use management. *Science of the Total Environment* **382**, 165-190.

De Leeuw, J. W., Versteegh, G. J. M., and Van Bergen, P. F., (2006). Biomacromolecules of algae and plants and their fossil analogues. *Plant Ecology* **182**, 209-233.

DeGryze, S., Six, J., Paustian, K., Morris, S. J., Paul, E. A., and Merckx, R., (2004). Soil organic carbon pool changes following land-use conversions. *Global Change Biology* **10**, 1120-1132.

del Río, J. C., Gutiérrez, A., Rodríguez, I. M., Ibarra, D., and Martínez, A. T., (2007). Composition of non-woody plant lignins and cinnamic acids by Py-GC/MS, Py/TMAH and FT-IR. *Journal of Analytical and Applied Pyrolysis* **79**, 39-46.

del Río, J. C., Martin, F., and Gonzalez-Vila, F. J., (1996). Thermally assisted hydrolysis and alkylation as a novel pyrolytic approach for the structural characterization of natural biopolymers and geomacromolecules. *TrAC Trends in Analytical Chemistry* **15**, 70-79.

Delarue, F., Laggoun-Défarge, F., Buttler, A., Gogo, S., Jassey, V. E. J., and Disnar, J. R., (2011). Effects of short-term ecosystem experimental warming on water-extractable organic matter in an ombrotrophic *Sphagnum* peatland (Le Forbonnet, France). *Organic Geochemistry* **42**, 1016-1024.

Derrien, D., Marol, C., Balabane, M., and Balesdent, J., (2006). The turnover of carbohydrate carbon in a cultivated soil estimated by ^{13}C natural abundances. *European Journal of Soil Science* **57**, 547-557.

Dignac, M. F., Bahri, H., Rumpel, C., Rasse, D. P., Bardoux, G., Balesdent, J., Girardin, C., Chenu, C., and Mariotti, A., (2005). Carbon-13 natural abundance as a tool to study the dynamics of lignin monomers in soil: An appraisal at the Closeaux experimental field (France). *Geoderma* **128**, 3-17.

Dijkstra, E. F., Boon, J. J., and Van Mourik, J. M., (1998). Analytical pyrolysis of a soil profile under Scots pine. *European Journal of Soil Science* **49**, 295-304.

Dise, N. B., (2009). Peatland response to global change. *Science* **326**, 810-811.

Dixon, R. K., Brown, S., Houghton, R. A., Solomon, A. M., Trexler, M. C., and Wisniewski, J., (1994). Carbon pools and flux of global forest ecosystems. *Science* **263**, 185.

Dorrestijn, E., Laarhoven, L. J. J., Arends, I. W. C. E., and Mulder, P., (2000). Occurrence and reactivity of phenoxyl linkages in lignin and low rank coal. *Journal of Analytical and Applied Pyrolysis* **54**, 153-192.

Du Rietz, G. E. and Nannfeldt, J. A., 1925. *Ryggmossen und stigsbo rödmosse, die letzen lebenden hochmoore der gegend von Uppsala*, Svenska Växtsociologiska Sällskapets Handlingar. pp 1-21.

Dungait, J. A. J., Hopkins, D. W., Gregory, A. S., and Whitmore, A. P., (2012). Soil organic matter turnover is governed by accessibility not recalcitrance. *Global Change Biology* **18**, 1781-1796.

Eriksson, H., (1991). Sources and sinks of carbon dioxide in Sweden. *Ambio* **20**, 146-150.

Ertel, J. R., Hedges, J. I., Devol, A. H., Richey, J. E., and Ribeiro, M. d. N. G., (1986). Dissolved Humic Substances of the Amazon River System. *Limnology and Oceanography* **31**, 739-754.

Esmeijer-Liu, A. J., Kürschner, W. M., Lotter, A. F., Verhoeven, J. T. A., and Goslar, T., (2012). Stable carbon and nitrogen isotopes in a peat profile are influenced by early stage diagenesis and changes in atmospheric CO_2 and N deposition. *Water, Air, and Soil Pollution* **223**, 2007-2022.

Estournel-Pelardy, C., Delarue, F., Grasset, L., Laggoun-Défarge, F., and Amblés, A., (2011). Tetramethylammonium hydroxide thermochemolysis for the analysis of cellulose and free carbohydrates in a peat bog. *Journal of Analytical and Applied Pyrolysis* **92**, 401-406.

Evans, M. G. and Warburton, J., (2010). Peatland Geomorphology and Carbon Cycling. *Geography Compass* **4**, 1513-1531.

Fabbri, D., Chiavari, G., and Galletti, G. C., (1996). Characterization of soil humin by pyrolysis(/methylation)-gas chromatography/mass spectrometry: structural relationships with humic acids. *Journal of Analytical and Applied Pyrolysis* **37**, 161-172.

Fabbri, D. and Helleur, R., (1999). Characterization of the tetramethylammonium hydroxide thermochemolysis products of carbohydrates. *Journal of Analytical and Applied Pyrolysis* **49**, 277-293.

Farmer, R., 2011. *Active Blanket Bogs in Wales*. EU LIFE. pp 58.

Farmer, R. A. and Nisbet, T. R., (2004). An overview of forest management and change with respect to environmental protection in the UK. *Hydrology and Earth System Sciences* **8**, 279-285.

Fenner, N. and Freeman, C., (2011). Drought-induced carbon loss in peatlands. *Nature Geoscience* **4**, 895-900.

Ferris, R., Peace, A. J., Humphrey, J. W., and Broome, A. C., (2000). Relationships between vegetation, site type and stand structure in coniferous plantations in Britain. *Forest Ecology and Management* **136**, 35-51.

Filley, T. R., (2003). Assessment of fungal wood decay by lignin analysis using tetramethylammonium hydroxide (TMAH) and ^{13}C-labeled TMAH thermochemolysis. In: Goodell, B., Nicholas, D. D., and Schultz, T. P. Eds.)*ACS Symposium Series. pp 119-139*.

Filley, T. R., Cody, G. D., Goodell, B., Jellison, J., Noser, C., and Ostrofsky, A., (2002). Lignin demethylation and polysaccharide decomposition in spruce sapwood degraded by brown rot fungi. *Organic Geochemistry* **33**, 111-124.

Filley, T. R., Hatcher, P. G., Shortle, W. C., and Praseuth, R. T., (2000). The application of ^{13}C-labeled tetramethylammonium hydroxide (^{13}C-TMAH) thermochemolysis to the study of fungal degradation of wood. *Organic Geochemistry* **31**, 181-198.

Filley, T. R., Minard, R. D., and Hatcher, P. G., (1999). Tetramethylammonium hydroxide (TMAH) thermochemolysis: Proposed mechanisms based upon the application of ^{13}C-labeled TMAH to a synthetic model lignin dimer. *Organic Geochemistry* **30**, 607-621.

Filley, T. R., Nierop, K. G. J., and Wang, Y., (2006). The contribution of polyhydroxyl aromatic compounds to tetramethylammonium hydroxide lignin-based proxies. *Organic Geochemistry* **37**, 711-727.

Frazier, S. W., Kaplan, L. A., and Hatcher, P. G., (2005). Molecular characterization of biodegradable dissolved organic matter using bioreactors and [^{12}C/^{13}C] tetramethylammonium hydroxide thermochemolysis GC-MS. *Environmental Science and Technology* **39**, 1479-1491.

Freeman, C., Evans, C. D., Monteith, D. T., Reynolds, B., and Fenner, N., (2001a). Export of organic carbon from peat soils. *Nature* **412**, 785.

Freeman, C., Ostle, N. J., Fenner, N., and Kang, H., (2004). A regulatory role for phenol oxidase during decomposition in peatlands. *Soil Biology and Biochemistry* **36**, 1663-1667.

Freeman, C., Ostle, N. J., and Kang, H., (2001b). An enzymic 'latch' on a global carbon store. *Nature* **409**, 149.

FSCC, 2006. Manual IIIa: Sampling and analysis of soil, *ICP Forests, 2006: Manual on the methods and criteria for harmonised sampling, assessment, monitoring and analysis of the effects of air pollution on forests*. UNECE ICP Forests Programme Co-Ordinating Centre, Hamburg. pp 26 + annexes. Available at: http://icp-forests.org/Manual.htm.

Gallet, C. and Lebreton, P., (1995). Evolution of phenolic patterns in plants and associated litters and humus of a mountain forest ecosystem. *Soil Biology and Biochemistry* **27**, 157-165.

Garnier, N., Richardin, P., Cheynier, V., and Regert, M., (2003). Characterization of thermally assisted hydrolysis and methylation products of polyphenols from modern and archaeological vine derivatives using gas chromatography-mass spectrometry. *Analytica Chimica Acta* **493**, 137-157.

Geib, S. M., Filley, T. R., Hatcher, P. G., Hoover, K., Carlson, J. E., Jimenez-Gasco, M. D. M., Nakagawa-Izumi, A., Sleighter, R. L., and Tien, M., (2008). Lignin degradation in wood-feeding insects. *Proceedings of the National Academy of Sciences of the United States of America* **105**, 12932-12937.

Gimingham, C. H., 1972. *Ecology of Heathlands*. Chapman and Hall, London. pp 266.

Gleixner, G., Bol, R., and Balesdent, J., (1999). Molecular insight into soil carbon turnover. *Rapid Communications in Mass Spectrometry* **13**, 1278-1283.

Gleixner, G., Poirier, N., Bol, R., and Balesdent, J., (2002). Molecular dynamics of organic matter in a cultivated soil. *Organic Geochemistry* **33**, 357-366.

Gold, M. H., Wariishi, H., and Valli, K., (1989). Extracellular peroxidases involved in lignin degradation by the white rot: *Basidiomycete Phanerochate chrysosporium*. Publ by ACS, Toronto, Ont, Canada. pp 127-140.

Goñi, M. A. and Hedges, J. I., (1992). Lignin dimers: Structures, distribution, and potential geochemical applications. *Geochimica et Cosmochimica Acta* **56**, 4025-4043.

González-Pérez, J. A., González-Vila, F. J., Almendros, G., and Knicker, H., (2004). The effect of fire on soil organic matter—a review. *Environment International* **30**, 855-870.

Gorham, E., (1991). Northern Peatlands: Role in the Carbon Cycle and Probable Responses to Climatic Warming. *Ecological Applications* **1**, 182-195.

Grasset, L. and Amblès, A., (1998). Structural study of soil humic acids and humin using a new preparative thermochemolysis technique. *Journal of Analytical and Applied Pyrolysis* **47**, 1-12.

Guo, L. B. and Gifford, R. M., (2002). Soil carbon stocks and land use change: A meta analysis. *Global Change Biology* **8**, 345-360.

Hájek, T., Ballance, S., Limpens, J., Zijlstra, M., and Verhoeven, J., (2011). Cell-wall polysaccharides play an important role in decay resistance of *Sphagnum* and actively depressed decomposition in vitro. *Biogeochemistry* **103**, 45-57.

Haraguchi, A., (1991). Effects of Water-Table Oscillation on Redox Property of Peat in a Floating Mat. *Journal of Ecology* **79**, 1113-1121.

Harborne, J. B., (1997). Recent advances in chemical ecology. *Natural Product Reports* **14**, 83-98.

Hargreaves, K. J., Milne, R., and Cannell, M. G. R., (2003). Carbon balance of afforested peatland in Scotland. *Forestry* **76**, 299-317.

Hatcher, P. G., (1990). Chemical structural models for coalified wood (vitrinite) in low rank coal. *Organic Geochemistry* **16**, 959-968.

Hatcher, P. G. and Minard, R. D., (1995). Comment on the origin of benzenecarboxylic acids in pyrolysis methylation studies. *Organic Geochemistry* **23**, 991-994.

Hatcher, P. G., Nanny, M. A., Minard, R. D., Dible, S. D., and Carson, D. M., (1995). Comparison of two thermochemolytic methods for the analysis of lignin in decomposing gymnosperm wood: the CuO oxidation method and the method of thermochemolysis with tetramethylammonium hydroxide (TMAH). *Organic Geochemistry* **23**, 881-888.

Hättenschwiler, S. and Vitousek, P. M., (2000). The role of polyphenols in terrestrial ecosystem nutrient cycling. *Trends in Ecology and Evolution* **15**, 238-242.

Hayward, P. M. and Clymo, R. S., (1982). Profiles of water content and pore size in Sphagnum and peat, and their relation to peat bog ecology. *Proceedings of the Royal Society of London - Biological Sciences* **215**, 299-325.

Hedges, J. I., Ertel, J. R., and Leopold, E. B., (1982). Lignin geochemistry of a Late Quaternary sediment core from Lake Washington. *Geochimica et Cosmochimica Acta* **46**, 1869-1877.

Hedges, J. I. and Mann, D. C., (1979a). The characterization of plant tissues by their lignin oxidation products. *Geochimica et Cosmochimica Acta* **43**, 1803-1807.

Hedges, J. I. and Mann, D. C., (1979b). The lignin geochemistry of marine sediments from the southern Washington coast. *Geochimica et Cosmochimica Acta* **43**, 1809-1818.

Hedges, J. I. and Parker, P. L., (1976). Land-derived organic matter in surface sediments from the Gulf of Mexico. *Geochimica et Cosmochimica Acta* **40**, 1019-1029.

Heim, A. and Schmidt, M. W. I., (2007). Lignin turnover in arable soil and grassland analysed with two different labelling approaches. *European Journal of Soil Science* **58**, 599-608.

Heinselman, M. L., (1970). Landscape Evolution, Peatland Types, and the Environment in the Lake Agassiz Peatlands Natural Area, Minnesota. *Ecological Monographs* **40**, 235-261.

Hernes, P. J. and Benner, R., (2003). Photochemical and microbial degradation of dissolved lignin phenols: Implications for the fate of terrigenous dissolved organic matter in marine environments. *Journal of Geophysical Research C: Oceans* **108**, 7-1.

Hernes, P. J. and Hedges, J. I., (2000). Determination of condensed tannin monomers in environmental samples by capillary gas chromatography of acid depolymerization extracts. *Analytical Chemistry* **72**, 5115-5124.

Hernes, P. J. and Hedges, J. I., (2004). Tannin signatures of barks, needles, leaves, cones, and wood at the molecular level. *Geochimica et Cosmochimica Acta* **68**, 1293-1307.

Hernes, P. J., Robinson, A. C., and Aufdenkampe, A. K., (2007). Fractionation of lignin during leaching and sorption and implications for organic matter "freshness". *Geophysical Research Letters* **34**.

Higuchi, T., 1980. Lignin structure & Morphological distribution in plant cell walls. In: Kirk, T. K., Higuchi, T., and Chang, H.-m. Eds.), *Lignin biodegradation: microbiology, chemistry, and potential applications*. CRC Press, Florida. pp 1-20.

Hillman, G. R., (1992). Some hydrological effects of peatland drainage in Alberta's boreal forest. *Canadian Journal of Forest Research* **22**, 1588-1596.

Holden, J., Shotbolt, L., Bonn, A., Burt, T. P., Chapman, P. J., Dougill, A. J., Fraser, E. D. G., Hubacek, K., Irvine, B., Kirkby, M. J., Reed, M. S., Prell, C., Stagl, S., Stringer, L. C., Turner, A., and Worrall, F., (2007). Environmental change in moorland landscapes. *Earth-Science Reviews* **82**, 75-100.

Hornibrook, E. R. C., Longstaffe, F. J., Fyfe, W. S., and Bloom, Y., (2000). Carbon-isotope ratios and carbon, nitrogen and sulfur abundances in flora and soil organic matter from a temperate-zone bog and marsh. *Geochemical Journal* **34**, 237-245.

Hu, Y. L., Zeng, D. H., Fan, Z. P., Chen, G. S., Zhao, Q., and Pepper, D., (2008). Changes in ecosystem carbon stocks following grassland afforestation of semiarid sandy soil in the southeastern Keerqin Sandy Lands, China. *Journal of Arid Environments* **72**, 2193-2200.

Huang, Y., Bol, R., Harkness, D. D., Ineson, P., and Eglinton, G., (1996). Post-glacial variations in distributions, ^{13}C and ^{14}C contents of aliphatic hydrocarbons and bulk organic matter in three types of British acid upland soils. *Organic Geochemistry* **24**, 273-287.

Huang, Y., Eglinton, G., Van Der Hage, E. R. E., Boon, J. J., Bol, R., and Ineson, P., (1998). Dissolved organic matter and its parent organic matter in grass upland soil horizons studied by analytical pyrolysis techniques. *European Journal of Soil Science* **49**, 1-15.

IPCC, (2000). Land use, land use change and forestry. In: (Watson, R. T., Noble, I. R., Bolin, B., Ravindranath, N. H., Verando, D. J., and Dokken, D. J. Eds.)*Special report of the intergovernmental panel on climate change*. Cambridge University Press, Cambridge University Press, Cambridge, UK. pp 375.

IPCC, (2001a). Climate Change 2001: Synthesis Report. A Contribution of Working Groups I, II, and III to the Third Assessment Report of the Integovernmental Panel on Climate Change, edited by: Watson, R.T. and the Core Writing Team. In: Watson, R. T. a. t. C. W. T. (Ed.). Cambridge University Press, Cambridge, United Kingdom, and New York, NY, USA. pp 398.

IPCC, (2001b). Climate Change: the scientific basis. Contribution of Working Group I to the Third Assessment Report of the Intergovernmental Panel on Climate Change, edited by: Houghton, J.T.,Y. Ding, D.J. Griggs, M. Noguer, P.J. van der Linden, X. Dai, K. Maskell, and C.A. Johnson. In: Houghton, J. T., Y. Ding, D.J. Griggs, M. Noguer, P.J. van der Linden, X. Dai, K. Maskell, and C.A. Johnson (Ed.). Cambridge University Press, Cambridge, United Kingdom and New York, NY, USA. pp 881.

IPCC, (2007). The Physical Science Basis, Contribution of Working Group I to the Fourth Assessment Report of the Intergovernmental Panel on Climate Change, edited by: Solomon, S., Qin, D., Manning, M., Chen, Z., Arquis, M., Averyt, K. B., Tignor, M., and Miller, H. L.,. Cambridge University Press, Cambridge, UK and New York, USA. pp 996.

Ise, T., Dunn, A. L., Wofsy, S. C., and Moorcroft, P. R., (2008). High sensitivity of peat decomposition to climate change through water-table feedback. *Nature Geoscience* **1**, 763-766.

Jandl, R., Lindner, M., Vesterdal, L., Bauwens, B., Baritz, R., Hagedorn, F., Johnson, D. W., Minkkinen, K., and Byrne, K. A., (2007). How strongly can forest management influence soil carbon sequestration? *Geoderma* **137**, 253-268.

Jassey, V. E. J., Chiapusio, G., Gilbert, D., Buttler, A., Toussaint, M. L., and Binet, P., (2011). Experimental climate effect on seasonal variability of polyphenol/phenoloxidase interplay along a narrow fen-bog ecological gradient in *Sphagnum fallax*. *Global Change Biology* **17**, 2945-2957.

Jia, G., Dungait, J. A. J., Bingham, E. M., Valiranta, M., Korhola, A., and Evershed, R. P., (2008). Neutral monosaccharides as biomarker proxies for bog-forming plants for application to palaeovegetation reconstruction in ombrotrophic peat deposits. *Organic Geochemistry* **39**, 1790-1799.

JNCC, (2011). Towards an assessment of the state of UK Peatlands. JNCC report No. 445. pp 82. Available at: http://jncc.defra.gov.uk/pdf/jncc445_web.pdf.

Johnson, L. C. and Damman, A. W. H., (1991). Species-Controlled *Sphagnum* Decay on a South Swedish Raised Bog. *Oikos* **61**, 234-242.

Joll, C. A., Huynh, T., and Heitz, A., (2003). Off-line tetramethylammonium hydroxide thermochemolysis of model compound aliphatic and aromatic carboxylic acids: Decarboxylation of some ortho- and/or para-substituted aromatic carboxylic acids. *Journal of Analytical and Applied Pyrolysis* **70**, 151-167.

Jones, C. G., Lawton, J. H., and Shachak, M., (1994). Organisms as Ecosystem Engineers. *Oikos* **69**, 373-386.

Jones, M. B. and Alison, D., (2004). Carbon Sequestration in Temperate Grassland Ecosystems and the Influence of Management, Climate and Elevated CO_2. *New Phytologist* **164**, 423-439.

Kaal, E. and Janssen, H. G., (2008). Extending the molecular application range of gas chromatography. *Journal of Chromatography A* **1184**, 43-60.

Kalbitz, K., Kaiser, K., Bargholz, J., and Dardenne, P., (2006). Lignin degradation controls the production of dissolved organic matter in decomposing foliar litter. *European Journal of Soil Science* **57**, 504-516.

Kang, H. and Freeman, C., (1999). Phosphatase and arylsulphatase activities in wetland soils: Annual variation and controlling factors. *Soil Biology and Biochemistry* **31**, 449-454.

Karhu, K., Fritze, H., Tuomi, M., Vanhala, P., Spetz, P., Kitunen, V., and Liski, J., (2010). Temperature sensitivity of organic matter decomposition in two boreal forest soil profiles. *Soil Biology and Biochemistry* **42**, 72-82.

Karroum, M., Guillet, B., Lottier, N., and Disnar, J. R., (2004). Importance and fate of biopolymers (lignins and polysaccharides) in soils of *Fagus sylvatica* stands of various ages in Fougeres forest (Brittany-France). *Annals of Forest Science* **61**, 221–233.

Kay, B. D. and Angers, D. A., 2000. Ch 7. Soil Structure. In: Sumner, M., E (Ed.), *Handbook of Soil Science*. Taylor & Francis Ltd CRC Press Inc, Florida. pp A229–A276.

Kendall, C., 1998. Tracing nitrogen sources and cycling in catchments. In: (Kendall, C. and McDonnell, J. J. Eds.), *Isotope Tracers in Catchment Hydrology*. Elsevier Science B.V, Amsterdam, The Netherlands. pp 519-576.

Kennedy, F. M., (2002). The identification of soils for forest management. Forest Commission Field Guide, Edinburgh. pp 56.

Kettunen, A., Kaitala, V., Lehtinen, A., Lohila, A., Alm, J., Silvola, J., and Martikainen, P. J., (1999). Methane production and oxidation potentials in relation to water table fluctuations in two boreal mires. *Soil Biology and Biochemistry* **31**, 1741-1749.

Kiem, R. and Kögel-Knabner, I., (2003). Contribution of lignin and polysaccharides to the refractory carbon pool in C-depleted arable soils. *Soil Biology and Biochemistry* **35**, 101-118.

Kirk, T. K. and Farrell, R. L., (1987). Enzymatic "combustion": the microbial degradation of lignin. *Annual Review of Microbiology* **41**, 465-505.

Kishimoto, T., Chiba, W., Saito, K., Fukushima, K., Uraki, Y., and Ubukata, M., (2010). Influence of syringyl to guaiacyl ratio on the structure of natural and synthetic lignins. *Journal of Agricultural and Food Chemistry* **58**, 895-901.

Kleber, M., Nico, P. S., Plante, A., Filley, T., Kramer, M., Swanston, C., and Sollins, P., (2011). Old and stable soil organic matter is not necessarily chemically recalcitrant: implications for modeling concepts and temperature sensitivity. *Global Change Biology* **17**, 1097-1107.

Klingberg, A., Odermatt, J., and Meier, D., (2005). Influence of parameters on pyrolysis-GC/MS of lignin in the presence of tetramethylammonium hydroxide. *Journal of Analytical and Applied Pyrolysis* **74**, 104-109.

Klotzbücher, T., Filley, T. R., Kaiser, K., and Kalbitz, K., (2011). A study of lignin degradation in leaf and needle litter using ^{13}C-labelled tetramethylammonium hydroxide (TMAH) thermochemolysis: Comparison with CuO oxidation and van Soest methods. *Organic Geochemistry* **42**, 1271-1278.

Knill, C. J. and Kennedy, J. F., (2003). Degradation of cellulose under alkaline conditions. *Carbohydrate Polymers* **51**, 281-300.

Knorr, W., Prentice, I. C., House, J. I., and Holland, E. A., (2005). Long-term sensitivity of soil carbon turnover to warming *Nature* **433**, 298-301.

Kögel-Knabner, I., (2002). The macromolecular organic composition of plant and microbial residues as inputs to soil organic matter. *Soil Biology and Biochemistry* **34**, 139-162.

Kögel, I., (1986). Estimation and decomposition pattern of the lignin component in forest humus layers. *Soil Biology and Biochemistry* **18**, 589-594.

Kraus, T. E. C., Dahlgren, R. A., and Zasoski, R. J., (2003). Tannins in nutrient dynamics of forest ecosystems - A review. *Plant and Soil* **256**, 41-66.

Kraus, T. E. C., Zasoski, R. J., Dahlgren, R. A., Horwath, W. R., and Preston, C. M., (2004). Carbon and nitrogen dynamics in a forest soil amended with purified tannins from different plant species. *Soil Biology and Biochemistry* **36**, 309-321.

Kuroda, K. I. and Nakagawa-Izumi, A., (2005). Tetramethylammonium hydroxide thermochemolysis of guaiacyl-syringyl and guaiacyl dehydrogenation polymers. *Organic Geochemistry* **36**, 53-61.

Kuroda, K. I., Nishimura, N., Izumi, A., and Dimmel, D. R., (2002). Pyrolysis of lignin in the presence of tetramethylammonium hydroxide: A convenient method for S/G ratio determination. *Journal of Agricultural and Food Chemistry* **50**, 1022-1027.

Kyoto Protocol, (1997). Kyoto Protocol to the United Nations Framework Convention on Climate Change. Dec. 10, 1997. FCCC/CP/1997/7/Add.1. reprinted in (1998) 37 ILM. 22. UN. Available at: http://unfccc.int/kyoto_protocol/items/2830.php.

Lal, R., (2004). Soil carbon sequestration impacts on global climate change and food security. *Science* **304**, 1623-1627.

Lamers, L. P. M., Bobbink, R., and Roelofs, J. G. M., (2000). Natural nitrogen filter fails in polluted raised bogs. *Global Change Biology* **6**, 583-586.

Limpens, J., Berendse, F., Blodau, C., Canadell, J. G., Freeman, C., Holden, J., Roulet, N., Rydin, H., and Schaepman-Strub, G., (2008). Peatlands and the carbon cycle: From local processes to global implications - A synthesis. *Biogeosciences Discussions* **5**, 1379-1419.

Lindberg, B. and Theander, O., (1952). Studies on *Sphagnum* peat. II. Lignin in *Sphagnum*. *Acta chemica Scandinavica* **6**, 311-312.

Lindsay, R., (2010). Peatbogs and carbon: a critical synthesis to inform policy development in oceanic peat bog conservation and restoration in context of climate change. pp 315. Available at: http://www.rspb.org.uk/Images/Peatbogs_and_carbon_tcm9-255200.pdf.

Lorenz, K., Lal, R., Preston, C. M., and Nierop, K. G. J., (2007). Strengthening the soil organic carbon pool by increasing contributions from recalcitrant aliphatic bio(macro)molecules. *Geoderma* **142**, 1-10.

Lorenz, K., Preston, C. M., Raspe, S., Morrison, I. K., and Feger, K. H., (2000). Litter decomposition and humus characteristics in Canadian and German spruce ecosystems: Information from tannin analysis and ^{13}C CPMAS NMR. *Soil Biology and Biochemistry* **32**, 779-792.

Macko, S. A., Engel, M. H., Hartley, G., Hatcher, P., Helleur, R., Jackman, P., and Silfer, J. A., (1991). Isotopic compositions of individual carbohydrates as indicators of early diagenesis of organic matter in peat. *Chemical Geology* **93**, 147-161.

Malmer, N. and Holm, E., (1984). Variation in the C/N-quotient of peat in relation to decomposition rate and age determination with ^{210}Pb. *Oikos* **43**, 171-182.

Marschner, B., Brodowski, S., Dreves, A., Gleixner, G., Gude, A., Grootes, P. M., Hamer, U., Heim, A., Jandl, G., Ji, R., Kaiser, K., Kalbitz, K., Kramer, C., Leinweber, P., Rethemeyer, J., Schäffer, A., Schmidt, M. W. I., Schwark, L., and Wiesenberg, G. L. B., (2008). How relevant is recalcitrance for the stabilization of organic matter in soils? *Journal of Plant Nutrition and Soil Science* **171**, 91-110.

Martínez, A. T., Rencoret, J., Nieto, L., Jiménez-Barbero, J., Gutiérrez, A., and Del Río, J. C., (2011). Selective lignin and polysaccharide removal in natural fungal

decay of wood as evidenced by in situ structural analyses. *Environmental Microbiology* **13**, 96-107.

Mason, S. L., 2009. Polyphenolic degradation and turnover in model and natural systems, PhD Thesis. Newcastle University, Newcastle-Upon-Tyne, UK.

Mason, S. L., Filley, T. R., and Abbott, G. D., (2009). The effect of afforestation on the soil organic carbon (SOC) of a peaty gley soil using on-line thermally assisted hydrolysis and methylation (THM) in the presence of ^{13}C-labelled tetramethylammonium hydroxide (TMAH). *Journal of Analytical and Applied Pyrolysis* **85**, 417-425.

Mason, S. L., Filley, T. R., and Abbott, G. D., (2012). A comparative study of the molecular composition of a grassland soil with adjacent unforested and afforested moorland ecosystems. *Organic Geochemistry* **42**, 1519-1528.

McClymont, E. L., Bingham, E. M., Nott, C. J., Chambers, F. M., Pancost, R. D., and Evershed, R. P., (2011). Pyrolysis GC-MS as a rapid screening tool for determination of peat-forming plant composition in cores from ombrotrophic peat. *Organic Geochemistry* **42**, 1420-1435.

McKinney, D. E., Bortiatynski, J. M., Carson, D. M., Clifford, D. J., De Leeuw, J. W., and Hatcher, P. G., (1996). Tetramethylammonium hydroxide (TMAH) thermochemolysis of the aliphatic biopolymer cutan: Insights into the chemical structure. *Organic Geochemistry* **24**, 641-650.

McKinney, D. E. and Hatcher, P. G., (1996). Characterization of peatified and coalified wood by tetramethylammonium hydroxide (TMAH) thermochemolysis. *International Journal of Coal Geology* **32**, 217-228.

Metzger, R. A. and Benford, G., (2001). Sequestering of atmospheric carbon through permanent disposal of crop residue. *Climatic Change* **49**, 11-19.

Milne, R. and Brown, T. A., (1997). Carbon in the vegetation and soils of Great Britain. *Journal of Environmental Management* **49**, 413-433.

Minkkinen, K., Byrne, K. A., and Trettin, C., 2008. Climate impacts of peatland forestry. In: Strack, M. (Ed.), *Peatlands and climate change*. International Peat Society, Jyväskylä. Finland. 98-122.

Moers, M. E. C., Boon, J. J., de Leeuw, J. W., Baas, M., and Schenck, P. A., (1989). Carbohydrate speciation and Py-MS mapping of peat samples from a subtropical open marsh environment. *Geochimica et Cosmochimica Acta* **53**, 2011-2021.

Mojeremane, W., Rees, R. M., and Mencuccini, M., (2010). Effects of site preparation for afforestation on methane fluxes at Harwood Forest, NE England. *Biogeochemistry* **97**, 89-107.

Morison, J., Vanguelova, E., Broadmeadow, S., Perks, M., Yamulki, S., and Randle, T., (2010). Understanding the GHG implications of forestry on peat soils in Scotland. *Forest Research. pp 55. Available at: http://www.forestry.gov.uk/pdf/FCS_forestry_peat_GHG_final_Oct13_2010.pdf/$FILE/FCS_forestry_peat_GHG_final_Oct13_2010.pdf*.

Morris, S. J., Bohm, S., Haile-mariam, S., and Paul, E. A., (2007). Evaluation of carbon accrual in afforested agricultural soils. *Global Change Biology* **13**, 1145-1156.

Mounsey, S. C., 2000. Hydrological pathways and acid episodes in the Coalburn catchment, PhD Thesis. Newcastle University, Newcastle-Upon-Tyne, UK.

Natelhoffer, K. J. and Fry, B., (1988). Controls On Natural Nitrogen-15 And Carbon-13 Abundances In Forest Soil Organic Matter. *Soil Sci. Soc. Am. J.* **52**, 1633-1640.

Natural England, (2009). Vital uplands: a 2060 vision for England's upland environment, Crown Copyright. pp 14.

Nichols, J., Booth, R. K., Jackson, S. T., Pendall, E. G., and Huang, Y., (2010). Differential hydrogen isotopic ratios of *Sphagnum* and vascular plant biomarkers in ombrotrophic peatlands as a quantitative proxy for precipitation-evaporation balance. *Geochimica et Cosmochimica Acta* **74**, 1407-1416.

Nierop, K. G. J., (2001). Temporal and vertical organic matter differentiation along a vegetation succession as revealed by pyrolysis and thermally assisted hydrolysis and methylation. *Journal of Analytical and Applied Pyrolysis* **61**, 111-132.

Nierop, K. G. J. and Buurman, P., 2007. Thermally assisted hydrolysis and methylation of organic matter in two allophanic volcanic ash soils from the Azores Islands. In: Arnalds, Ó., Bartoli, F., Buurman, P., Óskarsson, H., Stoops, G., and García-Rodeja, E. Eds.), *Soils of Volcanic Regions of Europe.* Springer Verlag, Berlin, Heidelberg. pp 411-422.

Nierop, K. G. J. and Filley, T. R., (2007). Assessment of lignin and (poly-)phenol transformations in oak (*Quercus robur*) dominated soils by ^{13}C-TMAH thermochemolysis. *Organic Geochemistry* **38**, 551-565.

Nierop, K. G. J. and Filley, T. R., (2008). Simultaneous analysis of tannin and lignin signatures in soils by thermally assisted hydrolysis and methylation using ^{13}C-labeled TMAH. *Journal of Analytical and Applied Pyrolysis* **83**, 227-231.

Nierop, K. G. J., Preston, C. M., and Kaal, J., (2005). Thermally assisted hydrolysis and methylation of purified tannins from plants. *Analytical Chemistry* **77**, 5604-5614.

Nierop, K. G. J., Van Lagen, B., and Buurman, P., (2001). Composition of plant tissues and soil organic matter in the first stages of a vegetation succession. *Geoderma* **100**, 1-24.

Nierop, K. G. J. and Verstraten, J. M., (2003). Organic matter formation in sandy subsurface horizons of Dutch coastal dunes in relation to soil acidification. *Organic Geochemistry* **34**, 499-513.

Nordbakken, J. F., Ohlson, M., and Högberg, P., (2003). Boreal bog plants: nitrogen sources and uptake of recently deposited nitrogen. *Environmental Pollution* **126**, 191-200.

Novák, M., Buzek, F., and Adamová, M., (1999). Vertical trends in $\delta^{13}C$, $\delta^{15}N$ and $\delta^{34}S$ ratios in bulk *Sphagnum* peat. *Soil Biology and Biochemistry* **31**, 1343-1346.

Oades, J. M., (1988). The Retention of Organic Matter in Soils. *Biogeochemistry* **5**, 35-70.

Okland, R. H., Okland, T., and Rydgren, K., (2001). A scandinavian perspective on ecological gradients in north-west European mires: Reply to Wheeler and Proctor. *Journal of Ecology* **89**, 481-486.

Olenin, A. S., (1980). Geographical distribution and agricultural use of peatland. *International Peat Society: Proceedings of the 6th International Peat Congress*, Duluth. pp 75-78.

Paavilainen, E. and Päivänen, J., 1995. *Peatland forestry - ecology and principles*. Springer, Berlin. pp 248.

Pancost, R. D., Baas, M., van Geel, B., and Sinninghe Damsté, J. S., (2002). Biomarkers as proxies for plant inputs to peats: an example from a sub-boreal ombrotrophic bog. *Organic Geochemistry* **33**, 675-690.

Pandey, M. P. and Kim, C. S., (2011). Lignin Depolymerization and Conversion: A Review of Thermochemical Methods. *Chemical Engineering & Technology* **34**, 29-41.

Paul, K. I., Polglase, P. J., Nyakuengama, J. G., and Khanna, P. K., (2002). Change in soil carbon following afforestation. *Forest Ecology and Management* **168**, 241-257.

Pearsall, W. H., 1971. *Mountains and Moorlands*. Collins, London. pp 312.

Peregon, A., Uchida, M., and Shibata, Y., (2007). Sphagnum peatland development at their southern climatic range in West Siberia: Trends and peat accumulation patterns. *Environmental Research Letters* **2**.

Peri, P. L., Gargaglione, V., Martínez Pastur, G., and Lencinas, M. V., (2010). Carbon accumulation along a stand development sequence of Nothofagus antarctica forests across a gradient in site quality in Southern Patagonia. *Forest Ecology and Management* **260**, 229-237.

Peterken, G. F., Ausherman, D., Buchenau, M., and Forman, R. T. T., (1992). Old-growth Conservation within British Upland Conifer Plantations. *Forestry* **65**, 127-144.

Pitman, R. M., Vanguelova, E. I., and Benham, S. E., (2010). The effects of phytophagous insects on water and soil nutrient concentrations and fluxes through forest stands of the Level II monitoring network in the UK. *Science of the Total Environment* **409**, 169-181.

Post, W. M., Emanuel, W. R., Zinke, P. J., and Stangenberger, A. G., (1982). Soil carbon pools and world life zones. *Nature* **298**, 156-159.

Post, W. M., Izaurralde, R. C., Mann, L. K., and Bliss, N., (2001). Monitoring and Verifying Changes of Organic Carbon in Soil. *Climatic Change* **51**, 73-99.

Powlson, D. S., Riche, A. B., Coleman, K., Glendining, M. J., and Whitmore, A. P., (2008). Carbon sequestration in European soils through straw incorporation: Limitations and alternatives. *Waste Management* **28**, 741-746.

Puget, P., Angers, D. A., and Chenu, C., (1999). Nature of carbohydrates associated with water-stable aggregates of two cultivated soils. *Soil Biology and Biochemistry* **31**, 55–63.

Ragan, M. A. and Glombitza, K. W., (1986). Phlorotannins, brown algal polyphenols. *Progress in Phycological Research* **4**, 129-241.

Rasmussen, S., Wolff, C., and Rudolph, H., (1995). Compartmentalization of phenolic constituents in *Sphagnum*. *Phytochemistry* **38**, 35-39.

Rasse, D. P., Dignac, M. F., Bahri, H., Rumpel, C., Mariotti, A., and Chenu, C., (2006). Lignin turnover in an agricultural field: From plant residues to soil-protected fractions. *European Journal of Soil Science* **57**, 530-538.

Riedo, C., Scalarone, D., and Chiantore, O., (2009). Advances in identification of plant gums in cultural heritage by thermally assisted hydrolysis and methylation. *Analytical and Bioanalytical Chemistry* **396**, 1559-1569.

Robertson, S., 2008. Degradation of three lignin containing substrates by the oyster mushroom (*Pleurotus ostreatus* [Jacq:Fr.] Kummer. Division: Basidiomycota, class: Agaricomysetes, order: Agaricales, family Pleuorotaceae), PhD Thesis. Newcastle University, Newcastle-Upon-Tyne, UK.

Robinson, M., (1998). 30 years of forest hydrology changes at Coalburn: water balance and extreme flows. *Hydrology & Earth System Sciences* **2**, 233-238.

Robinson, M., Moore, R. E., Nisbet, T. R., and Blackie, J. R., (1998). From Moorland to forest: the Coalburn catchment experiment. Institute of Hydrology. pp 72. Available at http://nora.nerc.ac.uk/7372/1/IH_133.pdf

Rochefort, L., Vitt, D. H., and Bayley, S. E., (1990). Growth, Production, and Decomposition Dynamics of *Sphagnum* under Natural and Experimentally Acidified Conditions. *Ecology* **71**, 1986-2000.

Rose, K., (1994). Facile synthesis of homogeneous artificial proteins. *Journal of the American Chemical Society* **116**, 30-33.

Rudolph, H. and Samland, J., (1985). Occurrence and metabolism of sphagnum acid in the cell walls of bryophytes. *Phytochemistry* **24**, 745-749.

Rumpel, C., Kögel-Knabner, I., and Bruhn, F., (2002). Vertical distribution, age, and chemical composition of organic carbon in two forest soils of different pedogenesis. *Organic Geochemistry* **33**, 1131-1142.

Saiz-Jimenez, C., (1994). Analytical pyrolysis of humic substances: Pitfalls, limitations, and possible solutions. *Environmental Science and Technology* **28**, 1773-1780.

Sarkanen, K. V. and Hergert, H. L., 1971. Classification and distribution. In: Sarkanen, K. V., Ludwig, C.H. (Ed.), *Lignins: Occurrence, Formation, Structure, and Reactions*. Wiley-Interscience, New York, NY. pp 43-94.

Sauheitl, L., Glaser, B., and Bol, R., (2005). Short-term dynamics of slurry-derived plant and microbial sugars in a temperate grassland soil as assessed by compound-specific ^{13}C analyses. *Rapid Communications in Mass Spectrometry* **19**, 1437-1446.

Schouwenaars, J. M., (1988). The impact of water management upon groundwater fluctuations in a disturbed bog relict. *Agricultural Water Management* **14**, 439-449.

Schultz, J. C., Hunter, M. D., and Appel, H. M., (1992). Antimicrobial activity of polyphenols mediates plant-herbivore interactions. *Plant Polyphenols: Synthesis, Properties, Significance* **59**, 621-637.

Schwarzinger, C., 2002. Thermally Assisted Hydrolysis and Methylation of Carbohydrates and Related Materials, PhD Thesis. Johannes Kepler Universitat Linz.

Schwarzinger, C., (2003). On the mechanism of thermally assisted hydrolysis and methylation of carbohydrates: The contribution of aldol and retroaldol reactions. *Journal of Analytical and Applied Pyrolysis* **68-69**, 137-149.

Schwarzinger, C., (2004). Identification of methylated saccharinolactones and partially methylated saccharinic acids in the thermally assisted hydrolysis and methylation of carbohydrates. *Journal of Analytical and Applied Pyrolysis* **71**, 501-514.

Schwarzinger, C., Tanczos, I., and Schmidt, H., (2002). Levoglucosan, cellobiose and their acetates as model compounds for the thermally assisted hydrolysis and methylation of cellulose and cellulose acetate. *Journal of Analytical and Applied Pyrolysis* **62**, 179-196.

Shadkami, F. and Helleur, R., (2010). Recent applications in analytical thermochemolysis. *Journal of Analytical and Applied Pyrolysis* **89**, 2-16.

Six, J., Callewaert, P., Lenders, S., De Gryz, S., Morris, S. J., Gregorich, E. G., Paul, E. A., and Paustian, K., (2002). Measuring and understanding carbon storage in afforested soils by physical fractionation. *Soil Science Society of America Journal* **66**, 1981-1987.

Sjors, H., (1980). Peat on Earth: Multiple Use or Conservation? *Ambio* **9**, 303-308.

Sollins, P., Homann, P., and Caldwell, B. A., (1996). Stabilization and destabilization of soil organic matter: Mechanisms and controls. *Geoderma* **74**, 65-105.

Spaccini, R., Piccolo, A., Haberhauer, G., and Gerzabek, M. H., (2000). Transformation of organic matter from maize residues into labile and humic fractions of three European soils as revealed by ^{13}C distribution and CPMAS-NMR spectra. *European Journal of Soil Science* **51**, 583-594.

Srebotnik, E., Jensen Jr, K. A., Kawai, S., and Hammel, K. E., (1997). Evidence that Ceriporiopsis subvermispora degrades nonphenolic lignin structures by a one-electron-oxidation mechanism. *Applied and Environmental Microbiology* **63**, 4435-4440.

SSSA, Soil Science Society of America, (2001). *Glossary of Soil Science Terms. pp 135*.

Suzuki, S., Tuyet Lam, T. B., and Iiyama, K., (1997). 5-Hydroxyguaiacyl nuclei as aromatic constituents of native lignin. *Phytochemistry* **46**, 695-700.

Tanczos, I., Rendl, K., and Schmidt, H., (1999). The behavior of aldehydes—produced as primary pyrolysis products—in the thermochemolysis with tetramethylammonium hydroxide. *Journal of Analytical and Applied Pyrolysis* **49**, 319-327.

Tanczos, I., Schwarzinger, C., Schmidt, H., and Balla, J., (2003). THM-GC/MS analysis of model uronic acids of pectin and hemicelluloses. *Journal of Analytical and Applied Pyrolysis* **68-69**, 151-162.

Tarnocai, C. and Stolbovoy, V., 2006. Northern Peatlands: their characteristics, development and sensitivity to climate change. In: (Martini, I. P., Martinez, C., and Chesworth, W. Eds.), *Peatlands. Evolution and records of environmental and climate changes*. Elsevier. pp 17-51.

Taylor, J. A., (1964). Distribution and development of the world's peat deposits. *Nature* **201**, 454-456.

Taylor, P., 1960. *British Ferns and Mosses*. The Chiswick Press, London. pp 231.

Templier, J., Derenne, S., Croué, J.-P., and Largeau, C., (2005). Comparative study of two fractions of riverine dissolved organic matter using various analytical pyrolytic methods and a ^{13}C CP/MAS NMR approach. *Organic Geochemistry* **36**, 1418-1442.

Thormann, M. N., Currah, R. S., and Bayley, S. E., (2002). The relative ability of fungi from Sphagnum fuscum to decompose selected carbon substrates. *Canadian Journal of Microbiology* **48**, 204-211.

Thormann, M. N., Szumigalski, A. R., and Bayley, S. E., (1999). Aboveground peat and carbon accumulation potentials along a bog-fen-marsh wetland gradient in southern boreal Alberta, Canada. *Wetlands* **19**, 305-317.

Thuille, A., Buchmann, N., and Schulze, E. D., (2000). Carbon stocks and soil respiration rates during deforestation, grassland use and subsequent Norway spruce afforestation in the Southern Alps, Italy. *Tree Physiology* **20**, 849-857.

Tiessen, H. and Stewart, J. W. B., (1983). Particle-size Fractions And Their Use In Studies Of Soil Organic Matter: II. Cultivation Effects On Organic Matter Composition In Size Fractions. *Soil Sci. Soc. Am. J.* **47**, 509-514.

Tomassen, H. B. M., Smolders, A. J. P., Lamers, L. P. M., and Roelofs, J. G. M., (2003). Stimulated growth of *Betula pubescens* and *Molinia caerulea* on ombrotrophic bogs: Role of high levels of atmospheric nitrogen deposition. *Journal of Ecology* **91**, 357-370.

Tomassen, H. B. M., Smolders, A. J. P., Limpens, J., Lamers, L. P. M., and Roelofs, J. G. M., (2004). Expansion of invasive species on ombrotrophic bogs: Desiccation or high N deposition? *Journal of Applied Ecology* **41**, 139-150.

Trumbore, S. E., (1997). Potential responses of soil organic carbon to global environmental change. *Proceedings of the National Academy of Sciences* **94**, 8284-8291.

Trumbore, S. E., Bonani, G., and Wölfli, W., 1990. The rates of carbon cycling in several soils from AMS ^{14}C measurements of fractionated soil organic matter. In: Bouwman, A. F. (Ed.), *Soils and the Greehouse Effect*. John Wiley and Sons, Chichester, U.K. pp 407-417.

Turetsky, M. R., (2003). The Role of Bryophytes in Carbon and Nitrogen Cycling. *The Bryologist* **106**, 395-409.

Turetsky, M. R., Crow, S. E., Evans, R. J., Vitt, D. H., and Wieder, R. K., (2008). Trade-offs in resource allocation among moss species control decomposition in boreal peatlands. *Journal of Ecology* **96**, 1297-1305.

Umezawa, T. and Higuchi, T., (1987). Mechanism of aromatic ring cleavage of β-O-4 lignin substructure models by lignin peroxidase. *FEBS Letters* **218**, 255-260.

UNFCCC, (2001). The Marrakesh Accords and the Marrakesh Declaration, Available at: http://unfccc.int/cop7/documents/accords_draft.pdf.

van Breemen, N., (1995). How *Sphagnum* bogs down other plants. *Trends in Ecology & Evolution* **10**, 270-275.

van der Heijden, E., 1994. A combined anatomical and pyrolysis mass spectrometric study of peatified plant tissues, PhD Thesis. Universiteit van Amsterdam.

van der Heijden, E. and Boon, J. J., (1994). A combined pyrolysis mass spectrometric and light microscopic study of peatified Calluna wood isolated from raised bog peat deposits. *Organic Geochemistry* **22**, 903-919.

van der Heijden, E., Boon, J. J., Rasmussen, S., and Rudolph, H., (1997). Sphagnum acid and its decarboxylation product isopropenylphenol as biomarkers for fossilised *Sphagnum* in peats. *Ancient Biomolecules* **1**, 93-107.

van der Molen, P. C. and Wijmstra, T. A., (1994). The Thermal Regime of Hummock-Hollow Complexes on Clara Bog, Co. Offaly. *Biology and Environment: Proceedings of the Royal Irish Academy* **94B**, 209-221.

van Smeerdijk, D. G. and Boon, J. J., (1987). Characterisation of subfossil *Sphagnum* leaves, rootlets of ericaceae and their peat by pyrolysis-high-resolution gas

chromatography-mass spectrometry. *Journal of Analytical and Applied Pyrolysis* **11**, 377-402.

Vancampenhout, K., Wouters, K., De Vos, B., Buurman, P., Swennen, R., and Deckers, J., (2009). Differences in chemical composition of soil organic matter in natural ecosystems from different climatic regions - A pyrolysis-GC/MS study. *Soil Biology and Biochemistry* **41**, 568-579.

Vane, C. H., Drage, T. C., and Snape, C. E., (2003). Biodegradation of Oak (*Quercus alba*) Wood during Growth of the Shiitake Mushroom (*Lentinula edodes*): A Molecular Approach. *Journal of Agricultural and Food Chemistry* **51**, 947-956.

Vane, C. H., Martin, S. C., Snape, C. E., and Abbott, G. D., (2001). Degradation of lignin in wheat straw during growth of the oyster mushroom (Pleurotus ostreatus) using off-line thermochemolysis with tetramethylammonium hydroxide and solid-state ^{13}C NMR. *Journal of Agricultural and Food Chemistry* **49**, 2709-2716.

Vanguelova, E., (2012). A new evaluation of carbon stocks in British forest soils. *Soil Use and Management* **In Press**.

Vanguelova, E. I., Benham, S., Pitman, R., Moffat, A. J., Broadmeadow, M., Nisbet, T., Durrant, D., Barsoum, N., Wilkinson, M., Bochereau, F., Hutchings, T., Broadmeadow, S., Crow, P., Taylor, P., and Durrant Houston, T., (2010). Chemical fluxes in time through forest ecosystems in the UK – Soil response to pollution recovery. *Environmental Pollution* **158**, 1857-1869.

Verhoeven, J. T. A. and Liefveld, W. M., (1997). The ecological significance of organochemical compounds in *Sphagnum*. *Acta Botanica Neerlandica* **46**, 117-130.

Villada, A., Shaw, L., Verhoef, A., and Vanguelova, E., (2012). Effect of three species and soil type on chemical and physical carbon fractions in UK forest Soils (poster).

Vitt, D. H., Wieder, R. K., Scott, K. D., and Faller, S., (2009). Decomposition and peat accumulation in rich fens or boreal Alberta, Canada. *Ecosystems* **12**, 360-373.

von Arnold, K., Weslien, P., Nilsson, M., Svensson, B. H., and Klemedtsson, L., (2005). Fluxes of CO_2, CH_4 and N_2O from drained coniferous forests on organic soils. *Forest Ecology and Management* **210**, 239-254.

von Lützow , M., Kogel-Knabner, I., Ekschmitt, K., Matzner, E., Guggenberger, G., Marschner, B., and Flessa, H., (2006). Stabilization of organic matter in

temperate soils: Mechanisms and their relevance under different soil conditions - A review. *European Journal of Soil Science* **57**, 426-445.

Wang, S., Wang, K., Liu, Q., Gu, Y., Luo, Z., Cen, K., and Fransson, T., (2009). Comparison of the pyrolysis behavior of lignins from different tree species. *Biotechnology Advances* **27**, 562-567.

Watson, R. T. and Noble, I. N., 2005. The global imperative and policy for carbon sequestration. In: (Griffiths, H. and Jarvis, P. G. Eds.), *The Carbon Balance of Forest Biomes*. Thomson Publishing Services. pp 356.

Weng, J. K. and Chapple, C., (2010). The origin and evolution of lignin biosynthesis. *New Phytologist* **187**, 273-285.

White, T., (1957). Tannins—their occurrence and significance. *Journal of the Science of Food and Agriculture* **8**, 377-385.

Wieder, R. K. and Yavitt, J. B., (1994). Peatlands and global climate change: insights from comparative studies of sites situated along a latitudinal gradient. *Wetlands* **14**, 229–238.

Williams, C. J., Yavitt, J. B., Wieder, R. K., and Cleavitt, N. L., (1998). Cupric oxide oxidation products of northern peat and peat-forming plants. *Canadian Journal of Botany* **76**, 51-62.

Wysocki, L. A., Filley, T. R., and Bianchi, T. S., (2008). Comparison of two methods for the analysis of lignin in marine sediments: CuO oxidation versus tetramethylammonium hydroxide (TMAH) thermochemolysis. *Organic Geochemistry* **39**, 1454-1461.

Yeloff, D. and Mauquoy, D., (2006). The influence of vegetation composition on peat humification: Implications for palaeoclimatic studies. *Boreas* **35**, 662-673.

Yu, Z., Loisel, J., Brosseau, D. P., Beilman, D. W., and Hunt, S. J., (2010). Global peatland dynamics since the Last Glacial Maximum. *Geophysical Research Letters* **37**, L13402.

Zaccone, C., Said-Pullicino, D., Gigliotti, G., and Miano, T. M., (2008). Diagenetic trends in the phenolic constituents of *Sphagnum*-dominated peat and its corresponding humic acid fraction. *Organic Geochemistry* **39**, 830-838.

Zanella, A., Jabiol, B., Ponge, J. F., Sartori, G., De Waal, R., Van Delft, B., Graefe, U., Cools, N., Katzensteiner, K., Hager, H., Englisch, M., Brethes, A., Broll, G., Gobat, J. M., Brun, J. J., Milbert, G., Kolb, E., Wolf, U., Frizzera, L., Galvan, P., Kolli, R., Baritz, R., Kemmers, R., Vacca, A., Serra, G., Banas, D., Garlato, A.,

Chersich, Klimo, E., and Langohr, R., (2011). European humus forms reference base., Available at: http://hal.archives-ouvertes.fr/hal-00541496.

Zerva, A., Ball, T., Smith, K. A., and Mencuccini, M., (2005). Soil carbon dynamics in a Sitka spruce (*Picea sitchensis (Bong.) Carr.*) chronosequence on a peaty gley. *Forest Ecology and Management* **205**, 227-240.

Zerva, A. and Mencuccini, M., (2005). Carbon stock changes in a peaty gley soil profile after afforestation with Sitka spruce (Picea sitchensis). *Annals of Forest Science* **62**, 873-880.

APPENDIX

A1: The equations used to determine the original aromatic methoxyl/hydroxyl content of 3,4-dimethoxy- (guaiacyl, 1 and 2) and 3,4,5-trimethoxy (syringyl, 3 and 4) compounds (taken from Filley et al., 2006)

% Hydroxyl (G6, G5 and G18)

$$= 100 \text{ x } \left[\frac{(M_{L+1} - (M_{L+1})_{calc})}{M_L + M_{L+1} - (M_{L+1})_{calc}}\right]$$

Where

$$(M_{L+1})_{calc} = M_L \text{ x } \left(\frac{M_{UL+1}}{M_{UL}}\right) \text{ x } \left(\frac{N_L}{N_{UL}}\right)$$

% Hydroxyl (G4)

$$= 100 \text{ x } \left[\frac{(M_{L+2})_{calc}}{(M_L)_{calc} + (M_{L+2})_{calc}}\right]$$

Where

$$(M_L)_{calc} = \left(M_{L-1} \text{ x } \left(\frac{M_{UL}}{M_{UL-1}}\right) \text{ x } \left(\frac{N_L}{N_{UL}}\right)\right)$$

Where

$$(M_{L+1})_{calc} = \left(M_L \text{ - } \left(M_{L-1} \text{ x} \frac{M_{UL+1}}{M_{UL}}\right) \text{ x } \left(\frac{N_L}{N_{UL}}\right)\right)$$

$$- \left(\left(M_{L+1} \text{ - } \left(M_{L+2} \text{ x} \frac{M_{UL+1}}{M_{UL}}\right) \text{ x } \left(\frac{M_{UL-1}}{M_{UL}}\right)\right) x \left(\frac{M_{UL-1}}{M_{UL}}\right)\right)\left(\frac{N_{L+1}}{N_{UL}}\right)\left(\frac{M_{UL+1}}{M_{UL}}\right)$$

Where

$$(M_{L+2})_{calc} = M_{L+1} \text{ - } \left(M_{L+2} \text{x } \frac{M_{UL-1}}{M_{UL}}\right) \text{ x } \left(\frac{N_{L+1}}{N_{UL}}\right) - (M_{L+1})_{calc}$$

% Hydroxyl (S6 and S5)

% 1 Hydroxyl

$$= 100 \text{ x } \left[\frac{(M_L)}{M_L + [M_{L+1} - (M_{L+1})_{calc}] + [M_{L+2} - (M_{L+2})_{calc}]}\right]$$

% 2 Hydroxyl

$$= 100 \text{ x } \left[\frac{M_{L+1} - (M_{L+1})_{calc}}{M_L + [M_{L+1} - (M_{L+1})_{calc}] + [M_{L+2} - (M_{L+2})_{calc}]}\right]$$

% 3 Hydroxyl

$$= 100 \text{ x } \left[\frac{M_{L+2} - (M_{L+2})_{calc}}{M_L + [M_{L+1} - (M_{L+1})_{calc}] + [M_{L+2} - (M_{L+2})_{calc}]}\right]$$

Where

$$(M_{L+1})_{calc} = \left(M_L \text{ x } \left(\frac{M_{UL+1}}{M_{UL}}\right) \text{ x } \left(\frac{N_L}{N_{UL}}\right)\right)$$

Where

$$(M_{L+2})_{calc} = \left([M_{L+1} - (M_{L+1})_{calc}] \text{ x } \left(\frac{M_{UL+1}}{M_{UL}}\right) \text{ x } \left(\frac{N_L}{N_{UL}}\right)\right)$$

% Hydroxyl (S4)

% 1 Hydroxyl

$$= 100 \text{ x } \left[\frac{(M_{L-1})}{(M_{L-1}) + [(M_{L+1})_{calc}] + [M_{L+2} - (M_{L+2})_{calc}]}\right]$$

% 2 Hydroxyl

$$= 100 \text{ x } \left[\frac{(M_{L+1})_{calc}}{(M_{L-1}) + [(M_{L+1})_{calc}] + [(M_{L+2})_{calc}]}\right]$$

% 3 Hydroxyl

$$= 100 \text{ x } \left[\frac{(M_{L+2})_{calc}}{(M_{L-1}) + [(M_{L+1})_{calc}] + [(M_{L+2})_{calc}]}\right]$$

Where

$$(M_{L+1})_{calc} = M_{L+1} - \left[\left(M_L - M_{L-1} \text{ x } \left(\frac{M_{UL}}{M_{UL-1}}\right)\right) \text{ x } \left(\frac{M_{UL-1}}{M_{UL}}\right) \text{ x } \left(\frac{N_L}{N_{UL}}\right) + \left(M_{L+2} - M_{L+3} \text{ x } \frac{M_{UL+1}}{M_{UL}}\right) \text{ x } \left(\frac{M_{UL+1}}{M_{UL}}\right) x \left(\frac{N_{L+1}}{N_{UL}}\right)\right]$$

Where

$$(M_{L+2})_{calc} = M_{L+2} - \left[M_{L+1} - \left(M_{L+2} - M_{L+3} \text{ x } \frac{M_{UL+1}}{M_{UL}}\right) \text{ x } \left(\frac{M_{UL+1}}{M_{UL}}\right) \text{ x } \left(\frac{N_{L+1}}{N_{UL}}\right) \text{ x } \left(\frac{M_{UL}}{M_{UL-1}}\right)\right.$$

A2: The equations used to determine the original aromatic methoxyl/hydroxyl content of sphagnum acid thermochemolysis products

% Hydroxyl (**I**, **IIa/b**, **III**)

$$= 100 \text{ x } \left[\frac{(M_{L+1} - (M_{L+1})_{calc})}{M_L + M_{L+1} - (M_{L+1})_{calc}}\right]$$

Where

$$(M_{L+1})_{calc} = M_L \text{ x } \left(\frac{M_{UL+1}}{M_{UL}}\right) \text{ x } \left(\frac{N_L}{N_{UL}}\right)$$

Table A2: The first set of data required to ascertain the methoxyl/hydroxyl content of sphagnum acid thermochemolysis products

	m/z	**I**	*m/z*	**IIa**	**IIb**	*m/z*	**III**
NL		9		10	10		10
NUL		10		12	12		12
MUL	148	137625	206	12945	52201	206	21411
MUL+1	149	18615	207	2842	9446	207	4002
ML	149	126222	208	4953	14358	208	4992
ML + 1	150	15823	209	799	2023	209	769
(ML + 1)calc		15365.4		906.2	2165.1		777.56

4-Isopropenyl phenol

So to determine (ML+1)calc

= 126222 x (18615 / 137625) x (9 / 10)

= 126222 x 0.1352589 x 0.9

= 15365.38

So to determine the percentage of **I** that has one hydroxyl group (i.e. derived from sphagnum acid):

= 100 x (15823 – 15365.38) / (126222 + 15823 – 15365.38)

= 100 x (457.62 / 126679.62)

= 100 x $3.61x10^{-3}$

= 0.36

=100-0.36

= <u>99.64%</u>

(E) and (*Z*)- 3-(4'-hydroxyphen-1-yl)but-2-enoic acid

Isomer 1:

So to determine (ML+1)calc

= 4953 x (2842 / 12944) x (10 / 12)

= 4953 x 0.219544 x 0.8333

= 906.17

So to determine the percentage of **IIa** that has two hydroxyl groups (i.e. derived from sphagnum acid):

= 100 x (799 – 906.2) / (4953+ 799 – 906.2)

= 100 x (-107.17/ 4845.8)

= 100 x -0.0221

= -2.21

=100-2.21

= <u>97.79%</u>

Isomer 2:

So to determine (ML+1)calc

= 14358 x (9446 / 52201) x (10 / 12)

= 14358 x 0.18095 x 0.8333

= 2165.12

So to determine the percentage of **IIb** that has two hydroxyl groups (i.e. derived from sphagnum acid):

= 100 x (2023 – 2165.12) / (14358+ 2023 – 2165.12)

= 100 x (-142.12/ 14215.9)

= 100 x $-9.9x10^{-5}$

= -0.999

=100-0.999

= <u>99.001%</u>

3-(4'-hydroxyphen-1-yl)but-3-enoic acid

So to determine (ML+1)calc

= 4992 x (4002/21411) x (10/12)

= 4992 x 0.1869 x 0.8333

= 777.559

So to determine the percentage of **III** that has two hydroxyl groups (i.e. derived from sphagnum acid):

= 100 x (769 – 777.56) / (4992+ 769 – 777.56)

= 100 x (-8.56/ 4983.44)

= 100 x $-1.72x10^{-3}$

= -0.17

=100-0.17

= <u>99.83%</u>